

REDESIGN OF COLLAGEN CASINGS FOR HIGH QUALITY PERFORMANCE USING FOOD GRADE POLYSACCHARIDES

Motolani Oluwafunmilayo Sobanwa, MSc

Thesis Submitted to the University of Nottingham for
the degree of Doctor of Philosophy

Division of Food, Nutrition and Dietetics
School of Biosciences
University of Nottingham
Loughborough
LE12 5RD

July 2021

Abstract

Collagen film (casings) obtained from acid-swollen collagen fibres is widely used as an alternative to natural casings for sausage production. However, collagen casings possess weak properties such as low mechanical properties (tensile strength and stiffness) and thermal stability compared to natural casings. Therefore, there is a need industrially to improve these properties. The main purpose of this work was to study the effects of polysaccharides on the properties of acid-swollen collagen pastes and films as a function of collagen paste concentrations (2.5 %, 3.5 % and 4 %wt/wt). In this work, polysaccharides dispersions: cellulose fibres of different length and waxy (WS) and high amylose (HAS) maize starch granules and molecular solutions: Hydroxypropylmethylcellulose (HPMC), Methylcellulose (MC), high molecular weight (GH), low molecular weight guar gum (GM) and Carboxymethylcellulose (CMC) were blended with acid-swollen collagen paste to fabricate collagen films with improved properties such as mechanical properties (tensile strength, stiffness and flexibility) and thermal stability. The viscoelastic of the blend pastes and denaturation of collagen was studied by rheological and thermal techniques. The pure and composite films were studied by sorption, mechanical, spectroscopic, structural, and thermal techniques.

The focus of the first part of this study is to investigate the effect of uncharged and negatively charged molecular solutions at comparable low-shear viscosity on the viscoelastic and thermal properties of acid-swollen collagen paste. Dynamic rheological data indicated that the addition of non-charged hydrocolloids: HPMC, MC, GH and GM increased the storage modulus (G') and loss modulus (G'') of the acid-swollen collagen paste. By contrast, negatively charged CMC decreased the G' and G'' of the collagen pastes. At the level of addition of non-charged solutions (HPMC,

MC, GH and GM) considered in this study, the denaturation temperature of collagen as determined by DSC was not affected while negatively charged CMC increased the denaturation temperature.

Composite films containing blends of collagen paste with the individual molecular solutions were formed. Films were characterised for their mechanical, thermal, sorption and structural properties. Collagen/CMC films were not tested due to the difficulty in analysing the films. The thickness of the films increased and was dependent on the collagen concentration as well as the hydrocolloid concentration in the film network. Mechanical data revealed that the addition of hydrocolloids increased the tensile strength (TS), stiffness (YM), and elongation at break (EAB) of the films. Derivatised cellulose showed higher enhancement than the guar. Consistent with the mechanical data, DSC revealed an increase in peak temperature and a decrease in enthalpy of the films with the addition of the polymers. An increase in TS, YM, and EAB and an increase in peak temperatures were dependent on the collagen concentration. XRD data of the composite film showed a reduction in the intensity of the crystalline peak of collagen. FTIR spectra of the films helped to understand the structural changes and the interaction between the collagen and hydrocolloids. The thermal degradation temperature of collagen was not affected, as evidenced by the TGA curves. Furthermore, the composite films showed lower moisture uptake than the pure collagen films.

The next study focused on investigating the effect of polysaccharide dispersions, cellulose with different fibre length, waxy and high amylose maize starches at comparable dispersed phase volume on the rheological and thermal properties of acid-swollen collagen paste. The dynamic rheological measurement revealed the dominant

elastic behaviour ($G' > G''$) of the blend and control pastes. Cellulose fibres, waxy and high amylose starch granules increased the storage and loss modulus, and values increased with increasing collagen content. The starches exhibited a higher value due to the high concentration used. According to the DSC data, the denaturation of collagen and enthalpy of melting was not affected by the addition of the dispersions. On the other hand, on reheating the blend pastes, the starches lowered the enthalpy of the denatured collagen. Films were made from the blend pastes and were characterised for their mechanical, thermal, sorption and structural properties. The surface of composite films appeared rough because of the protrusion of the cellulose fibres and starch granules. The thickness of the films increased with the addition of the cellulose fibres and starch granules. Values increased with increasing levels of collagen and dispersions concentration in the film-forming paste. Reinforcing collagen films with cellulose fibres increased the mechanical properties (TS, YM and EAB) of the films. The mechanical properties of collagen with starch granules films could not be tested due to the brittleness of the films. DSC data showed that cellulose fibres increased the peak temperature of the films. By contrast, starch granules decreased the peak temperature. The enthalpy of the films was significantly reduced with the addition of cellulose fibres and starch granules. Collagen with starch granules films had the lowest enthalpy values. XRD data showed a decrease in the intensity of the crystalline peak of collagen in the blend films. The thermal stability of collagen was reduced, as evidenced by the TGA data. Additionally, the water uptake of the films decreased with the addition of cellulose fibres and starch granules.

For the final study, the effect of collagen pastes (2.5%, 3.5% and 4 % wt) on the pasting properties of waxy (WS), high amylose (HAS) and normal (NS) maize starches were studied using Rapid Viscous Analyser (RVA) at conventional (up to 95 °C) and

high-temperature (up to 140 °C) heating modes. Results showed that collagen pastes modified the pasting properties of the starches. At conventional heating mode, high amylose did not show a noticeable pasting profile. The pasting temperature of waxy starch was unaffected by the addition of collagen paste. By contrast, the addition of collagen paste lowered the pasting temperature of normal starches. The viscosities (peak, setback, and breakdown) of NS and WS increased. The final viscosity of WS decreased while that of NS increased with the increase in collagen paste concentration. When the samples are heated to temperatures 140 °C higher, HAS showed a noticeable pasting profile. The pasting temperature of HAS decreased with increasing levels of collagen paste addition. Peak and breakdown viscosities of NS, WS, and HAS increased with increasing collagen paste levels. In contrast, setback and final viscosities reduced.

Acknowledgement

This research was funded by Engineering, Physical Science Research Council (EPSRC) and DEVRO Plc.

Thanks be to God almighty for the strength and for making this journey possible.

My profound gratitude goes to my supervisors, Prof Tim Foster, Dr Nicolas Watson, and Dr Gleb Yakubov, for their encouragement, the wealth of knowledge, patience and support offered to me during this study. I want to thank Devro Plc for funding this PhD and Dr Gordon Paul for his support and valuable suggestions about the project.

Special thanks to Dr William Macnaughtan for his support, training, guidance, and scientific discussion of my experimental results. I would like to thank Darrell Cobon for helping perform the DSC and TGA experiments of my film samples.

I would also like to thank Dr Melvin Holmes, my MSc supervisor at the University of Leeds, for recommending me for this PhD.

Many thanks to my friends and colleagues for making my time at the University of Nottingham memorable. Thanks to Dr Toba Sanni for helping to proofread my work.

A big thanks to my parents and siblings for their constant support and prayers during this PhD. Also, thanks to my husband Isaiah Fasanya for his love, support and patience.

List of abbreviations and symbols

ANOVA	Analysis of variance
ATR-FTIR	Attenuated total reflectance Fourier transform infrared spectroscopy
CMC	Carboxymethylcellulose
CNC	Cellulose nanocrystals
DSC	Differential Scanning Calorimeter
DVS	Dynamic vapor sorption
EAB	Elongation at break
G'	Storage modulus
G''	Loss modulus
GAB	Guggenheim, Anderson and de Boer
GH	High molecular weight guar gum
GM	Medium molecular weight guar gum
HAS	High amylose starch
HPMC	Hydroxypropylmethylcellulose
M ₀	Monolayer moisture content
MC	Methylcellulose
MFC	Microfibrillated cellulose
Na CMC	Sodium carboxymethylcellulose
NS	Normal starch
RH	Relative humidity
RVA	Rapid viscous analyser
SEM	Scanning electron microscopy
tan δ	Tan delta
TGA	Thermogravimetric analysis

T_{peak}	Maximum melting temperature
TS	Tensile strength
WS	Waxy starch
XRD	X-ray diffraction
$\dot{\gamma}$	Shear rate (1/s)
YM	Young's modulus
ΔH	Enthalpy (J/g)
η	Shear Viscosity
η_0	zero-shear viscosity (Pas)
τ	Shear stress (Pa)
ω	Angular Frequency (rad/s)

List of publications

Sobanwa, M., T.J.Foster, and N.J.Watson. "The effect of cellulose and starch on the viscoelastic and thermal properties of acid-swollen collagen paste". *Food Hydrocolloids* 101, 105460 <https://doi.org/10.1016/j.foodhyd.2019.105460>.

Sobanwa, M., T.J.Foster, Gleb Yakubov and N.J.Watson. The impact of hydrocolloids addition on viscoelastic and thermal properties of acid-swollen collagen paste. *Food Hydrocolloids*, manuscripts in preparation.

Sobanwa, M., T.J.Foster, Gleb Yakubov and N.J.Watson. Effect of acid-swollen collagen paste on the pasting properties of corn starch at different heating modes *Carbohydrate polymer*, manuscripts in preparation.

Presentations

M. Sobanwa, N.J.Watson, T.J. Foster. Redesign of collagen casings for high quality performance using food grade polysaccharides. *University of Nottingham, School of Biosciences symposium, 19th – 21st April 2018*. Poster presentation.

M. Sobanwa, N.J.Watson, T.J. Foster. Redesign of collagen casings for high quality performance using food grade polysaccharides. *3rd EPNOE International Junior Scientists Meeting, Maribor, Slovenia, 14th – 15th May 2018*. Poster presentation.

M. Sobanwa, N.J.Watson, G.Paul, T.J. Foster. The impact of cellulose on the rheological and thermal properties of collagen paste used for sausage casing. *17th Food colloids conference, Leeds, UK, 8th – 11th April 2019*. Poster presentation.

M. -Sobanwa, N.J.Watson, T.J. Foster. Effect of cellulose and starch on viscoelastic and thermal properties of collagen paste used for sausage casing. *University of Nottingham, School of Biosciences symposium, 26th – 27th June 2019*. Oral presentation.

M. Sobanwa, N.J.Watson, T.J. Foster. Effect of cellulose and starch on viscoelastic and thermal properties of collagen paste. *The 20th Gums & Stabilisers for the Food Industry Conference, Spain, San Sebastian, 11th – 14th June 2019*. Oral presentation

M. Sobanwa, N.J.Watson, T.J. Foster. Thermal, mechanical and structural properties of collagen with cellulose/starch films. *4th UK Hydrocolloids Symposium, Leeds, UK, 12th September 2019*. Oral and Poster presentation.

M. Sobanwa, N.J.Watson, T.J. Foster. Thermal, mechanical and structural properties of collagen with cellulose/starch films. *6th EPNOE International polysaccharide conference, Aveiro, Portugal, 21st – 25th October 2019*. Poster presentation.

M. Sobanwa, N.J.Watson, T.J. Foster, G. Yakubov. The impact of hydrocolloids on the viscoelastic and thermal properties of acid-swollen collagen paste. *Food Physics virtual conference, 2nd – 3rd February 2021*. Poster presentation.

Table of contents

Abstract	i
Acknowledgement	v
List of abbreviations and symbols	vi
List of publications	viii
Presentations	viii
Table of contents.....	x
List of figures.....	xvii
List of tables	xxiii
1 INTRODUCTION	1
1.1 Background and relevance of the study	2
1.2 Research Aim and Objectives	5
1.3 Thesis Structure	5
2 LITERATURE REVIEW	8
2.1 Sausage Casings	9
2.2 Casing functionalities	10
2.3 Types of Casings	11

2.3.1	Natural casings.....	11
2.3.2	Cellulose casings.....	12
2.3.3	Collagen casings	13
2.4	Collagen.....	15
2.4.1	Collagen structure	17
2.4.2	Collagen Applications	19
2.4.3	Collagen sources.....	20
2.5	Hydrocolloids.....	22
2.5.1	Guar gum.....	22
2.5.2	Cellulose.....	24
2.5.3	Cellulose ethers.....	26
2.5.4	Starch	29
2.6	Collagen-hydrocolloid films	36
3	THE IMPACT OF HYDROCOLLOIDS ADDITION ON VISCOELASTIC AND THERMAL PROPERTIES OF ACID-SWOLLEN COLLAGEN PASTE.....	40
3.1	Abstract.....	41
3.2	Introduction	42
3.3	Materials and Methodology	45

3.3.1	Materials	45
3.3.2	Methodology	46
3.4	Results and Discussions	52
3.4.1	Flow behaviour of hydrocolloids	52
3.4.2	Dynamic Frequency sweep	55
3.4.3	Dynamic Temperature sweep	63
3.4.4	Thermal properties	69
3.5	Conclusions.....	78
4	CHARACTERISATION OF MIXED COLLAGEN-HYDROCOLLOID COMPOSITE FILMS.....	80
4.1	Abstract.....	81
4.2	Introduction	82
4.3	Materials and Methods.....	84
4.3.1	Materials	84
4.3.2	Methodology	85
4.3.3	Film characterisation	85
4.4	Results and Discussion.....	90
4.4.1	Differential scanning calorimeter (DSC).....	90

4.4.2	Mechanical properties.....	96
4.4.3	Thermogravimetric analysis.....	100
4.4.4	X-ray diffraction	106
4.4.5	FTIR spectra of films.....	110
4.4.6	Moisture content and Thickness.....	115
4.4.7	Dynamic Vapour sorption	121
4.5	Conclusion	126
5	THE EFFECT OF CELLULOSE AND STARCH ON THE VISCOELASTIC AND THERMAL PROPERTIES OF ACID-SWOLLEN COLLAGEN PASTE.....	128
5.1	Abstract.....	129
5.2	Introduction	130
5.3	Materials and Methods.....	133
5.3.1	Materials.....	133
5.3.2	Methodology	133
5.4	Results and Discussion.....	139
5.4.1	Dynamic Frequency sweep	139
5.4.2	Dynamic Temperature sweep.....	144
5.4.3	Thermal properties	150

5.5	Conclusions.....	159
6	STRUCTURAL, THERMAL, MECHANICAL AND SORPTION PROPERTIES OF COLLAGEN-CELLULOSE AND COLLAGEN-STARCH FILMS	160
6.1	Abstract.....	161
6.2	Introduction	162
6.3	Materials and Methods.....	166
6.3.1	Materials.....	166
6.4	Methodology.....	166
6.4.1	Determination of dispersion phase volume (Φ).....	166
6.4.2	Preparation of collagen-cellulose and collagen-starch pastes	166
6.4.3	Preparation of collagen-cellulose and collagen-starch films	166
6.4.4	Film characterisation	166
6.5	Result and Discussion.....	172
6.5.1	Microstructure.....	172
6.5.2	Moisture content and thickness	174
6.5.3	Water interaction determined by dynamic vapour sorption	179
6.5.4	Mechanical properties.....	183

6.5.5	Attenuated total reflectance-Fourier Transform Infrared Spectroscopy (ATR-FTIR).....	187
6.5.6	X-ray Diffraction of films.....	193
6.5.7	Differential Scanning Calorimetry	198
6.5.8	Thermogravimetric analysis.....	204
6.6	Conclusions.....	210
7	EFFECT OF ACID-SWOLLEN COLLAGEN PASTE ON STARCH GELATINISATION USING STANDARD AND HIGH-TEMPERATURE HEATING MODES	212
7.1	Abstract.....	213
7.2	Introduction	215
7.3	Material and Methods.....	218
7.3.1	Materials.....	218
7.3.2	Measurement of pasting properties	218
7.3.3	Microscopy	219
7.3.4	Statistical Analysis.....	219
7.4	Results and discussions.....	220
7.4.1	Pasting properties of starch/collagen blends measured in standard heating mode (up to 95 °C).....	220

7.4.2	Pasting properties of starch/collagen blends measured in High-Temperature mode (up to 140 °C).....	230
7.5	Conclusion	238
8	CONCLUSIONS AND FUTURE WORK	241
8.1	Conclusions.....	242
8.2	Future work	248
	REFERENCES	250
	APPENDICES.....	287

List of figures

Figure 2-1: Schematic representation of collagen structure from molecular to supramolecular level (https://www.gold-collagen.com/ae/en/skincare-science-and-research).	19
Figure 2-2: Structure of guar gum (Mudgil et al., 2012).....	23
Figure 2-4: Supramolecular organisation of cellulose (Adapted https://alevelbiology.co.uk/notes/cellulose/).	25
Figure 2-3: Molecular structure of cellulose derivatives (Jones, 1992), where R represents the substituents CH ₃ in methylcellulose and CH ₃ -OHCH-CH ₂ is hydroxypropylmethylcellulose.	28
Figure 2-5: The chemical structures of (a) amylose and (b) amylopectin.	30
Figure 2-6: Schematic representation of the molecular organisation of the starch granule (A) single granule made from concentric growth rings (Bb) crystalline and amorphous lamellae (C) amylopectin cluster structure (Jenkins et al., 1994).	31
Figure 2-7: Typical pasting profile and schematic representation of starch behaviour under heating and cooling (Schirmer et al., 2015).....	35
Figure 3-1: Flow curves of Hydroxypropylmethylcellulose (HPMC) (●), Methylcellulose (MC) (▲), Medium Guar gum (GM) (◆), High Guar gum (GH) (—) and Sodium carboxymethylcellulose (CMC) (■) solutions measured at 20 °C. Cross-Williamson fit is the solid orange line.....	54
Figure 3-2: Storage modulus G' (closed symbol) and Loss modulus G'' (open symbol) as a function of angular frequency for COLLMC (▲), COLLHPMC (●), COLLGH (—), COLLGM (◆), COLLCMC (●) and COLLAGEN (■) pastes at (A) 4% (B) 3.5% (C) 2.5% collagen concentrations, 0.1 % strain at 20 °C.....	58

Figure 3-3: Loss factor ($\tan \delta$) as a function of angular frequency COLLMC (\blacktriangle), COLLHPMC (\bullet), COLLGH (—), COLLGM (\blacklozenge), COLLCMC ($*$) and COLLAGEN (\blacksquare) pastes at (A) 4% (B) 3.5% (C) 2.5% collagen concentrations, angular frequency of 10 rad s⁻¹, 0.1 % strain at 20 °C. 60

Figure 3-4: Phase-contrast light micrographs of collagen with hydrocolloid pastes (A) COLLAGEN (B) COLLCMC (C) COLLGH (D) COLLGM (E) COLLHPMC (F) COLLMC at 4% collagen concentration X10. 62

Figure 3-5: Temperature dependence of the storage modulus (G') during heating for COLLMC (blue line), COLLHPMC (grey line), COLLGH (red line), COLLGM (orange line), COLLCMC (black line) and COLLAGEN (green line) pastes at (A) 4% (B) 3.5% (C) 2.5% collagen concentrations, angular frequency of 10 rad s⁻¹ and 0.1 % strain. 65

Figure 3-6: Loss factor ($\tan \delta$) as a function of temperature for COLLMC (blue line), COLLHPMC (grey line), COLLGH (red line), COLLGM (orange line), COLLCMC (black line) and COLLAGEN (green line) pastes at (A) 4% (B) 3.5% (C) 2.5% collagen concentrations, angular frequency of 10 rad s⁻¹ and 0.1 % strain. 68

Figure 3-7: DSC thermograms (first heating) for COLLMC (blue line), COLLHPMC (grey line), COLLGH (red line), COLLGM (orange line), COLLCMC (black line) and COLLAGEN (green line) pastes at (A) 4% (B) 3.5% (C) 2.5% collagen concentrations. 72

Figure 3-8: DSC thermograms (second heating) for COLLMC (blue line), COLLHPMC (grey line), COLLGH (red line), COLLGM (orange line), COLLCMC (black line) and COLLAGEN (green line) pastes at (A) 4% (B) 3.5% (C) 2.5% collagen concentrations. 76

Figure 4-1: DSC thermograms of pure collagen (black line), COLLMC (orange line), COLLHPMC (blue line), COLLGH (yellow line) and COLLGM (grey line) at (A) 4 % (B) 3.5% (C) 2.5 % wt/wt collagen concentrations. 94

Figure 4-3: DTG curves of pure collagen (black line), COLLMC (blue line), COLLHPMC (orange line), COLLGH (green line) and COLLGM (red line) at (A) 4 % (B) 3.5% (C) 2.5 % wt/wt collagen concentrations. 104

Figure 4-4: XRD of pure collagen (black), COLLMC (blue), COLLHPMC (yellow), COLLGH (grey) and COLLGM (orange) at (A) 4 % (B) 3.5% (C) 2.5 % wt/wt collagen concentrations..... 108

Figure 4-5: FTIR spectra of COLLHPMC (orange line), COLLMC (blue line), COLLGM (green line), COLLGH (red line) and pure collagen (black line) films at (A) 2.5% (B) 3.5% (C) 4% collagen concentrations. 113

Figure 4-6: Moisture content of collagen films with and without hydrocolloid addition at different collagen concentrations, (A) 4% wt/wt (B) 3.5% wt/wt (C) 2.5% wt/wt in the pre-dried acid-swollen collagen pastes. The different letter means a significant ($P < 0.05$) difference between the films. The error bars represent the standard deviation..... 118

Figure 4-7: Thickness of collagen films with and without hydrocolloid addition at different collagen concentrations (A) 4% wt/wt (B) 3.5% wt/wt (C) 2.5% wt/wt in the pre-dried acid-swollen collagen pastes. The different letter means a significant ($P < 0.05$) difference between the films. The error bars represent the standard deviation..... 121

Figure 4-8: (A) Sorption isotherm, and (B) Desorption isotherms of COLLHPMC (blue line), COLLMC (yellow line), COLLGM (orange line), COLLGH (grey line) and pure

collagen (black line) films at 2.5% collagen concentration at 25 °C. The graph presented here is an average of duplicate measurements..... 124

Figure 5-1: Storage modulus G' (closed symbols) and loss modulus G'' (open symbols) as a function of angular frequency for COLLSF3 (●), COLLSF9 (—), COLLWS (■), and COLLHAS (◆) and COLLAGEN (▲). At (A) 4%, (B) 3.5% and (C) 2.5% Collagen concentrations at 20 °C..... 142

Figure 5-2: Loss factor $\tan \delta$ as a function of angular frequency for COLLSF3 (●), COLLSF9 (—), COLLWS (■), and COLLHAS (◆) and COLLAGEN (▲) pastes at different collagen concentrations (A) 4% collagen (B) 3.5% collagen (C) 2.5% collagen..... 143

Figure 5-3: Storage modulus G' as a function of temperature during heating for COLLHAS (grey line), COLLWS (orange line), COLLSF3 (green line), COLLSF9 (blue line) and COLLAGEN (black line) pastes at different collagen concentrations (A) 4% collagen (B) 3.5% collagen and (C) 2.5% collagen concentrations. 146

Figure 5-4: Loss factor $\tan \delta$ as a function of temperature for COLLHAS (grey line), COLLWS (orange line), COLLSF3 (orange line), COLLSF9 (blue line) and COLLAGEN (black line) pastes at different collagen concentrations (A) 4% collagen (B) 3.5% collagen and (C) 2.5% collagen concentrations. 150

Figure 5-5: DSC thermograms of first heating for COLLHAS (Blue line), COLLWS (orange line), COLLSF3 (green line), COLLSF9 (red line) and pure collagen (black line) at different acid-swollen collagen paste concentration (A) 4% (B) 3.5% and (C) 2.5%. 154

Figure 5-6: DSC thermograms of second heating for COLLHAS (Blue line), COLLWS (orange line), COLLSF3 (green line), COLLSF9 (red line) and pure collagen (black) 157

Figure 6-1: SEM images of surface morphology of (A) COLLAGEN (B) COLLWS (C) COLLHAS (D) COLLSF9 (E) COLLSF3. The scale bar is 100µm for each image. 173

Figure 6-2: Moisture content of collagen with cellulose (COLLSF3 and COLLSF9), Collagen with starch (COLLWS and COLLHAS) and pure collagen films at (A) 3.5% (B) 2.5% collagen concentrations. The different letter means significant ($P < 0.05$) difference between the pastes. The error bars represent the standard deviation... 175

Figure 6-3: Thickness of collagen with cellulose (COLLSF3 and COLLSF9), Collagen with starch (COLLWS and COLLHAS) and pure collagen films at (A) 3.5% (B) 2.5% collagen concentrations. The different letter means significant ($P < 0.05$) difference between the pastes. The error bars represent the standard deviation. 178

Figure 6-4: (A) Sorption isotherm, and (B) Desorption isotherms of pure collagen, collagen- cellulose (COLLSF3 and COLLSF9) and collagen-starch (COLLWS and COLLHAS) films at 2.5% collagen concentration at 25 °C. The graph presented here is an average of duplicate measurements..... 181

Figure 6-5: FTIR spectra of COLLSF3 (orange line), COLLSF9 (red line), COLLWS (green line), COLLHAS (blue line) and pure collagen (black) films at (A) 3.5% (B) 2.5% collagen concentrations..... 191

Figure 6-6. X-ray diffraction patterns of pure collagen (black line) COLLSF3 (blue line) and COLLSF9 (green line) films at (A) 2.5% (B) 3.5% collagen concentration. 196

Figure 6-7. X-ray diffraction patterns of pure collagen (black line) COLLWS (red line) and COLLHAS (blue line) films at (A) 2.5% (B) 3.5% collagen concentration. 197

Figure 6-8. DSC thermograms of pure collagen (black line), COLLSF9 (green line), COLLSF3 (orange line), COLLWS (Blue line) and COLLHAS (red line) collagen with and without cellulose fibres/starch granules at (A) 3.5% (B) 2.5% collagen concentrations..... 203

Figure 6-9. . TGA curves of pure collagen (black line), COLLSF3 (orange line), COLLSF9 (grey line), COLLWS (red line) and COLLHAS (blue line) films at (A) 2.5% (B) 3.5% collagen concentrations..... 207

Figure 6-10. DTG curves of pure collagen (black line), COLLSF3 (orange line), COLLSF9 (grey line), COLLWS (red line) and COLLHAS (blue line) films at (A) 2.5% (B) 3.5% collagen concentrations..... 208

Figure 7-1: Pasting profile of (A) WS (B) NS (C) HAS in water (blue line) and different collagen concentrations: 4%w/w (green line), 3.5%w/w (red line) and 2.5%w/w (yellow line) studied under standard RVA heating mode (to 95 °C). The temperature profile (black line)..... 228

Figure 7-2: Pasting profile of (A) WS (B) NS (C) HAS in water (blue line) and different collagen concentrations: 4%w/w (green line), 3.5%w/w (red line) and 2.5%w/w (yellow line) studied under standard RVA heating mode (to 140 °C). The temperature profile is (black line). 233

Figure 7-3: Light microscopy of (A) HAS + WATER (B) HAS + 4% COLL (C) NS + WATER (D) NS + 4% COLL (E) WS + WATER (F) WS + 4% COLL after standard-temperature RVA mode (up to 95 °C). 236

Figure 7-4: Light microscopy of (A) HAS + WATER (B) HAS + 4% COLL (C) NS + WATER (D) NS + 4% COLL (E) WS + WATER (F) WS + 4% COLL after high-temperature RVA mode (up to 140 °C). 237

List of tables

Table 3-1: Substitution ranges of Cellulose ethers (Sarkar 1979)	46
Table 3-2: Concentration (%w/w) of hydrocolloids required for a zero-shear viscosity of 300 mPas.	47
Table 3-3: Summary of the concentration of the stock hydrocolloid solutions and stock collagen paste their mixing ratios and final concentrations in the mixture.	49
Table 3-4: Cross-Williamson model for hydrocolloid solutions	54
Table 3-5: DSC parameters after first heating of collagen with and without hydrocolloids pastes at different collagen paste concentrations and mixing ratios. T_{peak} = peak temperature; T_o = Onset temperature; T_e = endset temperature and ΔH = enthalpy.....	73
Table 3-6: DSC parameters after second heating of collagen with and without hydrocolloids pastes at different collagen paste concentrations and mixing ratios. T_P = peak temperature; T_o = Onset temperature; T_e = endset temperature and ΔH = enthalpy.....	77
Table 4-1: Onset temperature (T_o), endothermic peak (T_{peak}), Endset (T_{end}), enthalpy (ΔH) of collagen with and without hydrocolloid films at different collagen concentrations.....	95
Table 4-2: Mechanical properties of collagen films with and without hydrocolloids at different collagen concentrations.....	99
Table 4-3: Thermal degradation temperature (T_d) and weight loss (%) of collagen with and without hydrocolloid films at different collagen concentrations.	105
Table 4-4. Percentage crystallinity of collagen films with and without hydrocolloids at different collagen concentrations.....	109

Table 4-5: Wavenumber of the bands in the FTIR spectra of the films.....	114
Table 4-6: FTIR absorption ratios of A1111/A1450 for collagen films with and without cellulose hydrocolloids at different collagen concentrations.	115
Table 4-7: GAB fitting parameters of sorption isotherm of collagen films with and without hydrocolloids.	125
Table 5-1: Concentration of cellulose and starches required at 15% dispersed phase volume.....	134
Table 5-2: Formulation of collagen-cellulose and collagen-starch blends at various mixing ratios and different concentrations of collagen. SF3 = Solka floc 300, SF9 = Solka floc 900, WS = Waxy starch, HAS = High amylose starch, Φ = phase volume.	135
Table 5-3: DSC parameters after first heating of collagen/cellulose and collagen/starch pastes at different collagen paste concentrations. T_p = peak temperature, T_o = Onset temperature, T_{end} = endset temperature and ΔH = enthalpy.	155
Table 5-4: DSC parameters (second heating) of collagen/cellulose and collagen/starch pastes at various collagen concentrations (4%, 3.5% and 2.5%). T_p = peak temperature; T_o = Onset temperature; T_e = end set temperature and ΔH = enthalpy.	158
Table 6-1: GAB fitting parameters of sorption isotherm of collagen films with and without cellulose fibres/starch granules. SF9 (Solka floc 900), SF3 (Solka floc 300), WS (Waxy starch) and HAS (high amylose starch).....	183
Table 6-2: Mechanical properties of collagen films with and without cellulose fibres/starch granules at different collagen concentrations.....	187
Table 6-3. Wavenumber of the bands in the FTIR spectra of the films.....	192

Table 6-4. FTIR absorption ratios of AIII/A1450 for collagen films with and without cellulose fibres/starch granules at different collagen concentrations.....	193
Table 6-5: Percentage crystallinity of collagen films with and without cellulose/starch at different collagen concentrations.....	198
Table 6-6. Onset temperature (T_o), endothermic peak (T_{peak}), Endset (T_{end}), enthalpy (ΔH) of collagen with and without cellulose/starch films at different collagen concentrations.....	204
Table 6-7. Thermal degradation temperature (T_d) and weight loss (%) of collagen with and without cellulose fibres/starch granules at different collagen concentrations. .	209
Table 7-1: Pasting parameters of WS, NS and HAS with and without different collagen concentrations at standard RVA heating mode (95 °C).....	229
Table 7-2: Pasting parameters of WS, NS and HAS with and without different collagen concentrations at high-temperature RVA heating mode (140 °C).	234

1 INTRODUCTION

1.1 Background and relevance of the study

This PhD is sponsored by Devro plc, one of the world's leading manufacturers of collagen casings and films for the manufacturing of different sausages and meat products. Casings provide the sausage with its definite shape and protect it from environmental factors such as moisture, UV light and microbial contamination. Traditionally, sausages are made from casings obtained from the intestines of animals such as goats, sheep, and pigs. However, to meet the growing population needs, the increasing costs, lack of intestine, problems associated with natural casings, such as bacterial contamination and lack of uniformity in thickness, colour, and diameter (Barbut, 2010). It has been necessary to develop casings made from alternative sources such as cellulose, collagen, alginate and synthetic materials. Collagen casings are widely used for sausage production because they provide the sausage with consistent shape, length, sizes, are easy to process, flexible, and are edible and of natural origin. Collagen possesses good film-forming capacity, and the casings have high tensile strength and good thermal stability resulting from collagen's fibrous hierarchical structure.

Collagen casings are made from collagen extracted from the corium layer of bovine hides. Once the hides are removed, decalcification and grinding steps follow. Acid, either hydrochloric acid or acetic, is added at a pH of about 3.0 to induce collagen fibres swelling. The subsequent swollen collagen 'dough' or 'paste' is then extruded into a tubular shape. The extraction process changes the hierarchical structure of collagen due to the prolonged alkaline treatment of the bovine hide. As a result, the reconstituted collagen materials possess inferior mechanical properties such as tensile strength, stiffness, and low thermal stability than the native materials (Xiao et al., 2020). For example, the casings may break easily during the filling of the meat

batter, separate from meat stuffing during cooking compared to animal intestine casings. Consequently, collagen casing manufacturers and researchers must understand how collagen casings can be adapted to provide the same properties as casings made from natural intestines. The mechanical properties (tensile strength, stiffness, and elongation at break) are among the most important physical properties of collagen films (casings). In particular, the casing must have enough strength and elasticity to withstand the resulting deformation caused during processing operations, such as filling of the meat batters. Consequently, researchers have made many efforts to improve these properties, notably the tensile strength of collagen films/casings. Methods explored include physical, chemical, enzymatic crosslinking and the blending of hydrocolloids with collagen (Shi et al., 2019; Chen et al., 2020; Ahmad et al., 2016).

Among these techniques, the mixing of hydrocolloids offers great opportunities for strengthening collagen mechanical properties. It is assumed that by combining hydrocolloids into the collagen paste, the physical and tensile properties of edible films can be enhanced compared to the film made from collagen alone (Chen et al., 2008). Some researchers have attempted to improve the mechanical and thermal properties of collagen by adding hydrocolloids such as chitosan (Ahmad et al., 2016), microfibrillated cellulose (Wang et al., 2016b), starch (Wang et al., 2017a), and hydrocolloid proteins such as casein, soy protein isolate and keratin (Wu et al., 2019). Collagen is insoluble; though, it contains some fractions that can be solubilised. It is important to note that most of the research so far has been done using acid or pepsin soluble collagen. This differs from the acid-swollen fibrous collagen used in this study due to differences in the hierarchical length scales. Different treatment such as the extent of liming or extraction method alters collagen to different structural levels, which may affect the properties of the resulting films. Acid or pepsin soluble collagen consists

of mostly loose procollagen molecules, whereas acid swollen collagen paste is made up of a mixture of collagen fibrils and fibres. Also, some reports on collagen films with hydrocolloids are made using collagens from tendon and marine animals. The amino acid composition differs among different animal species, which determines the final properties of collagen and the final film properties (Suurs and Barbut, 2020). In this study, the films are made of fibrous acid-swollen collagen paste are extracted from the corium layer of bovine hides.

However, little is known about the effect of adding hydrocolloids on the properties of collagen films (casings) prepared from the fibrous acid-swollen collagen paste. Therefore, in this research, fillers such as cellulose fibres, corn starches and soluble hydrocolloids such as guar gums (of different molecular weights) and derivatised celluloses (hydroxypropylmethylcellulose and methylcellulose) were blended with acid-swollen fibrous paste to develop collagen films with a view to enhance their properties. The hydrocolloids mentioned above were chosen because of their high availability, low cost, and different functionalities. The cellulose fibres and corn starches are dispersions (combined cold to the collagen paste), while the guar and derivatised celluloses are water-soluble, imparting viscosity as a function of molecular space-filling and entanglement. The insight into how these hydrocolloids mix and interact with collagen in the paste, and then through subsequent drying and film formation, is crucial as it would allow the correct selection of hydrocolloids to change collagen film properties, thus optimising the finished product performance. This will provide scientific knowledge for further developing collagen films and open up the possibility of developing enhanced properties such as tensile strength and thermal stability. Also, new functionalities might be identified, e.g., cooking performance.

1.2 Research Aim and Objectives

This PhD research aimed to inform future collagen film design (casings) with improved quality performance in cooking, manufacturing, and machinery efficiencies by adding food-grade polysaccharide ingredients.

The following objectives were set out to be achieved during this project.

1. To investigate the effect of different polymer types, i.e., neutral, negatively charged, hydrophobic, polymer molecular weight on acid-swollen pastes and films. Five different polymers were selected: starch, cellulose, derivatised cellulose (HPMC and MC) and guar gums. These were chosen because of their functionalities, low cost, and abundance.
2. To investigate the rheological properties of the polysaccharides when added to acid-swollen collagen pastes using small deformation measurements.
3. To study the material structure and functionality using thermal, spectroscopic and microscopy techniques while the main structural component of collagen is maintained.
4. To establish structures within the paste relevant to efficient processing by exploring the thermodynamic compatibility of collagen polysaccharides.

1.3 Thesis Structure

This thesis is written in a publication format. The general structure of the study takes the form of eight chapters, including the introductory chapter. Chapter 2 presents a general literature review. The results of this project are presented in five separate chapters. A specific literature review and a materials and methods section are presented in each results chapter.

The work presented in Chapter 3 investigates neutral and negatively charged non-gelling and gelling hydrocolloids at comparable low-shear viscosity (viscosifying effect) on the viscoelastic and thermal properties of acid swollen collagen paste. The neutrally charged and hydrophobic hydrocolloids selected were hydroxypropylmethylcellulose and methylcellulose, which are water-soluble at low temperatures and are known for their heat-set gelation properties, while the non-gelling hydrocolloid used was guar gum of high and low molecular weights. The effect of negatively charged carboxymethylcellulose was also investigated. The low-shear viscosity of the hydrocolloids was fixed whilst changing the collagen paste concentration in the mixtures.

Chapter 4 will focus on understanding the effects of the different polymers examined in chapter 3 on the mechanical, thermal, structural, spectroscopic, and physical and sorption characteristics of collagen fibrous films.

The work in Chapter 5 will focus on the effect of dispersions of cellulose with different fibre lengths and normal, waxy and high amylose maize starch, acting as fillers on the viscoelastic and thermal properties of acid swollen collagen paste. The starches were chosen because of their different amylose and amylopectin ratios. Also, cellulose with varying lengths of fibre was chosen to investigate the effect of cellulose fibre lengths on collagen properties. The dispersed phase volume of the cellulose fibres and starch granules was fixed whilst changing collagen concentration in the mixtures.

Chapter 6 is a follow-on study from chapter 5; this work describes the effect of cellulose with different fibre length and starch granules with different amylose and amylopectin content on the mechanical, thermal, spectroscopy, structural and physical properties

of collagen fibrous films. The effect of these inert fillers on the moisture isotherms of collagen fibrous films was also studied.

In Chapter 7, the effect of collagen fibrous paste at different concentrations on the pasting properties for normal, waxy and high amylose corn starches was studied. The pasting profile was studied using both conventional RVA (up to 95 °C) and high temperature (up to 140 °C) heating modes.

Finally, Chapter 8 presents the general conclusions and suggestions for future work.

2 LITERATURE REVIEW

2.1 Sausage Casings

Casings are thin tubular skins or films enclosing the sausage meat batter. The casings consist of composites showing mechanical and other functional properties related to each constituent's performance (Savic and Savic, 2002). The casings determine the shape, size and integrity of the sausages. Also, they protect the meat product from environmental factors such as moisture, UV light and microbial contamination (Feiner, 2006). The casing also influences volumetric, structural and chemical changes in sausages. Edible and non-edible casings are made from animal intestines, natural polymers such as cellulose, collagen and alginate, and synthetic polymers such as polyvinylidene chloride (PVDC), polyamide, polyolefin and polyester (Savic and Savic, 2016). Some researchers have studied the use of other biopolymers for sausage casings. Adzaly (2014) studied the use of chitosan to develop a casing for commercial application. Films made with chitosan were found to be used as an alternative to collagen casings for sausage production. The films showed high tensile strength, increasing barrier to water, oxygen, liquid smoke and UV light, and they were more transparent (Ioi, 2013; Adzaly, 2014). Liu et al. (2007) reported pectin and mixtures of gelatin with sodium alginate for sausage casing production. However, casings made from animal intestines, collagen and cellulose are mainly used industrially for sausage production due to their hierarchal structures, which provide increased tensile strength and thermal stability. (Osburn, 2002; Wang et al., 2017a).

2.2 Casing functionalities

The quality of the finished sausage product is determined by the functional properties of the casing, which depend on the structural organisation of the natural or synthetic polymers they are made from. During casing fabrication, the materials processing is essential to achieve a casing with the appropriate properties necessary for sausage processing. From an industrial standpoint, the mechanical, thermal, permeability, and optical characteristics of the casings are essential; they affect the end product's quality. The casings thickness and flexibility also play a key role (Savic and Savic, 2002; Ioi, 2013).

Among the most crucial properties of the casings are the mechanical properties such as tensile strength, elongation, toughness and elasticity. The evaluation of these properties provides casing manufacturers with the amount of stress and deformation that a casing can withstand before breaking during sausage manufacturing, in addition to enabling predictions of casing success (Hernandez, 1997; Savic and Savic, 2002; Simelane and Ustunol, 2005; Ioi, 2013). The casing elasticity and tensile strength are important because they affect sausage size, shape, structure and behaviour during processing. Sausage processing involves high pressure; therefore, the casing must have enough strength and elasticity to withstand the resulting deformation caused during processing operations such as filling and cooking. Additionally, the meat batter undergoes some increase in volume during processing and storing. Therefore, the casing must be stretchable and shrinkable to accommodate the expansion and contraction of meat batter (Savic and Savic, 2002; Ioi, 2013).

Permeability is another essential property relating to the transfer rate of permeates such as moisture, gas, light and aroma into the enclosed interior wall (Savic and Savic,

2002; Ioi, 2013). Casings are used as a barrier to moisture and other substances that cause changes in the sausage quality. The extent of permeability of a material depends on its polarity. Protein and polysaccharides films are highly permeable to water due to their hydrophilic nature. However, such casings are less permeable to substances with low polarities, such as oxygen, aroma compounds and oils (Krochta, 2002; Ioi, 2013).

In addition to the already discussed properties, optical properties such as light scattering affects are also important, resulting in varying degrees of opacity. The casing should be transparent to allow easy transmission of light, thereby allowing visual observation of the product's meat interior (Crooks, 1985).

2.3 Types of Casings

2.3.1 Natural casings

Traditionally, casings are made from pigs, sheep, horses and cattle. Sheep casings are made from the small intestine, while casings from pigs can be made from the stomach, bungs, small and large intestines (Feiner, 2006; Suurs and Barbut, 2020). These casings are made by separating submucosa from the animal's small intestine, followed by the cleaning and drying of the guts. Additionally, they require preservation by curing or salt addition before packaging and distribution (Bakker et al., 1999; Harper et al., 2012). These casings are preferred because of the many benefits they offer, including edibility/naturalness and easy digestibility, high permeability to smoke and humidity that prevents the separation of components such as water and fat from the meat product. They have good thermal stability; they shrink and give the snap texture of cooked sausages such as frankfurters. They adhere well to the meat batter, thus preventing separation during cooking (Savic and Savic, 2016). Although natural

casings from animal intestines have many advantages as listed above, they have the following disadvantages (i) high risk of bacterial contamination, (ii) they need to be preserved either by the addition of salt only or refrigerated, (iii) lack uniformity in thickness, colour, and diameter, and (v) lack consistency in size, length and diameter (Osburn, 2002; Savic and Savic, 2002).

Regardless of these disadvantages, natural casings are extensively used in the food industry. Koolmees et al. (2004) estimated that about \$2.5 billion was generated from the annual sales of natural casings globally, with sheep casings consisting of about 60% of the total sales. It is reported that 55% of the edible casings produced in 2018 were from animal intestines (Devro, 2019). Even with impressive sales figures for natural casings in the food industry, the challenges of using natural casings require the development of alternative sausage casings. Currently, available alternative casings are made from either natural biodegradable hydrocolloid such as collagen and cellulose or synthetic materials.

2.3.2 Cellulose casings

Casings from regenerated cellulose date back to the early nineteenth century. They are used to produce emulsion-type sausages where uniform size is desired. Meat products such as skinless hot dogs, cooked ham, frankfurters, and spreadable raw sausages are examples of products wrapped in cellulose casings (Feiner, 2006). The production of cellulose casings involves using raw cellulose, which has been subjected to several processing steps, which include (i) chemical treatment with alkali, (ii) derivatisation, and (iii) regeneration through solvent exchange (Feiner, 2006). Cellulose casings are an appealing alternative to natural casings because they have good mechanical strength. They can also be produced in various sizes, and casing uniformity is not problematic.

Moreover, they are permeable to smoke which improves the flavour and extends the shelf life of the final product. They are also easy to use in comparison with natural casings. However, the use of cellulose casings is limited as they are not edible and must be removed from finished products (Adzaly, 2014).

2.3.3 Collagen casings

The development of collagen casings (tubular collagen films) started as an alternative to natural casings because of the limited supply of animal casings, their high price, and the problems associated with the use of natural casings. Collagen casings received much attention in the food industry because of their mechanical and physical characteristics. They are now seen as a good alternative to producing sausage casings and edible films because of their many advantages compared to natural casings. These include: (i) being less prone to microbial contamination and longer shelf-life. (ii) having high mechanical strength and high resistance to breakage during processing operations because of their hierarchical fibrous structure, (iii) being uniform, consistent in sizes and flexible to allow high throughput, and (iv) they are also thermally stable, i.e., can withstand different processing temperatures (Harper et al., 2012).

Collagen also enhances the texture and chewing properties of meat products wrapped in edible collagen casings (Savic and Savic, 2016). According to Devro plc Annual Reports and Accounts 2018, the global usage of collagen casings for sausage manufacturing increased from 30% to 45% from 2008 to 2018 (Devro, 2019).

2.3.3.1 Collagen casing manufacturing

Regenerated edible and non-edible collagen casings for sausage manufacturing are made from the mechanical extraction of fibrous type 1 collagen, which is the main structural component of connective tissues in animals. Type 1 collagen used for sausage casings is obtained from animal hide corium, preferably bovine or porcine. The hide corium of bovine animals aged 18 – 36 months is mainly used for sausage casing manufacturing because they are more fibrous, strong and contains less soluble collagen. Industrially, collagen casings are produced by two different processes, namely wet or dry methods. Generally, the production stages for collagen casings include collagen extraction, decalcification, regeneration, homogenisation, extrusion, drying, and shirring (Ioi, 2013; Savic and Savic, 2016). Collagen extraction is performed at a low temperature of approximately 4 °C, to avoid the denaturation of the collagen molecules into random coils and prevent bacterial contamination.

Bovine skins are delimed with alkali to remove impurities and then buffered using acid to reduce the pH value near the isoelectric point of bovine or porcine, about 4.8 and 5, respectively. When this pH is achieved, the hides are washed thoroughly with water and ground into small fibres that are then dispersed in water to form a pulp. Acid, either a hydrochloric or acetic acid, is then added to induce fibre swelling, containing a total solid content of about 4-5 % for the wet process and 12 – 15 % for the dry process. Industrially, hydrochloric acid is the preferred acid as it yields a more viscous paste and improves the rate of swelling of collagen pulp (Ratanavaraporn et al., 2008; Ioi, 2013). According to (Ratanavaraporn et al., 2008), the difference in the ionic strength of acetic and hydrochloric acids affects the collagen self-assembly. In HCL solution,

the positive charge regions of the collagen molecules swell to a greater degree than in acetic acid solution.

The paste is then homogenised and extruded at high pressures using a wet or dry extrusion process. In the wet process, extruded casings are passed through a coagulation bath of sodium or ammonium salt at a pH of about 12, aiming to neutralise the acid and shrink collagen fibres. Then the casings are treated with plasticisers such as glycerol and sorbitol and cross-linking agents such as glutaraldehyde or liquid smoke to improve casing strength and reduce brittleness. The casings are further inflated with air and dried at a low temperature to a final moisture content of about 13-18 %. In the dry process, the plasticising and cross-linking agent is added before extrusion. The casings are extruded in sodium or ammonium salt at a lower pH of about 5.5, after which they are dried to a moisture content of about 12 %, conditioned and neutralised. The casings are finally reeled and packed. The major difference between the two processes is the type of hierarchical fibre structures formed, which affects the casing strength. In the dry process, the fibres are long and cross-hatched; hence the casings formed are thick, while in the wet process, the fibres are aligned/parallel (Savic and Savic, 2016).

2.4 Collagen

Collagen is the most abundant fibrous protein found in the Extracellular matrix (ECM). It is the main structural component of connective tissues such as bones, skin, ligaments, cornea, and tendons in mammals. Collagen makes up approximately 30 % of the total protein found in the body. Due to its unique properties such as abundance, biodegradability and biocompatibility, the usage of collagen is increasing in food,

cosmetics, tissue engineering and pharmaceutical industries ((Hashim et al., 2015). To date, about 29 types of collagens have been identified, and they are classified into different groups based on their amino acid composition, structure size and function (Pataridis et al., 2008). The collagens are classified into Fibril-forming collagen (Type I, II, III, IV and V), network-forming collagen (Type IV, VIII and X), fibril-associated collagens (IX, XII, XIV, XVI and XIX), transmembrane collagens (type XIII and XVII) and basement membrane collagen (type IV) (Prockop and Kivirikko, 1995; Gelse et al., 2003). The collagen has a right-handed triple helical structure made of three polypeptide alpha chains. These chains can either be identical (homotrimeric) as seen in collagen type II, III, VII, VIII, X or different (heterotrimeric) in types I, IV, V, VI, IX and XI (Gelse et al., 2003). The functionalities of the collagens are different, which is due to their different amino acid compositions and their location in the body. Amongst all the collagens, the most common ones are:

- Collagen type I: found in skin, tendon, organs and bone tissues.
- Collagen type II: the main component of cartilage.
- Collagen type III: the main component of reticular fibres, alongside type I.
- Collagen type IV: Forms the bases of the cell basement membrane.
- Collagen type V: the main component of cell surfaces, hair and placenta.

Among all the collagen type, the fibrillar collagens account for about 80 – 90% of the mammalian body's collagen. Collagen type I accounts for about 90% of the collagen in the skin, bones, tendons, ligaments and tendons. Collagen type I is the most used for sausage casings because it forms insoluble fibres with intense intra and intermolecular forces, which provide higher tensile strength and stability.

2.4.1 Collagen structure

Collagen type I is a rigid rod with a molecular weight of around 300 kDa, a length of 300 nm and a diameter of 1.5 nm (Stenzel et al., 1974). The collagen molecule comprises of three polypeptide α -chains, each twisted in a left-handed helix, coiled around each other to form a right-handed triple helix. As mentioned earlier, depending on the collagen type, the chains are either homotrimeric or heterotrimeric. Collagen type I explored in this study consists of two identical $\alpha_1(I)$ chains and one $\alpha_2(I)$ – chain, each containing more than 1000 amino acids. The collagen polypeptide chains consist of repeating units of Gly-X-Y amino acid sequence where Gly represents Glycine, X and Y are proline and 4-hydroxyproline, respectively. One-third of the amino acids present in collagen is glycine. Glycine being the smallest amino acid, occupies every third position of polypeptide chains and allows folding of polypeptide chains and tightly packing of the triple helix. Imine acids, proline and hydroxyproline, make up approximately 25% of the collagen triple helix's amino acids and play a vital role in triple helix stabilisation. They are found outside the surface of the protein, allowing a single collagen monomer to interact with an adjacent monomer to form cross-linkages (Friess, 1998). The cyclic nature and hydrogen bond formation between the amine nitrogen and the imino acids carboxyl groups stiffen the α - chains and limits their rotation (Piez, 1984). The collagen molecules can self-assemble to form a complex macromolecular structure via intermolecular hydrogen bonding (Pauling and Corey, 1951; Ramachandran and Kartha, 1954). The triple helix is stabilised by inter-and intramolecular hydrogen bonding between chains. Bella et al. (1995) reported that multiple hydrogen bonding patterns stabilise the triple helix. These include, i) direct hydrogen bonding among the peptides (i.e., the NH group in glycine in each polypeptide chain forms H-bonds with adjacent peptide CO groups of the other

chains), ii) water-mediated hydrogen bonding linking carbonyl groups, and iii) water-mediated hydrogen bonding, which links hydroxyproline OH groups and carbonyl groups.

Additionally, the molecule contains short non-helical region of about 9-26 amino acids at the amino (N) and carboxyl (C) terminal end of the molecule that is not part of the helical structure. These non-helical regions are called telopeptide; the C-terminus is involved in the initiation of triple helix formation, while the N-terminus is involved in regulating the fibril diameters. The telopeptides are primary sites for intermolecular cross-linking (Gelse et al., 2003). Through the process of fibrillogenesis, about four to eight collagen molecules align in a quarter-stagger arrangement and aggregate to form microfibrils and subsequently into fibrils of about 10 – 500 nm in diameter. Once the fibrils are formed, the structure is stabilised and reinforced by covalent lysine-hydroxylysine crosslinks between the tropocollagen. The fibrils further organise to form fibres with high tensile strength and elasticity (Figure 2-1) (Friess, 1998; Savic and Savic, 2002). The collagen structure is rich in the hydroxyl, carboxylic acid groups, and amide and amine groups; thus, it is highly hydrophilic (Greene, 2003). Additionally, collagen is insoluble in an aqueous solvent due to the strong inter-and intramolecular hydrogen bonds, ionic bonds, Van der Waals' force and hydrophobic bonds between the polar and non-polar groups, which limits the application of collagen in the food industry. As mentioned earlier, fibrous acid swollen collagen, which consists of fibrils and fibres, is used for collagen casings.

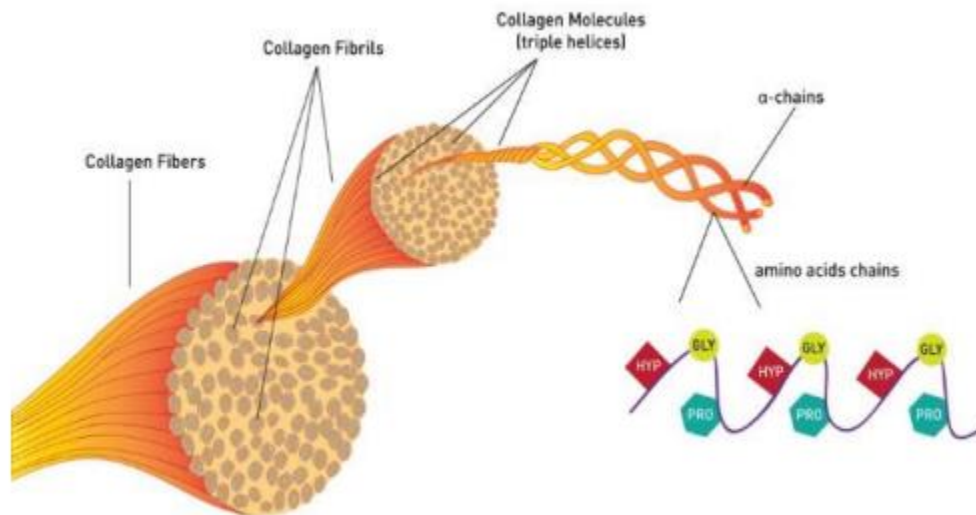


Figure 2-1: Schematic representation of collagen structure from molecular to supramolecular level (<https://www.gold-collagen.com/ae/en/skincare-science-and-research>).

2.4.2 Collagen Applications

Collagen has unique properties, such as biocompatibility, biodegradability, non-toxic, film-forming capacity, high hydrophilicity, weak antigenicity, texturisation, and thickening properties. For this reason, it has been used in food, leather, pharmaceuticals, cosmetics and tissue engineering and biomedical applications (Bae et al., 2008; Gómez-Guillén et al., 2011; Hashim et al., 2015). According to Noorzai and Verbeek (2020), the global demand for collagen increases to approximately 20% annually, owing to the increase in the cost of natural casings. Collagen can be processed into pastes or solutions further formulated into different forms, including powders, solutions, fibres, sponges (Friess, 1998). Collagen is insoluble in an aqueous solvent at low temperature, below that of thermal degradation of the fibrillar and helical structures; however, it can be solubilised with an acidic medium such as acetic acid and hydrochloric acid (Lee et al., 2001). It is mainly used in the meat industry for sausage casings due to collagen fibres with high-sized strength formed by triple-helical

structure (Wu et al., 2018). Collagen is also used as a supplement to improve hair, skin, body and nails. It is used in sports nutrition products such as protein bars and shakes for weight management, muscle recovery and muscle contraction. In the cosmetic industry, collagen is used in skincare formulation for anti-age and anti-wrinkle products and helps reduce marks from skin burns and skin wounds (Oliveira et al., 2021). Also, collagen is extensively used for biomedical applications such as for drug delivery systems and collagen shields in ophthalmology (Kaufman et al., 1994), sponges for the dressing of burns and wounds due to its homeostatic properties (Panduranga Rao, 1996), mini-pellets and tablets for protein and gene delivery carrier (Lucas et al., 1990), hydrogels coated with liposomes for controlled drug delivery (Joséfonseca et al., 1996) and nanoparticles for gene delivery (Rössler et al., 1994). Additionally, collagen interacts with cells and modulates biological activities, increasing its use for tissue engineering applications, including scaffolds for bone regeneration and matrices for cell growth and proliferation (Wallace and Rosenblatt, 2003; Yang et al., 2004).

2.4.3 Collagen sources

Collagen can be extracted from a variety of mammals (cow, pig, buffalo, rats, equine, and rabbits), marine invertebrates and vertebrates (cuttlefish, jellyfish, starfish, and whale) and poultry (turkey and chicken feet). The amino acid composition is different in each animal species, which determines the final properties of the collagen (Silvipriya et al., 2015b). However, collagen from bovine skin, porcine skin, rat-tail tendons are commonly used for industrial use. In specific, fibrous collagen type 1 extracted from bovine and porcine skins are used for sausage casings. Bovine collagen, commonly obtained from cowhides, has several advantages over other collagen sources, such

as higher thermal stability than collagen from marine sources (Hashim et al., 2015). However, safety concerns associated with the risk of transmission of zoonotic diseases such as bovine spongiform encephalopathy (BSE), transmissible spongiform encephalopathy (TSE) and foot and mouth disease (FMD) from bovines and religious concerns related to the use of porcine collagen, have heightened the need for alternative sources of collagen (Zhang et al., 2010). Recently, researchers have shown an increased interest in collagen obtained from marine sources. Moreover, marine sources have several advantages: low inflammatory response, less immunogenic, less regulatory and quality control problems over animal sources (Silvipriya et al., 2015a). However, a major problem with marine collagen is low thermal stability resulting from its lower hydroxyproline content, which has limited its industrial application.

On heating, collagen fibrils undergoes a denaturation process which involves the disruption of the non-covalent bonds and the transition from the triple-helix structure to a randomly coiled form in which the three α -chains are separated (Miles and Bailey, 2001). Depending on the extent of heating, the denaturation can be reversible or irreversible. Moderate heating result in an unfolding within the protein, which appears to regain its native structure upon the restoration of normal temperatures. This unfolding may be due to the breaking of a small number of consecutive hydrogen bonds. Severe heating results in a time-dependent irreversible transformation of the native triple helical structure into a more random (coiled) structure. The transformation resulting from severe heating occurs primarily via the breaking of longer sequences of hydrogen bonds that stabilize the triple helix; particular subdomains along the molecule (Wright and Humphrey, 2002). The stability of collagen has been linked to the hydroxyproline content, which according to Ramachandran et al. (1973) is due to

the intermolecular hydrogen-bonding involving the hydroxyl group of hydroxyproline. The thermal stability of collagen increases with increase hydroxyproline content(Hashim et al., 2015).

2.5 Hydrocolloids

Hydrocolloids (proteins and polysaccharides) are groups of naturally occurring polymers widely used in several industries due to their functionalities, including thickening, gelling, stabilisation, emulsifying and controlled release of flavours (Saha and Bhattacharya, 2010). Notably, in the food industry, they are primarily used to modify food rheological and textural characteristics. Due to the increasing consumer demand for ready-to-eat foods and choice of healthier/nutritious diets, hydrocolloids are increasingly being explored to improve food products' texture and quality (Williams and Phillips, 2009). Hydrocolloids are widely used to prepare edible films due to their excellent film-forming capability. Owing to their extended functionalities, the mixing of hydrocolloids into collagen matrix can be an effective strategy to change collagen films physicochemical, thermal and mechanical properties.

2.5.1 Guar gum

Guar gum is a galactomannan obtained from the guar beans (*Cyamopsis tetragonoloba*). It is a non-gelling, neutral, hydrophilic polysaccharide and formed of a linear chain of (1-4)-linked β -D-mannanopyranosyl units with (1-6)-linked α -D-galactopyranosyl residues as side chains (Mudgil et al., 2014). Guar gum has a mannose to galactose ratio of about 2:1. The chemical structure of guar gum is shown in Figure 2-2. Guar gum is widely used as a rheology modifier for many food

applications. It has a great hydration capacity due to its high molecular weight and intense hydrogen bonding activity. At lower concentrations, the solutions have a high viscosity and high pseudoplastic behaviour, and this is due to their long, soluble chains. (Kim and Yoo, 2011a). The pseudoplasticity and viscosities of Guar gum solution increase with increasing polymer concentration and molecular weight (Robinson et al., 1982). Guar gum solution viscosity and hydration properties are affected by temperature, pH, solute, and concentration. Guar gum solutions are stable across a broad spectrum of pH between 1.0-10.5, and this was attributed to its non-ionic and uncharged behaviour (Carlson et al., 1962). Also, it is highly soluble in both cold and hot water due to its high galactose content in the side chain, which prevents the strong molecular associations of the backbone (Goycoolea et al., 1995) and the formation of extensive crystalline regions, so that water can easily penetrate between the single molecules or hydrate or dissolve the gum (Phillips and Williams, 2009).

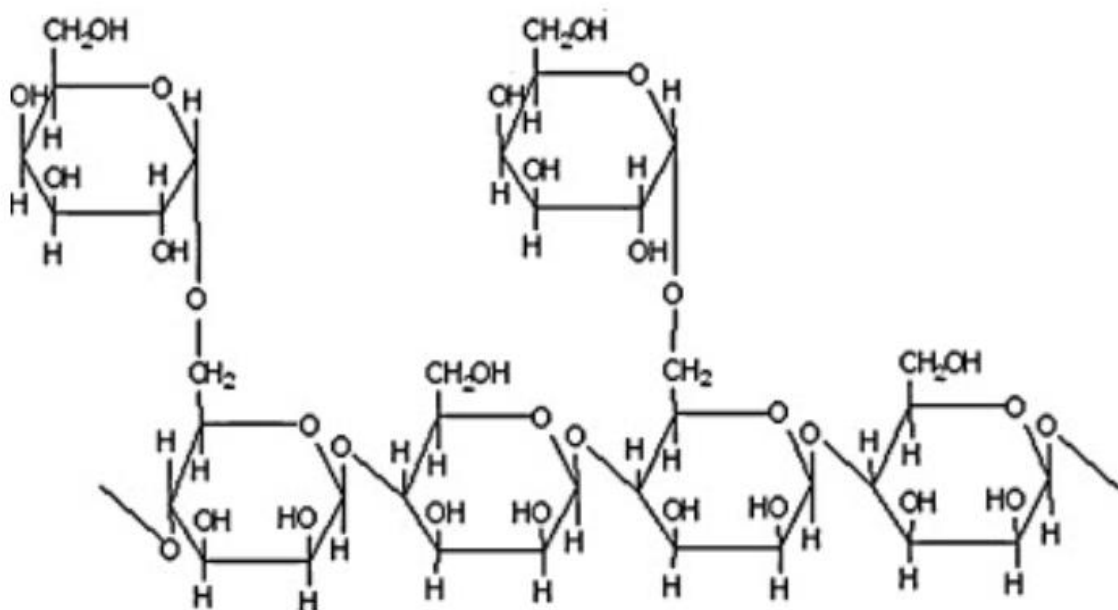


Figure 2-2: Structure of guar gum (Mudgil et al., 2012).

2.5.2 Cellulose

Cellulose is a natural fibre obtained from plants that possess remarkable properties, including abundance, biodegradability, high tensile strength, increased thermal stability and low cost (Ding et al., 2015). Cellulose is a high molecular weight linear polymer that consists of β -1,4- linked anhydro-D-glucose units. It is the major structural component of the plant cell wall and makes up about 30-35% of the plant dry weight (Stephen, 1995). Cellulose can also be found in microorganisms, including aerobic bacteria (*Acetobacter xylinum*), algae and fungi (Klemm et al., 2005; Petersen and Gatenholm, 2011). Based on the properties mentioned above, cellulose is used widely in the paper, building, mining and allied industries.

Cellulose has a highly ordered structure stabilised by strong intramolecular and intermolecular hydrogen bonding. Accordingly, cellulose fibres have high strength, high thermal stability and are insoluble in aqueous solvents, particularly water (Kroon-Batenburg and Kroon, 1997). Cellulose is semi-crystalline as it is made up of highly ordered (crystalline) and less ordered (amorphous) regions. In the ordered regions, cellulose chains are tightly packed in crystallites held by strong hydrogen bonding (in-plane) and Van der Waals interactions (between planes). Depending on the source, extraction procedure and treatment, cellulose exists in four different polymorphs: cellulose I, II, III and IV, respectively. These polymorphs have different chain arrangements with different intermolecular hydrogen bonds (Klemm et al., 2005).

Like collagen, cellulose has a complex and highly ordered structure with hierarchical levels from molecules, microfibrils and fibres (Figure 24), which can provide the casing

with increased stiffness, strength and elasticity when added to collagen pastes. Due to extensive hydrogen bonding, the microfibrils can further associate to form macrofibrils which combine to form large cellulose fibres (Brown Jr and Saxena, 2000). The plant cellulose fibres are 1-2 mm long and about 30-60 microns in diameter. These fibres are made from microfibrils 1-10 microns in length and approximately 35 Å in diameter, and these microfibrils are composed of 30-40 cellulose chains (Pérez and Mazeau, 2005). The entire structure is stabilised by intermolecular hydrogen bonding between the glucose units of neighbouring chains. The applicability of cellulose is limited due to the insolubility in aqueous solvents. To increase cellulose application, cellulose is converted to its derivatives, which involves substituting three OH groups in each anhydroglucose unit (AGU). This leads to the formation of water-soluble cellulose derivatives, with new functionalities that is greatly employed for industrial applications (Clasen and Kulicke, 2001b).

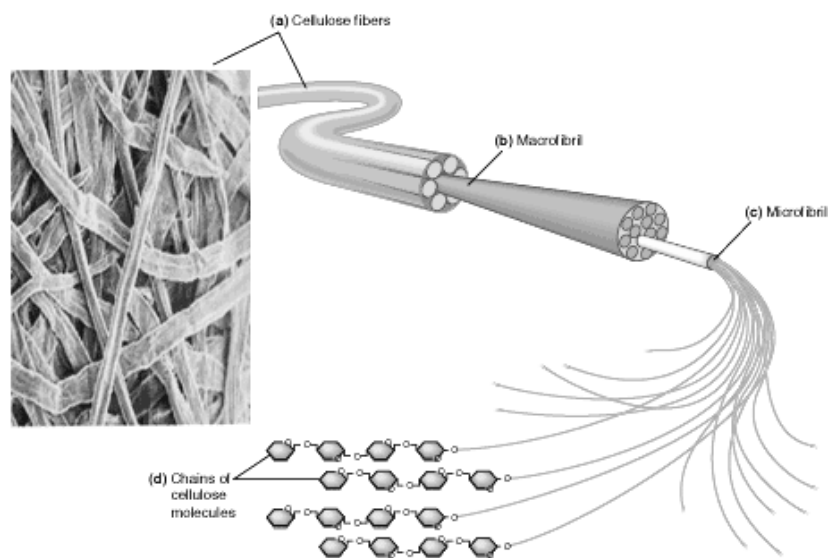


Figure 2-3: Supramolecular organisation of cellulose
(Adapted <https://alevelbiology.co.uk/notes/cellulose/>).

2.5.3 Cellulose ethers

Native cellulose is highly crystalline, characterised by strong intra and intermolecular hydrogen bond interactions between cellulose chains in the fibrils. Consequently, cellulose is insoluble in water, limiting its industrial application (Klemm et al., 2005). Modifications of the crystalline regions of native cellulose by chemical substitution of hydroxyl groups in each anhydroglucose unit within the region by other functional groups result in water-soluble cellulose derivatives (cellulose esters or ethers) (Pérez et al., 2006). Cellulose ethers are a group of cellulosic derivatives widely used in the food, pharmaceutical, textile industries. In particular, they are used as film-formers, emulsifiers, stabilisers and thickeners in the food industry. Among the cellulose ethers, hydroxypropylmethylcellulose (HPMC), methylcellulose (MC), and sodium carboxymethylcellulose (CMC) are the most used due to their availability, film-forming ability, biocompatibility and biodegradability (Silva et al., 2008). Industrially, cellulose ethers are produced from alkali cellulose, which involves treating cellulose powders with strong sodium hydroxide (NaOH) (Heinze and Petzold, 2008). This process disrupts hydrogen bonds in crystalline regions, thus allowing hydroxyl groups more accessibility for alkylation. Once the alkali cellulose is formed, several chemicals are added based on the type of cellulose ether. For the formation of MC, the alkali cellulose is reacted with methyl chloride. For HPMC, a further reaction takes place with propylene oxide. For CMC, chloroacetic acid is used or its sodium salts to give sodium carboxymethylcellulose (Na CMC) (Jones, 1992; Klemm et al., 2005). The available reactive hydroxyl groups for substitution are located at C2, C3 and C6 atoms on the glucose unit. The degree of substitution (DS) is the average number of substitutions per glucose unit, while the molar substitution (MS) is the average number of moles added per sugar unit. Factors such as molecular weight, concentration and

temperature (below gelation temperature) affect cellulose ether viscosity (Williams and Phillips, 2009).

2.5.3.1 Methylcellulose and Hydroxypropylmethylcellulose

Methylcellulose (MC) and hydroxypropylmethylcellulose (HPMC) (Figure 2-4) are non-ionic cellulose ethers produced by methyl and hydroxypropyl substitution groups with the three hydroxyl groups found on each glucose residue. MC has a degree of substitution between 1.3 -2.6 methyl groups per anhydroglucose unit. MC is highly hydrophobic with less substituted hydrophilic regions, whereas the hydroxypropyl substituents increase the HPMC hydrophilicity (Desbrieres et al., 2000). HPMC and MC solutions possess a unique thermoreversible gelation property; they gel upon heating and revert to a solution on cooling (Sarkar, 1979). The gelation of MC and HPMC is attributed to hydrophobic interaction between polymer chains regions with heavily substituted methoxylated groups (Sarkar, 1979; Haque et al., 1993a; Desbrieres et al., 2000; Silva et al., 2008). The gelation temperature, gel strength and precipitation temperature of MC and HPMC depend on molecular weight, degree of methyl and hydroxypropyl substitution, concentration and presence of additives (Sarkar, 1995).

Different explanations have been proposed for the mechanism of thermogelation of MC and HPMC. Early studies by Heymann (1935) suggested that the thermal gelation of methylcellulose occurs by dehydration of particles followed by clotting and loose gel network formation with a strong tendency to syneresis. However, the most accepted mechanism was proposed by Haque et al. (1993a). During the initial heating stage, the strands at the ends of the bundles separate, leading to the exposure of the hydrophobic methyl substituents, resulting in the formation of water cages. As the

temperature increases, the water cages are disturbed, which causes polymer-polymer hydrophobic association and leads to the formation of a strong cross-linked gel network. An increase in viscosity indicates gelation, and the temperature at which it occurs is influenced by the type of cellulose ether (Sarkar, 1995). The temperature of gelation of MC occurs at a lower temperature and forms stronger gels than HPMC. The hydroxypropyl groups inhibit the aggregation of HPMC due to the hydrophilic character of the hydroxypropyl groups.

Additionally, lowering methyl substitution and the presence of hydroxypropyl substituent in HPMC inhibits the association of the chains of hydrophobic methoxyl groups, leading to an increase in the gelation temperature and lower gel strength (Haque and Morris, 1993; Haque et al., 1993a).

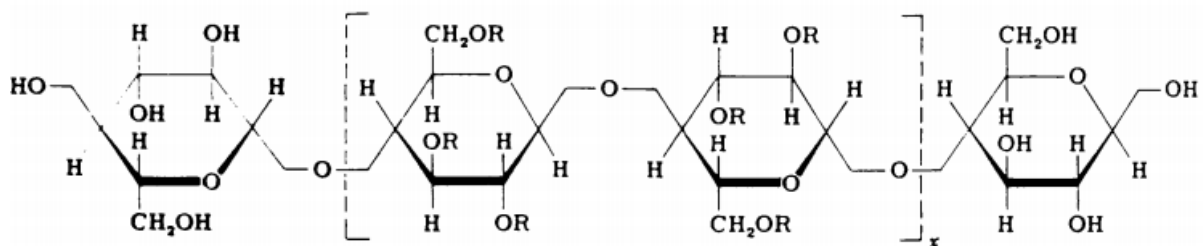


Figure 2-4: Molecular structure of cellulose derivatives (Jones, 1992), where R represents the substituents CH₃ in methylcellulose and CH₂-CH(OH)-CH₂ is hydroxypropylmethylcellulose.

2.5.3.2 Sodium carboxymethylcellulose (CMC)

Sodium carboxyl methylcellulose is a linear, long-chain, unbranched anionic water-soluble polysaccharide formed through alkali cellulose reaction with monochloroacetate or its sodium salt. It is a copolymer of two units: β-D- glucose and β-D- glucopyranose 2-O- (carboxymethyl)-monosodium salt (Florjancic et al., 2002; Yaşar et al., 2007), and is frequently used as an emulsifier, a thickener, water binder,

extrusion aid, texture modifier and film formers (Cheng et al., 1999). CMC is a polyelectrolyte when dissolved in water, and the molecules dissociate into sodium cations and polymer anions (Yang and Zhu, 2007). CMC rheological properties depend on the polymer concentration, degrees of substitution, molar mass, temperature, salt content, pH, presence of surfactants, and molecular structure (Gibis et al., 2015). CMC solutions exhibit pseudoplastic behaviour; the solutions have long entangled and looping molecular chains with irregular internal order that form a high resistance against the flow. However, on increasing shear rates, the chain molecules are disentangled and orientated parallel to the shearing force. The molecules aligning allows molecules to slip past each other more easily, and the viscosity is reduced. The solutions are stable between pH 2 and pH 10. Below pH 2, precipitation of solids occurs, whereas above pH 10, the viscosity decreases (Ghannam and Esmail, 1997). They also show thixotropic behaviour as the viscosity decreases with the shearing time (Benchabane and Bekkour, 2008).

2.5.4 Starch

Starch is the major energy storage polysaccharide and the second most abundant polymer after cellulose in nature. Starch granules are found in the seeds, roots, tubers, fruits and stems of plants, and they are produced via photosynthesis. The unique physicochemical and functional properties, including thickening, stabilising, gelling agent, and water retention properties of starch, have widened their application in different industries, including coating, pharmaceutical, building, food and packaging industries (Singh et al., 2003). Starch granules vary in size (about 1 -100 μm in diameter), shape (round, lenticular, polygonal), size distribution (uni- or bi-modal) and composition (α -glucan, lipid, moisture, protein and mineral content) depending on the

origin. The dimension of maize starches (used in this project) is in the range of 5 to 20 μm (Sullo, 2012). Starch granules are insoluble in water but can be solubilised in non-aqueous solvents such as ionic liquids (Koganti et al., 2011); To extend their application, the granules can be modified chemically, enzymatically, and physically for unique and enhanced properties (Tester et al., 2004).

2.5.4.1 Structure

Starch is semi-crystalline and comprises two types of polymers: amylose and amylopectin (Figure 2-5).

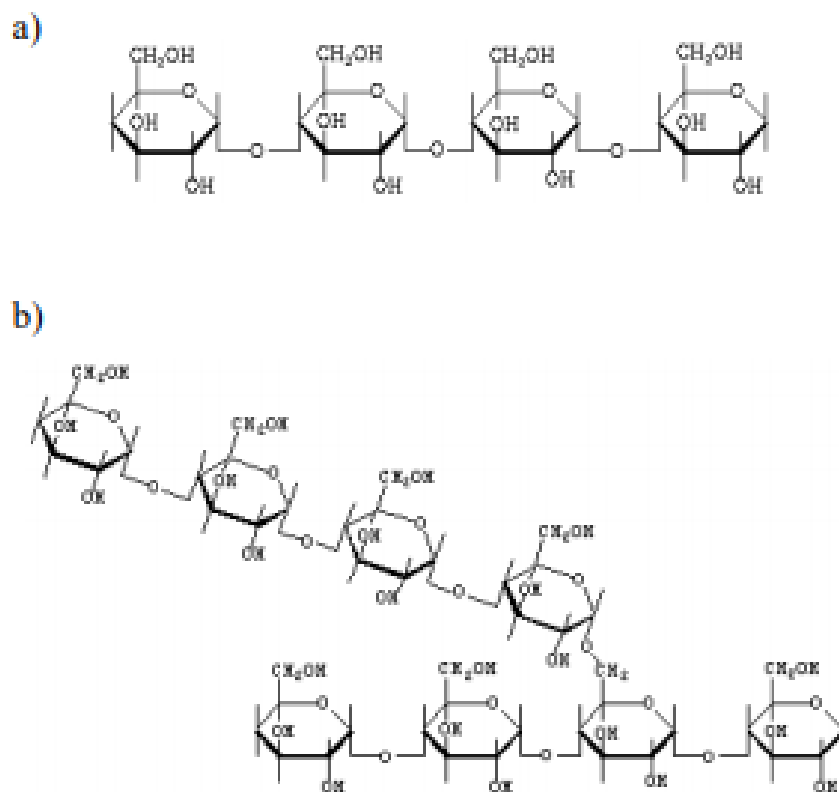


Figure 2-5: The chemical structures of (a) amylose and (b) amylopectin.

The ratio of amylose and amylopectin varies with the botanical origin of the starch (Tester et al., 2004). Generally, the native starch granule comprises 20-25% amylose

and 75-80% amylopectin, respectively. However, some modified starches, called waxy or high amylose starches, contains less than 5% or more than 40% amylose, respectively (Coultate, 2009). Amylose is contained the amorphous region of a starch granule and is a linear polymer composed of glucopyranose units linked by α -D-(1-4) linkages, with a molecular weight of about $1 \times 10^5 - 10^6$ Da. Amylopectin, the main component of the crystalline region, is a highly branched polymer consisting of shorter chains of (1-4) α -D-glucopyranose linked with (1-6)- α -D-glycosidic branched linkages. The average molecular weight of amylopectin is about $1 \times 10^7 - 10^9$. According to the widely accepted cluster model (French, 1972), amylopectin molecule has a supramolecular structure consisting of alternating crystalline and amorphous regions. The structure contains different chains: A, B, and C. A single C-chain exists in the amylopectin molecule, which contains the only free reducing end. The A-chain is attached to the main structure by a single linkage, while B-chains holds at least one A-chain and forms the link between the A and C-chains (Figure 2-6).

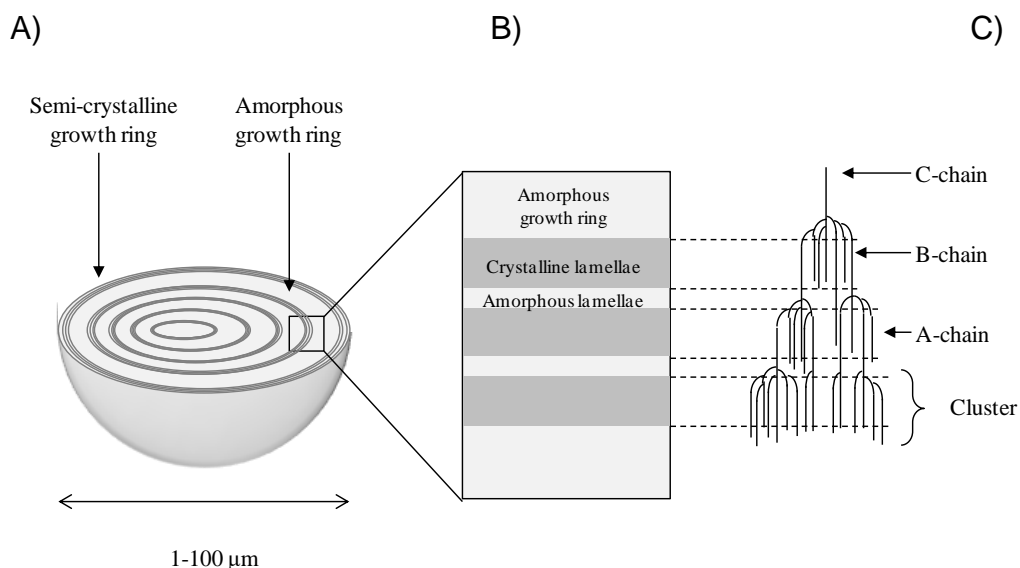


Figure 2-6: Schematic representation of the molecular organisation of the starch granule (A) single granule made from concentric growth rings (Bb) crystalline and amorphous lamellae (C) amylopectin cluster structure (Jenkins et al., 1994).

X-ray diffraction analysis revealed that starch granules from different sources show different polymorphic forms depending on their amylose/amylopectin ratio and amylopectin branch length (Zobel, 1988; Hoover, 2001). The A-type X-ray pattern is found in cereal starches, and it is arranged in a monoclinic unit cell. The B-type pattern is predominant in tubers such as potato and high amylose cereal starches, arranged into a hexagonal unit cell. The C-type pattern, a combination of the A and B-type patterns, is found in legumes such as pea and bean starches (Singh et al., 2003). Normal cereal and waxy starches show an A-type XRD pattern, whereas high-amylose starches display a B-type pattern. The ratio of amylose to amylopectin in normal starches such as maize, rice is between 20-35% and 70-80%, respectively (Pérez and Bertoft, 2010). X-ray diffraction analysis of amylose and amylopectin showed that polymorphs A and B are made of ordered arrays of left-handed double helices with parallel strands (Cooke and Gidley, 1992).

2.5.4.2 Starch gelatinisation

Native starch granules are insoluble in cold water because of the intra- and intermolecular hydrogen bonds stabilising the starch molecules in the structure (Tester and Morrison, 1990a). However, upon heating in excess water, starch granules undergoes an irreversible order to disorder transition known as gelatinisation. This process involves a series of irreversible physical changes consisting of granule swelling due to its hydration, loss of crystalline structure, loss of optical birefringence, and dissociation of double helices. These changes are followed by the separation of amylose and amylopectin, which results in the leaching of the amylose out of the granules (Singh et al., 2003). Techniques such as DSC, RVA, NMR, X-ray and optical

microscopy have been employed to study the changes that occur during the gelatinisation process.

Starch gelatinisation is found to be dependent on moisture content. Donovan (1979) proposed that in excess water, the swelling of the amorphous regions of the granule melts the crystallites, followed by unfolding and hydration of the crystallite's helices, which gives rise to a single endotherm in the DSC. However, in limited water contents, two endotherms are observed; only the crystallites located in areas of locally high-water concentrations get disrupted and give rise to the same endotherm as in the case of excess water. The remaining crystallites would melt at higher temperatures, giving rise to a second endotherm called 'M1' at high temperature. Biliaderis et al. (1980) proposed a similar explanation for the gelatinisation phenomenon of starches from different origin when heated at intermediate and high-water contents. An alternative explanation for the biphasic endothermic events at intermediate water contents was proposed by Waigh et al. (2000) using a side-chain liquid crystalline approach. The first was ascribed to the disassociation of double helices within the crystallites. The second endotherm was related to the unwinding and helix-coil transition of the double helices. Additionally, a third endotherm called M2 ascribed to the melting of amylose-lipid complexes is observed at higher temperatures in the DSC study of some starches (Tester and Morrison, 1990b; Liu et al., 2006).

Another widely used technique for monitoring the changes in starches during heating is the Rapid Visco Analyser (RVA). The RVA is used to measure the rheological properties, i.e., the changes in the viscosity of starch pastes/suspensions in excess water upon heating (gelatinisation) and cooling (retrogradation) under constant shearing. The process of viscosity development of the starch pastes is referred to as

“starch pasting”. A typical pasting profile (Figure 2-7) shows the viscosity changes of starch plotted as a function of temperature and time. Typically, the starch granules are slurried in excess water at low temperature (< 50 °C). When the temperature increases, the starch granules hydrate and swell, leading to a sharp increase in viscosity (number 2 in Figure 2-7). The temperature at which the granule swelling is initiated is taken as the pasting temperature (number 1 in Figure 2-7). As the viscosity of the granules increases, amylose molecules leach out of the swollen granules. Upon further increase in temperature, the swelling becomes easier, and it reaches a maximum, which is known as peak viscosity (number 3, Figure 2-7). Starch swelling properties have been directly correlated to the amylopectin content, whereas amylose and the internal lipids retard the swelling property (Tester and Morrison, 1990b).

As the temperature increases, the swollen granules become sensitive to shearing and lose their integrity, represented by a decrease in the viscosity, regarded as the breakdown viscosity (number 4 in Figure 2-7), which leads to a trough viscosity (number 5 in Figure 2-7). Upon cooling the gelatinised starch suspension, a turbid viscoelastic paste, at high starch concentrations (>6% w/w), a gel is formed. This is due to the leached amylose molecules interacting with one another and with amylopectin molecules to form a strong network, leading to a setback viscosity, a process known as retrogradation; this is represented by an increase in viscosity at the end of the RVA profile (number 6 in Figure 2-7) (Morris, 1990). The amylose retrogradation process is affected by the amylose: amylopectin ratio and lipid content of the starch. The retrogradation kinetics for each of the starch polymers follows different rates. Amylose has a shorter retrogradation period due to the chains recrystallising easily, while the chains of amylopectin take longer to re-associate due to the branched structure of the amylopectin. Starches with high amylose content

develop strong gels. However, starch pastes with high amylopectin form weak gels. When amylose leaches out of the granule, hydrogen bonds are formed between the chains to produce a rigid and opaque gel. However, due to the branched structure of amylopectin, the chains cannot interact easily via hydrogen bonding, and the solutions remain clear and liquid-like (Bahnassey and Breene, 1994).

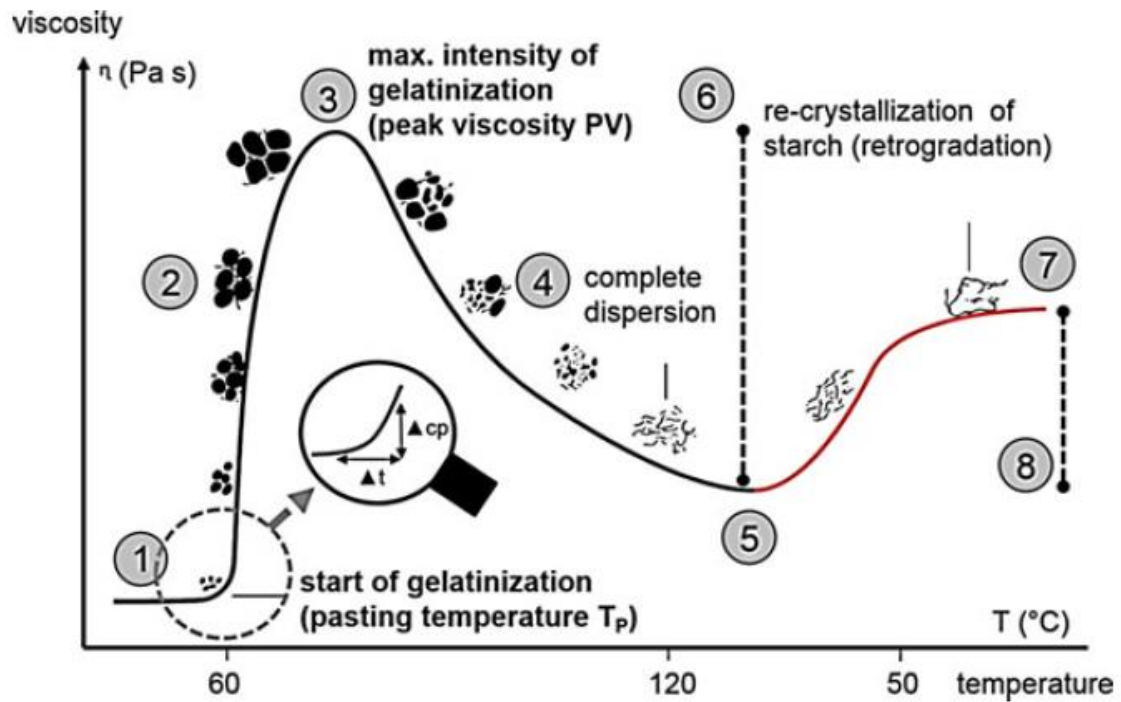


Figure 2-7: Typical pasting profile and schematic representation of starch behaviour under heating and cooling (Schirmer et al., 2015).

2.6 Collagen-hydrocolloid films

To increase the applications of collagen in the food industry, several methods have been explored to improve collagen film properties, particularly mechanical properties. This includes crosslinking of collagen via physical (Wang et al., 2015) or enzymatic (Wu et al., 2017; Cheng et al., 2019) methods and blending of collagen with other biopolymers (Ahmad et al., 2016; Long et al., 2018) or in-organic substances (Ma et al., 2018). Amongst these methods, collagen mixing with other biopolymers is the most widely explored and preferred method for producing films with increased tensile strength and broaden the range of collagen film application. It is important to mention that much of the literature on collagen-biopolymer films was performed using acid or pepsin soluble collagen, which is entirely different from the fibrous collagen used in this study. The different collagen treatment changes collagen to different structural levels, leading to different film properties.

Several studies on the improvement of collagen film properties have focused on using biopolymers such as gelatin, microfibrillated cellulose (MFC), and cellulose nanocrystals (CNCs) (Wang et al., 2016b; Long et al., 2018; Xiao et al., 2020). It should be noted that some of these studies have been done on collagen extracted from various animals. However, this review will only focus on collagen extracted from bovine. Moreover, the fibrous collagen used in this work is different to the type of collagen used in some of these studies.

Wang et al. (2016b) investigated the effect of incorporating carboxylated MFC as a reinforcing agent on the mechanical properties, thermal stability and morphological properties of acid-swollen collagen fibre film. Adding MFC led to the formation of an

interwoven film network, which increased in tensile strength, stiffness and thermal stability, but the opposite effect was observed for the film's elongation at break. The authors concluded that a strong interaction existed between the MFC and collagen fibres; the specific interaction was attributed to ionically crosslinking of MFC fibrils with collagen fibres in the composite films. It was also proposed that intermolecular hydrogen bonding occurred between the carboxyl groups of MFC and the amide groups of collagen fibres.

Wang et al. (2017a) studied the effects of ungelatinised waxy maize, normal and high amylose starch granules on heated and unheated collagen films in wet and dry states. It was reported that high amylose and normal corn starches increased the tensile strength of unheated wet and dried collagen films, whereas all the starches increased the tensile strength of the heated collagen films. On the contrary, adding starches reduced the elongation at break of heated and unheated films. Whether heated or not, the increase in tensile strength of the films was starch concentration-dependent. Higher concentrations (50 %) of the starch granules were found to decrease the tensile strength. This was attributed to the granules' aggregation in the film matrix, which disrupted the collagen fibres network. Additionally, collagen film thermal stability increased with the incorporation of starches. However, the various starches increased thermal stability to a different degree. The authors concluded the enhanced tensile strength and improved thermal stability were due to interactions between the collagen fibres and starch chains. This result was similar to the study of (Wang et al., 2018), where a lower amount (50 g Kg⁻¹) of anionic CNFs increased the higher tensile strength and EAB of collagen fibre films. On the contrary, it was shown that a higher amount (up to 200 g Kg⁻¹) of anionic CNFs led to a decrease in the higher tensile strength and EAB due to a reduction in the cohesion force in the film matrix.

Another study showed that the inclusion of cellulose nanocrystals as reinforcement fillers in the collagen led to an increase in the TS, YM and thermostability of collagen casings (Long et al., 2018). This enhancement was attributed to hydrogen bonding interaction between hydroxyl groups on the surface of CNCs and collagen and electrostatic interaction, creating a dense network structure. In a recent study by Wu et al. (2020), collagen fibre paste was immersed into anionic carboxymethylcellulose solution to form composite films. It was demonstrated that the interaction between CMC and collagen increased tensile strength, elongation at break, stiffness, and the thermal stability of films.

Animal and plant proteins have also been used to enhance collagen fibre film properties. Wu et al. (2018) found that adding soy proteins, casein that was crosslinked with transglutaminase and non-crosslinked caesin increased the TS, EAB and thermal stability of collagen fibre films. Their results also showed that the higher contents of the proteins led to a decrease of the mechanical properties; this correlates with the results obtained by (Wang et al., 2017a; Wang et al., 2018). The water vapour permeability of films was reduced, improving their potential for sausage casings. Additionally, the crosslinking of collagen resulted in enhancing the tensile strength and stiffness of the collagen fibre films.

Similarly, in a recent study by Xiao et al. (2020), it was reported that crosslinked and non-crosslinked type A and type B gelatin increased the mechanical properties, thermal stability and water barrier properties of collagen fibre films. From these studies, mixing hydrocolloids with acid-swollen collagen paste or solutions can create collagen films (casings) with enhanced mechanical and thermal stability properties. In this study, different hydrocolloids dispersions (cellulose fibres, starches with different

amylose and amylopectin ratio) and solutions (guar gums, HPMC, MC and CMC) are blended with fibrous acid-swollen collagen paste, and their effects on their resulting films are investigated. It is assumed that collagen films with improved properties can be designed by exploring the hydrocolloids functional properties, such as gelation and viscosifying effects.

3 THE IMPACT OF HYDROCOLLOIDS ADDITION ON VISCOELASTIC AND THERMAL PROPERTIES OF ACID- SWOLLEN COLLAGEN PASTE

3.1 Abstract

The interactions between proteins and polysaccharides are of considerable importance in the food industry. In this study, the effect of non-charged methylcellulose (MC), hydroxypropylmethylcellulose (HPMC), medium (GM) and high (GH) molecular weight guar gum and negatively charged sodium carboxymethylcellulose (CMC) at comparable low-shear viscosity (300 mPa.s) was investigated on the rheological and thermal properties of acid-swollen collagen paste as a function of collagen concentration. Dynamic frequency sweep showed that the addition of the hydrocolloids except for CMC increased the storage modulus (G'), loss modulus (G'') of collagen pastes at all collagen levels investigated. MC, HPMC, GH, and GM increased the collagen pastes' storage modulus to a similar extent. In contrast, the values of the loss moduli were found to be markedly different for each hydrocolloid. The loss factor ($\tan \delta$) showed that incorporating the hydrocolloids made the pastes less elastic than pure collagen pastes. The phase transition temperature of collagen measured during the temperature sweep tests was not affected by MC, HPMC, GH, and GM. However, CMC shifted the transition temperature of collagen to higher temperatures. Micro Differential scanning calorimeter (microDSC) results showed that the presence of MC, HPMC, and guar gums did not affect the denaturation temperature (T_d) and enthalpy (ΔH). In contrast, the addition of CMC increased the denaturation temperature and denaturation enthalpy of collagen pastes. By fixing the hydrocolloids' viscosifying power and changing the collagen concentration, collagen pastes with different hydrocolloids show different viscoelastic properties.

3.2 Introduction

There have been considerable research efforts in understanding the interaction between proteins and polysaccharides due to their role in developing food products such as gels, emulsions, and edible films (Anvari and Chung, 2016). Collagen is the most abundant fibrous protein found in connective tissues such as skins, bones, cartilages, and tendons of mammals. It makes up approximately 30% of the total protein in the body. The collagen molecule known as tropocollagen is a triple helix structure made up of three alpha chains. Each chain consists of a predominance of repeating units of GLY-X-Y amino acids sequence, GLY is glycine, X and Y are proline and hydroxyproline, respectively. The alpha chains interact together via intermolecular hydrogen bonding and further intertwine to form a right-handed triple helix structure (Stenzel et al., 1974; Friess, 1998).

About four to eight collagen molecules aggregate through fibrillogenesis into microfibrils and subsequently into collagen fibrils (cross-section diameter between 10 nm – 500 nm). The extra strength and stability stem from further self-aggregation and intermolecular crosslinks (Stenzel et al., 1974; Gelse et al., 2003). These fibrils further assemble to form collagen fibres, which give tensile strength and elasticity to animal tissues (Savic and Savic, 2002). Collagen fibres extracted from bovine or porcine skins are processed into a swollen fibrous paste using an acidic solvent, usually hydrochloric or acetic acid. One of the major applications of collagen pastes or gels in the food industry is films/casings. Due to the viscoelastic nature of solubilised collagen solutions and acid-swollen collagen pastes, extrusion is a preferred processing method to produce films for the edible casings (Wallace and Rosenblatt, 2003; Yang et al., 2016). High tensile strength is an essential property for extruded films to be

commercially useful, and this depends on the rheological properties of precursor dispersions or pastes (Zhang et al., 2013). Current research focuses on modifying the rheological and thermal properties of collagen pastes, with one approach to blend the pastes with hydrocolloids. Understanding the rheological properties of protein-polysaccharide mixtures and their relation to their structures is essential for their performance in commercial applications (Derkach et al., 2020).

Cellulose derivatives and guar gum are widely applied food hydrocolloids used as thickeners, binders, gelators, film formers, stabilisers and emulsifiers (Ghosh and Bandyopadhyay, 2012; Gałkowska et al., 2014). Methylcellulose (MC) and hydroxypropylmethylcellulose (HPMC) are water-soluble, non-ionic cellulose derivative ethers. MC is more hydrophobic than HPMC, and they show thermal gelation properties; their solutions form gels when heated, and the process is reversible upon cooling. For this reason, they are widely used as film-forming, thickening and gelling agents (Clasen and Kulicke, 2001a). Sodium carboxymethylcellulose is a linear, water-soluble anionic cellulose derivative produced by reacting alkali cellulose with sodium monochloroacetate (Feddersen and Thorp, 1993). It is primarily used as a stabiliser, emulsifying agent or, film former across a broad range of fast-moving consumer goods, such as foods, cosmetics and household products (Benchabane and Bekkour, 2008).

Guar gum is a galactomannan that is made up of a linear chain of β -(1-4) linked mannan backbone substituted by a single galactose (Gal) side chain through α -(1-6) linkages at a 2:1 molecular ratio of mannose: galactose (Funami et al., 2005; Choi and Chang, 2012). It is a non-gelling, water-soluble non-ionic polysaccharide extracted

from *Cyamopsis tetragonoloba* L. and are used mainly as a thickening and stabilising agent (Lee and Chang, 2015).

In binary admixtures of hydrocolloids, the rheological properties are determined by the interactions between the different components in the system. These interactions are dependent on each biopolymer's chemical nature (El Ghzaoui et al., 2001). Indeed Haug et al. (2003) showed that both phase separation and molecular electrostatic interactions could occur simultaneously in a system. Many of the preceding papers have explored the interactions of gelatin and water-soluble hydrocolloids (Alves et al., 1999; Antonov and Gonçalves, 1999; Harrington and Morris, 2009; Antonov and Gonçalves, 2015), whereas few have explored, in comparative detail, the interaction of acid-swollen collagen with such soluble polymers. Thus, understanding the interaction between acid-swollen collagen paste and these hydrocolloids when mixed is essential if they are to be used for industrial applications. The rheological properties of a mixed system might depend on the type of hydrocolloid, structure, concentration and the interaction between the hydrocolloid molecules. In this study, to determine the effect of different hydrocolloids on collagen paste properties, collagen pastes were mixed with water-soluble hydrocolloids to modify the paste's rheological properties.

So far, only one study exists to date describing the effect of HPMC on the rheology and thermal properties of soluble collagen (Ding et al., 2014a). The authors reported that the storage and loss modulus decreased, and the thermal stability of collagen solution increased with increased levels of HPMC. No study has been conducted to study the effects of methylcellulose, sodium carboxymethylcellulose, and guar gums on fibrous acid-swollen collagen rheological and thermal properties paste. To address this knowledge gap and consider how the additions of the hydrocolloids would impact

different application of collagen pastes, the present study investigates the effect of hydrocolloids additives on the rheological and thermal properties of the paste as a function of acid-swollen collagen concentration. The hydrocolloids concentrations were adjusted to render all solutions to have comparable low-shear viscosity (300 mPas). It was hypothesised that since the viscosifying potential of the solutions was matched, their effects on the overall viscoelastic nature of the pastes should be the same unless specific interactions between the collagen and hydrocolloids result in a synergistic rheological effect. Therefore, this work investigates the effect of non-gelling and gelling water-soluble hydrocolloids on the rheological and thermal properties of the paste as a function of acid-swollen collagen concentration. Also, the effect of hydrocolloid and molecular weight was considered.

Three different mixing ratios, requiring various stock pastes and solutions, were combined to produce mixtures with the same final concentration of each component. The final concentration of the individual hydrocolloids corresponding to a low-shear viscosity of 300 mPas was chosen. The final concentration of collagen paste was 4, 3.5 and 2.5 %w/w, respectively, from a starting stock concentration of 5 %w/w.

3.3 Materials and Methodology

3.3.1 Materials

Collagen pastes (5 %w/w collagen concentration-COLL) at pH of 2 was provided by Devro plc. Sodium carboxymethylcellulose (Na CMC) with the trade name BLANOSE 7MIF cellulose gum, a product of Aqualon, France, was provided to the project team; the degree of substitution was in the range of 0.70-0.95. Guar gum with a 'medium' molecular weight of 1649 kDa (GM) and a 'high' molecular weight of 2660 kDa (GH) was kindly provided by DuPont. Methylcellulose A4M (MC) and

hydroxypropylmethylcellulose K4M (HPMC) were kindly provided by Dow Chemical Co (trade name Methocel). The letter 'A' corresponds to MC, while 'K' is HPMC with different addition level of the two substituents. The letter 'M' indicates the value of viscosity in cPs for the solution of 2% at room temperature; for example, 4M = 4000 cPs. Their average degree of substitution (DS) and their average molar substitution (MS) adapted from (Sarkar, 1979) are shown in Table 3-1.

Table 3-1: Substitution ranges of Cellulose ethers (Sarkar 1979)

	MC (A4M)	HPMC (K4M)
Methoxyl degree of substitution (DS)	1.6 – 1.8	1.1 - 1.4
Hydroxypropyl molar substitution (MS)	0	0.1- 0.3

DS is the average number of hydroxyl groups substituted by alkyl groups on the anhydroglucose unit. MS is the average of the total number of substituted groups per anhydroglucose unit.

3.3.2 Methodology

3.3.2.1 Preparation of hydrocolloid solutions

To measure the effect of the hydrocolloids on acid-swollen collagen paste, the low-shear viscosity of methylcellulose (MC), hydroxypropylmethylcellulose (HPMC), medium molecular weight (GM), high molecular weight (GH) guar gums and sodium

carboxymethylcellulose (CMC) were matched at a low-shear viscosity of 300 mPas. The concentrations required are presented in Table 3-2. The MC, HPMC, GM, GH solutions were prepared based on the method described by Sullo and Foster (2010). The required concentration of derivatised cellulose was prepared by heating 1/3 of the required volume of water to at least 90 °C, followed by adding the powders carefully under agitation with the aid of a magnetic stirrer. The mixtures were agitated until the particles were dispersed properly, and to complete solubilisation, the remaining cold water was then added until hydration was achieved. Guar gum was prepared by dispersing the required amount of powder in distilled water using a magnetic stirrer. The solutions were stirred at 80 °C for 1 hour. CMC solution was prepared by dissolving the required amount of polymer powder under constant agitation in distilled water at room temperature.

Table 3-2: Concentration (%w/w) of hydrocolloids required for a zero-shear viscosity of 300 mPas.

Hydrocolloids	Conc. (%w/w) required for a low-shear viscosity of 300 mPas
Methylcellulose (MC)	1.0
Hydroxypropylmethylcellulose (HPMC)	1.0
High molecular weight Guar gum (GH)	0.5
Medium molecular weight Guar gum (GM)	0.76
Sodium carboxymethylcellulose (CMC)	2.7

3.3.2.2 Preparation of collagen pastes with and without hydrocolloids

Stock collagen paste (5% w/w) was mixed with hydrocolloid solutions at different collagen/hydrocolloids mixing ratios, i.e., 80:20, 70:30 and 50:50. The stock collagen paste was diluted with water at a similar mixing ratio of hydrocolloids to final concentrations of 4% (w/w), 3.5% (w/w) and 2.5% (w/w), respectively. The final concentrations of the hydrocolloids in the mixture are shown in Table 3-2. The stock collagen pastes, and hydrocolloid solutions were mixed by gently stirring at room temperature for 15 mins using an overhead stirrer (yellow line IKA OST 20 high torque overhead Stirrer). The pH of the final blends was between 2 and 2.5. Samples were degassed using an Audionvac VMS 53 multivac vacuum packager (Audion Elektron, Netherlands) to remove the air bubbles incorporated during mixing before further analyses were performed. The blends formulation and sample code are shown in Table 3-3.

Table 3-3: Summary of the concentration of the stock hydrocolloid solutions and stock collagen paste their mixing ratios and final concentrations in the mixture.

	Mixing ratio Collagen: hydrocolloid	Stock Conc.of collagen paste	Stock Conc. of solution	Conc. of collagen in the mixture	Conc. (% wt) of hydrocolloids in the mixture
COLLHPMC	80:20	5	5	4	1
	70:30	5	3.3	3.5	1
	50:50	5	2	2.5	1
COLLMC	80:20	5	5	4	1
	70:30	5	3.3	3.5	1
	50:50	5	2	2.5	1
COLLGM	80:20	5	3.8	4	0.76
	70:30	5	2.53	3.5	0.76
	50:50	5	1.52	2.5	0.76
COLLGH	80:20	5	2.5	4	0.5
	70:30	5	1.67	3.5	0.5
	50:50	5	1	2.5	0.5
COLLCCMC	80:20	5	13.5	4	2.7
	70:30	5	9	3.5	2.7
	50:50	5	5.4	2.5	2.7

3.3.2.3 Rheological measurements

The steady shear viscosity measurements for each hydrocolloid solution were performed at 20°C using a controlled stress rheometer (Anton Paar, Austria) equipped with concentric cylinder geometry over the shear rate ($\dot{\gamma}$) range from 0.1 to 1000 s⁻¹. The viscoelastic properties of the mixed pastes were performed by small-amplitude oscillatory measurements using a controlled stress rheometer (Anton Paar, Austria) equipped with parallel plate geometry (50 mm diameter; 1.5 mm gap). The

temperature was controlled using a Peltier system with the assistance of a water bath (R1, Grant, Shepreth UK). Before each measurement, samples were allowed to rest at 20 °C for 5 min for structure recovery and temperature equilibration. The edge of the samples was trimmed and covered with low viscosity mineral oil (Sigma, USA) to prevent the sample from drying. Amplitude sweeps were performed at 0.001 – 1000% strain at an angular frequency of 10 rad/s in order to determine the linear viscoelastic region. Frequency sweeps were performed from 0.1 to 100 rad/s at 0.1% strain, which is found to be within the linear viscoelastic region. Temperature sweep tests were performed at a constant strain (0.1%) and angular frequency (10 rad/s) with a temperature ramp from 10 °C to 95 °C at a heating rate of 5 °C/min. The storage modulus (G'), loss modulus (G'') and loss factor ($\tan \delta$) were recorded using the Rheoplus software (Anton Paar, Austria).

3.3.2.4 Thermal Analysis

The thermal transition of collagen pastes with and without hydrocolloids were studied using a micro differential scanning calorimeter (MicroDSC III, Setaram Instrumentation, France). Approximately 0.8 g of pastes were weighed in Hastelloy cells and sealed with O rings and Hastelloy screw tops. The samples were scanned over the range of temperature from 10 to 95 °C at a heating rate of 1 °C/min. The samples were reheated to check for a reversible peak. A Hastelloy cell filled with RO water was used reference. The melting temperature (T_m), the transition enthalpy (ΔH), onset temperature (T_o) and endset temperature (T_e) were processed using Calisto Processing software v1.43 (AKTS, Switzerland).

3.3.2.5 Microstructure

Images of the pastes were recorded using an EVOS phase-contrast light microscope (ThermoFisher). Samples were mounted on a glass slide; a coverslip was placed on the sample, and another slide was used to press the pastes to make it thin for easy imaging. Images were taken at magnifications of 10X.

3.3.2.6 Statistical Analysis

Analysis of variance ANOVA was used to determine the difference between samples using Statistical Package for Social Science Software (SPSS Inc.). When there were any differences between samples, Tukey's test was used to determine the significance of the means of the samples ($P < 0.05$).

3.4 Results and Discussions

3.4.1 Flow behaviour of hydrocolloids

Figure 3-1 shows the hydrocolloids viscosity curves at concentrations required to match a low-shear viscosity of 300 mPa.s. All the hydrocolloid solutions show a shear-thinning behaviour due to the molecular disentanglement of polysaccharides chains when subjected to shearing forces or increased orientation of the polymer chains in the direction of flow (Mezger, 2006; Benchabane and Bekkour, 2008). For the same low-shear viscosity, the shear-thinning behaviour was different for the hydrocolloid solutions. The Cross-Williamson model equation (3-1) was used to fit the rheological data of the hydrocolloid solutions.

$$\frac{\eta}{\eta_0} = \frac{1}{1 + k\gamma^{(1-n)}} \quad (3-1)$$

Where η is the viscosity at a specific rate γ , η_0 is the low shear viscosity, k is a time constant (which measures the consistency of the fluid), n is a dimensionless rate constant, indicating the flow behaviour index of the fluid, and a measure of the degree of pseudoplasticity. For a Newtonian fluid, n is equal to 1; for a dilatant, $n > 1$, for a pseudoplastic fluid, $n < 1$. The fits of the experimental data using the Cross-Williamson model are shown as the solid line in Figure 3-1. The resulting k , n and R^2 parameters are summarised in Table 3-4. As shown in Table 3-4, the values of the hydrocolloid solutions are less than 1, indicating the shear-thinning behaviour of the solution, where the viscosity decreases with increasing shear rates. The flow index (n) was found to follow the order $\text{GH} < \text{GM} < \text{HPMC} \sim \text{MC} \ll \text{CMC}$. High molecular weight guar gum (GH) shows the lowest n value, reflecting a more pronounced shear-thinning

behaviour. The lower concentration of GH (0.5%) might be the reason for having a greater shear-thinning. CMC shows the least degree of shear-thinning behaviour and higher viscosity at higher shear rates. Furthermore, the consistency coefficient (k) increases in the order GH > GM > HPMC ~ MC >> CMC as the flow behaviour index. The regression coefficients (R^2) shows that the Cross-Williamson model offers a suitable fit ($R^2 > 0.999$) for the experimental data of the hydrocolloids. The degree of shear-thinning behaviour of random coil polymers depends on the concentration, molecular weight, and chain stiffness of the polymers (Morris et al., 1981; Lapasin and Prici, 1995). Thus, the difference in the shear-thinning behaviour of the different hydrocolloid solutions may be due to the different concentrations used at comparable low-shear viscosity (300mPas) due to differences in polymers molecular weights. Lower concentrations are needed for guar gum solutions due to their higher molecular weight and greater chain mobility influencing hydration capacity resulting from their high degree of branching (Kim and Yoo, 2011a; Kim and Yoo, 2011b; Choi and Chang, 2012; Lee and Chang, 2015). Haque and Morris (1993) stated that the shear-thinning behaviour of methylcellulose and hydroxypropylmethylcellulose deviates from the normal random coil polysaccharides reported by Morris et al. (1981). The deviation of MC and HPMC was attributed to intact native cellulose remaining, which links several chains together into bundles. Interestingly, MC and HPMC show flow profiles, as expected from their industrial classification, and conform with Haque et al. (1993a). Having matched the different hydrocolloids for their low-shear viscosity and recorded their different shear-thinning behaviour, their effects on the properties of acid swollen collagen pastes will be studied.

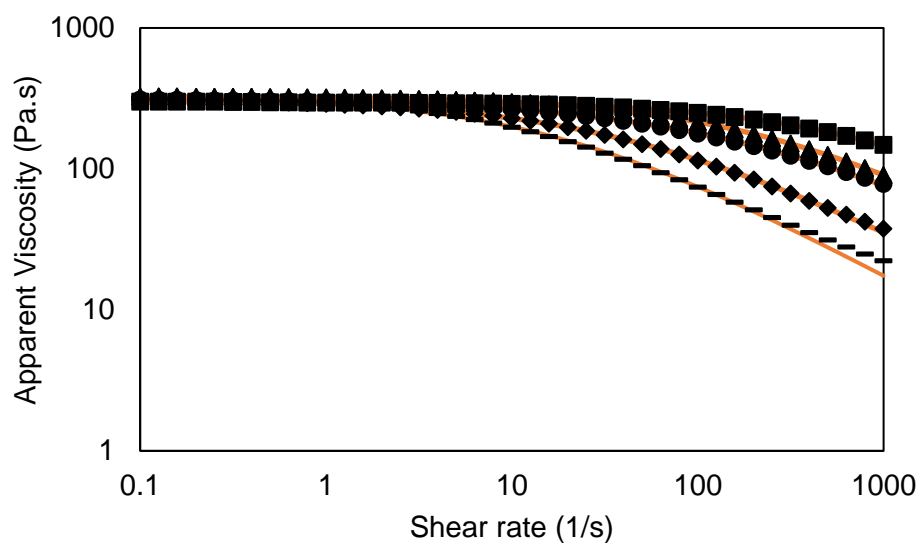


Figure 3-1: Flow curves of Hydroxypropylmethylcellulose (HPMC) (●), Methylcellulose (MC) (▲), Medium Guar gum (GM) (◆), High Guar gum (GH) (—) and Sodium carboxymethylcellulose (CMC) (■) solutions measured at 20 °C. Cross-Williamson fit is the solid orange line.

Table 3-4: Cross-Williamson model for hydrocolloid solutions

	n	K (Pa.S ⁿ)	R ²
GH	0.280 ± 0.004	0.120 ± 0.005	0.992
GM	0.337 ± 0.003	0.081 ± 0.009	0.999
HPMC	0.384 ± 0.138	0.044 ± 0.010	0.999
MC	0.390 ± 0.004	0.040 ± 0.002	0.999
CMC	0.416 ± 0.09	0.022 ± 0.010	0.999

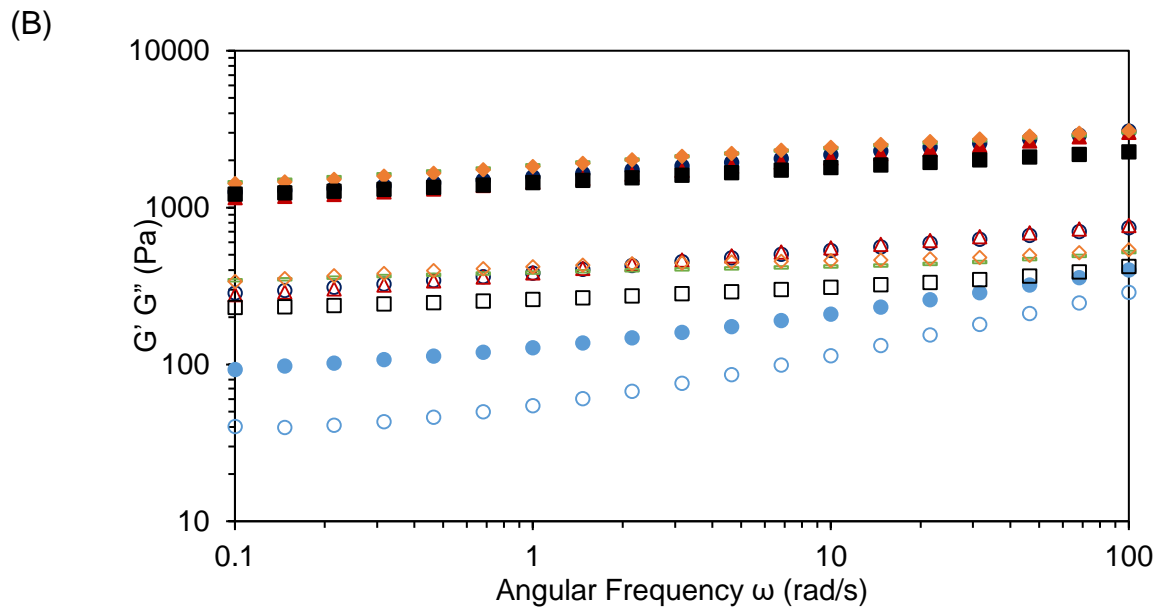
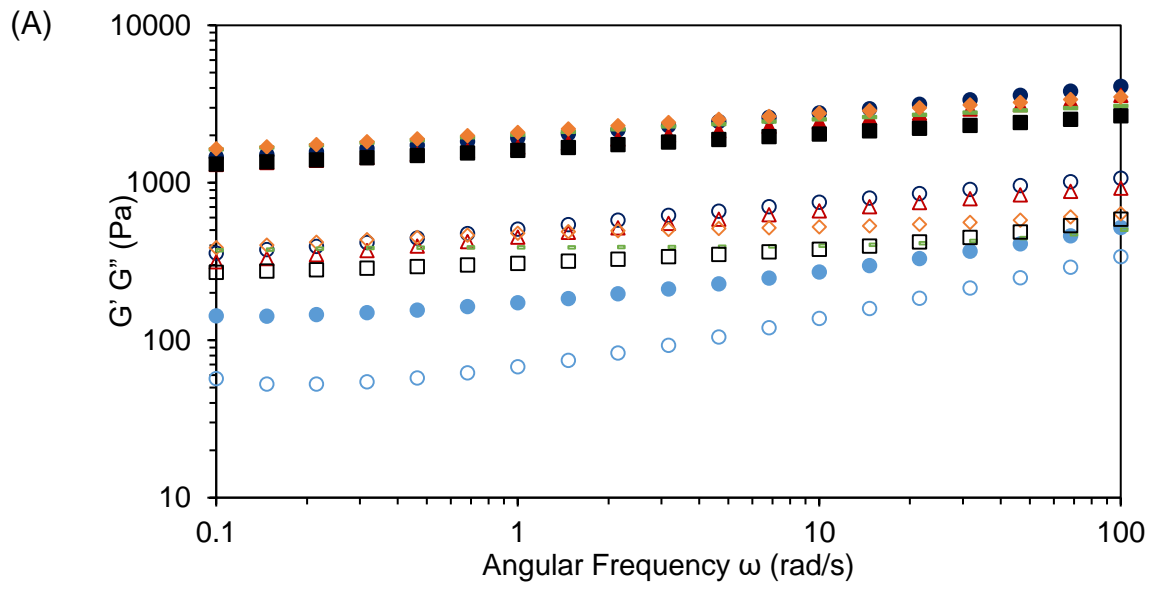
3.4.2 Dynamic Frequency sweep

The storage modulus (G'), loss modulus (G'') and loss factor ($\tan \delta$) as a function of angular frequency (ω) for the collagen pastes with and without hydrocolloids at different collagen concentrations are shown in Figure 3-2 and Figure 3-3, respectively. The mechanical spectra of all the pastes show a typical weak gel behaviour (Clark and Ross-Murphy, 1987), where G' were higher than G'' at the angular frequency range investigated. Both moduli increased in a manner dependent on angular frequency. A greater frequency dependency of G' and G'' moduli is evidenced for COLLCMC pastes. The addition of the hydrocolloids except for CMC (which will be discussed separately below) increased slightly the G' and G'' of the collagen pastes at the various levels of collagen investigated, and as expected, the values increased with increasing collagen concentration in the mixtures.

The G' curve is similar for COLLHPMC, COLLMC, COLLGM and COLLGH. This indicates that the hydrocolloid type did not affect the overall elastic properties of collagen paste, and indeed the increase in viscosity provided by the hydrocolloids is the reason for the slight increase of G' . However, the pastes show different G'' responses, where now the viscosity of the hydrocolloids also increases G'' to a greater extent than G' , with a concomitant increase in the loss factor ($\tan \delta$) at low angular frequencies. The G'' of the hydrocolloid solutions are similar at low shear, but with increasing angular frequencies, the difference between the samples becomes clearer. COLLHPMC and COLLMC retain higher G' values, whereas those of COLLGM and COLLGH tend towards the values for the collagen paste alone. The difference between the viscous portion of the samples (COLLHPMC and COLLMC gives a slightly higher G'' than COLLGM and COLLGH at high angular frequencies) might be due to difference in the viscosity of the hydrocolloids at high shear rates and phase

separation. This data shows the link between the flow profiles of the hydrocolloids and the viscoelastic properties of the pastes. This is a very important for material processing because by optimising the flow behaviour of the hydrocolloids, the viscoelastic properties of the paste can be altered.

In the case of COLLCMC pastes, the values of G' and G'' were lower than those of pure collagen pastes, indicating that the addition of CMC weakened the paste structure. A decrease in the storage and loss moduli of meat batter with the addition of CMC was reported by Schuh et al. (2013), although the authors did not explain the reason for the reduction in values. In this study, the collagen paste is positively charged under acidic conditions, while the CMC is negatively charged due to the presence of carboxyl groups. Upon mixing, the ionised carboxyl group of CMC and the positively charged amine ($-NH_2^+$) will lead to the formation of complexes due to charge interaction between the polymers which according to Wu et al. (2020) may lead to the inhibition of the swelling of the fibrous collagen structure, as a consequence, the elastic and loss modulus of the pastes decreases. The attractive electrostatic interaction between collagen and CMC molecules counteracts the swelling of collagen and leads to the formation of large visible collagen fibre aggregates (Figure 3-4B), consequently resulting in a non-homogeneous and loose structure.



(C)

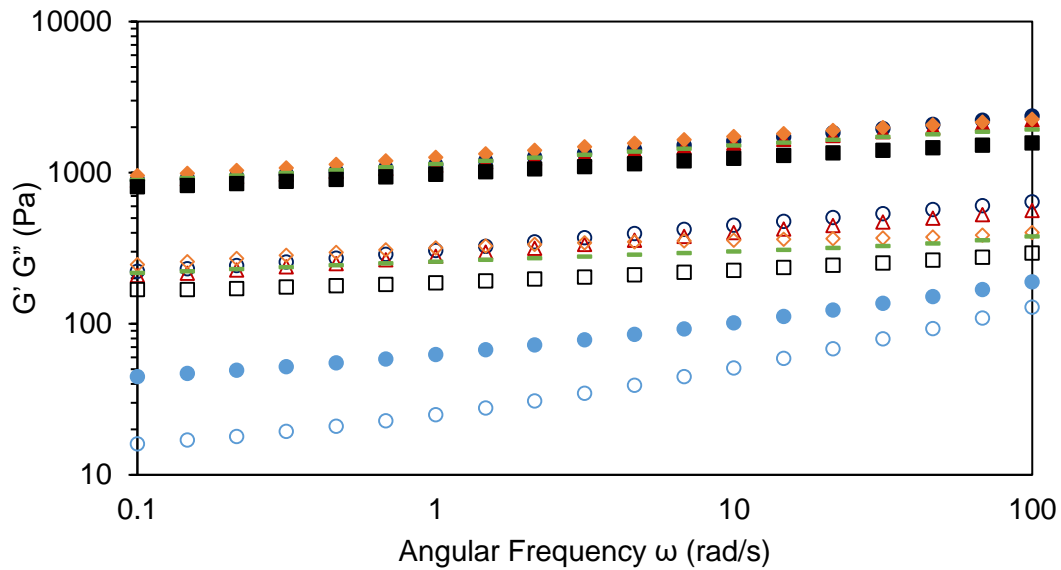


Figure 3-2: Storage modulus G' (closed symbol) and Loss modulus G'' (open symbol) as a function of angular frequency for COLLMC (\blacktriangle), COLLHPMC (\bullet), COLLGH (\blacksquare), COLLGM (\blacklozenge), COLLCMC (\bullet) and COLLAGEN (\blacksquare) pastes at (A) 4% (B) 3.5% (C) 2.5% collagen concentrations, 0.1 % strain at 20 °C.

Focusing further upon the loss factor ($\tan \delta$) used to show the differences in the viscoelastic behaviour of the pastes. A $\tan \delta$ value of less than one shows an elasticity-dominated behaviour, however, the higher value above 1 indicates more viscous properties (Mezger, 2006). Figure 3-3 shows that the $\tan \delta$ values of all the pastes were less than 1, with the $\tan \delta$ values of pure collagen pastes at the various collagen concentrations coincident with only a slight decrease seen for the lower concentration showing slight frequency dependence. This is indicative of a weak gel rather than a 'true' molecular three dimensions aggregated gel. The addition of the hydrocolloids increased the $\tan \delta$ values of the collagen pastes at all the levels of collagen investigated. Among the hydrocolloids studied, COLLCMC pastes has the highest $\tan \delta$ values, thought to be due to electrostatic interaction between collagen and CMC molecules which results in the de-swelling of reverse the swollen collagen fibrils.

The $\tan \delta$ of COLLMC, COLLHPMC, COLLGM and COLLGH is similar at low angular frequencies and higher than collagen paste alone. COLLMC and COLLHPMC show higher $\tan \delta$ values than COLLGM and COLLGH pastes as the angular frequency is increased, indicating a transition to a more fluid-like paste, and the values are similar irrespective of final collagen concentration. Overall, collagen pastes with the hydrocolloids show an increase in $\tan \delta$ values than the controls, indicating that the blend paste's overall structure became less elastic. However, it is interesting to note that these results cast a little more light on the impact of hydrocolloid molecular structure. At the higher collagen concentration (4%w/w), the differences between the hydrocolloids are more discerning, where the higher molecular weight guar reflects the $\tan \delta$ of collagen alone at lower frequencies, and there is a clear difference between the two guar, which in turn are quite different from the two derivatised celluloses. As collagen concentration decreases, the guar become more similar, and at 2.5%w/w collagen, all four hydrocolloids are similar up to higher frequencies (about 1 rad/s). Therefore, the higher the added hydrocolloid's molecular weight, the less fluid-like the composite paste becomes, particularly at higher frequencies. Whereas at lower frequencies, the hydrocolloids allow a network weakening and the hydrocolloid molecules themselves have sufficient time to rearrange regardless of molecular size or stiffness. Overall, the observed differences in moduli, and particularly in $\tan \delta$ between cellulose derivatives and guar are marginal, but they show a difference in the way that they influence on the sol fraction, which may stem on their molecular weight and overall degree of space occupancy.

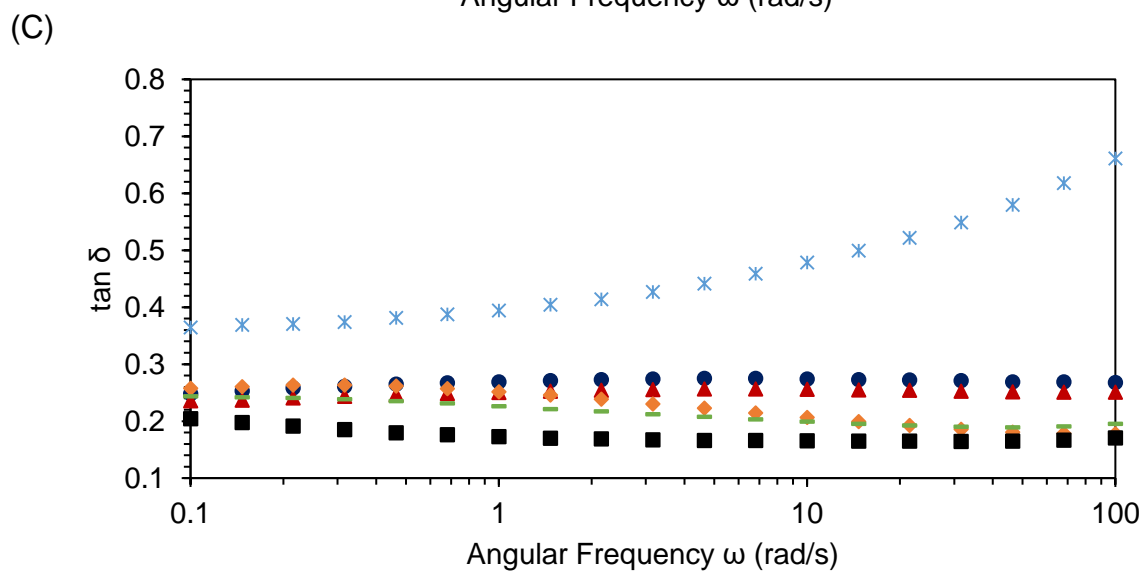
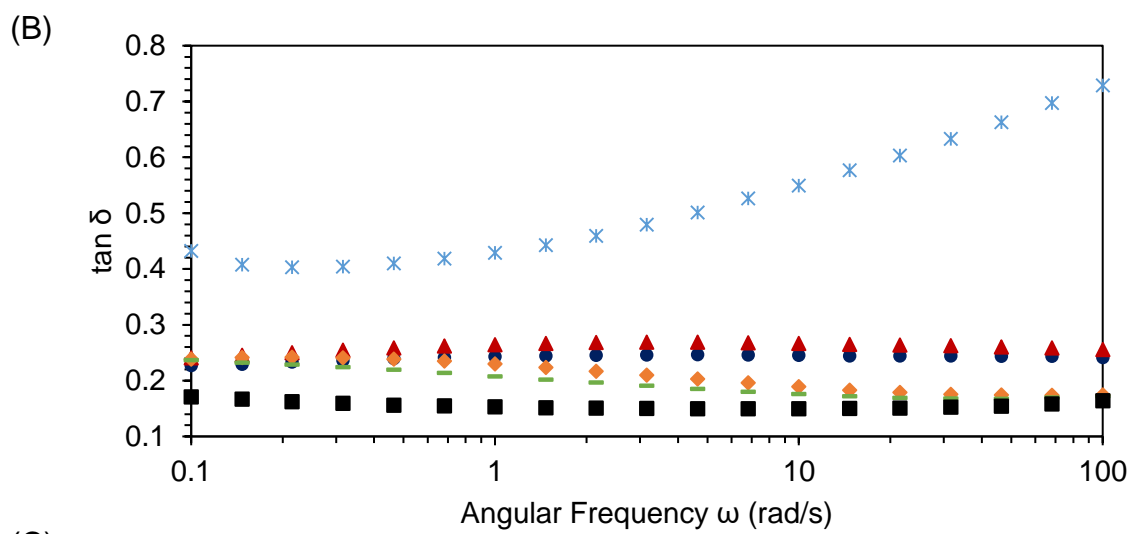
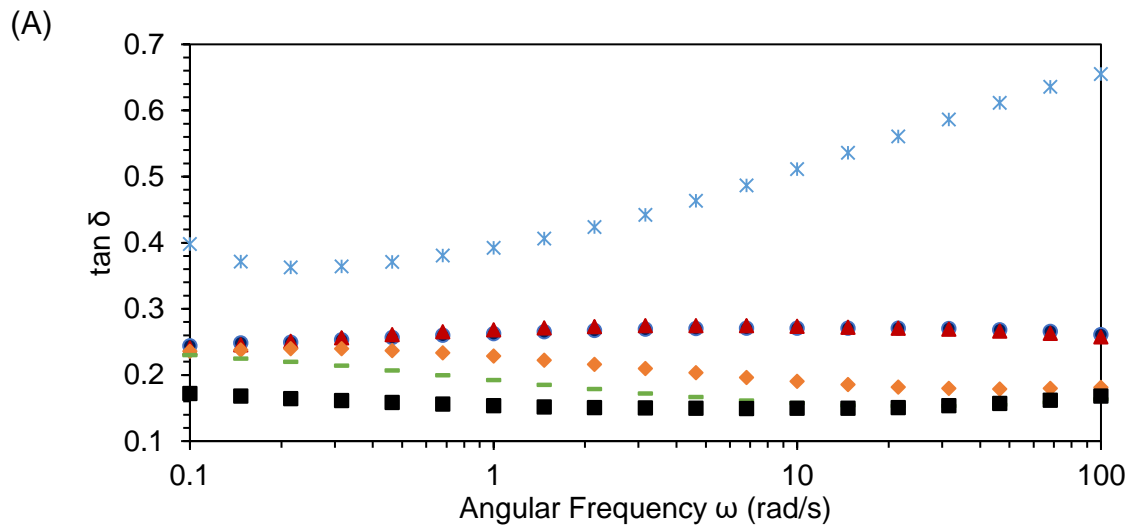


Figure 3-3: Loss factor ($\tan \delta$) as a function of angular frequency COLLMC (\blacktriangle), COLLHPMC (\bullet), COLLGH (—), COLLGM (\blacklozenge), COLLCMC ($*$) and COLLAGEN (\blacksquare)

pastes at (A) 4% (B) 3.5% (C) 2.5% collagen concentrations, angular frequency of 10 rad s⁻¹ , 0.1 % strain at 20 °C °C.

To gain insight into the structural organisation of the pastes upon the addition of hydrocolloids, the microstructures were examined using phase-contrast light microscopy. Figure 3-4 shows the micrographs of the pastes at 4% collagen concentrations obtained at a magnification of x10. Collagen paste is composed of highly entangled long fibres, responsible for the paste's high elastic properties (Figure 3-4A). The addition of CMC results in changes in the microstructure and shows large fibrous structures, which may be attributed to the CMC acting as tethers/bridges to promote aggregation (Oechsle et al., 2017). Conversely, collagen pastes with non-charged hydrocolloids (COLLMC, COLLHPMC, COLLGM, COLLGH), while difficult to see clearly, shows less of a 'bundled' structure of collagen fibrils and a more homogenous blend.

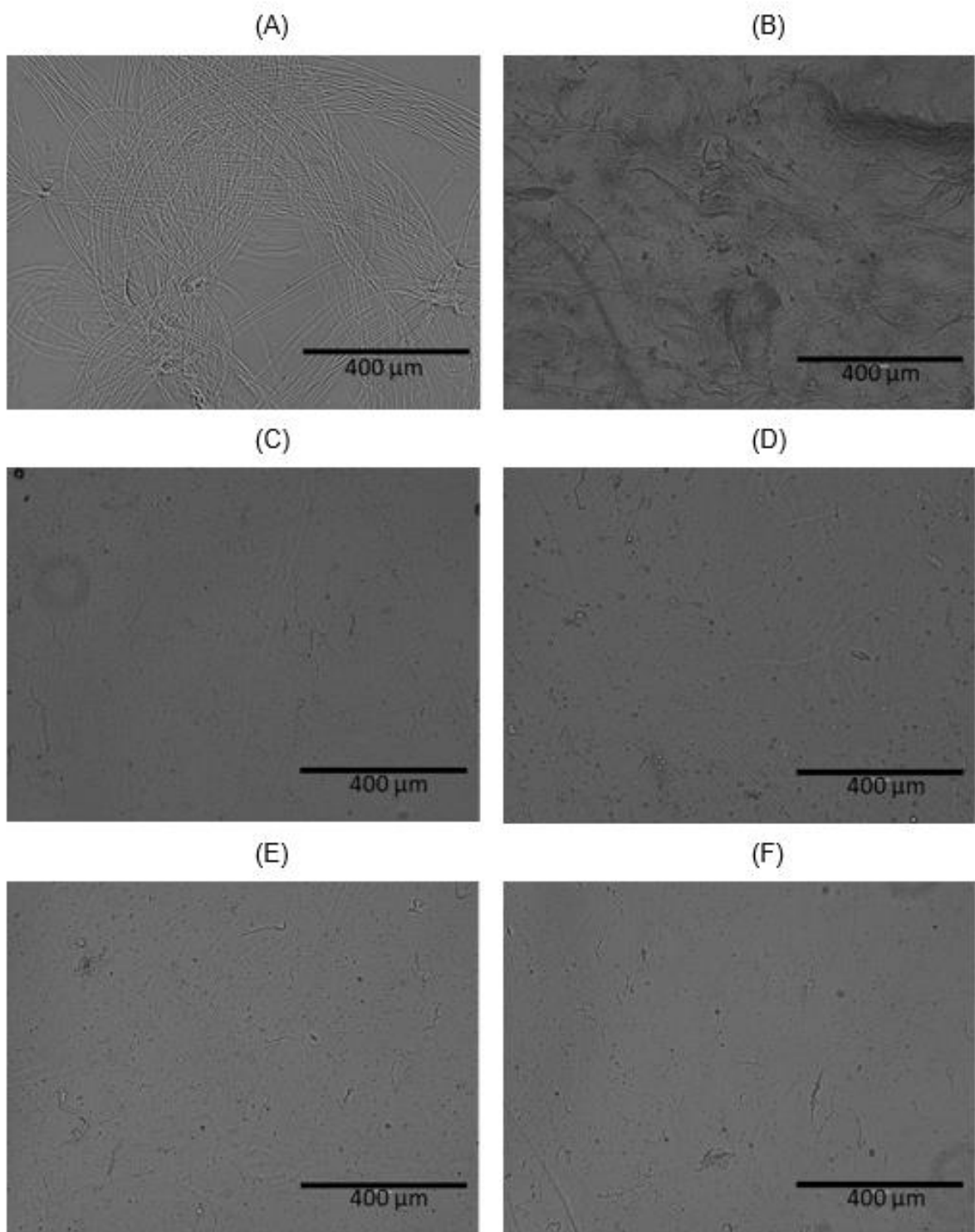


Figure 3-4: Phase- contrast light micrographs of collagen with hydrocolloid pastes (A) COLLG (B) COLLCMC (C) COLLGH (D) COLLGM (E) COLLHPMC (F) COLLMC at 4% collagen concentration X10.

3.4.3 Dynamic Temperature sweep

The temperature-dependent storage modulus G' and $\tan \delta$ for collagen paste with and without hydrocolloids at different collagen concentrations are displayed in Figure 3-5 and Figure 3-6, respectively. Concurrent with what was shown in Figure 3-2, the G' of COLLMC, COLLHPMC, COLLGM, and COLLGH are higher than for pure collagen pastes at the various collagen concentration investigated. Irrespective of the collagen concentration, the G' of COLLMC, COLLHPMC, COLLGM, COLLGH and pure collagen pastes show a plateau within the temperature range of 10 °C – 34 °C. In contrast, COLLMC shows a plateau up to a higher temperature of about 40 °C. A corresponding $\tan \delta$ plateau is observed for the pastes at similar temperatures, which suggests that the pastes' structure remains intact.

Upon further temperature increase, G' decreases with a corresponding increase in $\tan \delta$ at about 34 °C for COLLHPMC, COLLMC, COLLGH, COLLGM and pure collagen pastes. This temperature is consistent with the study of Xu et al. (2020a), where it was reported that the storage modulus of collagen fibre dispersions started to decrease at 33 °C. Whereas the decrease in G' and the corresponding increase in $\tan \delta$ occurred at a higher temperature of about 40 °C for COLLMC pastes, suggesting an increase in the thermal stability of the collagen within the pastes. Therefore, the electrostatic interaction between collagen and CMC, which led to the aggregation of collagen fibres, also leads to increased thermal stability. The decrease in G' and the corresponding increase in $\tan \delta$ indicates a softening of the paste structure, caused by the denaturation of the collagen triple helical structure, more specifically the disruption of the hydrogen bonds stabilising the collagen structure (Wright and Humphrey, 2002). The onset temperature of the decrease in G' for all the pastes is consistent with the DSC data onset temperature (Table 3-5).

With further increase in temperature, difference in G' response is due to the properties of the individual hydrocolloid present in the collagen paste. For collagen with guar gum (COLLGM and COLLGH), the G' values decreased continuously, indicating that the paste became highly viscous due to the molecules becoming mobile due to the melting of collagen molecules. In contrast, G' values increased for COLLHPMC and COLLMC; this is attributed to the thermal gelation of the cellulose ethers occurring at lower temperatures as the derivatised moiety becomes more hydrophobic (Sarkar, 1979; Haque et al., 1993a; Li et al., 2003; Sullo et al., 2013). A similar increase in G' was reported for starch dispersions mixed with MC and HPMC (Sullo and Foster, 2010). Interestingly, the initial decrease in G' (attributed to the denaturation of the collagen helices) is hydrocolloid type-dependent, with the guar gum being different to the celluloses at a collagen concentration of 4%w/w. In contrast, they converge in effect at the lower collagen concentrations. There appears to be a 'shallower' decrease in G' , thought to be due to the more homogeneous composite structure implied in Figure 3-5.

In the case of COLLMC pastes, the decrease in G' upon denaturation of collagen is lower, and a slight increase in G' was observed at about 53 °C, followed by a plateauing with increasing temperature. This might suggest that the electrostatic tethering between collagen and CMC molecules responsible for the increase in thermal stability of collagen is retained at higher temperatures, which led to the retention of a network with increased elasticity.

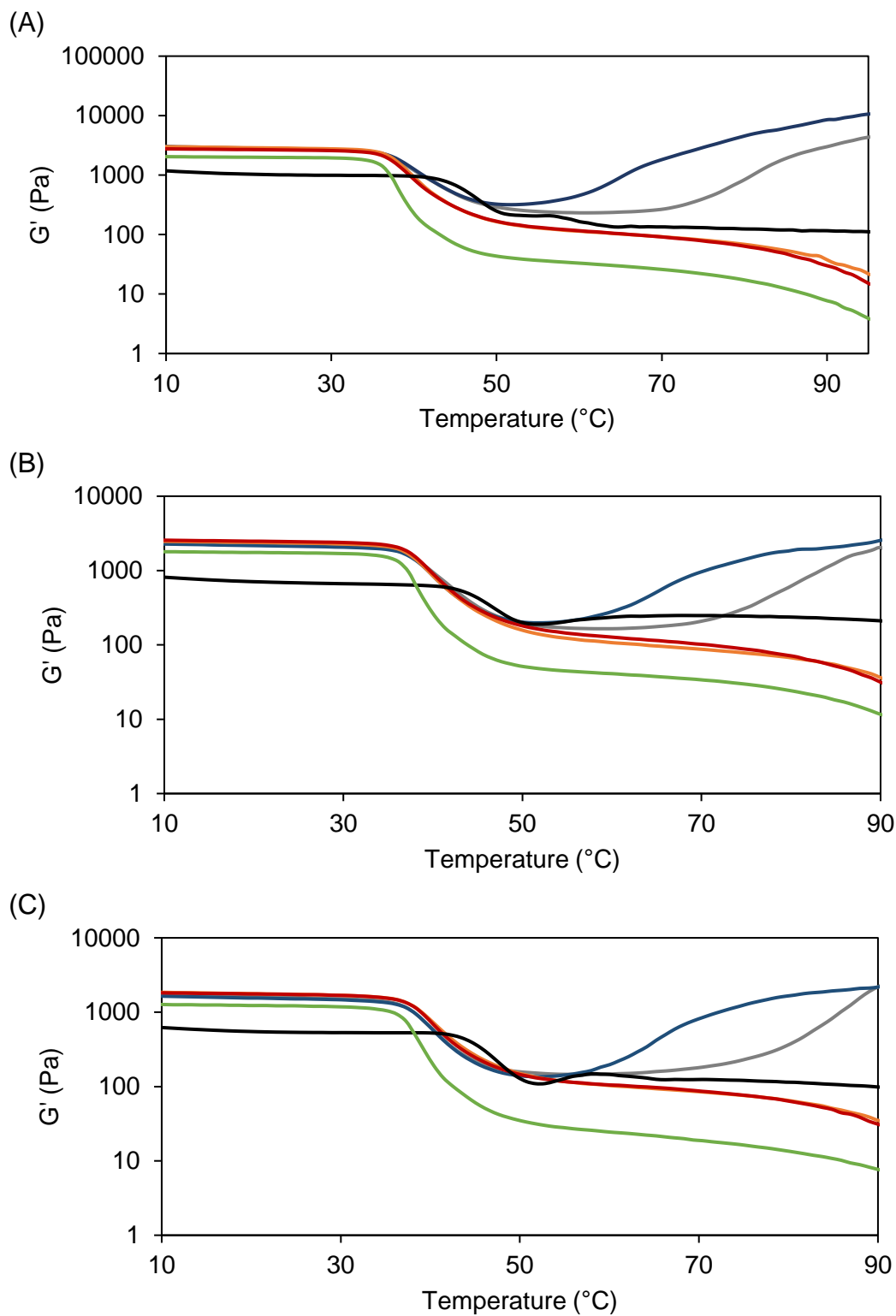


Figure 3-5: Temperature dependence of the storage modulus (G') during heating for COLLMC (blue line), COLLHPMC (grey line), COLLGH (red line), COLLGM (orange line), COLLCCMC (black line) and COLLAGEN (green line) pastes at (A) 4% (B) 3.5% (C) 2.5% collagen concentrations, angular frequency of 10 rad s⁻¹ and 0.1 % strain.

The $\tan \delta$ values of all the samples at 10 °C - 90 °C (Figure 3-6), including collagen alone, were less than 1, indicating that not all collagen fibres melted within the range of temperature investigated. At lower temperatures (10 – 34 °C), the $\tan \delta$ value of COLLMC and COLLHPMC were higher than COLLGM and COLLGH, as shown at the frequency of 10 rads^{-1} , suggesting that collagen with MC/HPMC has higher viscous components than those of collagen with guar gums and pure collagen pastes (3.5 % and 2.5 % wt/wt). For COLLCMC, higher values were observed between temperature ranges of 10 – 42 °C, indicating that the pastes were more viscous than other pastes.

On further increase in temperature, pure collagen shows a peak in $\tan \delta$ at about 40 °C, ascribed to a loosening of the bundle structure upon the onset of collagen denaturation. The $\tan \delta$ curve of pure collagen paste is similar to those reported by Zheng et al. (2021) for pure collagen solution. However, with a subsequent increase in hydrodynamic volume and the strain used in the experiment being low enough, $\tan \delta$ then decreases until a progressive increase is seen at a higher temperature. Such a peak in $\tan \delta$ is not seen for COLLMC, COLLHPMC, COLLGM, and COLLGH thought to due to the more homogeneous structure of these composites, discussed earlier. For collagen with guar gum pastes (COLLGH and COLLGM), the $\tan \delta$ values increased with increasing temperatures and the values were higher than pure collagen pastes. This might be attributed to the guar dominating the thermodynamics and properties of the overall system. Similarly, for COLLMC and COLLHPMC, the drop in the $\tan \delta$ concurrent with the thermal gelation of the MC and HPMC chains and indicative of a homogeneous blend of collagen fibrils and hydrocolloids, where upon the denaturation of collagen structural collapse is not seen and the gelation of derivatised celluloses can take over and create a three-dimensional gel network. Moreover, the $\tan \delta$ values of COLLMC were higher than COLLHPMC due to its high

methyl substituents (Sarkar, 1995). For COLLCMC, a peak in the $\tan \delta$ values is again seen at about 49 °C. It then plateaus with increasing temperature below that of collagen alone, which again suggests the retention of an electrostatic network.

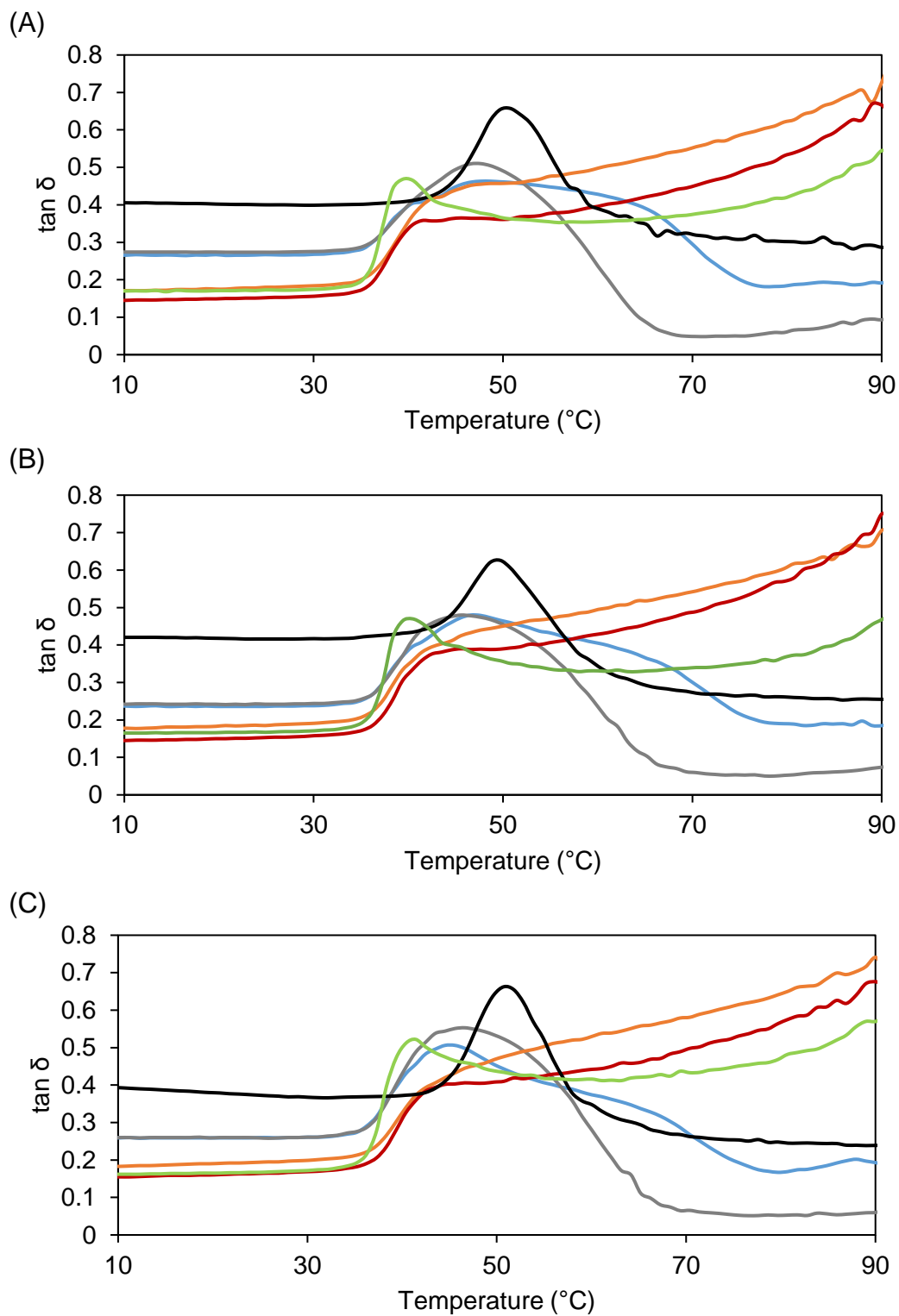


Figure 3-6: Loss factor ($\tan \delta$) as a function of temperature for COLLMC (blue line), COLLHPMC (grey line), COLLGH (red line), COLLGM (orange line), COLLCMC (black

line) and COLLAGEN (green line) pastes at (A) 4% (B) 3.5% (C) 2.5% collagen concentrations, angular frequency of 10 rad s⁻¹ and 0.1 % strain.

3.4.4 Thermal properties

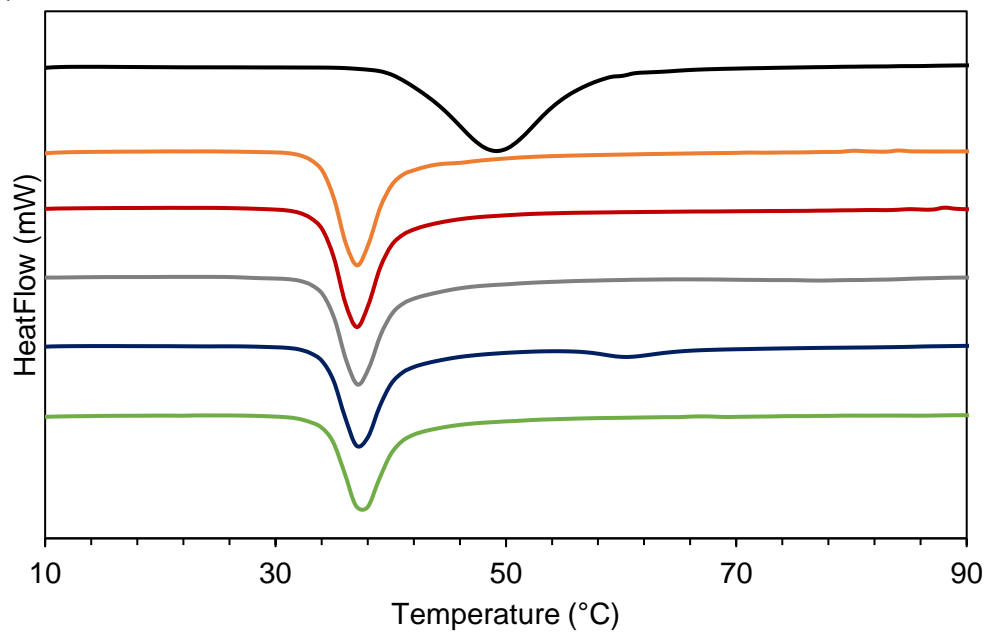
The DSC thermograms obtained for collagen pastes with and without hydrocolloids are shown in Figure 3-7. Their onset (T_o), peak (T_{peak}), endset (T_e) transition temperatures and enthalpies (ΔH) parameters at different levels of collagen are presented in Table 3-5. All the pastes show a single endothermic peak associated with the denaturation (helix-coil) transition temperature of collagen, which involves the disruption of the hydrogen bonds between the three polypeptide chains of collagen molecules the unfolding of the separated helices into random coils (Li et al., 2008). COLLMC pastes show two peaks where the second is associated with the thermal gelation of MC (the enthalpy of HPMC (K4M), which is known to be four times lower than MC and is thought to be lost in the baseline of these experiments) (Haque and Morris, 1993).

As seen in Table 3-5, the peak temperature (T_{peak}) for pure collagen pastes at 4%, 3.5% and 2.5% wt/wt collagen concentrations were observed at 37.4 °C, 37.4 °C and 37.9 °C, respectively. Nicoletti and Telis (2009) reported similar denaturation temperature for collagen powder extracted from bovine hides. For COLLHPMC, COLLMC, COLLGH and COLLGM, the denaturation temperatures (T_{peak}) values were in the range of 37.1 – 37.9 °C. Whereas the addition of CMC shifted the T_{peak} values to higher temperatures of about 49.2 - 50.4 °C. As stated earlier, the attractive electrostatic interaction between the cationic collagen and anionic CMC molecules resulted in the de-swelling of the collagen paste. Consequently, strongly associated

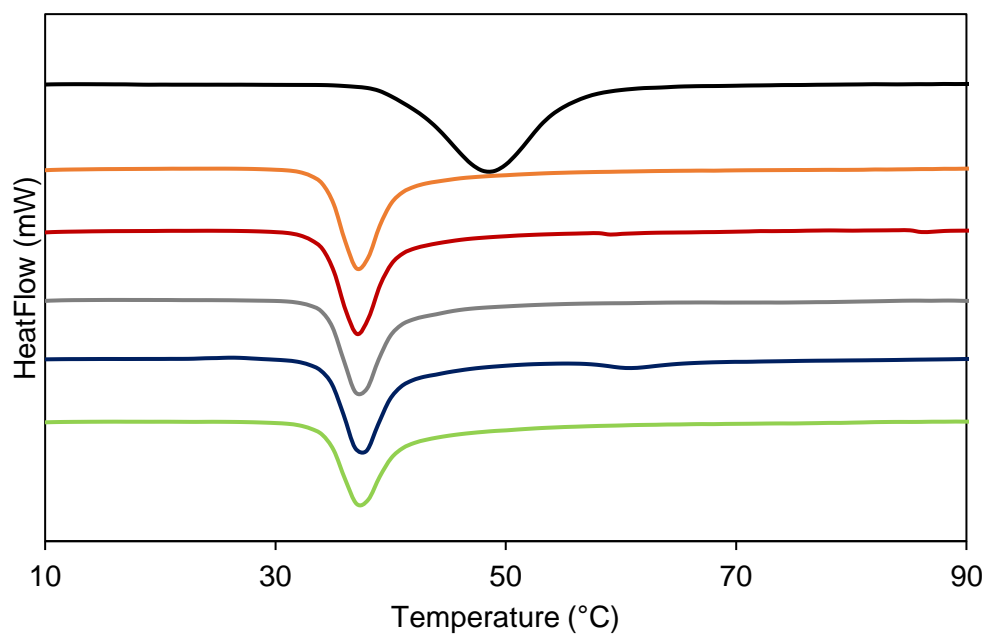
collagen fibrous structures that are more thermally stable were formed (Gioffrè et al., 2012).

With respect to the denaturation enthalpies (ΔH), which is the energy required for the breaking of the hydrogen bonds stabilising the collagen triple helices (Bigi et al., 2004; Ding et al., 2014b). The enthalpies of transition for the COLLMC, COLLHPMC, COLLGM and COLLGH are similar to those of the pure collagen pastes at all the levels of collagen studied (Table 3-5). This suggests that the hydrocolloids did not affect collagen helical content, which inferred that the same amount of energy is required to melt the collagen helices present in the blend pastes. It should be noted that there is an inconsistency in the enthalpy values recorded for the composites containing MC, where at the higher collagen concentration, a significant decrease is seen (not for the two lower collagen concentrations). This may be an anomaly, however, it could pose the question as to whether hydrophobic molecules could alter the properties of an acid swollen collagen paste. COLLMC pastes had higher enthalpies values than pure collagen pastes, indicating that higher energy is required to disrupt the hydrogen bonds. This is possibly due to the increased aggregation of the collagen fibres induced by the electrostatic cross-linking of collagen and CMC.

(A)



(B)



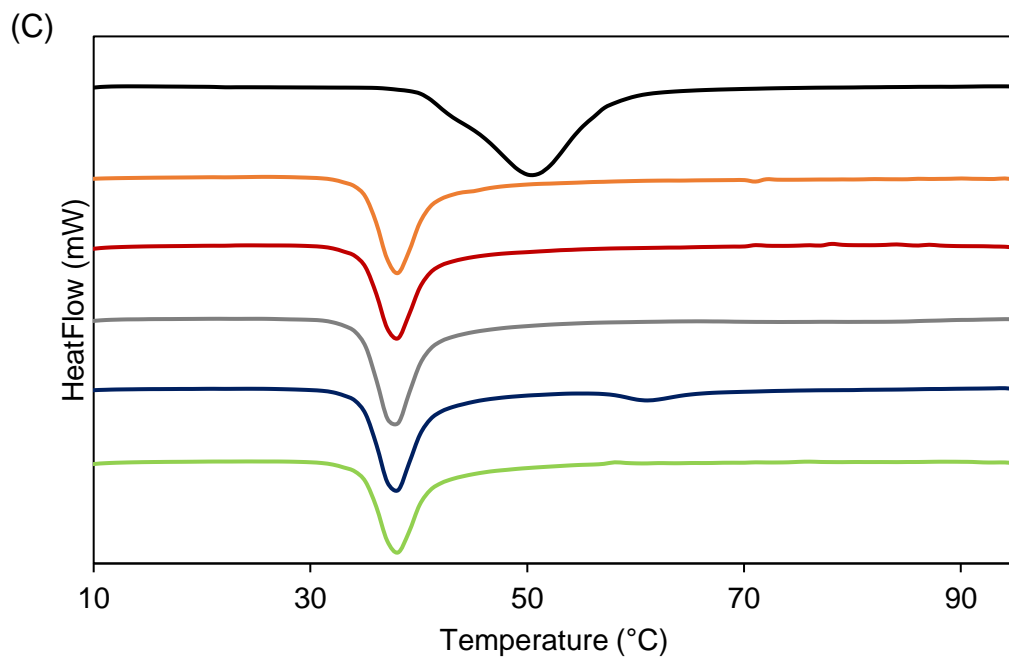


Figure 3-7: DSC thermograms (first heating) for COLLMC (blue line), COLLHPMC (grey line), COLLGH (red line), COLLGM (orange line), COLLCMC (black line) and COLLAGEN (green line) pastes at (A) 4% (B) 3.5% (C) 2.5% collagen concentrations.

Table 3-5: DSC parameters after first heating of collagen with and without hydrocolloids pastes at different collagen paste concentrations and mixing ratios. T_{peak} = peak temperature; T_o = Onset temperature; T_e = endset temperature and ΔH = enthalpy.

Samples	T_{onset} (°C)	T_{peak} (°C)	T_{offset} (°C)	ΔH (J/g)
4% COLLAGEN	34.36 ± 0.14^a	37.38 ± 0.17^a	40.94 ± 0.13^b	2.17 ± 0.09^b
COLL CMC	41.22 ± 0.26^b	49.20 ± 0.11^b	56.98 ± 0.05^b	3.11 ± 0.23^c
COLL GM	34.09 ± 0.02^a	37.08 ± 0.04^a	40.50 ± 0.09^a	2.18 ± 0.02^b
COLL GH	34.08 ± 0.02^a	37.06 ± 0.07^a	40.52 ± 0.08^a	2.24 ± 0.07^b
COLL HPMC	34.22 ± 0.01^a	37.20 ± 0.00^a	40.77 ± 0.05^{ab}	2.11 ± 0.02^{ab}
COLL MC	34.33 ± 0.07^a	37.29 ± 0.09^a	40.79 ± 0.10^{ab}	1.73 ± 0.04^a
3.5% COLLAGEN	34.30 ± 0.10^{ab}	37.40 ± 0.06^a	41.22 ± 0.08^c	1.92 ± 0.16^a
COLL CMC	41.99 ± 0.23^d	49.72 ± 0.06^b	56.81 ± 0.01^d	3.09 ± 0.04^b
COLL GM	34.25 ± 0.07^{ab}	37.27 ± 0.02^a	40.74 ± 0.02^{ab}	1.93 ± 0.04^a
COLL GH	34.07 ± 0.08^a	37.18 ± 0.02^a	40.62 ± 0.08^a	1.97 ± 0.07^a
COLL HPMC	34.36 ± 0.18^{bc}	37.35 ± 0.00^a	40.84 ± 0.03^{ab}	1.81 ± 0.09^a
COLL MC	34.45 ± 0.06^c	37.47 ± 0.00^a	41.03 ± 0.16^{bc}	1.74 ± 0.19^a
2.5% COLLAGEN	34.84 ± 0.08^a	37.89 ± 0.04^a	41.42 ± 0.08^a	1.29 ± 0.08^a
COLL CMC	41.64 ± 0.39^b	50.41 ± 0.06^b	57.64 ± 0.95^b	2.40 ± 0.52^b
COLL GM	34.90 ± 0.02^a	37.92 ± 0.04^a	41.43 ± 0.14^a	1.35 ± 0.00^a
COLL GH	34.74 ± 0.03^a	37.84 ± 0.02^a	41.30 ± 0.07^a	1.33 ± 0.09^a
COLL HPMC	34.65 ± 0.02^a	37.71 ± 0.00^a	40.84 ± 0.03^a	1.48 ± 0.04^a
COLL MC	34.75 ± 0.02^a	37.62 ± 0.26^a	41.26 ± 0.20^a	1.30 ± 0.04^a

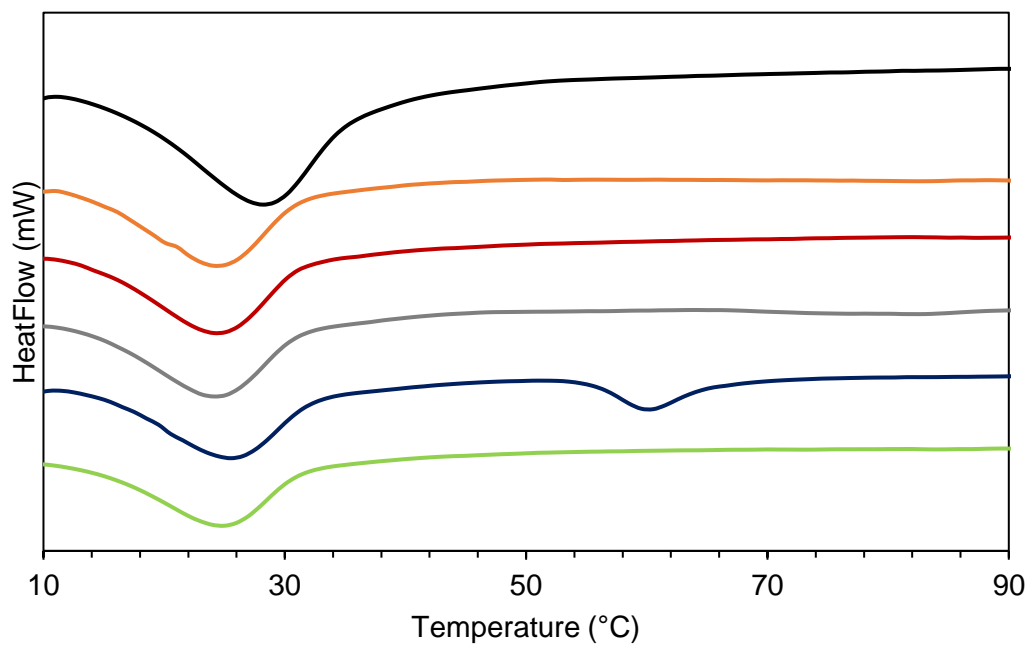
^{a-c}Mean \pm standard deviation. Means in the same column with different superscript letter are significantly different ($P < 0.05$).

Once the initial heating scan was completed, the samples were cooled and rescanned. As seen in Figure 3-8, the thermograms of the second heating cycle show that the endotherm peak occurred at lower temperatures than the original transition ascribed

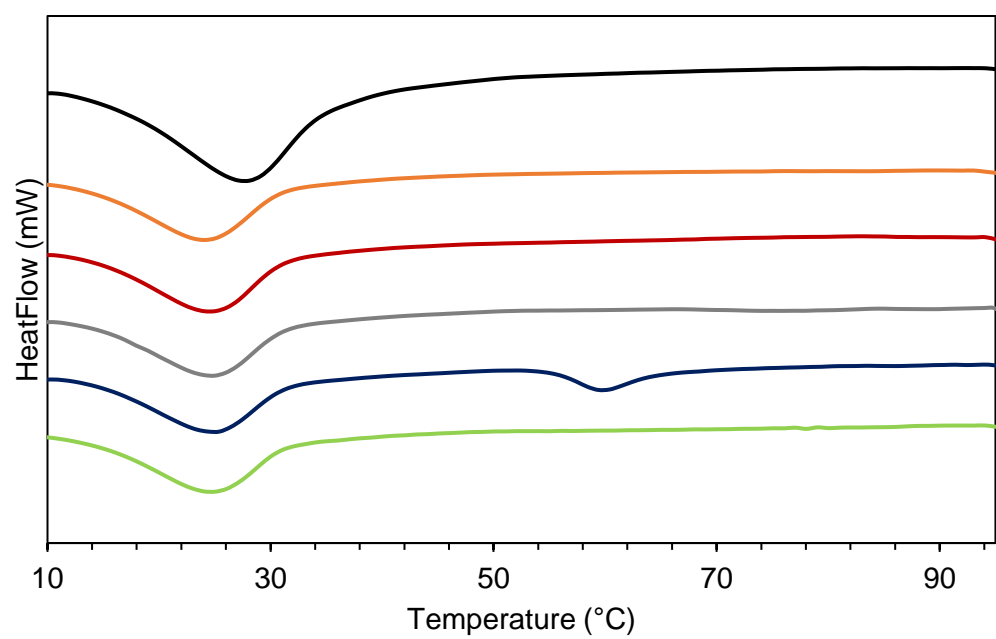
to the melting of renatured gelatin-like structures obtained from the denaturation of collagen helices (Badea et al., 2012). Also, the enthalpy of transition reduced when the pastes were subjected to reheating, which indicated less energy was required to melt the helices. Michon et al. (1997) reported that the thermal stability and energy needed for the melting of gelatin gels are related to the helices' length. Lower melting temperature reflects a smaller number of helical structures and a lower enthalpy value (Gilsenan and Ross-Murphy, 2000). Based on this, the lower melting temperature and enthalpies observed on reheating of the pastes suggests a less ordered structure and a reduced helix length. Also, the lower molecular weight of gelatin might account for the reduced melting temperature and enthalpies. Gilsenan and Ross-Murphy (2000) reported that low molecular weight gels melt at a lower temperature than high molecular weight gels. Hence, the lower temperature values observed on reheating are ascribed to the lower molecular weight of gelatin compared to collagen.

The melting temperatures and enthalpies values of the blend pastes were not different from those of the pure collagen pastes at the various collagen levels (Table 3-6). This indicates that the presence of the polysaccharides did not affect the thermal stability and energy of the melting of the renatured pastes. The decrease in enthalpy for COLLMC composites is not seen in any of the collagen concentrations for renatured pastes, indicating that no hydrophobic interaction is possible during renaturation, as at such temperatures, the MC would still be in its own hydrophobically driven gel structure. In contrast, CMC increases the melting temperature and enthalpy values of collagen pastes, which might indicate higher thermal stability of the renatured pastes in the presence of CMC.

(A)



(B)



(C)

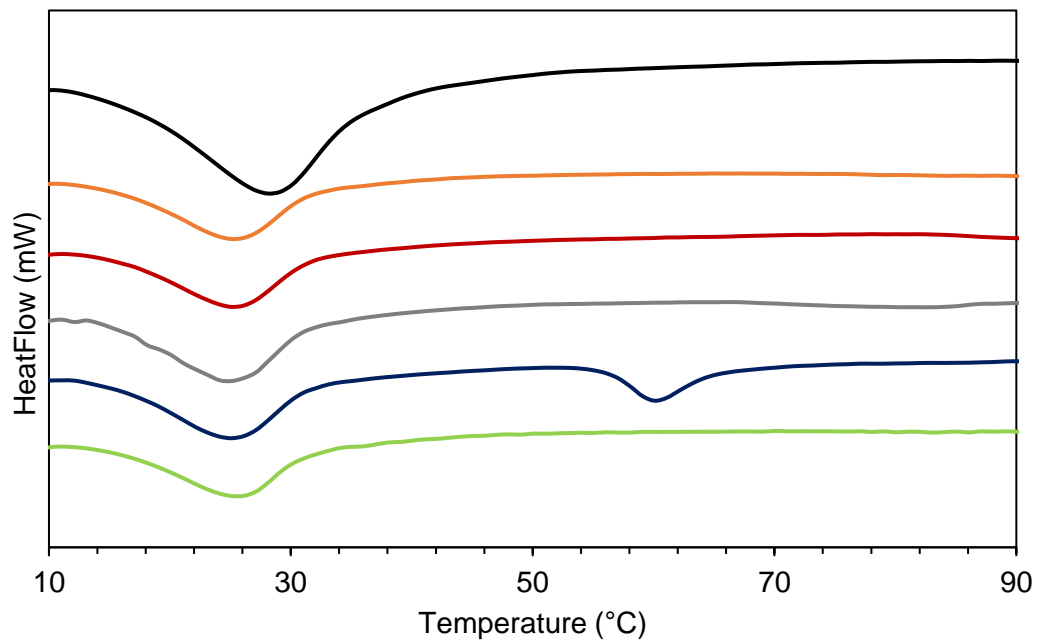


Figure 3-8: DSC thermograms (second heating) for COLLMC (blue line), COLLHPMC (grey line), COLLGH (red line), COLLGM (orange line), COLLCMC (black line) and COLLAGEN (green line) pastes at (A) 4% (B) 3.5% (C) 2.5% collagen concentrations.

Table 3-6: DSC parameters after second heating of collagen with and without hydrocolloids pastes at different collagen paste concentrations and mixing ratios. T_P = peak temperature; T_o = Onset temperature; T_e = endset temperature and ΔH = enthalpy.

Samples	T_{onset} (°C)	T_{peak} (°C)	T_{offset} (°C)	ΔH (J/g)
4% COLLAGEN	14.49 ± 0.42^a	24.72 ± 0.11^a	32.05 ± 0.01^a	0.80 ± 0.80^a
COLL CMC	15.47 ± 0.35^a	27.31 ± 0.04^b	35.7 ± 0.00^b	1.52 ± 0.10^b
COLL GM	13.29 ± 1.19^a	24.48 ± 0.02^a	31.88 ± 0.14^a	0.88 ± 0.02^a
COLL GH	15.37 ± 2.08^a	24.59 ± 0.11^a	31.81 ± 0.03^a	0.88 ± 0.03^a
COLL HPMC	15.24 ± 1.68^a	24.43 ± 0.13^a	31.92 ± 0.05^a	0.86 ± 0.03^a
COLL MC	17.74 ± 0.70^a	24.85 ± 0.48^a	31.94 ± 0.03^a	0.84 ± 0.04^a
3.5% COLLAGEN	14.24 ± 0.47^a	24.70 ± 0.2^a	32.14 ± 0.28^a	0.80 ± 0.05^a
COLL CMC	15.62 ± 0.11^a	27.28 ± 0.09^b	36.25 ± 0.10^a	1.50 ± 0.04^b
COLL GM	14.37 ± 0.18^a	$24.64 \pm .004^a$	31.91 ± 0.12^a	0.78 ± 0.00^a
COLL GH	14.43 ± 0.51^a	24.64 ± 0.08^a	31.83 ± 0.06^a	0.81 ± 0.06^a
COLL HPMC	15.40 ± 0.09^a	24.63 ± 0.02^a	31.96 ± 0.03^a	0.76 ± 0.00^a
COLL MC	15.37 ± 1.12^a	24.77 ± 0.15^a	32.05 ± 0.08^a	0.73 ± 0.04^a
2.5% COLLAGEN	16.12 ± 0.33^a	25.62 ± 0.19^b	31.88 ± 0.27^a	$0.43 \pm .001^a$
COLL CMC	16.45 ± 0.05^a	28.43 ± 0.00^c	37.00 ± 0.25^b	1.11 ± 0.22^b
COLL GM	16.05 ± 0.19^a	25.35 ± 0.11^{ab}	32.39 ± 0.20^a	0.45 ± 0.02^a
COLL GH	15.84 ± 0.03^a	25.35 ± 0.10^{ab}	32.27 ± 0.28^a	0.45 ± 0.00^a
COLL HPMC	17.24 ± 0.12^b	25.02 ± 0.09^a	32.07 ± 0.07^a	0.54 ± 0.01^a
COLL MC	16.80 ± 0.49^{ab}	25.11 ± 0.19^b	32.22 ± 0.00^a	0.50 ± 0.04^a

^{a-c}Mean \pm standard deviation. Means in the same column with different superscript letter are significantly different ($P < 0.05$).

3.5 Conclusions

Using water-soluble hydrocolloids at comparable low-shear viscosity and, therefore, a similar viscosifying effect, we explore the effect of hydrocolloids on the viscoelastic properties of collagen pastes and the effect of hydrocolloids on the dependency of the viscoelastic behaviour on temperature. Of the five hydrocolloid tested, it was found that CMC forms a complex with collagen, leading to a decrease in the viscoelasticity of the pastes, making them more viscous and heterogeneous (partial phase separation). The interaction between collagen and CMC may be further probed by the DSC, which results in the shift of the collagen melting peak to higher temperatures and energy needed for melting. Based on this finding, it would be interesting to study the effect of negatively charged water-soluble polymers such as pectin, xanthan and the sulphated lambda carrageenan on collagen paste properties.

The remaining four uncharged hydrocolloids may be considered an initial approximation of inert fillers that provide an appropriate matrix for collagen fibres. The hypothesis that the viscoelasticity of the collagen paste is a function of the shear thinning behaviour of filler hydrocolloids has been tested. The addition of hydrocolloids increases G' and G'' relative to pure collagen, which is consistent with the fact that composites have a more viscous matrix than water. For the derivatised celluloses, a very weak difference in the tan delta as a function of frequency is observed, while for guar gums show marked changes in tan delta behaviour as a function of oscillatory frequency was observed. At high frequencies, guar-based composites have the loss tangent similar to that of pure collagen, indicating that at higher frequencies the shear thinning behaviour begins to dominate the viscoelastic response. The dependency of G' on temperature shows that hydrocolloids can increase the collagen pastes' G' . For

derivatised cellulose, the effect of upper-point gelation was observed, whereby at the low temperature, the response is dominated by a collagen fibrillary network and at the higher temperatures, the effect of gelation of methyl and HPMC cellulose is observed. The effect of derivatised cellulose can also be seen on the DSC profiles, where a shallow peak associated with MC gelation can be observed. For HPMC, the heat flow peak was comparable with noise, but it would be expected to be similar to that observed in the MC-based composite.

Also, there is a slight indication that hydrophobic MC affects collagen pastes thermal properties, but it is not conclusive. Thus, based on this study's findings, uncharged polymers induce a homogeneous distribution of collagen fibrils in the mixed paste, and the properties of the added polymers determine the high frequency/flow characteristics. Negatively charged CMC induces a heterogeneous, collapsed collagen fibrillar microstructure, in which the fibrils are stabilised to high temperatures, requiring more energy to melt the fibrillar structure. Given these findings, it would be interesting to study positively charged polymers such as chitosan. The effect of polymers on collagen film properties will be reported in future chapters. To conclude, these findings suggest that different hydrocolloids induce different rheology responses within collagen pastes, which might be necessary for choosing hydrocolloids needed to modify collagen paste for industrial uses.

4 CHARACTERISATION OF MIXED COLLAGEN- HYDROCOLLOID COMPOSITE FILMS

4.1 Abstract

Collagen edible films are used for the manufacturing of meat products, such as sausages. However, there are opportunities to change the tensile strength and thermal properties of such films by adding hydrocolloids to acid-swollen collagen pastes pre-film formation. Herein, this study investigated the effects of Hydroxypropylmethylcellulose (HPMC), Methylcellulose (MC), high and medium molecular weight guar gum (GH and GM) (added at comparable viscosifying effect) on the following properties: mechanical - tensile strength (TS), elongation at break (EAB) and Young's Modulus (YM); thermal, structural and sorption of collagen films prepared from acid-swollen collagen paste. Mechanical properties show that the tensile strength, Young's Modulus, and elongation at break of the films increased with the addition of the hydrocolloids and increased collagen content in the starting pastes. This is important as the films (casings) must be sufficient to prevent breakage during processing. Films containing derivatised cellulose had higher tensile strength and stiffness than films with guar gums. Differential Scanning Calorimetry (DSC) showed a slight increase in the melting temperatures and decreased enthalpy values with the hydrocolloid's addition. X-ray diffraction results confirmed that the addition of the hydrocolloids decreased the crystalline ordered structure of the collagen in the films. Fourier transform infrared spectroscopy (FTIR) revealed a degree of interaction between the hydrocolloids and collagen. Thermogravimetric analysis showed that the hydrocolloids did not affect the degradation temperature of collagen films. Furthermore, the water sorption analysis revealed that the hydrocolloid addition decreased the water uptake of the composite films compared to pure collagen films. This study demonstrates that hydrocolloids can potentially improve collagen films (casings) for commercial applications.

4.2 Introduction

The growing concerns of environmental and safety issues related to synthetic films have led researchers to explore environmentally friendly options for making edible films (Ghanbarzadeh et al., 2010). Hydrocolloids, including proteins and polysaccharides, are now considered viable substitutes for synthetic polymers because they are renewable, biodegradable, low-cost, and plentiful (Wolf et al., 2009; Krystyjan et al., 2015; Esteghlal et al., 2018). One of the natural polymers used in making edible films, especially for sausage casings, is collagen. Collagen is the most abundant structural fibrous protein in mammalian connective tissues. To date, 28 types of collagens have been identified, of which collagen type 1 is the richest source in the mammalian body. Collagen has a complex hierarchical structure from tropocollagen (collagen molecules), microfibrils, fibrils, and fibres responsible for the high tensile strength and collagen stability (Sherman et al., 2015). Collagen has unique characteristics such as biodegradability, biocompatibility, easy film-forming ability, nontoxic, high thermal stability, and tensile strength. For this reason, collagen has received increased attention from the food, cosmetics, biomedical, and pharmaceutical industries (Wang et al., 2017c).

In the food industry, collagen type 1 fibres from bovine skins are mainly used to make edible collagen films such as sausage casings. Over the last few years, collagen casings are used as an alternative to sausage casings made from animal intestines due to the advantages they offer, which include low risk of microbial contamination, an increased structural homogeneity compared to the natural variation of intestine sources, providing uniformity in size providing and shapes of sausages (Arvanitoyannis et al., 1997; Harper et al., 2012; Shi et al., 2019). According to Amin

and Ustunol (2007), 80% of edible sausage casings used in the meat industry are made from collagen type 1 extracted from bovine skins.

Despite the extensive use of collagen, it still has some drawbacks that limit its wider use. During the collagen extraction process from the native source, the hierarchical structure of collagen is damaged. This leads to the reconstituted collagen materials having inferior mechanical and low thermal properties than native materials and also provide a degree of heterogeneity at the molecular and supramolecular level, determined by the effects of processing and source material (Xiao et al., 2020). For this reason, collagen casings show suboptimal tensile strength, stiffness and thermal stability compared to animal intestinal casings. Consequently, it is necessary to understand how collagen casings can provide similar properties to natural casings. Several methods are being explored to increase the tensile strength, stiffness, and thermal stability to overcome these drawbacks. One technique is blending collagen paste/solutions with hydrocolloids (Ding et al., 2015; Ahmad et al., 2016; Wang et al., 2017a) or inorganic materials (He et al., 2011; Ma et al., 2018). Another method is crosslinking either through physical crosslinking such as glutaraldehyde (Wang et al., 2015; Chen et al., 2020) or enzymatic crosslinking transglutaminase enzyme (Wu et al., 2017; Cheng et al., 2019).

Among the two methods mentioned, mixing is the most used to develop films with improved tensile, flexibility and stability. Combining proteins and polysaccharides with different properties, functionalities, and interactions between hydrocolloids can lead to films with unique properties. Several studies have confirmed the enhancement of edible films physical and mechanical tensile properties from the combination of different hydrocolloids compared to the film made from a single component (Ding et

al., 2015; Wu et al., 2019). Thus, understanding the interactions between collagen and hydrocolloid blends is critical to understanding the resulting films characteristics to allow designed functionalities. So far, various attempts have been made to increase the mechanical, thermal and physicochemical properties of collagen fibre films using natural and synthetic polymers such as chitosan (Andonegi et al., 2020), gelatin (Xiao et al., 2020), globular proteins such as casein, soy protein isolate, keratin (Ahmad et al., 2016; Wu et al., 2018), nano-hydroxyapatite (Wang et al., 2017c), sodium alginate (Wang et al., 2017d), apatite (Wang et al., 2016a). According to these authors, the enhancement in collagen film tensile strength was due to the interaction between the polymers and collagen chain. To date, no information regarding the effect of derivatised cellulose and guar gum on the properties of acid-swollen collagen-based fibre films has been reported.

The previous chapter demonstrated that adding these hydrocolloids increased acid-swollen collagen paste elasticity. Thus, understanding their effect upon dehydration to create collagen films is of practical and industrial significance, particularly for sausage casing production. Therefore, this study explores the feasibility of preparing composite films based on collagen-hydrocolloids blends where the hydrocolloids are used at comparable viscosifying potential, providing the same molecular space occupancy, and then understanding the effect of different collagen concentrations. The collagen concentration was varied between 2.5 to 4 % wt/wt, while the concentration of each hydrocolloid was kept constant within the blend.

4.3 Materials and Methods

4.3.1 Materials

The materials used for this study are described in Chapter 3, section 3.2.1.

4.3.2 Methodology

4.3.2.1 Preparation of collagen pastes with and without hydrocolloids.

The pastes preparation process has already been described in Chapter 3, section 3.2.2.2.

4.3.2.2 Preparation of collagen films with and without hydrocolloids.

The films were formed using the method described by Harper et al. (2013). Approximately 5g of collagen with and without hydrocolloid/cellulose/starch pastes were rolled on a stainless-steel board between two plastic sheet layers with a stainless roller with a recess of 0.50 mm to achieve uniform film thickness. The plastic sheet on the roller side was removed, and the sheet with the pastes was oven-dried at 20 °C for 24hrs. The formed films were peeled off from the plastic sheets. Films containing collagen with and without hydrocolloids were conditioned in a desiccator at $20 \pm 0.1^\circ$ C and 75% relative humidity (RH) for seven days before all analysis. Saturated sodium chloride solution was used to achieve the required relative humidity.

4.3.3 Film characterisation

4.3.3.1 Film thickness

The thickness of films was measured using a digital electronic micrometre (Mitutoyo Corp, Kawasaki-shi, Japan). The thickness values were obtained by the average of ten measurements from random locations on each film sample.

4.3.3.2 Moisture content

The water content of films pre-conditioned at 75% RH was determined gravimetrically upon drying in an oven at 105 °C until constant weight (dry sample weight). Samples

were analysed at least in triplicates and were calculated according to equation (4-1). The results were expressed as (%) of moisture content of samples.

$$\text{Moisture content (\%)} = \frac{\text{Initial weight of film} - \text{final weight after drying}}{\text{Initial weight of film}} \times 100 \quad (4-1)$$

4.3.3.3 Attenuated total reflectance Fourier Transform Infrared Spectroscopy (ATR-FTIR)

ATR-FTIR spectroscopy was used to characterise the molecular structure of collagen within the films. The spectra were obtained using a Bruker Tensor 27 spectrometer equipped with an attenuated total reflectance (ATR) accessory (Graseby-Space Ltd, Orpington, UK) at 25 °C. The FTIR spectra were recorded in the range of 4000 to 500 cm^{-1} collected in 128 scans at a 4 cm^{-1} spectral resolution against an empty background. Spectral data analysis was carried out using the OPUS 7.0 software (Bruker, UK). Before data analysis, the spectra were baseline corrected and normalised. The spectra plots represent an average of 6 repeats.

4.3.3.4 Differential Scanning Calorimetry

The thermal transitions of the films were determined using a Differential Scanning Calorimetry (Mettler Toledo, DSC 3+, UK). The instrument was calibrated with pure indium and cyclohexane. Approximately 10 mg of the equilibrated films (at 75% RH) were accurately weighed in stainless steel pans and were hermetically sealed. The samples were scanned from 25 °C to 140 °C at a heating rate of 10 °C/min under N_2 atmosphere. An empty stainless-steel pan was used as a reference. The transition temperature (T_m) related to the melting of collagen was determined as the maximum

peak temperature. The energy associated with the helix coil transition defined as the enthalpy (ΔH) change was determined from the area under the endothermic peak. All analyses were calculated using STAR^e Thermal Analysis Software Default (DB V15.00).

4.3.3.5 Thermogravimetric analysis (TGA)

The thermal degradation of the films was investigated using a thermogravimetric analyser (Mettler Toledo, UK) under an inert N₂ atmosphere at a flow rate (25ml/min). Films of approximately 10 mg were weighed in aluminium pans and were hermetically sealed. The pans and heated from 25 to 550 °C at a heating rate of 10 °C/min. The weight loss (mg) *versus* temperature plots were taken for Thermogravimetric Analysis (TGA). The Differential Thermogravimetric (DTG) analysis curves were obtained by differentiating the TGA data with respect to temperature. TGA and DTG data were analysed using STAR^e Thermal Analyses software (DB V15.00). Analyses were performed in duplicate.

4.3.3.6 Dynamic Vapour Sorption

The water sorption isotherm of the films was measured using a Dynamic Vapor Sorption Analyser DVS-1 (Surface Measurement Systems Ltd., London, U.K.) equipped with a microbalance (Cahn D200, UK). The experiments were carried out at 25 °C and RH values from 0 to 95%. Approximately 10 mg of the equilibrated samples were loaded into the sample pan and then pre-dried in the DVS-1 under a Nitrogen flow of 200 ml min⁻¹ (RH=0%); no further change was observed. The measurement cycle was then started at 0% RH and terminated at 95% RH with a step increase by equilibrating the sample weight at each step. The samples were considered

equilibrated when the equilibration time exceeded 200 min. All experiments performed at 25 °C, and duplicates tests were carried out for each sample. The moisture isotherms for each sample expressed on a dry weight basis were described using the Guggenheim, Anderson and de Boer (GAB) model (Guggenheim, 1966). The GAB model is widely applied to food materials as it fits water sorption data up to an RH of 90% (Lemus M, 2011) and also considers the properties of the absorbed water in the monolayer and multilayer region (Timmermann et al., 2001; Agrawal et al., 2004; Kristo and Biliaderis, 2006). The GAB model assumes that the water molecules are sorbed into primary sites and subsequently into multilayers and all that all multilayer states are identical (Yakimets et al., 2007). The GAB model is expressed mathematically as.

$$M = \frac{M_0 C K a_w}{(1 - K a_w)(1 - K a_w + C K a_w)} \quad (4-2)$$

Where M is the equilibrium moisture content (dry basis), M_0 is the moisture content at the monolayer (g water/100 g dry solids), a_w is the water activity (RH/100), C and K are temperature dependent. C is related to the heat of water sorption at the monolayer; and K is associated with the heat of water sorption at the multilayer (Van Den Berg and Bruin, 1981; Kent and Meyer, 1984; Sun et al., 2009).

4.3.3.7 Mechanical properties

The mechanical characteristics, including tensile strength (TS), Young's Modulus (E) and elongation at break (% EAB) of the films were evaluated using a Texture Analyser (Stable Microsystems, Surrey, UK) with a 5 kg Load Cell, using a miniature tensile grip

(A/MTG). The films were cut into a dumbbell-shaped specimen approximately 8 mm wide (centre of the dumbbell) x 75 mm in length. The tests were performed at ambient temperature at a crosshead speed of 1 mm/min with 50 mm gauge length. To evaluate the mechanical properties of the films, at least seven specimens were stretched. The values of TS and EAB of the samples were calculated using the following equations:

$$TS = \frac{F}{A} \quad (4-3)$$

$$EAB = \frac{\Delta L}{L_0} \times 100\% \quad (4-4)$$

Where F is the maximum load force (N), ΔL is the elongation length of the film, L_0 is the initial grip length of the film (50 mm), and A is the cross-sectional Area.

4.3.3.8 Wide-angle X-ray Diffraction

The X-ray Diffraction patterns of the films were carried out using an echo D8 Advance Bruker AXS powder-diffractometer (Bruker AXS, UK) equipped with a copper tube operating at 40 kV and 25 mA, copper K alpha (Cu K α) radiation of a wavelength of 0.1541 nm. The samples were scanned from $2\theta = 4 - 45^\circ$.

4.3.3.9 Statistical analysis

The data were presented as means \pm standard deviation. The results were subjected to analysis of variance (ANOVA) and means of samples of each level of collagen were compared by Tukey's mean comparison test, differences were considered significant when $P < 0.05$ using the Statistical Package for Social Sciences (SPSS for Windows, SPSS Inc., Chicago, IL, USA).

4.4 Results and Discussion

4.4.1 Differential scanning calorimeter (DSC)

The DSC thermograms of the films are shown in Figure 4-1 and their transition temperatures ($T_{\text{onset/peak/end}}$) and enthalpies (ΔH) are presented in Table 4-1. All films show only one endothermic peak, which is ascribed to the denaturation temperature (T_d) of collagen, and relates to collagen helix-coil transition temperature (Badea et al., 2012). This is caused by the disruption of the intramolecular and intermolecular forces stabilising the collagen structure (Chen et al., 2014). The thermal denaturation of pure collagen films made from 4%, 3.5%, and 2.5%wt/wt collagen concentrations occurs at 97.6 °C, 95.9 °C, and 94.5 °C, respectively, thereby showing a slight concentration dependence. This result is consistent with Wu et al. (2019), who reported that the peak temperature of collagen fibre films increases with higher collagen content. It was suggested that the more collagen fibres present, the more interaction forces available. The increase in the peak temperature may also be attributed to the fact that during the drying process, the loss of water results in the strong association of collagen fibres and as the collagen fibre concentration increases, the fibres become more tightly packed, requiring higher temperature for denaturation. The denaturation temperatures reported in this study are similar to those reported by Perumal et al. (2018) for collagen films, unlike those reported by (Wang et al., 2017a). This difference could be attributed to differences in collagen concentrations, film preparation methods, and the films water content. Miles and Ghelashvili (1999) demonstrated that the thermal stability of collagen fibres depends on the water content and that the denaturation temperature of collagen fibres increases with lower hydration degrees.

With the addition of hydrocolloids, the temperature corresponding to the melting peak (T_{peak}) increases slightly, indicating increased blend films thermal stability. These results agree with the finding of other studies in which hydrocolloids such as HPMC, corn-starches, CMC, and synthetic nano-hydroxyapatite and apatite were reported to increase the melting temperature of collagen fibre films (Ding et al., 2015; Wang et al., 2016a; Wang et al., 2017a; Wu et al., 2020). These authors suggested that the increased denaturation temperature of collagen in the presence of the polymers was due to the interactions between the polymer molecules and collagen fibres, resulting in the formation of a densely compact structure of the composite films. The same reasoning may be used to explain the increase in T_{peak} of collagen films with hydrocolloids compared to the pure collagen films. It may be that some level of interactions exists between collagen fibres and hydrocolloid molecules. As a result, the collagen-collagen interactions are interfered with and replaced by the formation of interactions between collagen fibres and hydrocolloids, which results in a stable film network (Andonegi et al., 2020). However, incompatibility of the polymers may also describe the effectiveness of the collagen to form more stable thermal structures. As mentioned above, increasing collagen concentration increases thermal stability, and in a system where the addition of a hydrocolloid would phase concentrate the collagen when drying, this can be mitigated further.

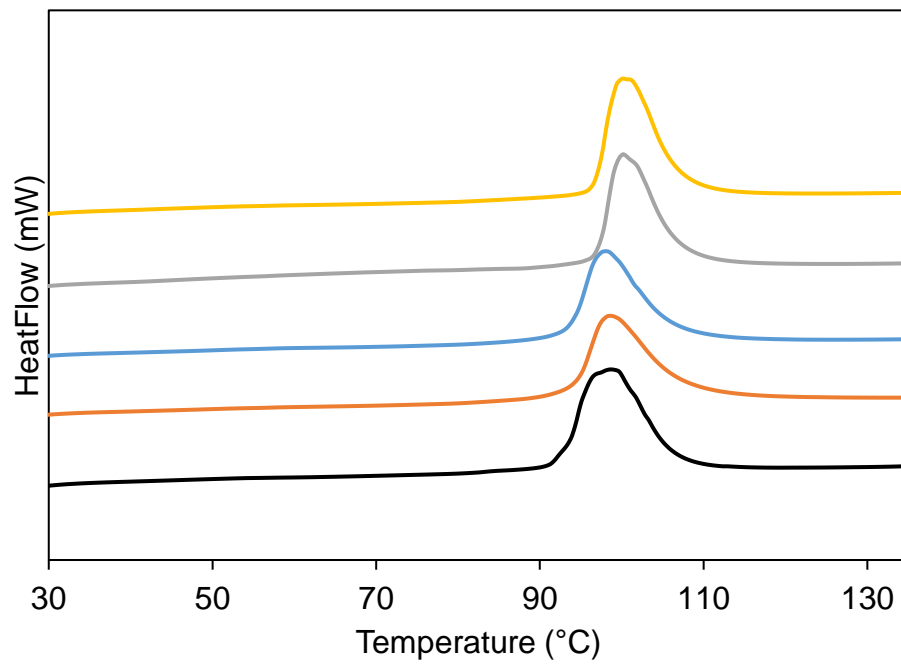
Meanwhile, the T_{peak} of collagen with guar films is slightly higher than that of collagen/derivatised celluloses films. This may be due to the higher molecular weight of the guar, which may have a greater effect of phase concentration, outweighing the increased stiffness of the derivatised cellulose (Haque and Morris, 1993). This could be explored further where the intrinsic viscosity of the celluloses and guar are matched, and thereby the effect of chain stiffness would be directly explored. COLLMC

shows the lowest T_{peak} at 3.5 and 2.5% collagen concentration, but the values are not statistically significant to other films. This may indicate that the hydrophobicity of the hydrocolloid may be influencing the thermal stability of collagen; further work will be needed to confirm this. Interestingly, when the derivatised cellulose in the form of negatively charged CMC was mixed with acid-swollen collagen fibrous paste, a deswelling of the pastes occurred, as shown in chapter 4. Consequently, films were not possible to be made. However, this result indicates that molecular weight, stiffness, hydrophobicity, and charge have a major effect on composite film properties.

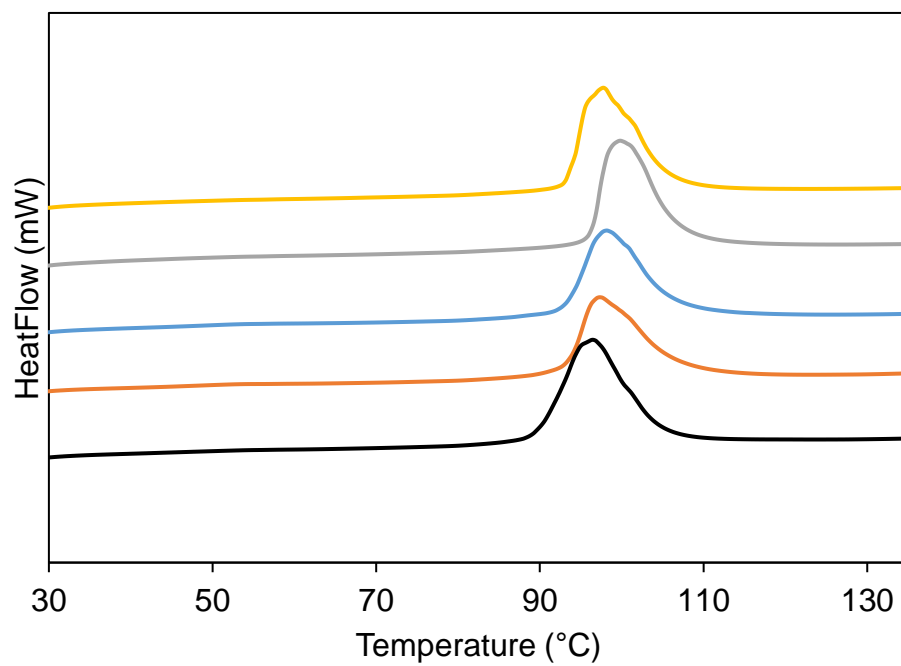
Contrary to the T_{peak} results, pure collagen films show higher enthalpy of transition but the values are not statistically significant ($p > 0.05$) to the composite films except COLLCMC films, indicating that more energy is required to break the intense cohesive forces stabilising the collagen hierarchical structure. Perumal et al. (2018) reported that in hydrated collagen films, the collagen fibrils are connected via water bridges, and the collagen molecules do not have direct contact with each other to form hydration bonds. However, during the drying process, the collagen fibrils come closer together and form strong intermolecular bonds that reduce the hydration bonds and stabilise the collagen structure, resulting in higher enthalpies. Similarly, Schroepfer and Meyer (2017) reported that the increase in collagen enthalpy upon dehydration was due to the direct interaction between the collagen molecules, leading to them being more tightly bound together. As a result, more energy is required to destroy the structure. It is unclear why the inclusion of hydrocolloids reduces the enthalpies of melting; however, it can be assumed that the hydrocolloid molecules, while potentially phase concentrating the collagen fibres and creating more thermally stable structures, prevent the collagen fibrils from coming close together to form intense interactions.

However, in this study, the enthalpies of collagen/guar films and collagen/derivatised cellulose films were not significantly different ($P < 0.05$).

(A)



(B)



(C)

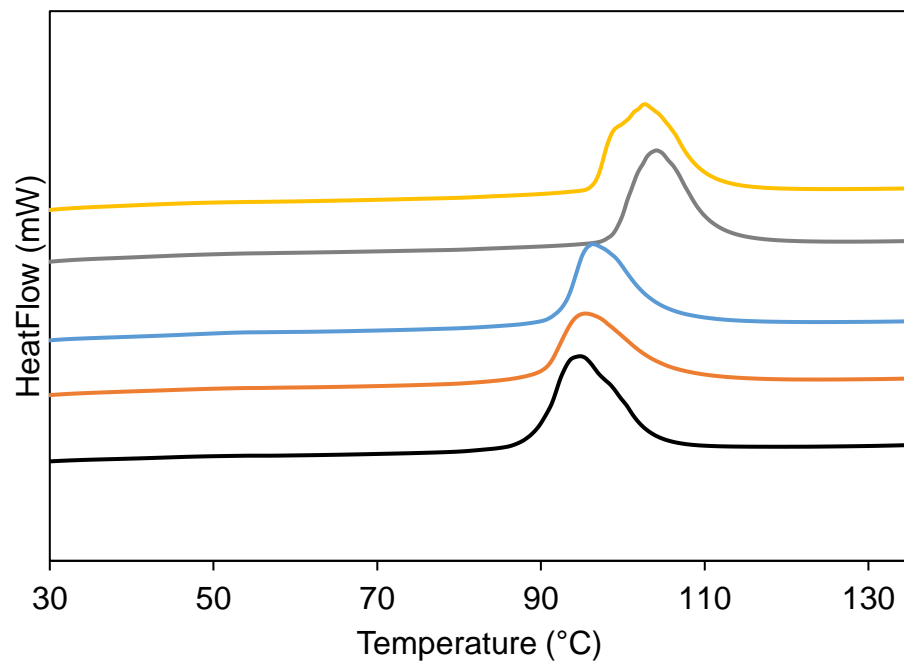


Figure 4-1: DSC thermograms of pure collagen (black line), COLLMC (orange line), COLLHPMC (blue line), COLLGH (yellow line) and COLLGM (grey line) at (A) 4 % (B) 3.5% (C) 2.5 % wt/wt collagen concentrations.

Table 4-1: Onset temperature (T_o), endothermic peak (T_{peak}), Endset (T_{end}), enthalpy (ΔH) of collagen with and without hydrocolloid films at different collagen concentrations.

Samples	Tonset (°C)	Tpeak (°C)	Tend (°C)	$\Delta H(J/g)$
4% COLLAGEN	92.99 ± 0.31 ^a	97.63 ± 2.54 ^a	107.65 ± 2.71 ^a	33.14 ± 0.81 ^d
COLLGM	97.01 ± 0.41 ^b	100.25 ± 0.16 ^a	107.16 ± 0.4 ^a	27.82 ± 0.71 ^a
COLLGH	96.68 ± 0.25 ^b	100.16 ± 0.37 ^a	107.17 ± 0.52 ^a	31.59 ± 0.49 ^{cd}
COLLHPMC	93.47 ± 0.52 ^a	98. ± 0.41 ^a	105.99 ± 0.92 ^a	28.82 ± 0.11 ^{ab}
COLLMC	94.10 ± 0.77 ^a	98.56 ± 0.72 ^a	108.16 ± 0.35 ^a	29.96 ± 0.24 ^{bc}
3.5% COLLAGEN	90.36 ± 1.56 ^a	95.91 ± 1.35 ^a	104.59 ± 1.13 ^a	34.71 ± 1.42 ^b
COLLGM	96.02 ± 0.17 ^b	99.76 ± 0.27 ^b	106.93 ± 0.43 ^a	30.97 ± 0.93 ^b
COLLGH	93.15 ± 0.41 ^{ab}	98.4 ± 0.97 ^{ab}	105.05 ± 0.81 ^a	30.94 ± 0.08 ^b
COLLHPMC	93.03 ± 0.82 ^{ab}	97.9 ± 0.81 ^{ab}	106.55 ± 0.14 ^a	29.29 ± 0.84 ^{ab}
COLLMC	93.18 ± 0.54 ^{ab}	95.30 ± 2.45 ^a	106.83 ± 0.84 ^a	27.04 ± 2.07 ^a
2.5% COLLAGEN	89.29 ± 0.82 ^a	94.50 ± 0.69 ^a	104.06 ± 0.13 ^a	31.83 ± 2.33 ^b
COLLGM	98.78 ± 0.16 ^d	98.78 ± 0.16 ^c	111.34 ± 0.76 ^c	28.38 ± 0.34 ^{ab}
COLLGH	96.40 ± 0.09 ^c	102.68 ± 0.07 ^d	110.37 ± 0.25 ^c	30.5 ± 1.39 ^{ab}
COLLHPMC	92.27 ± 0.95 ^b	96.33 ± 0.06 ^b	105.07 ± 0.61 ^{ab}	26.84 ± 0.12 ^{ab}
COLLMC	90.01 ± 0.00 ^{ab}	95.58 ± 0.41 ^{ab}	105.93 ± 0.21 ^b	26.7 ± 0.54 ^a

^{ad} Mean ± standard deviation. Different letters in the same column indicate significant differences.

4.4.2 Mechanical properties

Tensile strength (TS), elongation at break (EAB), and Young's modulus (YM) of collagen films are presented in Table 4-2. Hydrocolloid films mechanical properties are affected by factors such as the degree of interaction between the film-forming components, moisture content, plasticisers, and film microstructure (Arfat et al., 2014; Acosta et al., 2015). Pure collagen films at starting concentrations of 4%, 3.5%, and 2.5% wt/wt show TS of 17.27, 14.72, and 8.01 MPa, respectively. The YM of collagen films follow a similar trend to tensile strength, where the mechanical properties increase with increasing collagen fibre content. This indicates that the films mechanical properties relate to the collagen fibre contents, where higher collagen content results in a stronger and stiffer film network (Chen et al., 2019). This agrees with Savic and Savic (2016), who reported that the collagen casing's strength is affected by the collagen fibre content. As indicated earlier, this is also relevant to the extent to which the collagen fibres have been allowed to be reinforced during the drying process.

The addition of the hydrocolloids at the different collagen concentrations results in a significant ($p < 0.05$) increase in the TS and YM of the blend films. The composite films values increase concomitant to an increase in the collagen concentration, indicating that the collagen fibre content contributes to the enhanced tensile strength and stiffness of the composite films. This corroborates with the DSC data, which indicates increased denaturation temperature with increasing collagen content. As mentioned previously, the tightly packed structure formed due to the stronger association of the collagen fibres upon drying may result in films with increase strength and stiffness, and this effect will be enhanced with increasing collagen fibre content. The tensile

strength of the films is influenced by the interaction between the film components (Ding et al., 2015). A similar result was reported for collagen fibre film with CMC (Wu et al., 2020). These authors proposed that the electrostatic interactions between the collagen fibre and the CMC made the films more compact and resulted in increased tensile strength and stiffness. Therefore, it is plausible that during the drying process, some levels of interaction occurred between the collagen fibres and hydrocolloids which results in the formation of a complex matrix with enhanced strength and stiffness compared to the control films. Furthermore, collagen film with the addition of derivatised cellulose films (COLLMC and COLLHPMC) shows higher TS and EM values than collagen-guar films, indicating that the blend films with derivatised celluloses are stronger and stiffer. This might be because the more derivatised celluloses present in the film-forming matrix results in more interaction forces between the derivatised cellulose molecules and collagen fibres, thus improving the tensile and stiffness of the films.

The elongation at break (EAB) for pure collagen films follows a similar trend to the TS and EM, and the values decrease with decreasing collagen content in the films. The composite films show slightly higher EAB than the pure collagen films, but the increase was not significant at 4% collagen concentration. In contrast, the opposite is observed at collagen starting concentration of 3.5% and 2.5%, where COLLHPMC and COLLMC films were significantly different from pure collagen films alone. The strong covalent and non-covalent forces stabilising the collagen structure can prevent the chains from stretching, resulting in low elongation of collagen films (Ahmad et al., 2016). This result is similar to the study of Xiao et al. (2020), where the addition of gelatin increased the flexibility of collagen fibre film. Similarly, Ahmad et al. (2016) reported that collagen-chitosan films showed higher flexibility than pure collagen films. Therefore, it may be

deduced that the polymers interfering with the collagen-collagen intense interactions during drying allows the stretching of the films and increases the films extensibility and flexibility (Chen et al., 2008). Moreover, films containing derivatised cellulose shows higher elongation than collagen-guar films at the various collagen concentrations studied, though not significantly different ($p > 0.05$). This may be due to a higher amount of derivatised cellulose used at a comparable viscosifying effect. Although collagen with derivatised cellulose has a greater reinforcing effect than guar gums, they both impart similar elongation to the collagen films. Taking these results together, it can be concluded that adding hydrocolloids to collagen fibre films provides a feasible way to enhance the mechanical properties of collagen films (casing) as appropriate strength is needed for the casings to resist breakage during batter stuffing, cooking and transportation.

Table 4-2: Mechanical properties of collagen films with and without hydrocolloids at different collagen concentrations.

FILMS	TS (MPa)	EAB (%)	YM(Mpa)
4% COLLAGEN	17.27 ± 6.12 ^a	2.78 ± 1.92 ^a	1041.83 ± 142.68 ^a
COLLGM	22.41 ± 7.19 ^{ab}	3.11 ± 1.24 ^a	1072.22 ± 111.41 ^a
COLLGH	20.61 ± 8.63 ^{ab}	2.46 ± 1.31 ^a	1076.65 ± 133.59 ^a
COLLHPMC	28.20 ± 7.43 ^b	3.37 ± 1.57 ^a	1169.88 ± 134.94 ^{ab}
COLLMC	25.25 ± 5.35 ^{ab}	3.36 ± 1.27 ^a	1107.98 ± 129.37 ^a
3.5% COLLAGEN	14.72 ± 3.52 ^a	2.11 ± 0.73 ^a	707.15 ± 96.91 ^a
COLLGM	19.95 ± 7.59 ^{ab}	2.73 ± 1.26 ^{ab}	994.94 ± 152.93 ^b
COLLGH	18.59 ± 4.00 ^{ab}	2.54 ± 0.84 ^{ab}	984.41 ± 106.16 ^b
COLLHPMC	23.08 ± 3.59 ^b	3.37 ± 0.69 ^{bc}	1070.39 ± 67.11 ^b
COLLMC	22.96 ± 4.42 ^b	3.99 ± 1.49 ^c	1063.65 ± 120.73 ^b
2.5% COLLAGEN	8.01 ± 1.65 ^a	1.44 ± 0.24 ^a	567.76 ± 82.50 ^a
COLLGM	13.99 ± 5.99 ^{bc}	2.10 ± 1.44 ^{ab}	793.92 ± 72.92 ^b
COLLGH	11.84 ± 5.38 ^{ab}	2.17 ± 1.43 ^{ab}	802.67 ± 37.26 ^b
COLLHPMC	17.08 ± 2.28 ^c	3.03 ± 0.74 ^b	858.00 ± 68.44 ^b
COLLMC	16.30 ± 3.45 ^{bc}	2.61 ± 0.65 ^{ab}	878.03 ± 81.62 ^b

^{a-c} Mean ± standard deviation. Means in the same column with the different superscript letter are significantly different (P < 0.05).

4.4.3 Thermogravimetric analysis

The Thermogravimetric analysis (TGA) and corresponding differential thermogravimetric analysis (DTG) curves for the collagen films are shown in **Error! Reference source not found.** and Figure 4-2, their corresponding weight loss and degradation temperatures are presented in Table 4-3. Pure collagen films show a two-step degradation process while the blend films degrade in three steps. The degradation profile of pure collagen films agrees with Ding et al. (2015) and Meng et al. (2012). For all the films, the first weight-loss stage is observed around 100 °C, and the weight loss (Δw_1) values correlate with the moisture content values, as shown in Figure 4-5. This weight loss step is related to the evaporation of free and absorbed water from the films (Ding et al., 2015). The weight loss of pure collagen films was 21.1 %, 18.8 % and 18.0 % for pure collagen films at starting concentration of 4%, 3.5% and 2.5% wt/wt, respectively. This suggests that the rate at which the films absorb water during equilibration is affected by the proportion of collagen content (collagen starting concentration). Also, the more collagen fibre, the more polar sites for water molecular interaction. The composite films show weight loss between 17.0 % - 21.2 %, lower than the 4% collagen control during the first step. Interestingly, composite films have higher weight loss values at lower collagen concentration than pure collagen films. Considering that the concentration of each hydrocolloid is the same at all the collagen levels studied, it is hypothesised that the way the polymers thermodynamically interact with collagen may depend on the collagen concentration.

Collagen with derivatised cellulose films shows slightly lower weight loss values than collagen/guar films, which may occur due to derivatised cellulose hydrophobicity.

The second weight-loss stage for pure collagen films at 4%, 3.5%, and 2.5% wt/wt appears at temperature (T_{d2}) of 324.0 °C, 324.4 °C, and 323.3 °C, respectively with a weight loss between $\Delta w_2 = 54.2 - 56.0$ %, and relates to the thermal degradation of collagen, and agrees with the previous study (Ding et al., 2015). However, for the composite films, the second weight-loss stage may reflect the degradation of the side chains or substituting groups from the main backbone of the hydrocolloids. The derivatised celluloses show higher degradation temperatures, suggesting that they are more thermally stable than the guar. This may be due to a difference in molecular and structural conformation of the polymer. Compared to guar's flexible chains, the more rigid conformation of derivatised cellulose might require higher temperatures for degradation.

MC degrades at a higher temperature (265.5 – 295.0 °C) than HPMC (257.6 – 259.9 °C). This is suggested to be due to the higher degree of methoxylation of MC chains, thereby making the methylcellulose structure more thermally stable (Rodrigues Filho et al., 2007). In agreement, Zohuriaan and Shokrolahi (2004) reported that methylcellulose showed the highest degradation temperature amongst the derivatised cellulose investigated. For COLLGM and COLLGH films, the degradation temperature of medium and high molecular weight guar gum occurs at 214.6 – 218.6 °C and 218.0 - 222.1 °C, respectively. The degradation temperature of GH is higher than GM at 4% and 3.5% collagen concentration, whereas, at 2.5% collagen, the temperature difference is not evident. This difference may be ascribed to the difference in the molecular weight and degree of substitution of the guar gums. Calahorra et al. (1989)

reported that polymer molecular weight influences their thermal degradation temperature, as a polymer thermal stability decreases as molecular weight decreases. Also, high and medium molecular weight guar gums show a reduction in their degradation peak intensities, with high molecular weight guar gum showing a lower peak intensity, attributed to the lower polymer amount in the blend films.

The third degradation step of the composite films, which is the degradation temperature of collagen occurs at about 322.9 – 324.9 °C. These values were not significantly different ($P>0.05$) from pure collagen films, indicating that the thermal stability of collagen was not affected by the addition of hydrocolloids and suggesting that the different conformation of the hydrocolloids did not affect collagen degradation temperature.

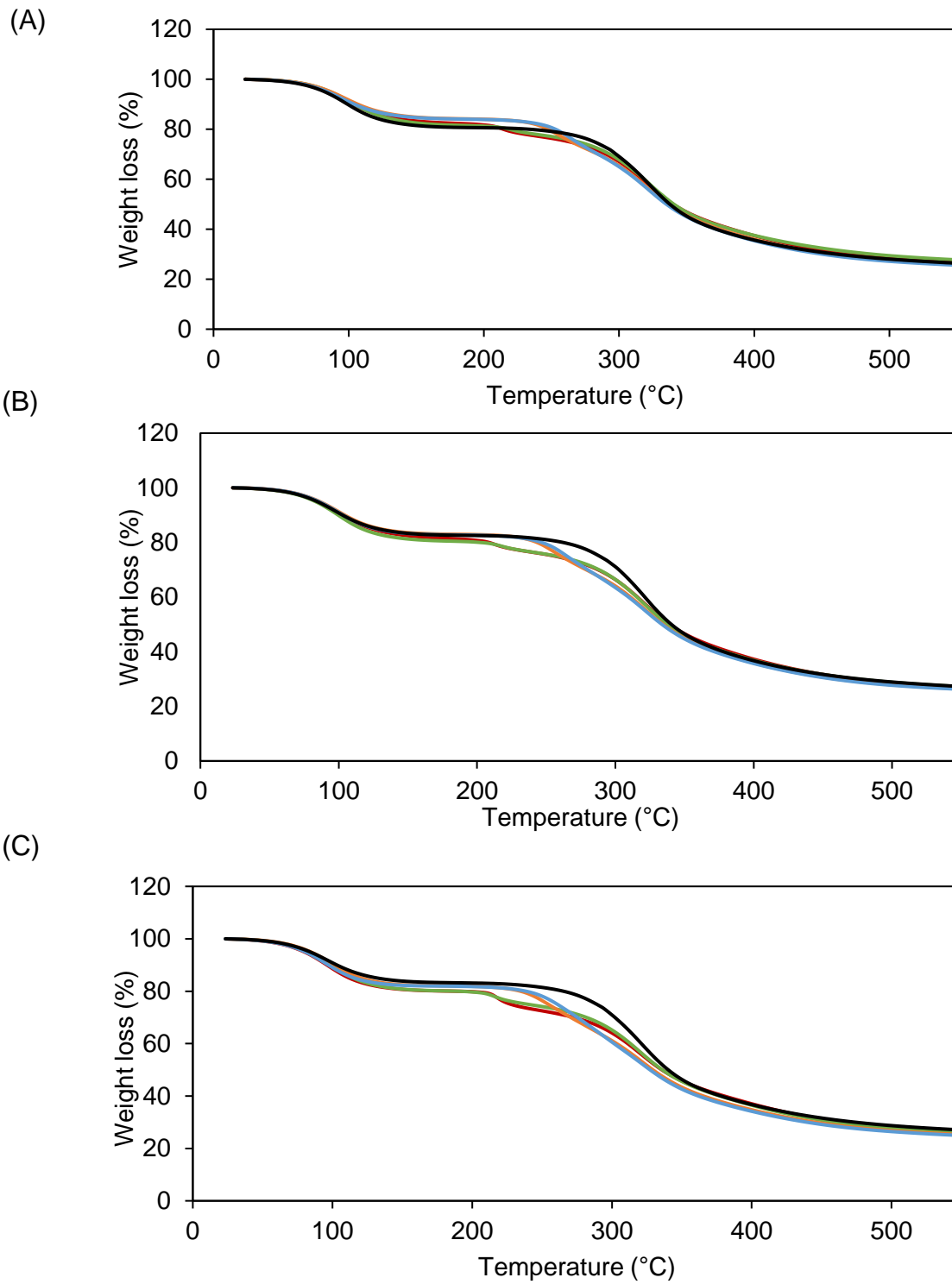
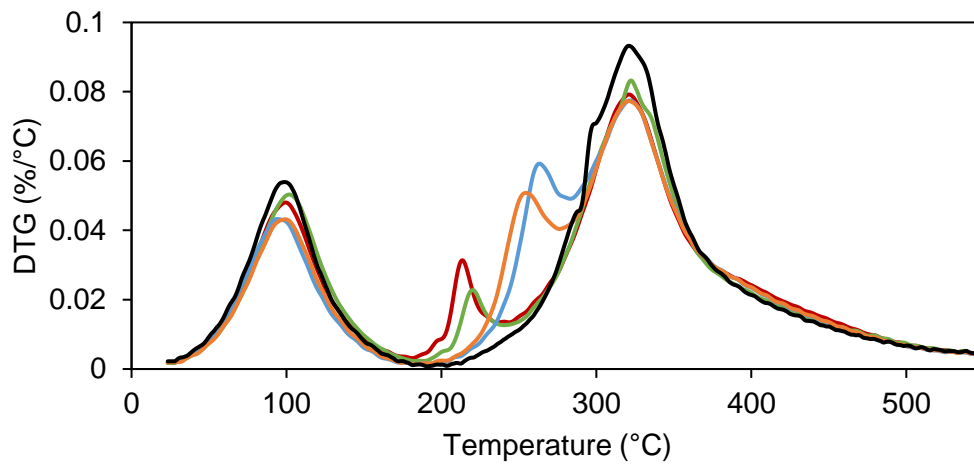
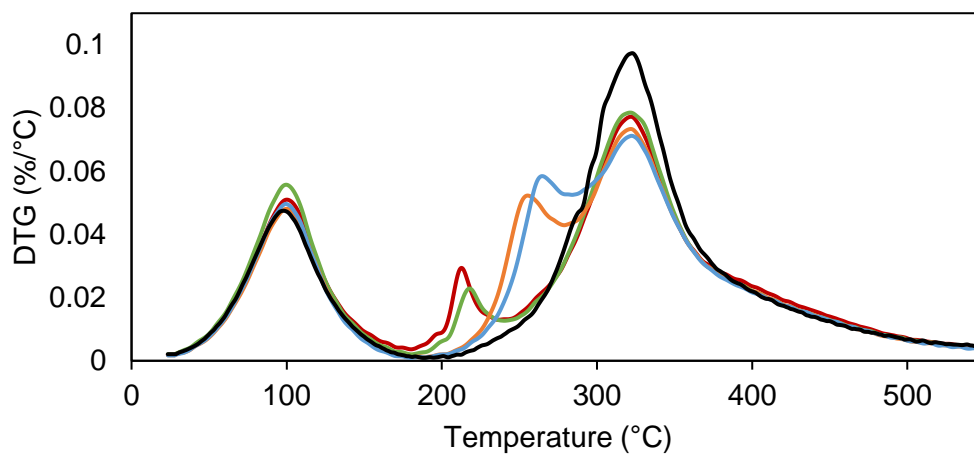


Figure 4 2: TGA curves of pure collagen (black line), COLLMC (blue line), COLLHPMC (orange line), COLLGH (green line) and COLLGM (red line) at (A) 4 % (B) 3.5% (C) 2.5 % wt/wt collagen concentrations.

(A)



(B)



(C)

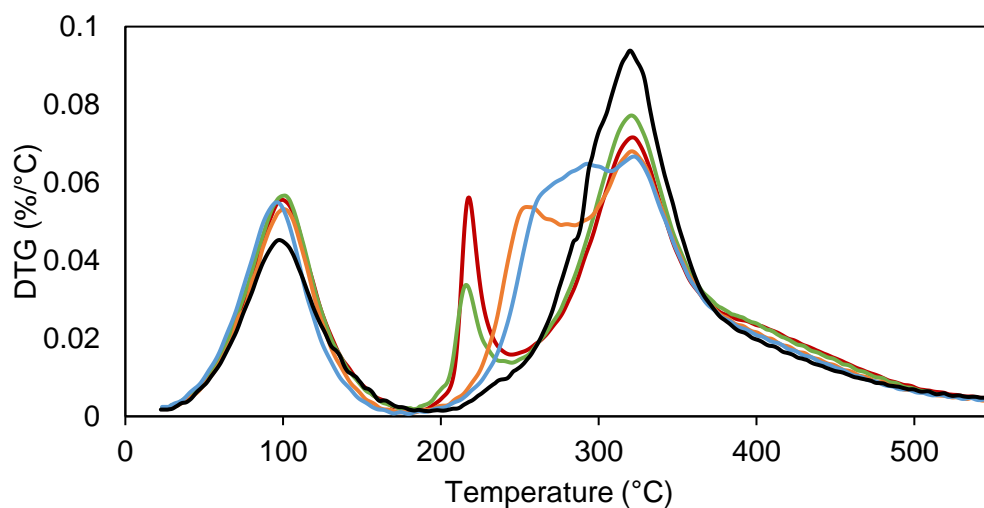


Figure 4-2: DTG curves of pure collagen (black line), COLLMC (blue line), COLLHPMC (orange line), COLLGH (green line) and COLLGM (red line) at (A) 4 % (B) 3.5% (C) 2.5 % wt/wt collagen concentrations.

Table 4-3: Thermal degradation temperature (Td) and weight loss (%) of collagen with and without hydrocolloid films at different collagen concentrations.

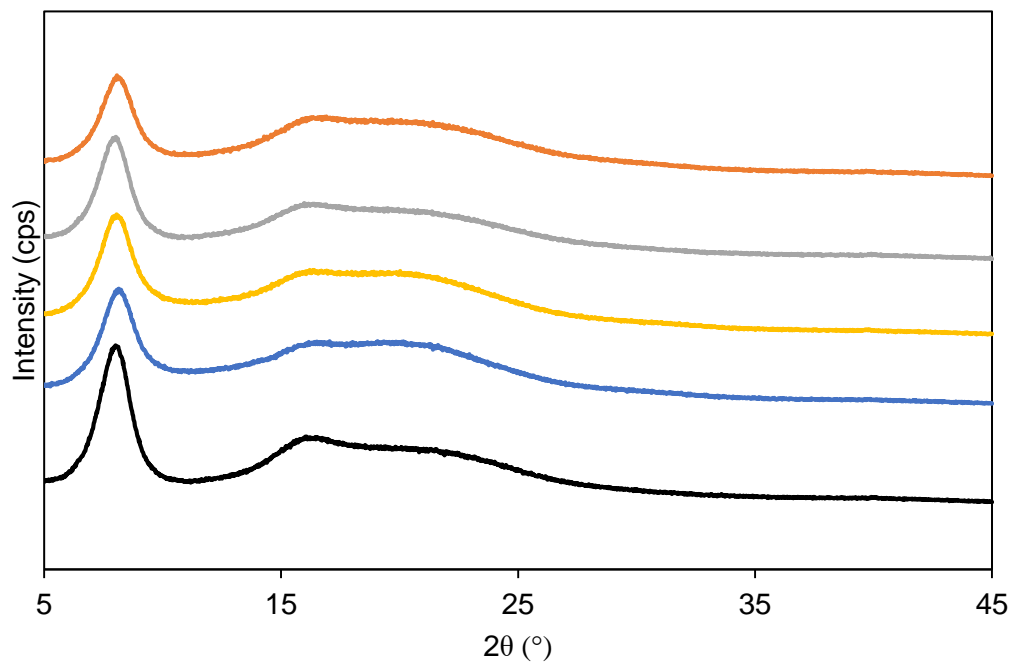
Sample	Δ_1		Δ_2		Δ_3	
	T _{d1} (°C)	Δ_{w1} (%)	T _{d2} (°C)	Δ_{w2} (%)	T _{d3} (°C)	Δ_{w3} (%)
4% COLLAGEN	102.0 ±1.9	21.1 ± 0.9	-	-	324.0 ±0.9	54.2 ± 0.9
COLLHPMC	102.3 ±1.4	17.0± 0.9	257.6 ±0.0	11.7 ±0.0	323.6 ±0.9	42.8 ± 1.8
COLLMC	97.3 ± 0.0	17.2 ± 0.9	265.5 ±0.0	10.9 ±0.0	324.2 ±0.0	44.7± 0.2
COLLGM	100.3 ± 1.4	18.8 ± 0.1	214.5 ±0.5	5.1 ± 0.0	322.9± 0.0	48.3± 1.0
COLLGH	104.8 ± 3.3	19.5 ± 0.3	222.1 ±0.0	3.5 ± 0.6	323.5 ±0.9	48.8 ± 0.2
3.5% COLLAGEN	103.5 ±0.9	18.8 ± 0.3	-	-	323.3 ±1.8	55.3 ± .5
COLLHPMC	102.5 ±1.9	17.7 ± 0.6	258.2 ±0.5	12.1 ±0.7	324.4 ±0.5	43.5 ± 0.6
COLLMC	102.4 ±1.7	17.9 ± 0.6	267.8 ±1.7	12.6 ±0.6	325.5 ±0.2	42.6 ± 0.7
COLLGM	102.4 ±1.9	19.9 ± 0.8	214.2 ±0.5	4.8 ± 0.2	324.1 ±0.5	48.6 ± 0.6
COLLGH	102.1 ±0.5	20.6± 1.1	220.2 ±0.5	3.9 ± 0.2	324.0 ±1.4	47.9 ± 0.2
2.5% COLLAGEN	100.2 ±1.0	18.0 ± 1.0			323.7 ± 0.1	56.0 ± 0.4
COLLHPMC	103.2 ±0.9	18.0 ± 0.2	259.9 ±0.5	12.9 ±1.0	323.3± 0.6	42.8 ± 1.1
COLMC	98.4 ± 0.6	19.0 ± 0.9	295.0 ±1.4	12.5 ±0.2	324.9 ±0.4	42.8 ± 1.1
COLLGM	103.4±5.2	21.2 ± 1.3	218.6 ±0.5	6.3 ± 0.5	324.9±0.6	46.1 ± 0.9
COLLGH	103.8 ±0.9	21.2 ± 0.5	218.0 ±0.9	4.9 ± 0.1	324.0±0.9	48.0 ± 0.1

^{ac} Mean ± standard deviation. Different letters in the same column indicate significant differences

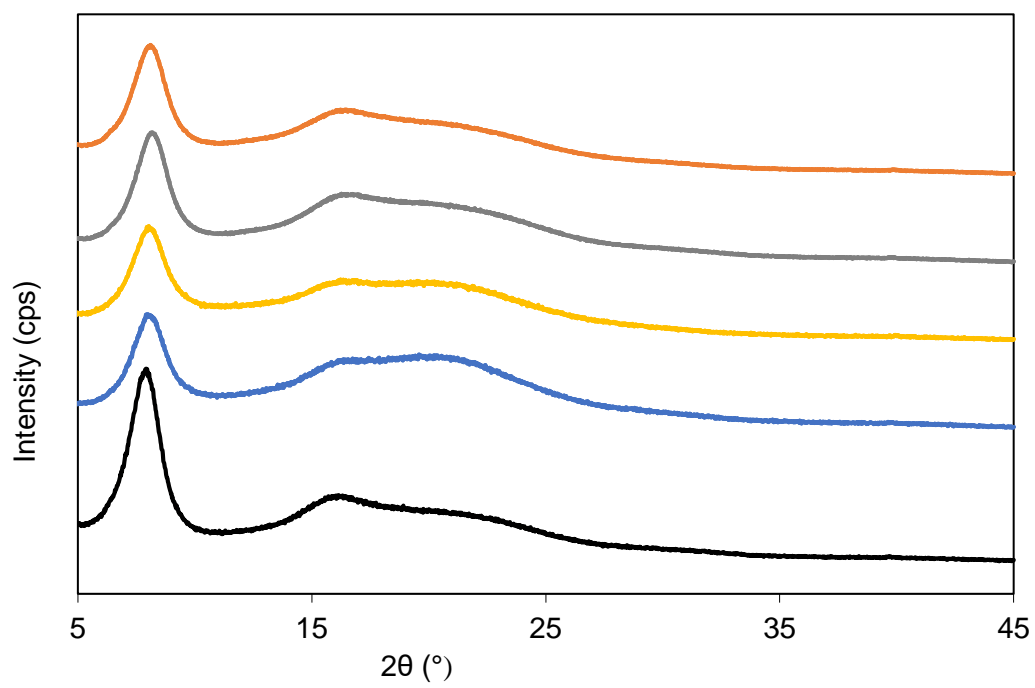
4.4.4 X-ray diffraction

The XRD diffractograms of collagen films are shown in Figure 4-3. All the films show a sharp diffraction peak at about $2\theta = 8^\circ$, corresponding to the intermolecular lateral packing distance between the molecular collagen chains. It also reflects the crystalline region of collagen's triple-helical structure (Rivero et al., 2010). This peak intensity is also related to the triple helix content in collagen (Bigi et al., 2004). The broad peak at $13^\circ - 27^\circ$ (2θ) is due to the amorphous scattering resulting from the disordered components within the collagen fibres (Meng et al., 2012). With the addition of the polymers, the sharp peak intensity at $2\theta = 8^\circ$ decreases slightly, relating to a decrease in collagen structural order. This confirms that the hydrocolloid molecules interfere with the collagen-collagen interactions during the drying process, thereby changing the structural order of the collagen. Additionally, a slight shift is seen for the broad peak at $13^\circ - 27^\circ$ (2θ), particularly for composite films with guar gums, indicative of a slightly more amorphous component.

(A)



(B)



(C)

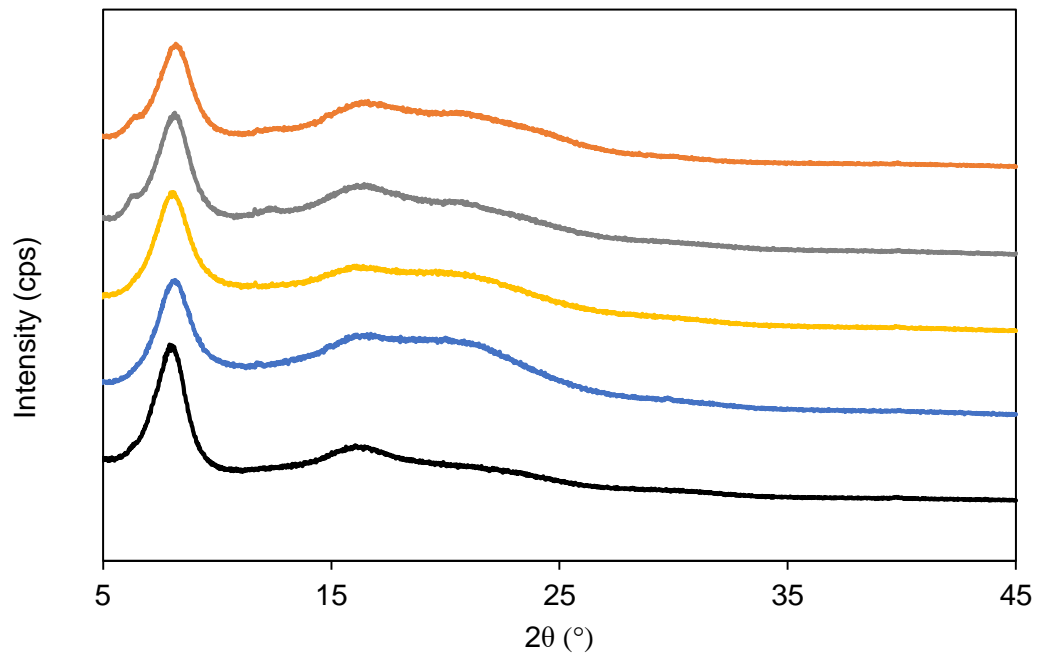


Figure 4-3: XRD of pure collagen (black), COLLMC (blue), COLLHPMC (yellow), COLLGH (grey) and COLLGM (orange) at (A) 4 % (B) 3.5% (C) 2.5 % wt/wt collagen concentrations.

Table 4-4. Percentage crystallinity of collagen films with and without hydrocolloids at different collagen concentrations.

Films	% Crystallinity
4% COLLAGEN	73.25 ± 2.62 ^b
COLLGM	60.00 ± 1.15 ^a
COLLGH	58.75 ± 1.50 ^a
COLLHPMC	56.75 ± 4.19 ^a
COLMC	58.50 ± 1.73 ^a
3.5% COLLAGEN	71.00 ± 1.63 ^c
COLLGM	59.25 ± 2.22 ^{ab}
COLLGH	60.75 ± 3.77 ^b
COLLHPMC	54.50 ± 2.38 ^a
COLMC	54.75 ± 0.50 ^a
2.5% COLLAGEN	70.25 ± 2.87 ^b
COLLGM	55.50 ± 5.25 ^a
COLLGH	53.00 ± 6.00 ^a
COLLHPMC	53.50 ± 1.73 ^a
COLMC	53.50 ± 2.38 ^a

^{a-c}Mean ± standard deviation. Means in the same column with different superscript letter are significantly different (P < 0.05).

4.4.5 FTIR spectra of films

The FTIR spectra of collagen films carried out in the wavenumber range of 500 – 4000 cm^{-1} are shown in Figure 4-4. The spectra of pure collagen films at 4%, 3.5%, and 2.5% collagen concentrations show characteristic absorption bands of collagen at 3293, 2929, 1627, 1546, and 1237 cm^{-1} corresponding to amide A, B, I, II and III, respectively. Amide A: N-H stretching coupled with O-H vibrations; amide B: asymmetric stretching vibration of $=\text{C}-\text{H}$ and NH_3^+ ; amide I, which is considered a marker of protein secondary structure, is linked to $\text{C}=\text{O}$ stretching/hydrogen bonding coupled with COO^- ; amide II arising from bending vibration of N-H groups and stretching vibrations of C-N groups; amide III: vibrations in plane of C-N and N-H bending vibrations from amide linkages, as well as the absorptions arising from wagging vibrations from CH_2 groups in the glycine backbone and proline side chains (He et al., 2011). Xu et al. (2020a) reported similar spectra for collagen fibre films prepared from acid-swollen collagen fibre with varying swelling degrees. The decrease in any of these amide peaks to a lower wavenumber indicates increased hydrogen bonding molecular interactions and collagen stability. In contrast, a shift to higher wavenumbers of these bands indicates structural rearrangements occurring in the film structure (Ben Slimane and Sadok, 2018). Upon the addition of the hydrocolloids, no substantial shift is found for the amide A bands of the composite films.

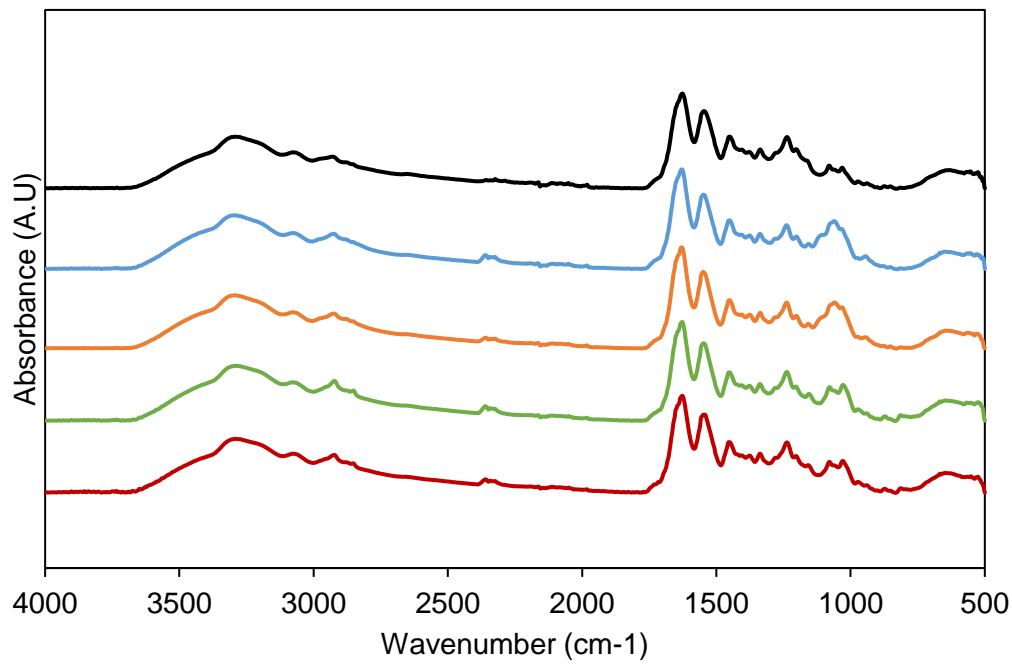
Meanwhile, the amide I and II bands shifted to higher wavenumbers, suggesting a change in the structural arrangement of collagen induced by the addition of the hydrocolloids. This may be related to the interference in the collagen-collagen interactions in the films during drying. This result was similar to those of Wang et al. (2017a), where the amide I band of collagen films shifted to higher wavenumbers with

the addition of starch. No substantial peak shift in amide III bands is seen for the composite films. Meanwhile, a decrease in the amide III bands intensity is observed for COLLHPMC and COLLMC compared to the pure collagen films. This slight reduction might be due to the higher concentration of the derivatised celluloses present in the films than guar gums.

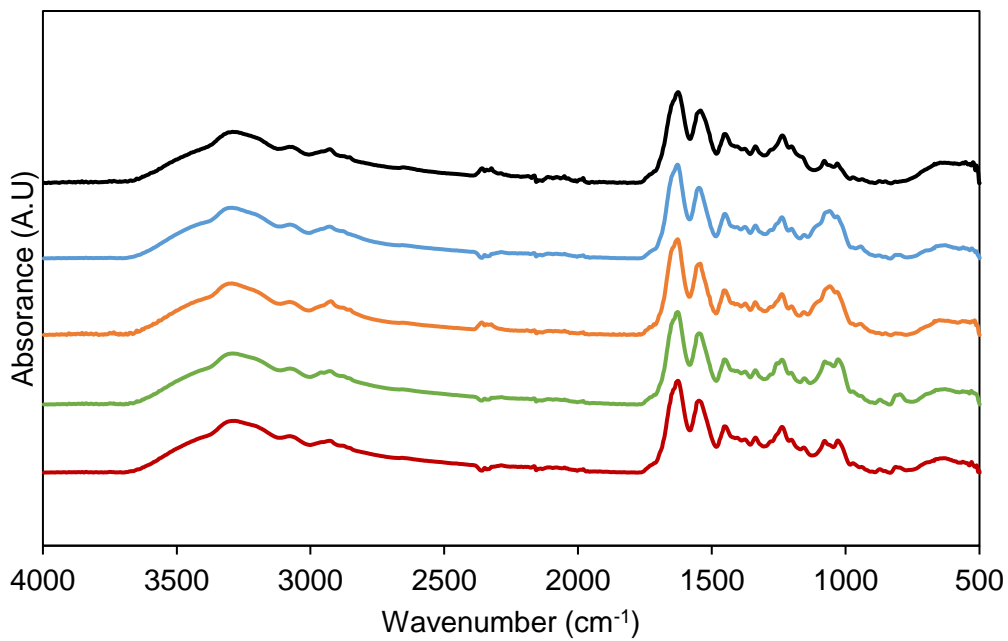
Additionally, the absorption ratio of Amide III to 1450 cm^{-1} (A_{III}/A_{1450}) is used for confirming the integrity of the collagen triple helical structure (Guzzi Plepis et al., 1996; He et al., 2011), a ratio closer or greater to 1 indicates better triple helix integrity. On the contrary, the structure is considered disordered when the ratio is about 0.6 which is the value for gelatin, the denatured form of collagen (He et al., 2011). As seen in Table 4-6, for the pure collagen films, the ratios at collagen paste concentrations of 4, 3.5, and 2.5% wt/wt were 1.00, 0.98, and 0.94, respectively. For the composite films, the values were above 0.6 but lower than pure collagen films, indicating that the triple helix of the collagen fibres are not altered significantly since a value of 0.6 or below indicates a loss in collagen structure (Hu et al., 2014). However, the reduction of absorption ratio values can be associated with changes in the structure of collagen, which agrees with the XRD results regarding the reduction in the structural order of collagen fibres in the composite films due to the presence of hydrocolloids in the film upon drying. A similar result was reported by He et al. (2011) for collagen films modified with procyanidin. The authors conclude that procyanidin molecules crosslinked the collagen by forming new hydrogen bond interactions with collagen without destroying the collagen backbone. Additionally, the values of the composite films decrease slightly with a decrease in collagen concentration. Since the concentration of each hydrocolloid is the same in the collagen films at the various collagen concentrations, this indicates an increased stabilisation and preservation of

collagen structure with increasing collagen fibre content. Furthermore, collagen with derivatised cellulose (COLLHPMC and COLLMC) show lower $A_{III}A_{1450}$ values, which may be due to the higher concentrations of the polymers in the film matrix.

(A)



(B)



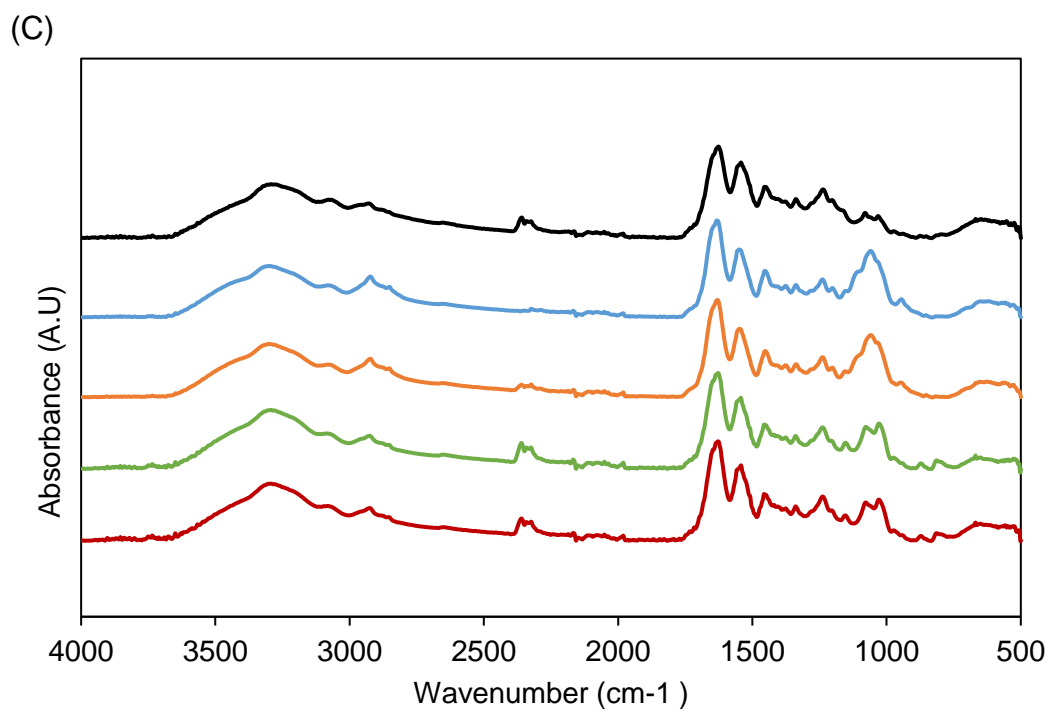


Figure 4-4: FTIR spectra of COLLHPMC (orange line), COLLMC (blue line), COLLGM (green line), COLLGH (red line) and pure collagen (black line) films at (A) 2.5% (B) 3.5% (C) 4% collagen concentrations.

Table 4-5: Wavenumber of the bands in the FTIR spectra of the films.

Samples	Amide A	Amide B	Amide I	Amide II	Amide III
COLLHPMC	3923	2926	1628	1548	1238
COLLMC	3292	2925	1628	1547	1238
COLLGH	3292	2923	1627	1548	1237
COLLGM	3292	2924	1627	1547	1238
4%	3292	2929	1626	1544	1237
COLLAGEN					
COLLHPMC	3293	2925	1629	1548	1238
COLLMC	3292	2926	1628	1548	1238
COLLGH	3292	2925	1628	1547	1237
COLLGM	3291	2926	1628	1547	1237
3.5%	3292	2928	1626	1543	1237
COLLAGEN					
COLLHPMC	3292	2924	1632	1548	1238
COLLMC	3292	2923	1630	1547	1239
COLLGH	3292	2926	1628	1543	1238
COLLGM	3292	2927	1628	1543	1238
2.5%	3292	2928	1626	1543	1237
COLLAGEN					

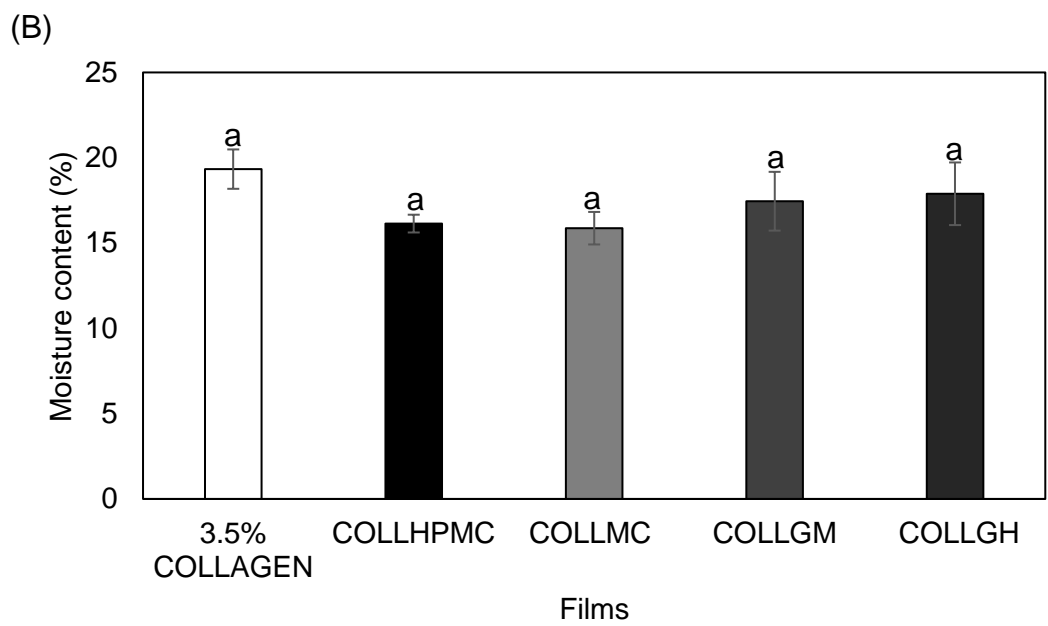
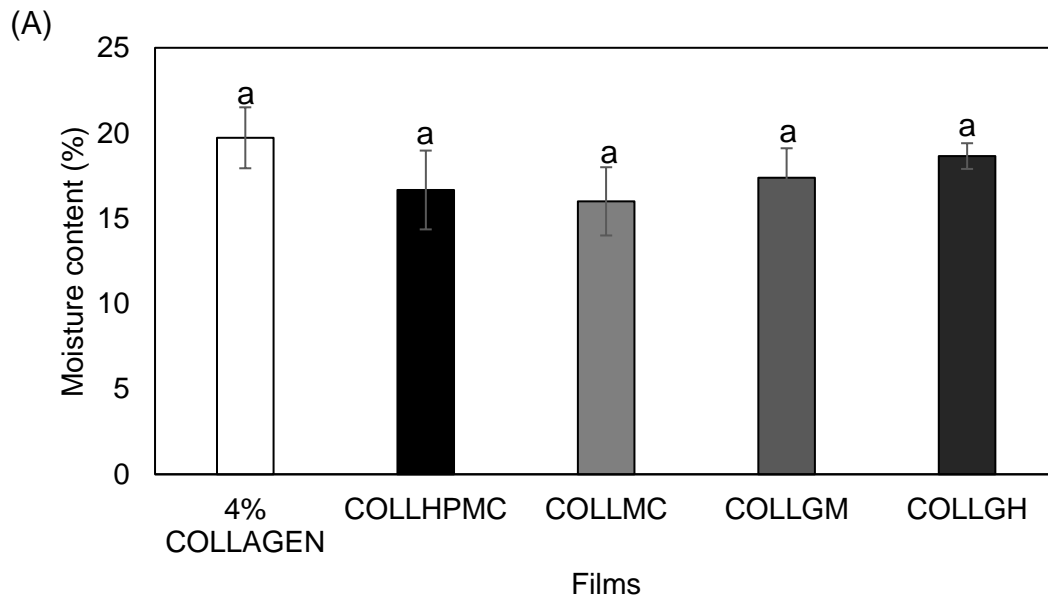
Table 4-6: FTIR absorption ratios of A_{III}/A₁₄₅₀ for collagen films with and without cellulose hydrocolloids at different collagen concentrations.

Films	A _{III} /A ₁₄₅₀ cm ⁻¹ Ratio
COLLHPMC	0.91
COLLMC	0.90
COLLGH	0.99
COLLGM	0.99
4% COLLAGEN	1.00
COLLHPMC	0.86
COLLMC	0.87
COLLGH	0.97
COLLGM	0.98
3.5% COLLAGEN	0.98
COLLHPMC	0.76
COLLMC	0.71
COLLGH	0.93
COLLGM	0.90
2.5% COLLAGEN	0.94

4.4.6 Moisture content and Thickness

Figure 4-5 shows the moisture content of collagen films with and without hydrocolloid addition. Collagen films alone show slightly higher moisture contents, although the values are not significantly different ($p > 0.05$) from the blend composite films. The slightly higher values of pure collagen films may be due to collagen's highly hydrophilic nature due to the abundance of polar groups in the structure, which increases

interactions with water molecules. Compared to the control collagen films, a decrease in moisture content upon the addition of hydrocolloids might indicate collagen-hydrocolloid molecular interaction occupying the polar sites of fibrous collagen structure, limiting the number of water molecules that can interact with said fibres. However, the state and nature of the collagen within the film may be changed, which would limit the uptake of water into the films, which could be due to molecular and supramolecular differences. No significant difference was found between collagen films containing either the derivatised cellulose (COLLMC and COLLHPMC) and guar gums (COLLGM and COLLGH). However, collagen/methylcellulose (COLLMC) films show slightly lower moisture values. The slightly lower moisture content of these films could be due to the enhanced hydrophobicity of the methyl groups, limiting the extent of the film of water uptake.



(C)

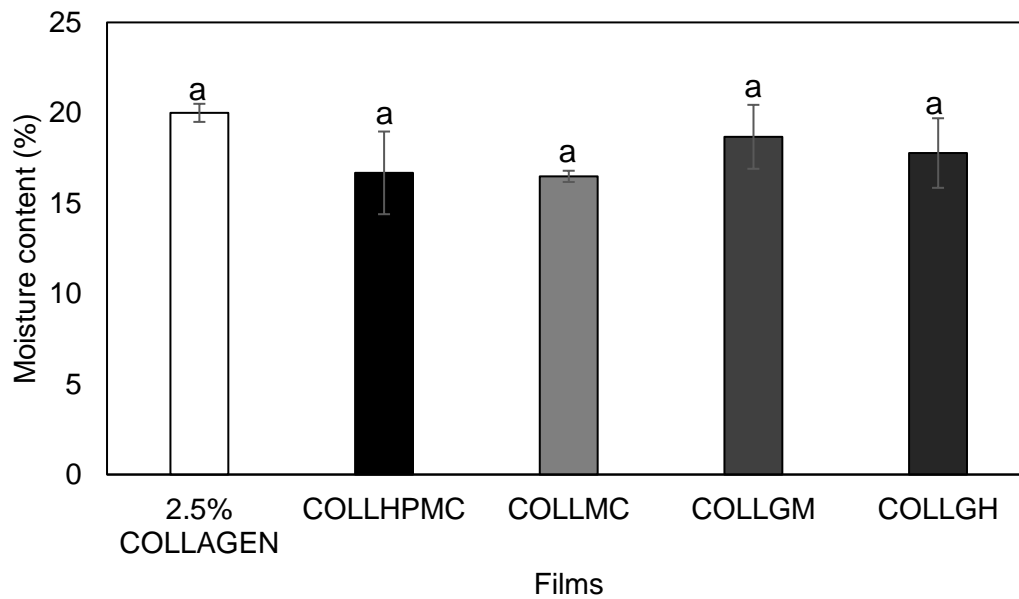


Figure 4-5: Moisture content of collagen films with and without hydrocolloid addition at different collagen concentrations, (A) 4% wt/wt (B) 3.5% wt/wt (C) 2.5% wt/wt in the pre-dried acid-swollen collagen pastes. The different letter means a significant ($P < 0.05$) difference between the films. The error bars represent the standard deviation.

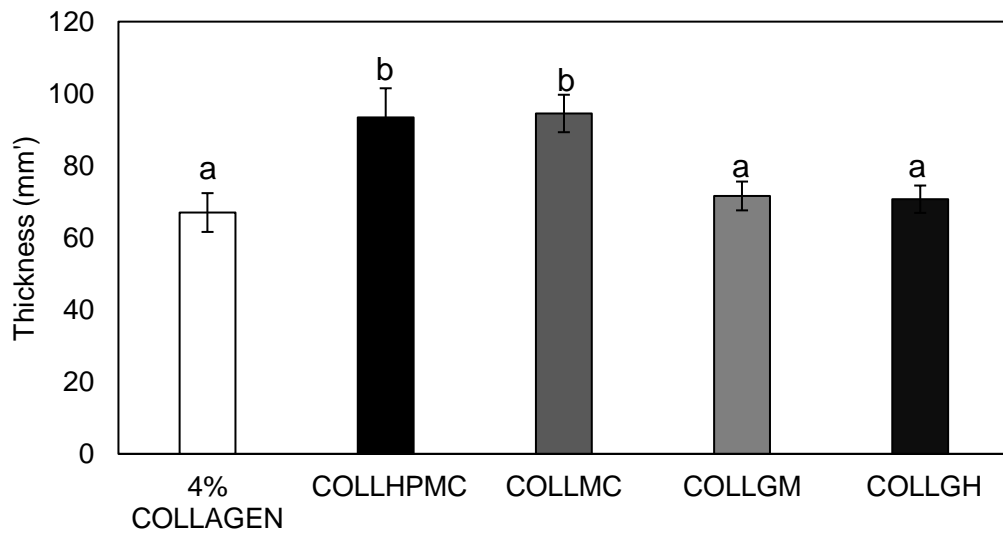
The thickness of collagen films with and without hydrocolloids prepared at various collagen paste concentrations are shown in Figure 4-6. In general, film thickness depends on preparation methods, drying conditions, film-forming solution composition, and the nature of film components (Ahmad et al., 2015). The thickness of the composite films increases substantially ($p < 0.05$) with the addition of the hydrocolloids compared to pure collagen films, and the values increase with an increase in collagen concentration. The increased film thickness upon incorporating hydrocolloids could be simply due to the initial increase in solid content. However, the ability of the collagen network to collapse during drying could also be influenced by changes in collagen molecular and supramolecular structure along with the possibility of binding the

collagen fibres with the added hydrocolloids. The thickness values of pure collagen films are higher than those reported by Wang et al. (2017c), who reported a thickness of 39.30 μm . However, the values were lower than those reported by Wu et al. (2018), with a thickness of 104 μm . The differences between those reported here are differences in the film-forming formulations, concentration of solutions or pastes, and film preparation procedures.

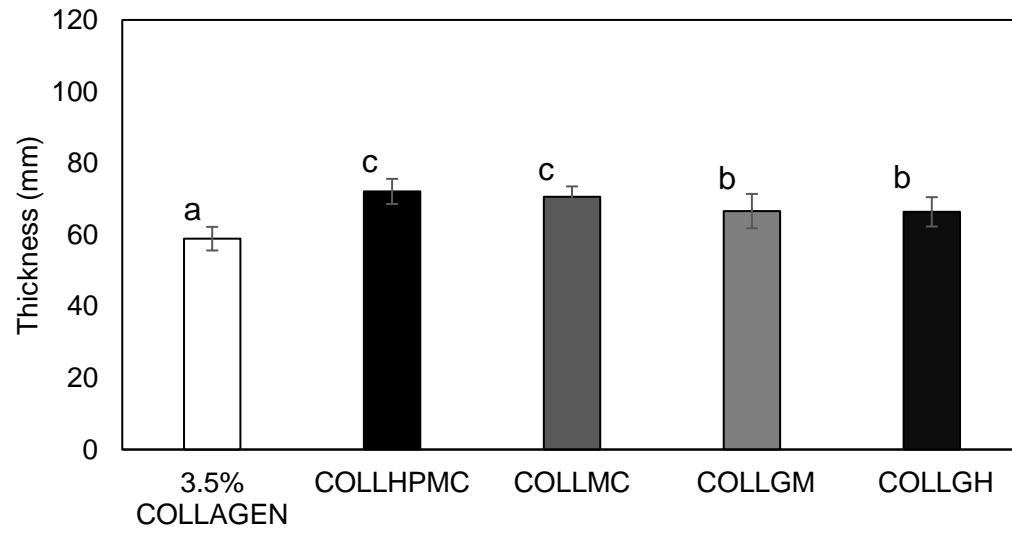
Meanwhile, among the different hydrocolloids used, collagen films containing derivatised cellulose (COLLMC and COLLHPMC) show greater thickness values than collagen films containing guar gums (COLLGM and COLLGH). This could be attributed to the higher concentrations of methylcellulose and hydroxypropylmethylcellulose in the film-forming paste and the differences they impose on the collagen structures during the drying process. While the low shear viscosity of the hydrocolloids added to the collagen pastes is the same, these film thickness differences indicate that upon drying, the molecular weight and chain stiffness of the different hydrocolloids play a role in how the collagen fibre networks can deform during water loss. Therefore, the indication is that the different molecules affect the thermodynamic incompatibility and water holding potential of the composite at the molecular and supramolecular level.

Furthermore, increasing the collagen concentration in the initial blend pastes (at constant respective hydrocolloid concentrations) also affects the thermodynamics during drying and contributes to the overall film thickness, where the lower the collagen concentration, the more impact the added hydrocolloids have. Such control of film thickness might be explored further, as the water removal rate may also play a role in the relative thermodynamic incompatibility and warrant further study.

(A)



(B)



(C)

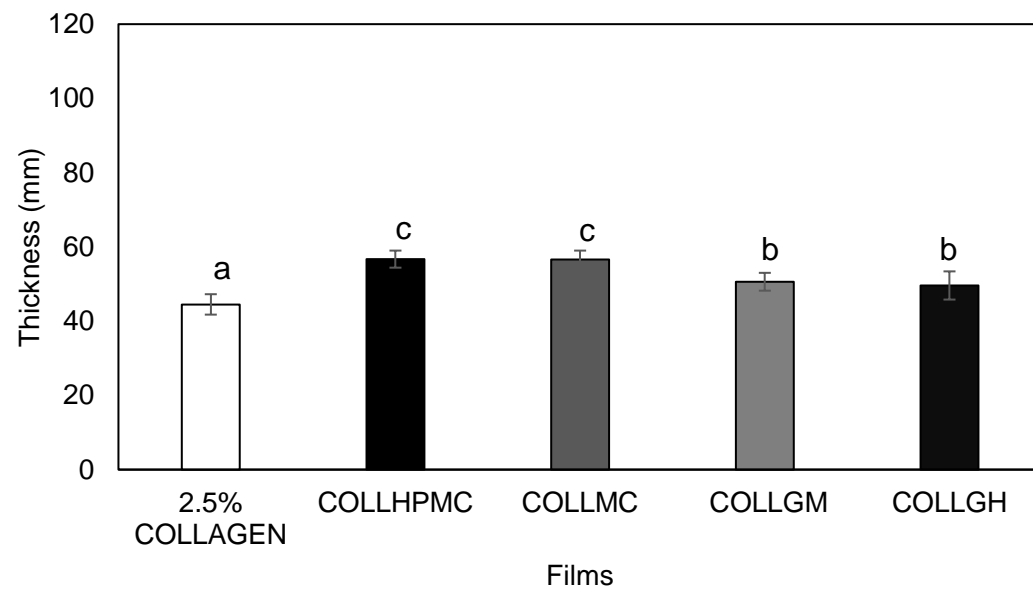


Figure 4-6: Thickness of collagen films with and without hydrocolloid addition at different collagen concentrations (A) 4% wt/wt (B) 3.5% wt/wt (C) 2.5% wt/wt in the pre-dried acid-swollen collagen pastes. The different letter means a significant ($P < 0.05$) difference between the films. The error bars represent the standard deviation.

4.4.7 Dynamic Vapour sorption

Figure 4-7 shows the moisture adsorption and desorption isotherms of the collagen films at 25 °C. All the films show a type II sigmoidal shape isotherm, typical for hydrophilic polymers (Belbekhouche et al., 2011), where the equilibrium moisture content increased with increasing RH. Pure collagen film shows slightly higher water affinity than the blend films at all the RH values, as seen in Figure 4-7 for a long time equilibrium due to the high amount of hydrophilic groups present in the collagen structure as well as the unaltered collagen structure. A similar trend is seen with the desorption curves (Figure 4-7B), indicating that the structures can take up moisture better and retain the moisture more effectively. The sorption isotherm profile obtained in this study was similar to those seen in films made from type 1 collagen and gelatin (Tanioka et al., 1974; Yakimets et al., 2007; Wolf et al., 2009; Pępczyńska et al., 2019). The composite films show slightly lower moisture uptake than pure collagen films, consistent with the moisture content values determined gravimetrically. As suggested earlier, the change in collagen structure in the films upon drying due to the presence of the hydrocolloids might affect how collagen takes up and losses water molecules. However, the effect of the hydrocolloids on reducing water uptake of the films is not pronounced, which may be due to the lower concentrations of hydrocolloids used. The equilibrium moisture content is similar for COLLHPMC, COLLGM, and COLLGH films.

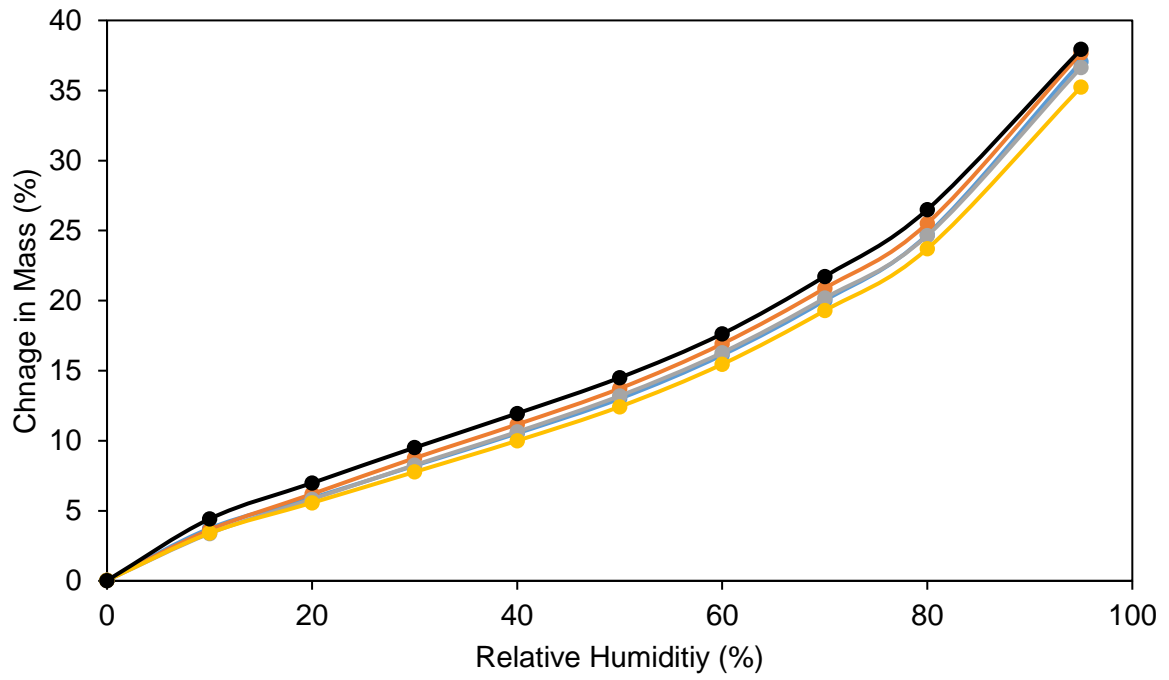
In contrast, COLLMC shows the lowest moisture sorption at all the RH investigated, which is in accordance with trend observed with the moisture content data.

The experimental data have been fitted with the Guggenheim, Anderson, and de Boer (GAB) model and the GAB parameters' values: the monolayer moisture content (cM_0), the sorption energy constants C and K are presented in Table 4-7. The GAB model fits the films adsorption isotherms very well with R^2 values > 0.999 . The monolayer (M_0) value is of particular interest as it indicates the amount of water that is adsorbed to active sites and indicates the number of sorption sites (Bilbao-Sáinz et al., 2010). As seen in Table 4-7, pure collagen film shows higher monolayer water content (M_0), attributed to the greater number of active sites available for water adsorption. This also suggests that collagen films can take up more water than the blend films and retain a higher amount of water upon drying.

The monolayer moisture content decreases slightly with the addition of hydrocolloids, suggesting reduced sorption sites, although this decrease was not statistically significant ($p > 0.05$). It is possible that due to the structural changes in collagen due to the presence of hydrocolloids interfering with the supramolecular structure of collagen, the total number of water-binding sites on collagen structure decreases. Collagen/guar films (COLLGH and COLLGM) show higher monolayer values (M_0) than collagen with derivatised cellulose films (COLLMC and COLLHPMC) films due to the increased hydrophilicity of the guar gums. Collagen with methylcellulose films (COLLMC) shows the lowest monolayer moisture content, which correlates with the moisture content data. As mentioned previously, this is due to the hydrophobicity of the methylcellulose molecules which decrease the interaction of water molecules and the film. The C parameter represents the strength of water binding to the primary sites

of the film (Villalobos et al., 2006). Pure collagen film shows a higher value of C , indicating the strength of binding of water molecules is higher in collagen films than the blend films. The K parameter, which corrects the properties of the multilayer water molecules with respect to the bulk liquid, was < 1 for all the samples, indicating the predominance of monolayer absorption and the formation of multilayers of water on the monolayer is similar for all the films (Basiak et al., 2017; Díaz-Calderón et al., 2017).

(A)



(B)

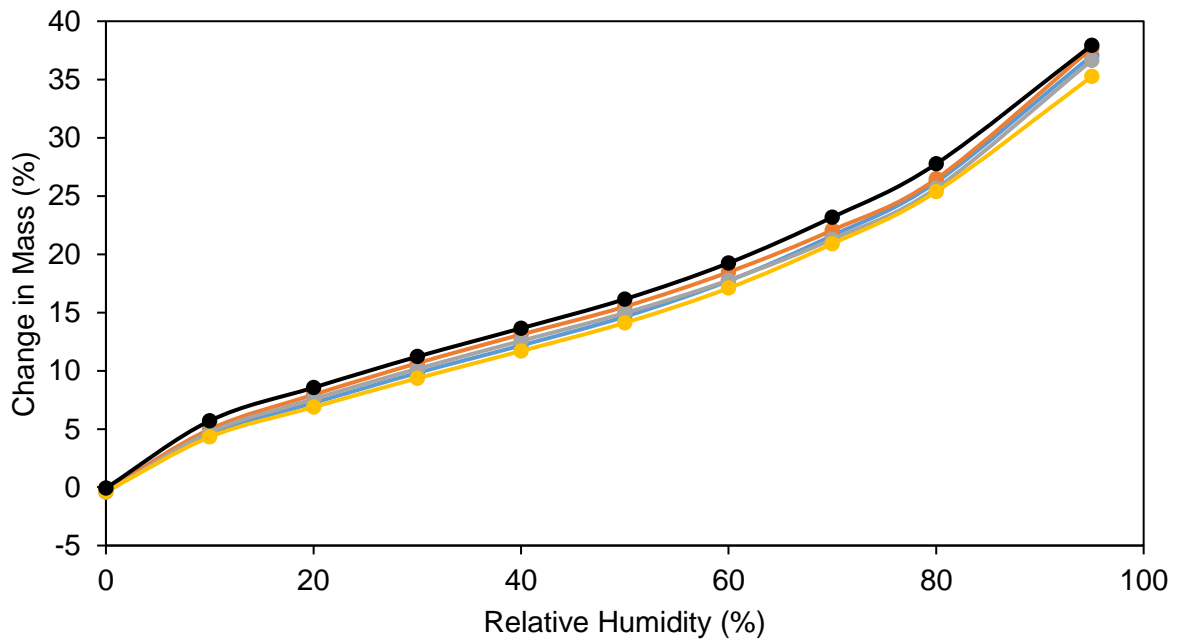


Figure 4-7: (A) Sorption isotherm, and (B) Desorption isotherms of COLLHPMC (blue line), COLLMC (yellow line), COLLGM (orange line), COLLGH (grey line) and pure

collagen (black line) films at 2.5% collagen concentration at 25 °C. The graph presented here is an average of duplicate measurements.

Table 4-7: GAB fitting parameters of sorption isotherm of collagen films with and without hydrocolloids.

Samples	M_0	K	C	R^2
COLLHPMC	10.80 ± 0.15	4.82 ± 0.18	0.77 ± 0.00	0.999
COLLMC	10.59 ± 0.10	4.56 ± 0.13	0.77 ± 0.01	0.999
COLLGM	11.49 ± 0.17	4.58 ± 0.29	0.76 ± 0.00	0.999
COLLGH	11.51 ± 0.29	4.36 ± 0.17	0.74 ± 0.01	0.999
2.5% COLLAGEN	11.93 ± 0.63	5.79 ± 0.86	0.74 ± 0.01	0.995

4.5 Conclusion

Development of composite films by mixing hydrocolloids with collagen is a potential approach to overcoming the shortcomings of pure collagen films' casings) and potentially providing new 'designer' properties. In this study, the effect of gelling and non-gelling hydrocolloids: HPMC, MC and high and medium molecular weight guar gums (at comparable viscosifying effect) on acid-swollen collagen films were investigated. The hydrocolloids showed a good dispersity in the collagen matrix, which led to films having homogenous surfaces. Compared to the pure collagen films, the composite films show higher tensile strength, stiffness, and elongation at break. This is particularly important for sausage casings as they must be able to withstand tensile stresses during processing operations and stretchable to allow the expansion and contraction of the meat batter. Meanwhile, derivatised cellulose films provided a higher level of reinforcement than guar gums. This is attributed to the high concentrations of derivatised celluloses used at comparable viscosity results in more interaction forces with the collagen fibre, consequently leading to stronger films.

The collagen concentrations played a significant role in the composite films mechanical properties as values increased with an increase in collagen concentrations. Thus, the increase in tensile strength and stiffness of the composite films depends on each hydrocolloid concentration in the film matrix, the interaction between the collagen fibre and the hydrocolloids, the-collagen fibre contents in the film matrix and the ability of collagen fibres to stabilise themselves upon drying.

Furthermore, the DSC results showed that the hydrocolloids presence increases the melting temperature of the films. This is ascribed to the interactions between

the hydrocolloids and collagen fibres, resulting in strong film networks, requiring high temperature to denature. Also, collagen films with guar gums showed higher values than collagen with derivatised cellulose films due to the higher molecular weight of the guar gums, requiring high melting energy. TGA results showed that the thermal stability of collagen fibre films was unaffected by the hydrocolloids. XRD results also demonstrated that the polymers decreased the collagens ordered structure, as shown by the blend films reduced crystalline peak. FTIR revealed a slight alteration in collagen structure, but the triple helical structure's overall integrity was not destroyed. Furthermore, the composite films moisture content values and sorption properties reduced slightly with the addition of the polymers. This was attributed to the change in the nature of collagen structure in the presence of 'he polymers. However, COLLMC showed lower sorption values of about 10.59%, which was attributed to the hydrophobicity of the MC chains.

This study has shown that the addition of hydrocolloids may serve as a potential approach to increase the mechanical properties of collagen casings for sausage manufacturing. Further studies would be required to determine the use of these films in industrial applications.

**5 THE EFFECT OF CELLULOSE AND STARCH ON THE
VISCOELASTIC AND THERMAL PROPERTIES OF ACID-
SWOLLEN COLLAGEN PASTE**

5.1 Abstract

Collagen pastes are processed by swelling minced bovine hides using acids into a swollen fibrous structure. Depending on the application, these pastes must be improved in terms of the final product's rheological properties and mechanical strength. In this work, the addition of cellulose fibres and starch granules as fillers in acid swollen collagen paste was investigated. The influence of cellulose fibre length and starch granules with different amylose and amylopectin content on the viscoelastic and thermal properties of acid swollen paste were studied as a function of collagen paste concentration. Adding cellulose and starch granules resulted in increased elastic modulus of collagen paste, with starch granules having the highest impact. Cellulose and starch also affected the $\tan \delta$ peak of collagen paste at different collagen concentrations as a function of temperature. The micro differential scanning calorimetry (microDSC) results indicated that collagen denaturation temperature was not influenced by cellulose and starch. However, when heating, the denaturation temperature of collagen pastes, with starch granules moved to lower temperatures.

5.2 Introduction

Collagen is the main structural protein of connective tissues such as tendons, bones, and skins. It consists of approximately 30% of the total protein in human and animal bodies (Hashim et al., 2015). At least 27 forms of collagen were identified in mammalian tissue, of which collagen type 1 was identified as the main structural component of connective tissue (Pati et al., 2010; Zhang et al., 2010; Wang et al., 2017a). Collagen's primary structure consists of repeating units of glycine (Gly)-proline (X)-hydroxyproline(Y). The collagen molecule made of three polypeptide chains coiled in a left-handed helix; these chains are further twisted into a right-handed superhelix stabilised by hydrogen bonds (Komsa-Penkova et al., 1996; Schroeffer and Meyer, 2017). Due to its unique characteristics, such as weak antigenicity, biodegradability, biocompatibility, bioactivity and tensile strength, collagen has been extracted into various forms such as gels, pastes, films, sponges and fibres. It is widely used in (Friess, 1998; Ding et al., 2014a). However, several challenges, such as low thermal stability and poor water vapour barrier properties, limit broader applications (Bigi et al., 2004; Mu et al., 2007). A possible means to circumvent collagen's suboptimal properties and increase its application is to incorporate other natural polymers such as polysaccharide fibres or fillers (Wang et al., 2018). These will reinforce the strength, barrier properties and thermal stability of the resulting composite structures (Wolf et al., 2009).

In the food industry, collagen type 1 extracted into a paste is used for sausage casings. Collagen casings have been applied successfully as an alternative to the relatively high cost of casings made from animal intestines (Barbut, 2010). Collagen casings possess weak mechanical properties compared to casings made from animal intestines. Consequently, there is an interest in modifying the mechanical properties

of collagen casings by adding natural biopolymers such as cellulose fibres and starch granules. These natural biopolymers are of particular interest as particulate fillers due to their natural abundance, biodegradability, and low cost (Ding et al., 2014a; Basiak et al., 2017). They have also been shown to provide great reinforcement to polymer matrices due to their high mechanical strength (Dufresne and Vignon, 1998; Bledzki and Gassan, 1999). Cellulose is the most abundant natural polymer on earth and is a significant component of higher plants' cell walls and some bacteria, such as *Acetobacter xylinum* strains. Cellulose has a complex and highly ordered chemical structure similar to collagen, albeit polysaccharide, not protein origin. It is a linear homopolymer composed of β -D-glucopyranose units linked with β -1, 4 glycosidic linkages. It is used in the food industry as a texturiser, non-caloric bulking agent, thickener, stabiliser and raising agent (Yoon and Lee, 1990; Ang and Miller, 1991; Harris and Smith, 2006).

Starch is a well-known storage carbohydrate in insoluble granules in plant cells (Sullo and Foster, 2010). Semi-crystalline starch granules are made up of two polysaccharides. The first is amylose, which contains the granule's amorphous region and has long linear (1-4) linked α -D-glucopyranose residues. The second is amylopectin, which is composed mainly in the crystalline region of the granule and is a highly branched molecule consisting of shorter chains of (1-4) α -D-glucopyranose residues with (1-6) - α -D-glycosidic branched linkages (Buléon et al., 1998; Jane et al., 1999). Starch is obtained from various sources such as cereal, tuber and root crops used in a wide range of applications, such as food, pharmaceutical, paper and plastic. Starch has unique physicochemical and functional properties; hence it is used as a thickener, colloidal stabiliser, gelling agent, adhesive and water retention agent in various industries (Singh et al., 2003; Copeland et al., 2009b).

In recent years, there has been an increased interest in blending collagen with other natural biopolymers to develop products with new and modified functional properties and provide cost and processing advantages. Several studies demonstrated that the addition of polysaccharides into collagen solutions could change the thermal and rheological properties of collagen solutions. Ding et al. (2014a) reports enhancement upon the hydroxypropyl methylcellulose (HPMC) improved the rheological and thermal stability of collagen solutions. It was attributed to a hydrogen bond interaction and compatibility between the collagen and HPMC molecules. Nicoletti and Telis (2009) reported that about 0.1% of xanthan gum increased the collagen solution's gel strength when heated. Increasing the concentration of xanthan to about 0.3% resulted in a weaker gel, while the addition of maltodextrin led to a more fluid-like structure, which was suggested to be due to the thermodynamic incompatibilities between the biopolymers.

Similarly, Oechsle et al. (2015) studied the influence of incorporating co-gelling biopolymers of different molecular weights; low molecular weight (whey protein isolate and blood plasma protein), or high molecular weight (soy protein isolate and gluten) into a collagen matrix, and they reported that they displayed effects when added to the collagen gels, affecting the collagen network and embedding within it. Therefore, this study aimed to understand how cellulose addition with different fibre lengths and starch granule fillers affects the viscoelastic and thermal properties of acid swollen collagen pastes. The viscoelastic properties were investigated using small oscillation rheological measurements, and the thermal changes were studied using a microDSC. Both rheological and thermal measurements were studied as a function of collagen paste concentration. The effect of biopolymer morphology and aspect ratios was also considered. It was hypothesised that matching the phase volume of the fillers will give

the same viscosity build-up and would have the same effect on collagen paste's viscoelasticity. A similar effect will be observed when the phase volumes of the polysaccharide are matched.

5.3 Materials and Methods

5.3.1 Materials

Collagen pastes (5 %w/w collagen concentration) at pH of 2 was provided by Devro plc. Cellulose fibres of different fibre lengths, Solka floc 300 (SF3; 22 μm) and Solka floc 900 (SF9; 100 μm), were supplied by the International Fibre Corporation (New York, USA). Amioca (waxy corn starch WS; pure amylopectin; contains only trace amounts of amylose) and Hylon VII (high amylose corn starch; HAS) were kindly donated by Ingredion (Manchester, UK).

5.3.2 Methodology

5.3.2.1 Determination of phase volume (ϕ)

The phase volume of cellulose and starch dispersions were measured by centrifugation (Thermo Electron Corporation, Ohio, USA) using a centrifugation force of 2000g for 20 mins at 20 °C. Cellulose and starch dispersions at a total solid concentration ranging from 1% to 7% were transferred into 50 ml conical bottom centrifuge tubes. After centrifugation, the total height H_T of the sample and the height of the sediment H_s were measured, and the phase volume of the cellulose and starch dispersions were calculated based on the method described by Hemar et al. (2011):

the height of the sediment divided by the total height multiplied by 100. The concentrations of cellulose and starch dispersions needed for a 15% phase volume (

Table 5-1) were extrapolated from a graph of phase volume against concentration (not shown).

Table 5-1: Concentration of cellulose and starches required at 15% dispersed phase volume

Dispersions	Concentration (% wt) for dispersed phase volume of = 15%
Solka floc 300 (SF3)	2.7
Solka floc 900 (SF9)	1.8
Waxy starch (WS)	7
High amylose starch (HAS)	6.6

5.3.2.2 Preparation of collagen-cellulose and collagen-starch blends

The concentrations of cellulose and starch (

Table 5-1) corresponding to a phase volume of 15% were prepared by dispersing the powders in deionised water. The dispersions were mixed with collagen paste at different collagen/cellulose (solka floc 300 and solka floc 900) and collagen/starch (waxy starch and high amylose starch) mixing ratios (w/w) i.e., 80:20, 70:30 and 50:50.

The final concentrations of the collagen pastes at the various mixing ratios were 4% (w/w), 3.5% (w/w) and 2.5% (w/w). The collagen paste with cellulose dispersions and starch dispersions were mixed by gently stirring at room temperature for 15 min using an overhead stirrer (yellow line IKA OST 20 high torque Overhead Stirrer). The pH of the final blends was between 2 and 2.5. Samples were degassed using an Audionvac VMS 53 multivac vacuum packager (Audion Elektron, Netherlands) to remove the air bubbles incorporated during mixing before further analyses were performed. The blends formulation and sample codes are shown in Table 5-2.

Table 5-2: Formulation of collagen-cellulose and collagen-starch blends at various mixing ratios and different concentrations of collagen. SF3 = Solka floc 300, SF9 = Solka floc 900, WS = Waxy starch, HAS = High amylose starch, Φ = phase volume.

	Mixing ratio Collagen: fillers dispersion	Stock Conc.of collagen paste	Stock Conc. of fillers dispersions	Conc. of collagen in the blends	Conc. (%wt) of cellulose/starch for Φ = 15% in the blends (%wt)
COLLSF3	80:20	5	13.5	4	2.7
	70:30	5	9	3.5	2.7
	50:50	5	5.4	2.5	2.7
COLLSF9	80:20	5	9	4	1.8
	70:30	5	5.6	3.5	1.8
	50:50	5	3.4	2.5	1.8
COLLWS	80:20	5	35	4	7
	70:30	5	23.3	3.5	7
	50:50	5	14	2.5	7
COLLHAS	80:20	5	33	4	6.6
	70:30	5	22	3.5	6.6

50:50

5

13.2

2.5

6.6

5.3.2.3 Measurement of paste viscoelasticity

Small amplitude oscillatory rheology of the collagen pastes with and without cellulose/starch was performed using a controlled stress rheometer (Physica MCR 301, Anton Paar, Austria), using a parallel plate (diameter 50 mm, gap 1.5 mm) geometry. After loading the samples, the excess pastes were trimmed. The edges of the exposed sample were covered with low viscosity mineral oil to prevent moisture evaporation and drying of pastes during the measurements. The samples were equilibrated for 5 mins before measurements were conducted; this was performed to avoid temperature variations within the samples. The dynamic viscoelastic measurements were performed by subjecting the samples to various profiles: (i) amplitude sweeps were conducted at a constant angular frequency (10 rad/s) to determine the maximum deformation attained by the sample in the linear viscoelastic range (ii) frequency sweeps were performed from 0.1-100 rad/s at 20 °C and a constant strain of 0.1% (selected from LVE region) (iii) dynamic temperature sweeps were conducted at a constant strain of 0.1% and frequency of 10 rad/s. Collagen pastes with/without cellulose and starch were heated from 5 to 80 °C at a rate of 5 °C/min. The storage modulus (G'), loss modulus (G''), and loss factor ($\tan \delta = G''/G'$) were recorded as a function of frequency or temperature. Each test was performed at least three times, and data were analysed using Anton Paar Rheoplus software (Physica, Anton Paar, Austria).

5.3.2.4 Differential Scanning Calorimeter (microDSC)

The pastes denaturation temperature (T_d) was determined using a micro-DSC (MicroDSC III, SETARAM Instrumentation, Calurie, France). Approximately 0.8 g of the samples were weighed into Hastelloy cells and sealed with O rings and Hastelloy

screw tops. Samples were loaded in the DSC instrument at 20°C and then cooled to 3°C at 1°C/min. Collagen pastes with/without cellulose and starch were heated up to 95 °C. Samples were then held at 95°C for 15 mins and cooled down to 3°C, and reheated to 95 °C at 1°C/min. A Hastelloy cell filled with RO water was used as a reference. The onset (T_O), offset, peak temperatures (T_{Peak}) and enthalpy of transition (ΔH) were processed using Calisto Processing software v1.43 (AKTS, Switzerland). The peak temperature of the thermogram was taken as the melting or denaturation temperature of collagen. Runs were performed in duplicate, and the average and standard deviation reported.

5.3.2.5 Statistical analysis

Analysis of variance ANOVA was used to determine the difference between samples using Statistical Package for Social Science Software (SPSS Inc.). When there were any differences between samples, Tukey's test was used to determine the significance of the means of the samples ($P < 0.05$).

5.4 Results and Discussion

5.4.1 Dynamic Frequency sweep

Figure 5-1 and Figure 5-2 shows the frequency dependency of the storage modulus (G'), the loss modulus (G'') and the loss tangent ($\tan \delta$) for COLLSF9, COLLSF3, COLLWS and COLLHAS pastes at the different collagen concentrations. The mechanical spectra of collagen pastes with starch granules and cellulose fibres at all mixing ratios show that all the pastes exhibit a solid-like behaviour as the storage modulus was higher than the loss modulus throughout the frequency range investigated. This is the typical behaviour of biopolymer gel where G' (storage modulus) is usually greater than the G'' (loss modulus) at the range of angular frequencies investigated (Ross-Murphy, 1995). The magnitude of the dynamic mechanical spectra of the collagen paste was modified after the addition of cellulose and starch, although the enhancement in G' was dependent on collagen concentration. Similar behaviour has also been reported by Oechsle et al. (2015), who studied the influence of gluten, soy isolate and blood plasma proteins on the viscoelastic properties of collagen gels. COLLWS and COLLHAS pastes had higher values of storage modulus than COLLSF3 and COLLSF9 pastes, which suggests that the addition of starch promoted a stronger network structure. However, at 4% collagen, the effect of starch is more pronounced than cellulose and this was attributed to the poor dispersibility of the cellulose fibres in the collagen matrix. Ahmed and Jones (1990) reported that the viscoelastic properties of composite materials are dependent on factors such as size, shape, concentration and distribution of the reinforcing polymers. Thus, the higher storage modulus observed for COLLWS and COLLHAS pastes might be due to the higher concentration of starch granules needed to match the phase volume of cellulose and differences in particle shape, sizes and packing.

Also, increasing filler content increases the modulus of a filled system (Ahmed and Jones, 1990). Tatsumi et al. (2002) reported that fibre suspensions would give higher elasticity than spherical suspensions when matched at equal volume concentration. In contrast, the results of this study show that when starch granules and cellulose fibres were compared at the same phase volume, starch granules were more effective at reinforcing the elastic modulus of acid swollen collagen pastes. Also, at all the collagen concentrations studied, cellulose fibres with longer (COLLSF9) and shorter (COLLSF3) fibre lengths both had similar effects on the G' and G'' of the pastes. This could be attributed to the fact that the volume fraction of the shorter fibre length (SF3) and longer fibre length (SF9) were matched in the final mixtures at all the mixing ratios studied. Hemar et al. (2011) indicated that the rheological behaviour of dispersions is related to the volume fraction that the particles occupy. Moreover, if the volume fraction of the cellulose fibres with different fibre lengths were not matched, differences in their packing densities and aspect ratios might affect the viscoelastic properties of collagen.

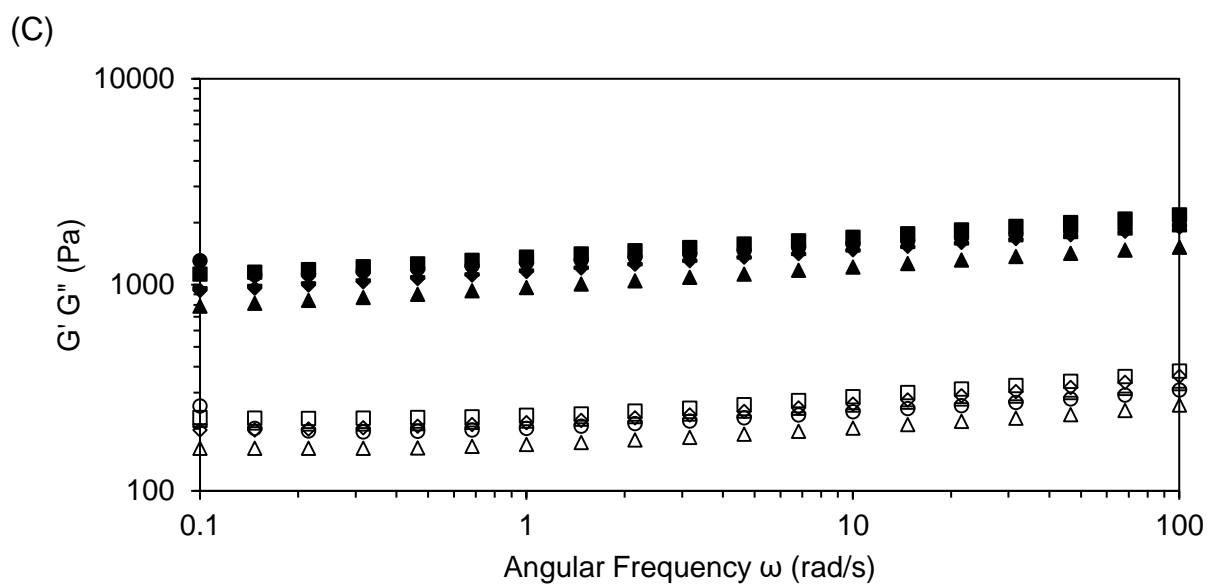
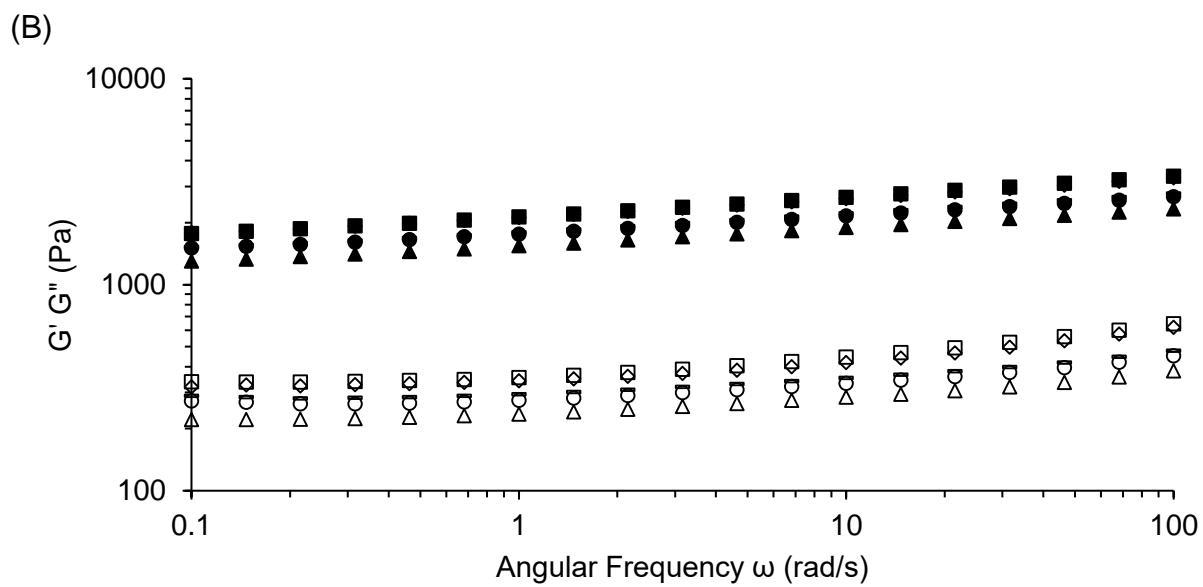
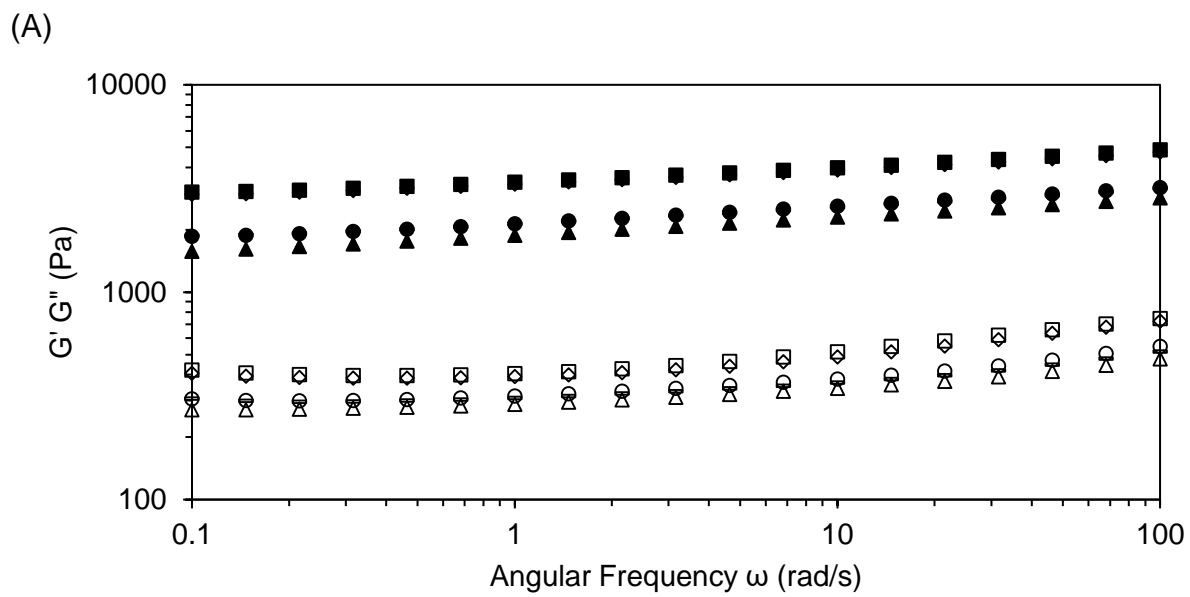


Figure 5-1: Storage modulus G' (closed symbols) and loss modulus G'' (open symbols) as a function of angular frequency for COLLSF3 (●), COLLSF9 (—), COLLWS (■), and COLLHAS (◆) and COLLAGEN (▲). At (A) 4%, (B) 3.5% and (C) 2.5% Collagen concentrations at 20 °C.

The $\tan \delta$ values of the blends at the various formulations were lower than one, indicating that the elastic component dominated over the viscous component (Figure 5-4A-C). The $\tan \delta$ value was dependent on the collagen concentrations; higher $\tan \delta$ values were observed for COLLSF3, COLLSF9, COLLWS, and COLLHAS pastes at a ratio of 50:50 (2.5% collagen concentration). This indicates that the pastes were weaker in structure than pastes at ratios 80:20 (4% collagen concentration) and 70:30 (3.5% collagen concentration). The most striking observation to emerge from the $\tan \delta$ data is the difference in the $\tan \delta$ shape at the various formulations. The $\tan \delta$ values of collagen with cellulose and starch mixed at a ratio of 80:20 and 70:30 decreased when the oscillation frequency increased from 0.1 to 1 angular frequency with a further increase in $\tan \delta$ values at higher frequencies. A similar frequency dependency of $\tan \delta$ was found for chicken-wheat flour doughs (Mohammed et al., 2011). However, at a ratio of 50:50, $\tan \delta$ values decreased when the frequency increased from 0.1 to 10 angular frequency and was almost constant at higher frequencies. This indicates that the pastes were solid-like when a slow change in stress is imposed, but when subjected to fast motions, the pastes behave more like a liquid.

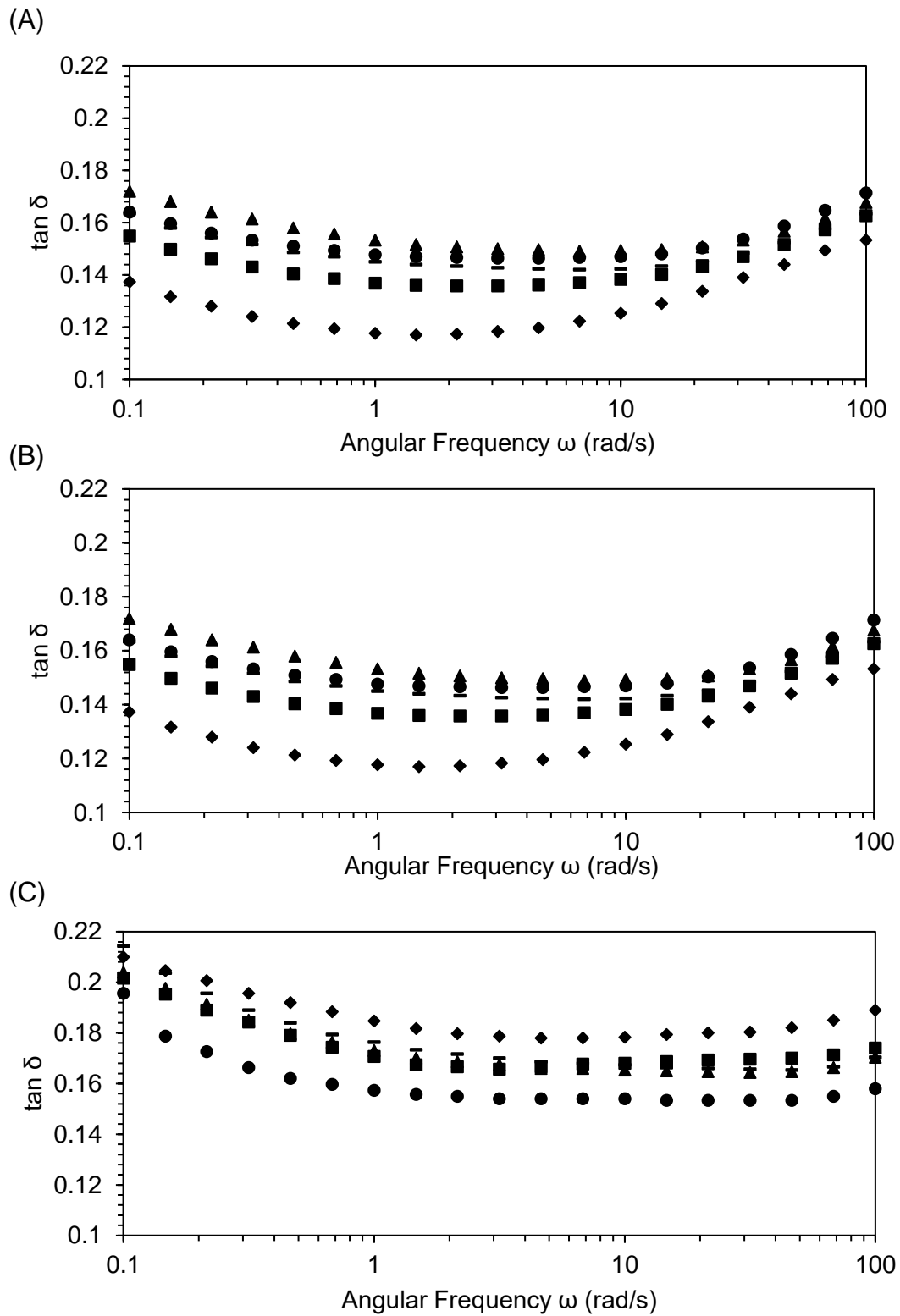


Figure 5-2: Loss factor $\tan \delta$ as a function of angular frequency for COLLSF3 (\bullet), COLLSF9 (—), COLLWS (\blacksquare), and COLLHAS (\blacklozenge) and COLLAGEN (\blacktriangle) pastes at

different collagen concentrations (A) 4% collagen (B) 3.5% collagen (C) 2.5% collagen.

5.4.2 Dynamic Temperature sweep

Figure 5-3 and Figure 5-4 shows the changes in storage modulus (G'), loss modulus (G'') and loss factor ($\tan \delta$) of COLLSF3, COLLSF9, COLLWS, and COLLHAS pastes at various collagen concentrations as a function of temperature. All the samples at the various mixing ratios showed no changes in G' with stable $\tan \delta$ values at temperatures from 10 °C to 33 °C. However, the G' rapidly decreased at approximately 34 °C (Figure 5-3), with a corresponding increase in $\tan \delta$ (Figure 5-4). Similar behaviour was observed when a collagen solution was studied as a function of concentration and temperature (Lai et al., 2008). This behaviour was due to the loss of mechanical strength due to the structural transition of the collagen triple helix to a random coil conformation. The temperature where G' decreased steeply closely matched the onset of denaturation (T_o about 34 °C) measured by the micro-differential scanning calorimeter, indicating helix to random coil transition (detailed later in section 5.3.3).

Furthermore, as depicted in Figure 5-3A-C, the addition of waxy starch to different concentrations of collagen pastes resulted in an increase in G' between 68 °C and 76 °C and a maximum at 76 °C with a corresponding decrease in $\tan \delta$ values at a temperature of 72 °C. This increase in G' and reduction of $\tan \delta$ can be ascribed to the swelling of the starch granules due to the melting of the amylopectin region (Donovan, 1979; Tester and Morrison, 1990b; Hsu et al., 2000). However, with further increases in temperature above 76 °C, a decrease in G' was observed for COLLWS pastes attributed to the loss of granule integrity and subsequent break down of the starch granules at a higher temperature. Similar findings were reported by Sullo and

Foster (2010) for waxy maize starch/hydrocolloid mixtures. It was shown in this work that the G' of the mixture increased at about 60 °C with a further decrease at higher temperatures (Sullo and Foster, 2010). On the contrary, the addition of high amylose starch to different concentrations of collagen paste did not increase G' at higher temperatures, which means that the granules of amylose starch did not swell under the range of temperatures the rheological measurements were performed. This is expected, as it has been reported that amylose molecules swell in the temperature range of 104 °C and 125 °C (Kibar et al., 2010).

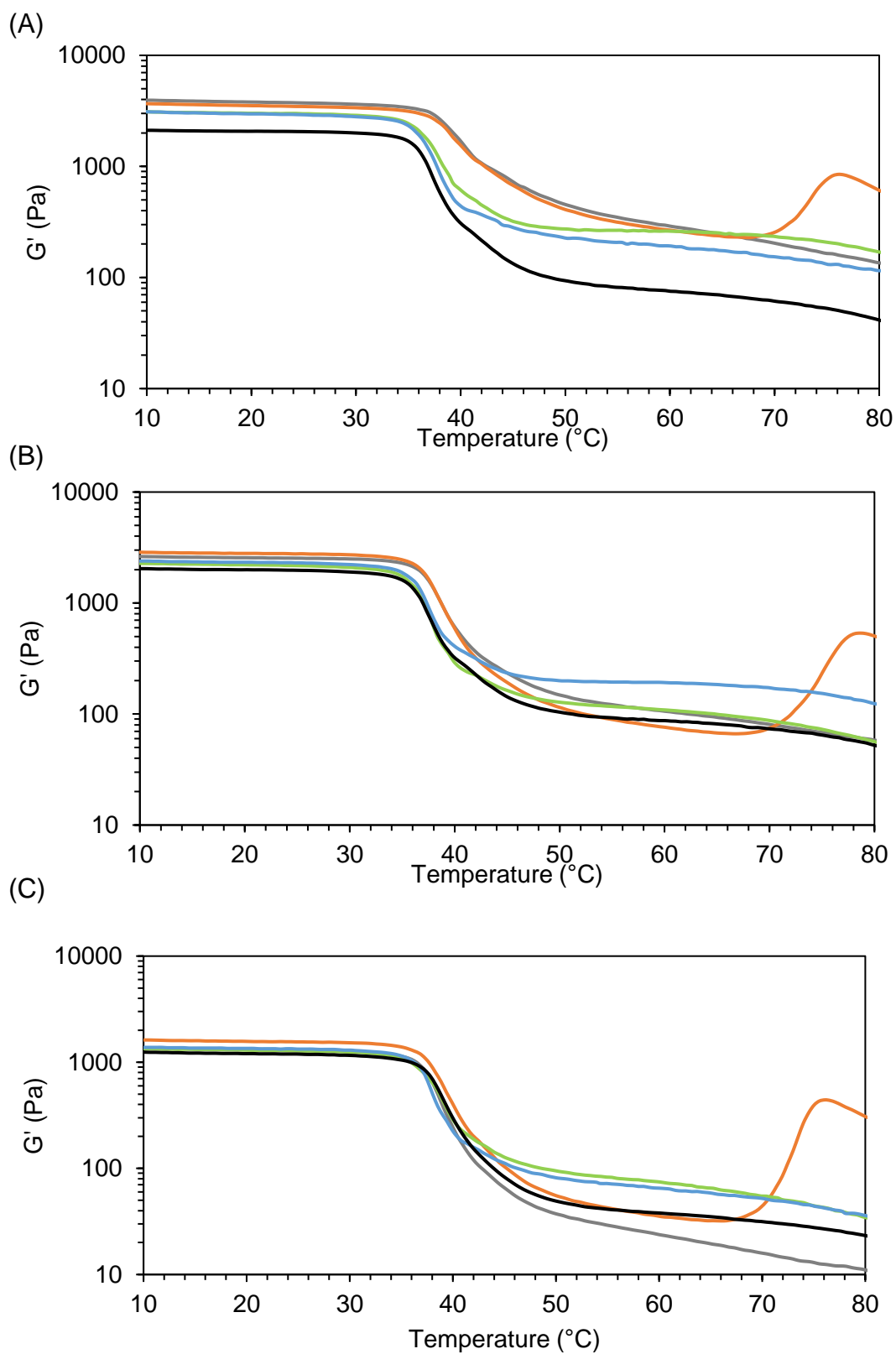


Figure 5-3: Storage modulus G' as a function of temperature during heating for COLLHAS (grey line), COLLWS (orange line), COLLSF3 (green line), COLLSF9 (blue

line) and COLLAGEN (black line) pastes at different collagen concentrations (A) 4% collagen (B) 3.5% collagen and (C) 2.5% collagen concentrations.

The loss factor ($\tan \delta$) values of collagen with and without cellulose/starch pastes (Figure 5-4) at the various collagen concentrations were lower than 1, indicating that their overall behaviour was solid-like. Some studies have reported that during oscillatory rheological measurements, the temperature at which $\tan \delta$ reached a peak value could be taken as the dynamic denaturation temperature of collagen (T_{dd}) (Lai et al., 2008; Zhang et al., 2010; Ding et al., 2014a). Hence the dynamic denaturation temperature of COLLSF3, COLLSF9, COLLWS and COLLHAS at the different collagen paste concentrations was recorded as 42 °C, which was slightly higher than that measured by microDSC (37 °C). Also, the different measurements report on the melting at different length scales. DSC report on the helix-coil transition directly, whereas the rheological measurement is dependent on the melting and softening of the helical aggregates as the helices melt. This result implies that differences could influence the thermal denaturation of the collagen triple helix in the heating rate used by each instrument.

Furthermore, a drastic drop in $\tan \delta$ was observed for all the samples at about 42 °C. This has been attributed to the glass/rubbery transition of the denatured collagen (Pietrucha, 2005). It is also interesting to note that the $\tan \delta$ peak value of COLLWS and COLLHAS pastes were lower than that of COLLSF3 and COLLSF9 pastes, indicating that the collagen pastes with starch granules were more rigid in comparison to collagen pastes with cellulose fibres. The lower $\tan \delta$ values observed for COLLWS and COLLHAS pastes might be due to the presence of closer packing of the starch granules in the collagen matrix, which reduced the molecular mobility of the collagen

triple helix molecules during heating. This is compared to cellulose fibres that were not closely attached to the collagen matrix, thus allowing the collagen chains' easy mobility. Another explanation is that the higher concentrations of starch granules resulted in a stronger network structure, which led to an increase in the restriction of the collagen chains and a reduction in the damping values. Mohanty suggested that the magnitude of the damping factor ($\tan \delta$) peak of composite materials is affected by incorporating fillers, the extent of packing and the concentration of the filler (Mohanty et al., 2006).

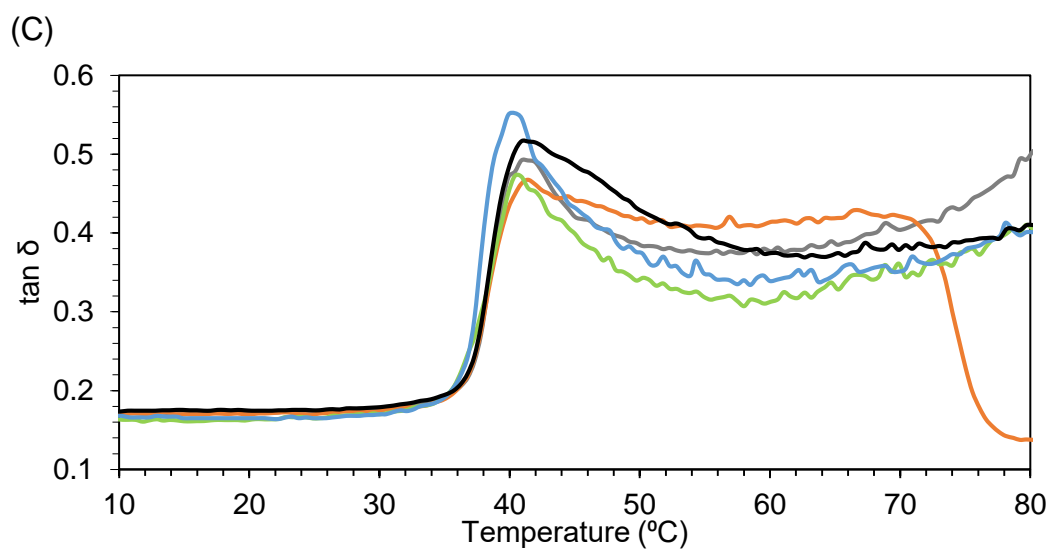
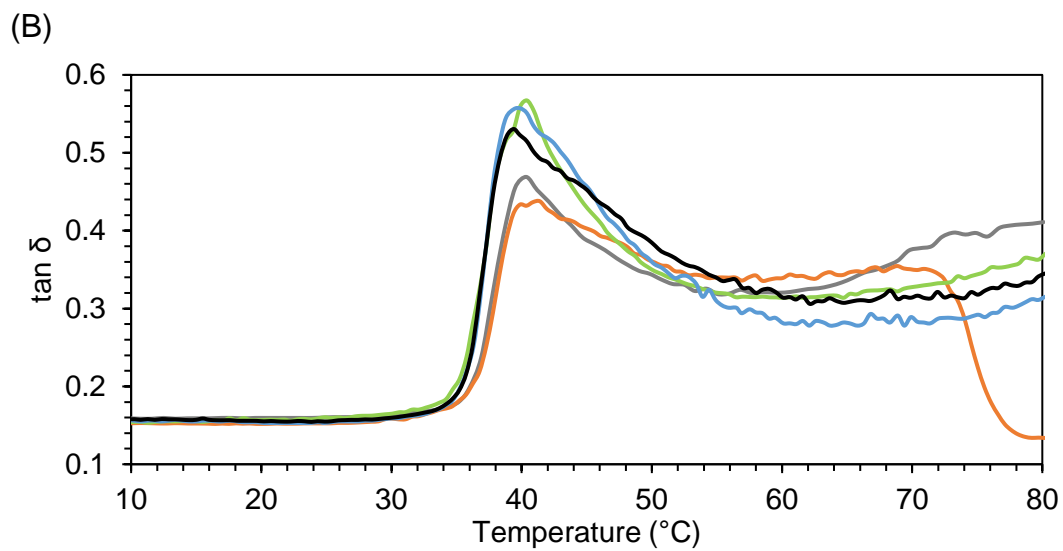
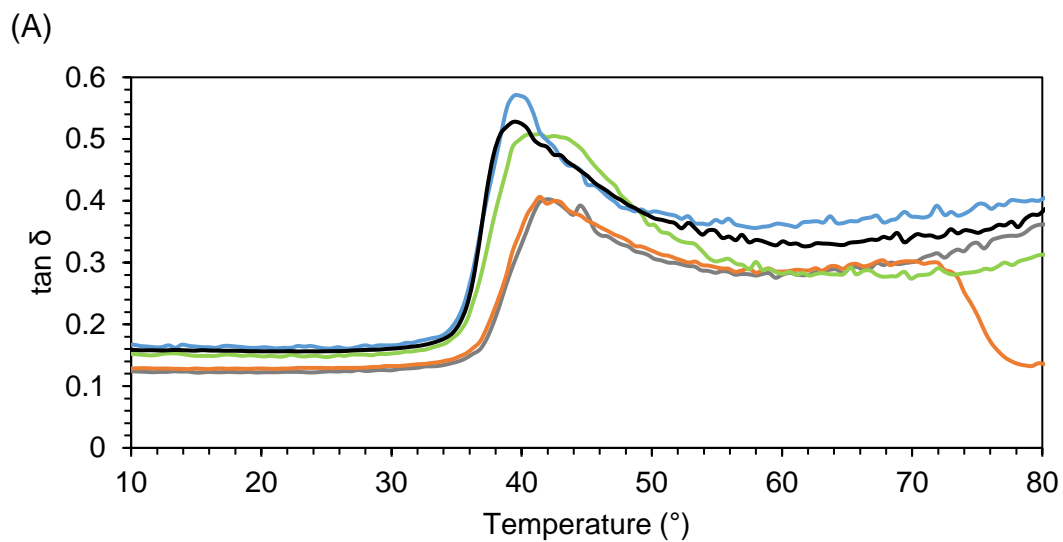


Figure 5-4: Loss factor $\tan \delta$ as a function of temperature for COLLHAS (grey line), COLLWS (orange line), COLLSF3 (orange line), COLLSF9 (blue line) and COLLAGEN (black line) pastes at different collagen concentrations (A) 4% collagen (B) 3.5% collagen and (C) 2.5% collagen concentrations.

5.4.3 Thermal properties

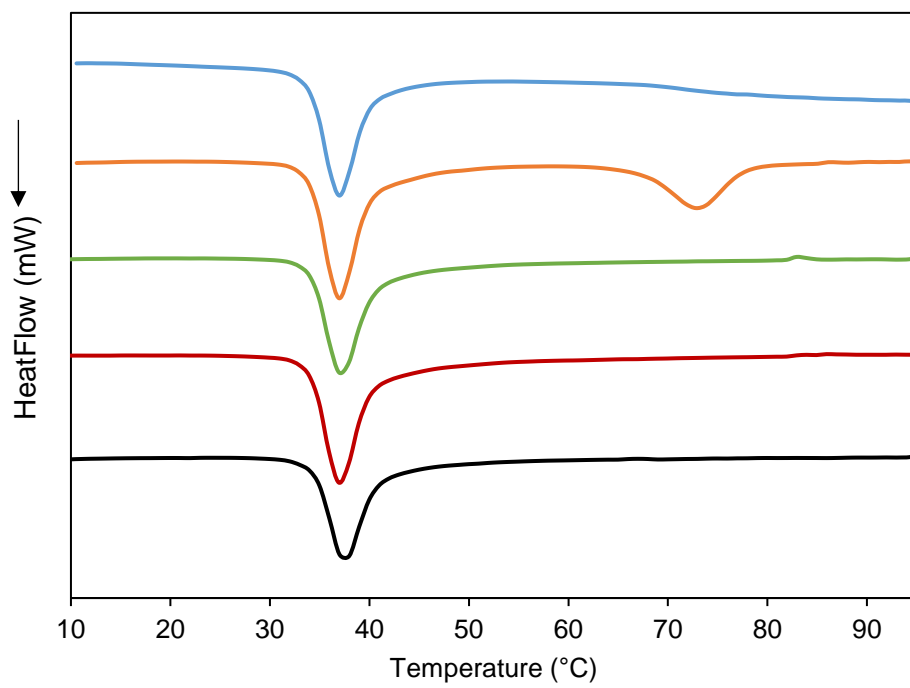
The thermal properties of the collagen pastes with and without the addition of cellulose and starch are summarised in Table 5-3. As depicted in Figure 5-5, pure collagen, COLLSF3 and COLLSF9 pastes (various formulations) exhibited a single endotherm at approximately 37 °C. The transition temperature was associated with the transition of collagen molecules from the triple helix to a randomly coiled conformation induced by the thermal disruption of hydrogen bonds in the collagen molecule (Bigi et al., 2004). In contrast, COLLWS and COLLHAS exhibited two endothermic peaks, the first peak was related to the denaturation of collagen and the second peak corresponds to gelatinisation of the starch granules (Figure 5-5). Starch gelatinisation involves the irreversible swelling of starch granules when heated in excess water (Tester and Morrison, 1990b; Morris, 1990). It was observed that the COLLWS showed a pronounced gelatinisation peak at 73°C, similar to previous reports (Liu et al., 2006). This endotherm can be attributed to the widely accepted gelatinisation of the amylopectin starch granules due to the disruption of the amylopectin crystallites (Donovan, 1979; Tester and Morrison, 1990b; Koganti et al., 2011). However, the endotherms for COLLHAS pastes were not as sharp as those of the waxy maize starch, which contains amylopectin; instead, the beginning of a broad endotherm can be observed from 68 °C. Such a broad peak was also observed previously for corn starch with high amylose content, within the temperature range of 65 to 115 °C (Liu et

al., 2006), suggesting it resulted from a composite consisting of both gelatinisation and a phase transition of the amylose lipid complex. In measurements of high amylose starch's pasting properties up to 140 °C, gelatinisation peaks beginning at 100 °C and peaking at 120 °C is observed (see chapter 7 section 7.3.2), supporting the fact that the broad peak seen in the DSC endotherms would be consistent with starch-lipid complexes. These results were expected because waxy maize contains about 99% amylopectin, which constitutes the crystalline regions of the starch. On the other hand, amylose restricts the swelling of the starch due to the leaching out of amylose during the gelatinisation and formation of complexes with the lipid's presence in starch granules, which limits the rate at which water penetrates the starch granules. Also, it was observed that decreasing the collagen concentrations from 4% to 2.5% resulted in a slight increase in the peak value temperatures of the collagen/cellulose and collagen/starch pastes. Overall, the transition temperatures of COLLSF3, COLLSF9, COLLWS and COLLHAS pastes were not significantly different ($P > 0.05$) from pure collagen pastes at the collagen concentrations studied. The endothermic peaks of the COLLSF3, COLLS9, COLLWS, and COLLHAS pastes at various collagen paste concentrations observed on reheating are shown in Figure 5-6, and the thermal transition parameters of all formulations are detailed in Table 5-4. The endothermic peak appeared at lower temperatures between 24 °C – 26 °C for all the samples. During the thermal denaturation of collagen, the triple helix is disrupted to give a random coil conformation (gelatin). However, on cooling (see supplementary figure 1), the random coils undergo a conformational disorder-order transition and partly renatures to a triple-helix structure similar to collagen but with a lower molecular weight (Machado et al., 2002; Bigi et al., 2004). Gilsenan and Ross-Murphy (2000) suggested that lower molecular weight gels melt at lower temperatures than high molecular

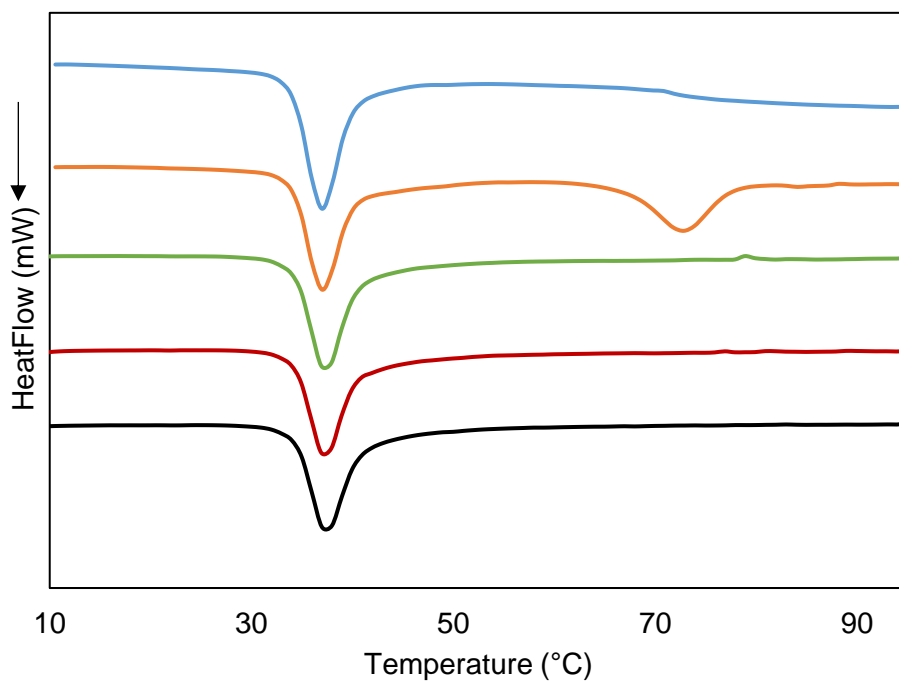
weight gels. Also, the lower transition temperature could indicate the formation of lower and less ordered helical bundles and reduced helix length (Michon et al., 1997; Aymard et al., 2001). Thus, this might explain the lower denaturation temperatures observed on the second DSC scans.

Furthermore, as shown in Table 5-4, the COLLWS and COLLHAS pastes enthalpies were significantly lower ($P < 0.05$) than those of the COLLSF3, COLLSF9 and pure collagen pastes. The decrease in the enthalpy can be related to a reduction in the ordering and semi-crystalline nature of the reformed gelatin-like matrix, after collagen melting, upon cooling. Such a decrease might not be expected if the two materials do not affect one another. Lorén et al. (2001) have shown that phase separation and subsequent phase concentration does not impact the amount of gelatin helices formed. Therefore, we do not expect that confinement effects would reduce the ability of the collagen to reform triple helices. Thus, an unexpected molecular interaction between collagen chains and starch may reduce the creation of a gelatin-like network. Indeed, when mixtures highlighted in Figure 5-4 are dried, mixtures containing starch also show a decrease in enthalpy. This is a phenomenon that is currently under further exploration. Finally, the transition enthalpy for COLLWS pastes was slightly higher than COLLHAS pastes. However, this increase in enthalpy for COLLWS was not significantly different ($P > 0.05$) from the enthalpy values of COLLHAS at 3.5% and 2.5% collagen concentration. An explanation for this might be due to the high molecular weight and branched chains of amylopectin, indicating a larger amount of energy was needed to melt the regenerated triple helix of the COLLWS paste. Also, waxy starch consists mostly of crystalline regions and requires more energy of melting than starches with high amylose starch (Koganti et al., 2011).

(A)



(B)



(C)

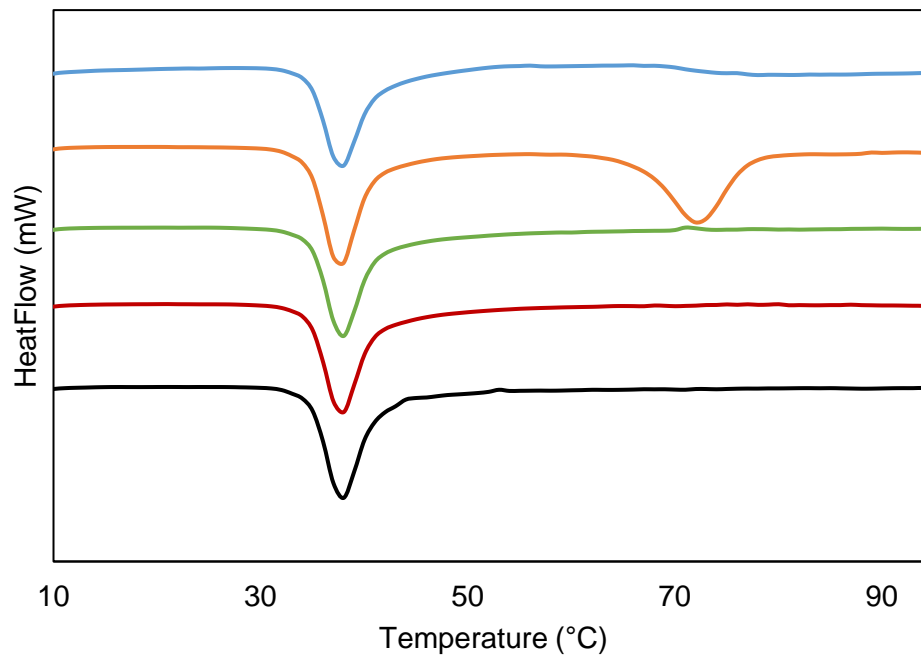


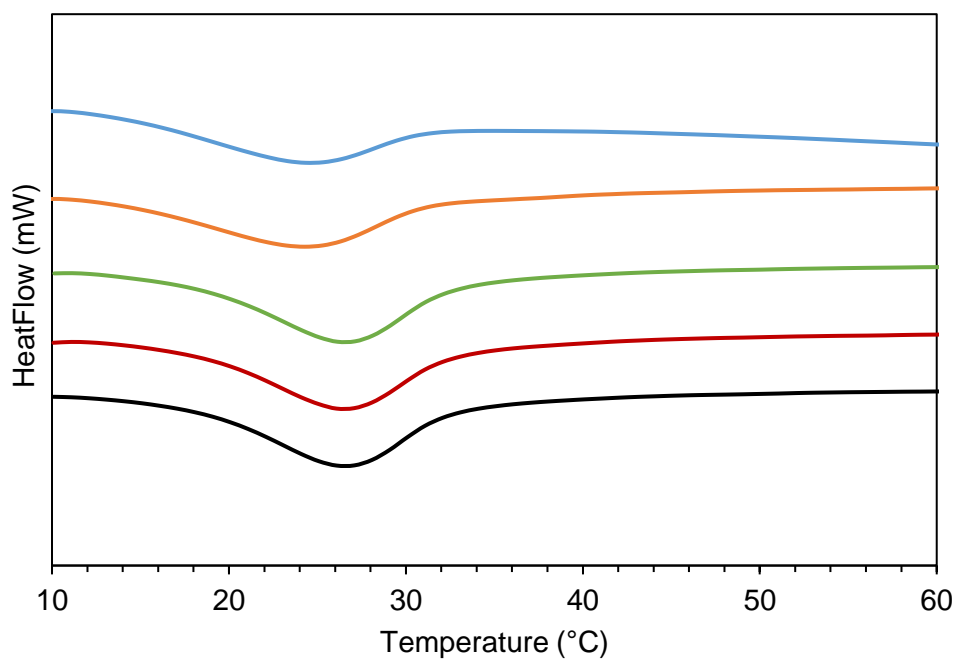
Figure 5-5: DSC thermograms of first heating for COLLHAS (Blue line), COLLWS (orange line), COLLSF3 (green line), COLLSF9 (red line) and pure collagen (black line at different acid-swollen collagen paste concentration (A) 4% (B) 3.5% and (C) 2.5%.

Table 5-3: DSC parameters after first heating of collagen/cellulose and collagen/starch pastes at different collagen paste concentrations. T_p = peak temperature, T_o = Onset temperature, T_{end} = endset temperature and ΔH = enthalpy.

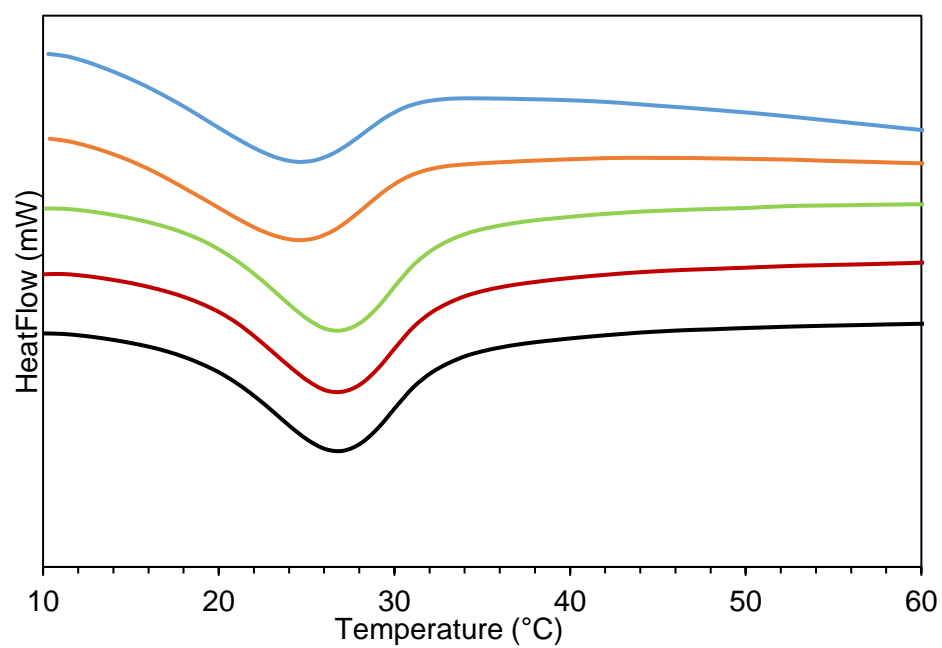
Samples	T_{onset} ($^{\circ}C$)	T_{Peak} ($^{\circ}C$)	ΔH (J/g of Collagen)	T_{end} ($^{\circ}C$)
4% COLLAGEN	33.90 ± 0.01^a	36.80 ± 0.02^a	46.75 ± 1.73^a	40.36 ± 0.02^a
COLLSF3	34.00 ± 0.05^a	37.01 ± 0.07^a	43.25 ± 0.74^{ab}	40.91 ± 0.05^a
COLLSF9	33.99 ± 0.01^a	37.01 ± 0.00^a	44.99 ± 1.755^{ab}	40.60 ± 0.23^a
COLLWS	34.05 ± 0.05^a	36.97 ± 0.02^a	45.67 ± 0.44^{ab}	40.38 ± 0.00^a
COLLHAS	34.03 ± 0.03^a	36.97 ± 0.02^a	40.96 ± 0.59^b	40.37 ± 0.06^a
3.5% COLLAGEN	34.16 ± 0.07^a	37.23 ± 0.05^{bc}	42.50 ± 5.64^a	40.91 ± 0.27^b
COLLSF3	34.10 ± 0.02^a	37.21 ± 0.07^{abc}	45.74 ± 0.37^a	40.96 ± 0.16^b
COLLSF9	34.17 ± 0.02^a	37.29 ± 0.07^c	48.55 ± 1.36^a	40.99 ± 0.99^b
COLLWS	34.12 ± 0.02^a	37.05 ± 0.04^a	44.56 ± 0.69^a	40.48 ± 0.12^{ab}
COLLHAS 70 : 30	34.01 ± 0.11^b	37.06 ± 0.02^{ab}	48.30 ± 2.11^a	40.30 ± 0.12^a
2.5% COLLAGEN	34.63 ± 0.05^a	37.77 ± 0.03^a	48.19 ± 0.08^b	41.63 ± 0.08^a
COLLSF3	34.46 ± 0.07^a	37.66 ± 0.09^a	44.56 ± 1.03^{ab}	41.08 ± 0.03^a
COLLSF9	34.62 ± 0.04^a	37.77 ± 0.07^a	43.56 ± 0.13^{ab}	41.49 ± 0.03^a
COLLWS	34.62 ± 0.02^a	37.79 ± 0.15^a	39.68 ± 1.36^a	41.02 ± 0.06^a
COLLHAS	34.63 ± 0.01^a	37.67 ± 0.02^a	42.19 ± 3.25^{ab}	41.01 ± 0.13^a

^{ac} Mean \pm standard deviation. Means in the same column with different superscript letters are significantly different ($P < 0.05$).

(A)



(B)



(C)

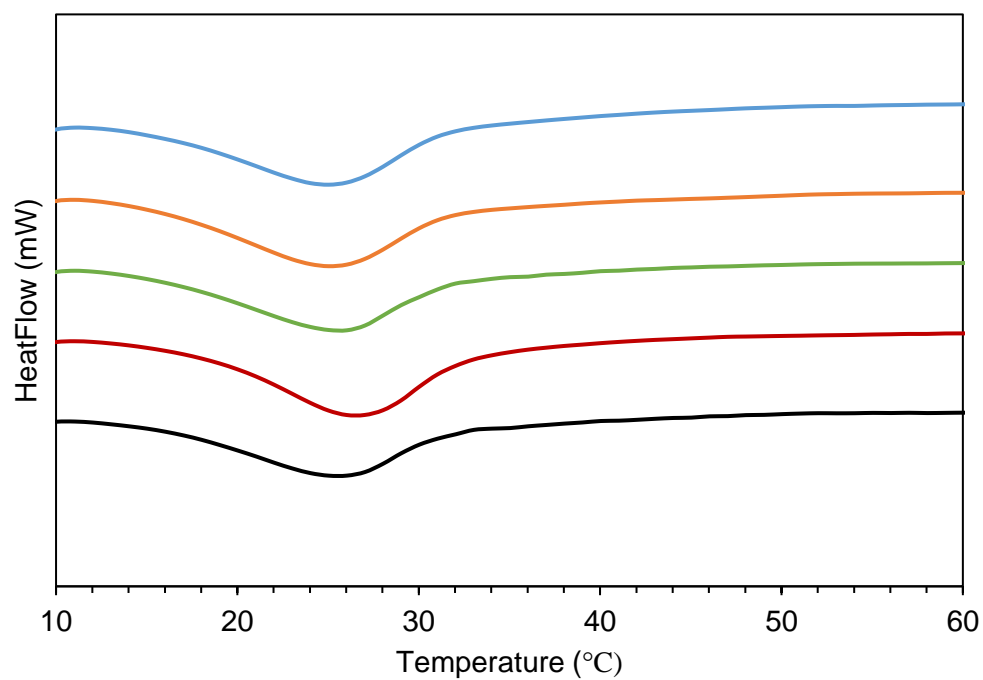


Figure 5-6: DSC thermograms of second heating for COLLHAS (Blue line), COLLWS (orange line), COLLSF3 (green line), COLLSF9 (red line) and pure collagen (black line) at different acid-swollen collagen paste concentration (A) 4% (B) 3.5% and (C) 2.5%.

Table 5-4: DSC parameters (second heating) of collagen/cellulose and collagen/starch pastes at various collagen concentrations (4%, 3.5% and 2.5%). TP = peak temperature; T_o = Onset temperature; T_e = end set temperature and ΔH= enthalpy.

Samples	T _{onset} (°C)	T _{Peak} (°C)	ΔH (J/g of collagen)	T _{end} (°C)
4% COLLAGEN	17.67 ± 0.11 ^b	26.66 ± 0.11 ^b	26.66 ± 1.05 ^c	33.29 ± 0.14 ^b
COLLSF3 80 : 20	18.13 ± 0.05 ^b	26.49 ± 0.05 ^b	26.61 ± 0.16 ^c	33.60 ± 0.04 ^b
COLLSF9 80 : 20	18.96 ± 0.04 ^b	26.55 ± 0.05 ^b	27.34 ± 0.64 ^c	33.98 ± 0.06 ^b
COLLWS 80 : 20	17.68 ± 0.13 ^b	24.37 ± 0.09 ^a	18.56 ± 0.06 ^b	33.38 ± 0.05 ^b
COLLHAS 80 : 20	17.46 ± 0.10 ^b	24.22 ± 0.00 ^a	14.22 ± 1.13 ^a	33.41 ± 0.05 ^b
3.5% COLLAGEN	13.76 ± 0.20 ^a	26.81 ± 0.04 ^b	26.49 ± 0.50 ^b	31.67 ± 0.00 ^a
COLLSF3 70 : 30	14.33 ± 0.42 ^a	26.79 ± 0.04 ^b	26.54 ± 0.17 ^b	31.33 ± 0.03 ^a
COLLSF9 70 : 30	18.09 ± 0.13 ^b	26.72 ± 0.02 ^b	26.67 ± 0.13 ^b	33.61 ± 0.02 ^b
COLLWS 70 : 30	19.07 ± 0.17 ^b	24.45 ± 0.02 ^a	17.55 ± 0.18 ^a	33.57 ± 0.00 ^b
COLLHAS 70 : 30	14.06 ± 0.37 ^a	24.22 ± 0.09 ^a	16.48 ± 0.86 ^a	31.47 ± 0.02 ^a
2.5% COLLAGEN	14.14 ± 0.37 ^a	27.32 ± 0.02 ^b	24.37 ± 1.68 ^b	31.41 ± 0.01 ^a
COLLSF3 50 : 50	19.21 ± 0.36 ^b	27.48 ± 0.09 ^b	23.20 ± 1.95 ^b	33.89 ± 0.16 ^b
COLLSF9 50 : 50	19.13 ± 0.02 ^b	27.38 ± 0.02 ^b	23.76 ± 0.47 ^b	34.02 ± 0.08 ^b
COLLWS 50 : 50	15.48 ± 0.07 ^a	25.08 ± 0.11 ^a	14.31 ± 0.54 ^a	31.80 ± 0.02 ^a
COLLHAS 50 : 50	15.98 ± 0.20 ^a	24.99 ± 0.06 ^a	11.91 ± 0.62 ^a	31.56 ± 0.13 ^a

^{a-c} Mean ± standard deviation. Means in the same column with different superscript letters are significantly different (P<0.05).

5.5 Conclusions

The viscoelastic properties of collagen pastes were modified by adding fillers, i.e. cellulose fibres and starch granules, at a range of different collagen concentrations. When matched for phase volumes, the results indicate that different materials have very different effects on the elastic properties of collagen pastes. Also, these materials did not affect the thermal stability of collagen. However, on reheating, the addition of starch granules impacted the melting of denatured collagen. The findings in this study may serve as a platform to improve the rheological properties and processing performance of collagen pastes. Further research is still necessary to understand the mechanisms or interactions underlying the effect of starch granules on the melting of denatured collagen.

**6 STRUCTURAL, THERMAL, MECHANICAL AND
SORPTION PROPERTIES OF COLLAGEN-CELLULOSE
AND COLLAGEN-STARCH FILMS**

6.1 Abstract

Collagen films are used for various applications in food, medicine, cosmetics and tissue engineering. It is of interest to explore whether their properties can be manipulated through the addition of other natural biopolymers. The objective of this study was to characterise the thermal, mechanical, sorption and structural properties of edible collagen films made from acid swollen collagen paste with cellulose fibres and corn starch granules (were considered as fillers) dispersions added at fixed and therefore comparable phase volume. The effect of filler type and shape on collagen films were characterised using Fourier transform infrared spectroscopy (FTIR), Differential scanning calorimetry (DSC), Thermogravimetric analysis (TGA), Wide-angle x-ray diffraction (XRD), Texture analyser, Scanning electron microscopy (SEM) and Dynamic vapour sorption (DVS). Film thickness increased with the addition of fillers and with increasing collagen concentrations. The surface morphology obtained from SEM Images showed that the blend films were rougher than pure collagen films. FTIR and XRD results demonstrated that cellulose fibres/starch granules also prevented the collagen structure's stabilisation upon drying. This was further confirmed by the reduced DSC enthalpy of transition and reduced thermal stability of the blend films, as evidenced in the TGA results. Also, tensile strength (TS), elongation at break (EAB) and Young's modulus (YM) of collagen films were increased with cellulose fibre additions. The collagen-starch films were not tested as they were too brittle. Moreover, the inclusion of cellulose fibres and starch granules reduced the water intake of the collagen films.

6.2 Introduction

There is a growing concern relating to food safety and its environmental impact due to the use of non-biodegradable synthetic polymeric materials as packaging films (Ghanbarzadeh et al., 2010; Krystijan et al., 2017). This has led scientists to study more environmentally friendly options to produce non-toxic and edible films, one of which involves the use of biodegradable and naturally occurring polymers of proteins and polysaccharides, often referred to as biopolymers (Shit and Shah, 2014; He et al., 2020). Collagen, the most abundant fibrous protein in the mammalian (Hoque et al., 2011). The unique characteristics of collagen, including high tensile strength, flexibility, biocompatibility, non-toxicity, biodegradability, and weak antigenicity, have allowed its widespread use in pharmaceuticals, cosmetics, tissue engineering, and the food industry. Collagen has been extracted and adapted for various forms or formulations such as gels, pastes, films, sponges and fibres. (Chak et al., 2013; Ding et al., 2014a; Ma et al., 2018).

In the Food Industry, collagen casings, a form of collagen film obtained from acid-swollen collagen fibres, are commonly used as an alternative to animal intestines for sausages due to their uniformity in shape, size, low cost, flexibility and high tensile strength resulting from the highly ordered triple helical structure of collagen (Arvanitoyannis et al., 1997; Simelane and Ustunol, 2005; Wang et al., 2015). However, compared to synthetic polymers, the use of collagen films in packaging applications is limited because of their poor tensile strength, thermal instability, and the tendency to degrade easily following the extraction and reprocessing (Cheng et al., 2019). To overcome these drawbacks, several approaches have been used to improve collagen suboptimal properties and overall performance. One approach relies on physical (Wang et al., 2018) and enzymatic (Wu et al., 2017) modifications using

other environmentally friendly and low-cost biopolymers. Over the years, various biopolymers such as chitosan, soy protein isolate, carboxymethylcellulose (CMC), globular proteins (casein and keratin), hydroxypropylmethylcellulose (HPMC), cellulose nanocrystals (CNCs), carboxylated cellulose nanofibres (CNF), microfibrillated cellulose (MFC), poly (lactic-co-glycolic-acid) (PLGA) have been used to improve the physicochemical and mechanical properties of collagen films (Jose et al., 2009; Li et al., 2014; Ding et al., 2015; Ahmad et al., 2016; Wang et al., 2016b; Wang et al., 2018; Wu et al., 2018; Bhuimbar et al., 2019; Wu et al., 2020). Ding et al. (2015) reported that the addition of HPMC increased the tensile strength and stiffness of collagen films, and they reasoned that the intermolecular hydrogen bonding interaction between collagen and HPMC was a key contributor. A different study also reported a significant increase in collagen films tensile properties and degradation temperature (Long et al., 2018). They explained the observation was due to the crosslinking via electrostatic and hydrogen bond interactions between the collagen and cellulose nanocrystals (CNCs). In a closely related study, Wang et al. (2018) found that electrostatic interaction between collagen fibre and CNF in the collagen matrix significantly increased its mechanical properties. Among the natural polymers, cellulose fibres and starch granules were chosen for this study due to their reinforcing capacity, abundance, non-toxic, low cost and biodegradability (Lee et al., 2009).

Cellulose, the richest natural polymer on earth, is found in wood, cotton, hemp, and other sources, the main structural component of the plant cell wall. It is a linear carbohydrate polymer chain consisting of D-glucopyranose units joined together by β -(1-4) glycosidic linkages (Khan et al., 2012). Cellulose has a hierarchical structure similar to collagen, where individual chains form microfibrils, fibrils and fibres, which are widely used as reinforcing polymers in several industries because of their high

aspect ratio, high tensile strength, high thermal stability and high stiffness (Tan et al., 2015; Haniffa et al., 2016).

Starch, a storage polysaccharide found in different plant sources, is a natural polymer made of two polymers, namely amylose and amylopectin arranged in granules with crystalline (amylopectin) and amorphous (amylose) regions. Amylose is a linear molecule also composed of D-glucopyranose units linked by α -(1-4) linkage, whereas amylopectin is a highly branched polymer of D-glucopyranose units linked with α -(1-4) with α -(1-6) branch linkages. However, the ratio of polymers varies by starch botanical source. (Tester and Morrison, 1990c; Pankaj et al., 2015; Ahmad et al., 2015). Starch granules possess unique physicochemical and functional properties hence are used as thickeners, colloidal stabilisers, gelling agents, adhesives and water retention agents in various industries as well as for the preparation of edible films, usually as a result of granule swelling (gelatinisation) (Singh et al., 2003; Soares et al., 2005; Copeland et al., 2009a).

Furthermore, starch has been successfully used as a reinforcing material for improving the physicochemical properties of biopolymer films (Wang et al., 2017b; Askari et al., 2018). The complex hierarchical structures of cellulose and starch can improve the physical and mechanical properties of the blend film. Previous research has demonstrated that the elastic properties of an acid swollen collagen paste were improved with cellulose fibre and corn starch granules (Sobanwa et al., 2020). However, the current lack of information and understanding of the reinforcement effect of cellulose fibres with varying lengths and corn starch granules on acid swollen collagen film is an understudied area with potential scope for new knowledge.

The main objective of this study was to understand how adding either cellulose fibres or starch granules (assumed as fillers) to collagen pastes to create composite films affected their mechanical, thermal, sorption and structural properties. The blend films were prepared from dispersions at different blend ratios allowing a fixed dispersed phase volume with a starting collagen paste at known collagen concentration, such that both dispersed phase volume and collagen concentration could be controlled. The hypothesis proposed here is that at fixed phase volume (the volume occupied by the dispersed phase), the composition and aspect ratios (length to width) of the cellulose fibres and starch granules will influence the film properties.

Furthermore, starting paste collagen concentration, cellulose fibre length and starch with different amylose and amylopectin content was also evaluated. Paste blends were prepared by mixing dispersions of cellulose/starch with collagen paste which were further rolled into films.

6.3 Materials and Methods

6.3.1 Materials

The materials used in this section has been described in Chapter 5, section 5.2.1.

6.4 Methodology

6.4.1 Determination of dispersion phase volume (Φ)

See Chapter 5, section 5.2.2.1.

6.4.2 Preparation of collagen-cellulose and collagen-starch pastes

See Chapter 5, section 5.2.2.2.

6.4.3 Preparation of collagen-cellulose and collagen-starch films

The films were formed using the method described by (Harper et al., 2013). Approximately 5g of collagen with and without hydrocolloid/cellulose/starch pastes were rolled on a stainless-steel board between two plastic sheet layers with a stainless roller with a recess of 0.50 mm to achieve uniform film thickness. The plastic sheet on the roller side was removed, and the sheet with the pastes was oven-dried at 20 °C for 24hrs. The formed films were peeled off from the plastic sheets. Films containing collagen with and without hydrocolloids were conditioned in a desiccator at $20 \pm 0.1^\circ$ C and 75% relative humidity (RH) for seven days before all analysis. Saturated sodium chloride solution was used to achieve the required relative humidity.

6.4.4 Film characterisation

6.4.4.1 Film thickness

The thickness of films was measured using a digital electronic micrometre (Mitutoyo Corp, Kawasaki-shi, Japan). The thickness values were obtained by the average of ten measurements from random locations on each film sample.

6.4.4.2 Moisture content

The film's water content pre-conditioned at 75% RH was determined gravimetrically upon drying in an oven at 105 °C until constant weight (dry sample weight). Samples were analysed at least in triplicates and were calculated according to equation (6-1). The results were expressed as (%) of moisture content of samples.

$$\text{Moisture content (\%)} = \frac{\text{Initial weight} - \text{Final weight} \times 100}{\text{Initial weight}} \quad (6-1)$$

6.4.4.3 Attenuated total reflectance Fourier Transform Infrared Spectroscopy (ATR-FTIR)

ATR-FTIR spectroscopy was used to characterise the molecular structure of collagen films with and without cellulose fibres and starch granules. The spectra were obtained using a Bruker Tensor 27 spectrometer (Germany) equipped with an attenuated total reflectance (ATR) accessory at 25 °C. The FTIR spectra were recorded in the range of 4000 to 500 cm⁻¹ collected in 128 scans at a resolution of 4 cm⁻¹ spectral resolution against an empty background. Spectral data analysis was carried out using the OPUS 7.2.139.1294 software (Bruker, UK). Before data analysis, the spectra were baseline corrected and normalised. The spectra plots represent an average of 6 repeats.

6.4.4.4 Differential Scanning Calorimetry

The thermal transitions of the films were determined using a Differential scanning calorimetry (Mettler Toledo, DSC 3+, UK). The instrument was calibrated with pure indium and cyclohexane. Approximately 10mg of films equilibrated at 75% RH were accurately weighed in stainless steel pans and were hermetically sealed. The samples

were scanned from 25 °C to 140 °C at a heating rate of 10°C/min under N₂ atmosphere. An empty stainless-steel pan was used as a reference. The transition temperature (T_m) related to the melting of collagen was determined as the peak temperature. The energy associated with the helix coil transition defined as change in enthalpy (ΔH), was determined from the area under the endothermic peak. All analyses were calculated using Mettler STARe Thermal Analysis Software Default (DB V15.00). Analyses were performed in duplicates, and the results were averaged.

6.4.4.5 Thermogravimetric analysis (TGA)

The thermal degradation of collagen/cellulose and collagen/starch films was investigated using a thermogravimetric analyser (Mettler Toledo, DSC 3+, UK) under an inert N₂ atmosphere at a flow rate (25 ml/min). Films of approximately 10 mg were weighed in aluminium pans and were sealed hermetically. The pans and heated from 25 °C to 550 °C at a heating rate of 10 °C/min. The weight loss (mg) *versus* temperature plots were taken for thermo-gravimetric analysis (TGA). The differential thermogravimetric (DTG) analysis curves were obtained by differentiating the TGA data with respect to temperature. TGA and DTG data were analysed using Mettler STARe Thermal Analysis Software Default (DB V15.00). Analyses were performed in duplicates.

6.4.4.6 Dynamic Vapour Sorption

The water sorption isotherm of collagen films with and without cellulose/starch was measured using a Dynamic Vapor Sorption Analyzer DVS-1 (Surface Measurement Systems Ltd., London, U.K.) equipped with a microbalance (Cahn D200, UK). The experiments were carried out at 25 °C and RH values from 0 to 95%. Approximately 10 mg of the sample was loaded into the sample pan and predried in the DVS-1 under

a nitrogen flow of 200 mlmin⁻¹ (RH=0%) until the dry weight of the sample showed no further change. The measurement was started at 0%RH and terminated at 95% RH with a step increase by equilibrating the sample weight at each step. The samples were considered equilibrated when the equilibration time exceeded 200 min. All experiments were run at 25 °C, and duplicate tests were carried out for each sample. The moisture isotherms for each sample expressed in a dry weight basis were described using the Guggenheim, Anderson and de Boer (GAB) model (Guggenheim, 1966). The GAB model is widely applied to food materials as it fits water sorption data up to an RH of 90% (Lemus M, 2011) and also considers the properties of the absorbed water in the monolayer and multilayer region (Timmermann et al., 2001; Agrawal et al., 2004; Kristo and Biliaderis, 2006). The GAB model assumes that the water molecules are sorbed into primary sites and subsequently into multilayers and that all multilayer states are identical (Yakimets et al., 2007). The GAB model is expressed mathematically as:

$$M = \frac{M_0 C K a_w}{(1 - K a_w)(1 - K a_w + C K a_w)} \quad (6-2)$$

Where M is the equilibrium moisture content (dry basis), M_0 is the moisture content at the monolayer (g water/100 g dry solids); a_w is the water activity (RH/100); C and K are temperature-dependent where C is related to the heat of sorption of water at the monolayer; and K is associated to the heat of sorption of water at the multilayer (Van Den Berg and Bruin, 1981; Kent and Meyer, 1984; Sun et al., 2009).

6.4.4.7 Mechanical properties

The mechanical characteristics, including tensile strength (TS), Young's Modulus (YM) and elongation at break (% EAB) of the films were evaluated using a Texture Analyser

(Stable Microsystems, Surrey, UK) with a 5 kg Load Cell, using miniature tensile grips (A/MTG). The films were cut into a dumbbell-shaped specimen approximately 8 mm wide (centre of the dumbbell) x 75 mm in length. The tests were performed at ambient temperature at a crosshead speed of 1 mm/min with 50 mm gauge length. To evaluate the mechanical properties of the films, at least seven specimens were stretched. The values of TS and EAB of the samples were calculated using the equations (6-3) and (6-4).

$$TS = \frac{F}{A} \quad (6-3)$$

$$EAB = \frac{\Delta L}{L_0} \times 100\% \quad (6-4)$$

Where F is the maximum load force (N), ΔL is the elongation length of the film, L_0 is the initial grip length of the film (50 mm), and A is the cross-sectional Area.

6.4.4.8 X-ray Diffraction

The X-ray Diffraction patterns of the films were carried out using an echo D8 Advance Bruker AXS powder-diffractometer (Bruker AXS, UK) equipped with a copper tube operating at 40 kV and 25 mA, using copper K alpha ($\text{Cu K}\alpha$) radiation of a wavelength of 0.1541 nm. The samples were scanned over the range of diffraction angle $2\theta = 4 - 45^\circ$. Crystallinity was calculated as the ratio of the crystalline area peaks to the total area of diffraction peaks (both amorphous and crystalline) using DIFFRAC.EVA Software (Bruker, UK).

6.4.4.9 Microstructure

The surface morphology of the prepared films was observed using (SEM JEOL 6060LV, Tokyo, Japan) at an accelerating voltage of 15kV. Before imaging, the films were fixed on conductive adhesive tape, coated with platinum and observed at a magnification of x140.

6.4.4.10 Statistical analysis

The results were presented as means \pm standard deviation. One-way analysis of variance (ANOVA) was performed using the Statistical Package for Social Sciences (SPSS for Windows, SPSS Inc., Chicago, IL, USA), and means of samples of each level of collagen were compared by Tukey's mean comparison test, and differences were considered significant when $P < 0.05$.

6.5 Result and Discussion

6.5.1 Microstructure

The surface morphology of collagen films with and without cellulose fibres/starch granules examined by SEM are shown in Figure 6-1. It is known that the microstructure of the film is affected by the components of the film-forming paste, the interaction of components in the film matrix and their molecular organisation during drying (Ahmad et al., 2015). The morphological difference between cellulose fibres and starch granules is clear. Cellulose fibres are bigger and rod-like, whereas starch granules are smaller and spherical. These differences in morphology and size play a vital role in the packing of the fillers during film formation and the overall films final properties. As shown in Figure 6-1A, pure collagen films show smooth and compact surfaces, indicating an ordered structure. Small circular pockets are seen on the surface of pure collagen films, which are air bubbles not removed during degassing. However, with the addition of cellulose fibres and starch granules, the surface of blend films are rougher due to starch granules and cellulose fibres protruding on the films' surface. The differences in microstructure of the films might indicate that during the film formation, the polymers arrange differently in the film network, thus enhancing the roughness of the film microstructure (Ahmad et al., 2015). Therefore, it can be assumed that the incorporation of cellulose fibres and starch granules reduced the rearrangement of collagen structure in the film network, which in turn increased film roughness. Similar microstructure has been reported in collagen films with chitosan (Ahmad et al., 2016). It was suggested that chitosan could not interact or disperse well, resulting in increased roughness and discontinuity of film microstructure.

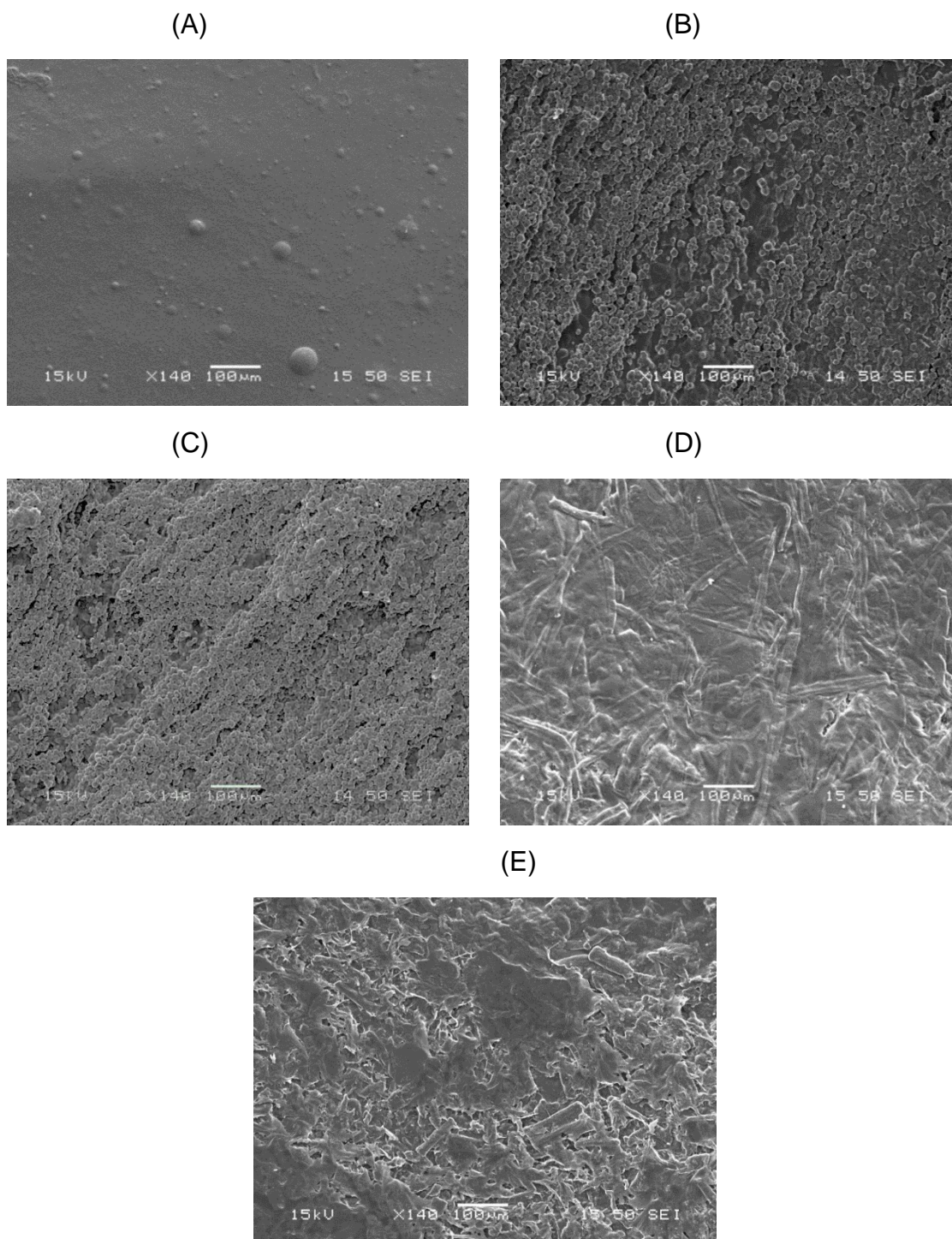
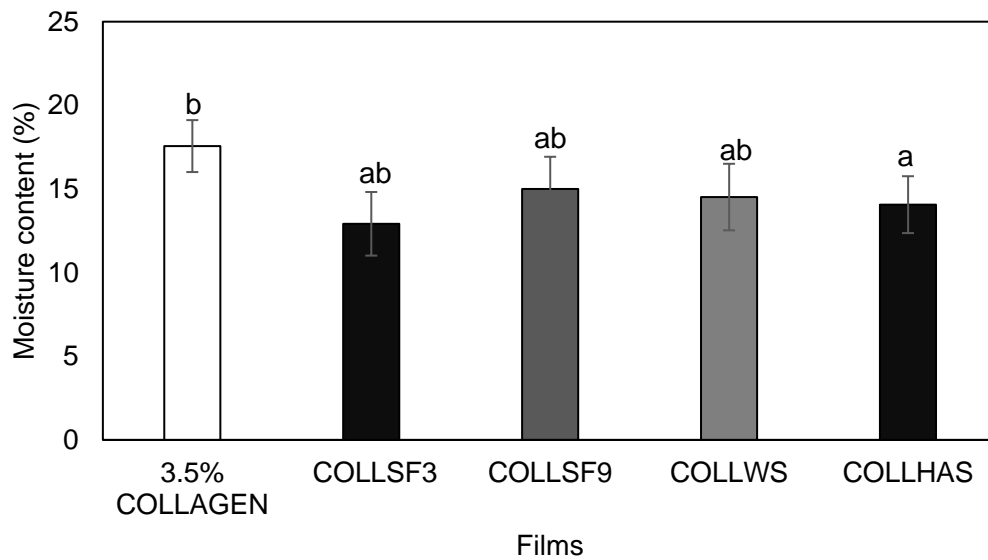


Figure 6-1: SEM images of surface morphology of (A) COLLAGEN (B) COLLWS (C) COLLHAS (D) COLLSF9 (E) COLLSF3. The scale bar is 100µm for each image.

6.5.2 Moisture content and thickness

The moisture content and thickness of collagen with and without cellulose/starch films prepared at different collagen concentrations are shown in Figure 6-2 and. Figure 6-2 shows the moisture contents of the films after equilibration at 75% RH over saturated sodium chloride solution. The moisture content of biopolymer films indicates the films hydrophilicity; higher moisture content values indicate more hydrophilic film (Bourbon et al., 2011). Pure collagen films show higher moisture content, although the values were not significantly different ($p>0.05$) to the blend films. The higher values of pure collagen films might be due to the greater hydrophilic nature of collagen, leading to more water absorption. However, the addition of cellulose fibres and starch granules reduced the moisture content of films at various collagen concentrations studied. Reduction in moisture content may result from macromolecular interactions involving collagen polar sites and cellulose/starch hydroxyl groups. As a result, fewer polar sites of collagen are exposed to interactions with water molecules, resulting in a reduced water intake of mixed films (Kanmani and Lim, 2013). These results were in accordance with those of Ahmad et al. (2016), who reported a decrease in water uptake with the addition of soy protein isolate to collagen films due to the interaction between the polar groups of collagen and SPI which reduced the hydrophilic sites that are exposed to water molecules.

(A)



(B)

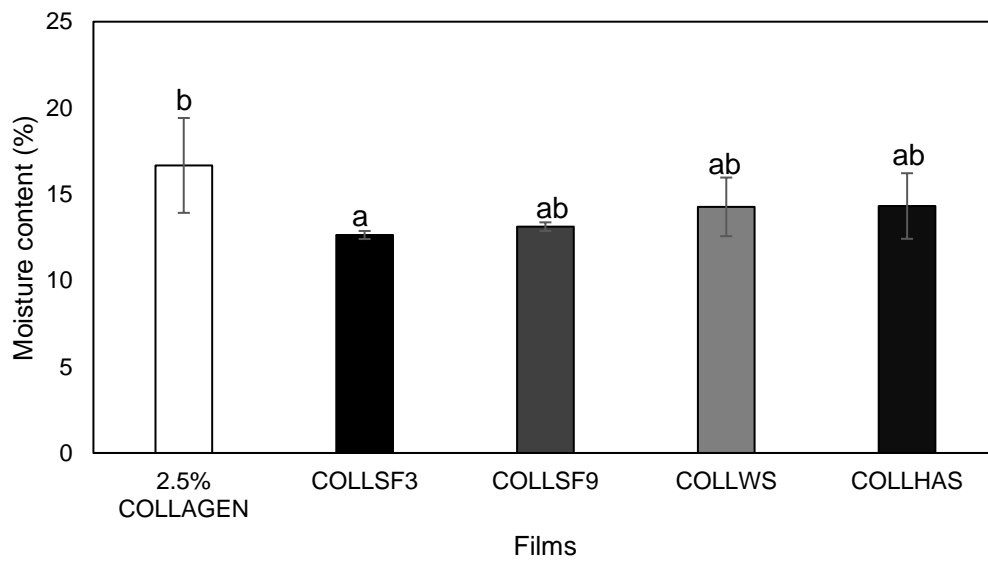


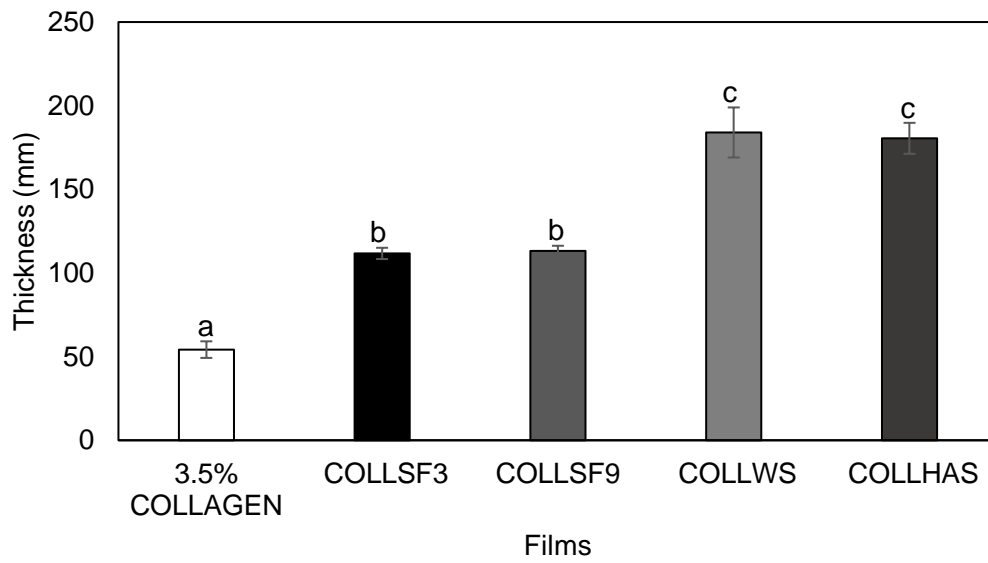
Figure 6-2: Moisture content of collagen with cellulose (COLLSF3 and COLLSF9), Collagen with starch (COLLWS and COLLHAS) and pure collagen films at (A) 3.5% (B) 2.5% collagen concentrations. The different letter means significant ($P < 0.05$) difference between the pastes. The error bars represent the standard deviation.

In the case of the thickness of the films (Figure 6-3), films with starch granules/cellulose fibres had higher thickness ($p < 0.05$) than the pure collagen films, and this depends on the type, shape of the fillers (cellulose fibres and starch granules) and concentration of collagen. Film thickness increases with increasing collagen concentration in film-forming pastes, which can be explained by increased dry matter in films. Meanwhile, among the blend films, collagen with starch films (COLLHAS and COLLWS) shows higher ($p < 0.05$) thickness values than those of pure collagen and collagen-cellulose films at the levels of collagen studied. According to Ahmad et al. (2016), differences in film thickness may depend on how the components of the film-forming solution influence the alignment, sorting and compacting of the molecules during the film drying process.

Therefore, it can be assumed that as water evaporates during the drying process, the chains of the pure collagen films align themselves to form a more compact and ordered structure with little or no protrusions, consequently resulting in thinner films (which interestingly have a higher water-binding capacity as shown for the moisture contents – above). However, the difference in cellulose and starch morphology, packing, and size may affect collagen fibres arrangement during film formation and contribute to the final film thickness. Cellulose fibrils can align to an extent with the rearranged collagen fibres upon drying. In contrast, the spherical starch granules do not align with the collagen fibrils, thereby preventing the ordered arrangement of collagen fibrils and not allowing a greater water uptake capacity. This results in a rough and protruded film network, as evidenced by the SEM images (Figure 6-1), and as a result, the thickness of collagen films increases. Also, differences in the dry matter of the films may explain the difference in thickness. Higher concentrations of starch granules were needed at comparable phase volume, resulting in higher dry matter and higher film thickness.

The thickness values of fibrous collagen-starch films were consistent with the range of film thickness previously reported by Wang et al. (2017a) for collagen films incorporating corn starch flour of different amylose and amylopectin content. The authors ascribed the increased thickness to the large surface area of the starch granules. In contrast, the results obtained in this study were higher than those reported by Ahmad et al. (2016) for collagen-chitosan and collagen-soy protein isolate films. The implication is that the properties of collagen films can be tailored if the interactions with the materials being incorporated are known and their impact on collagen network ordering on drying/film formation.

(A)



(B)

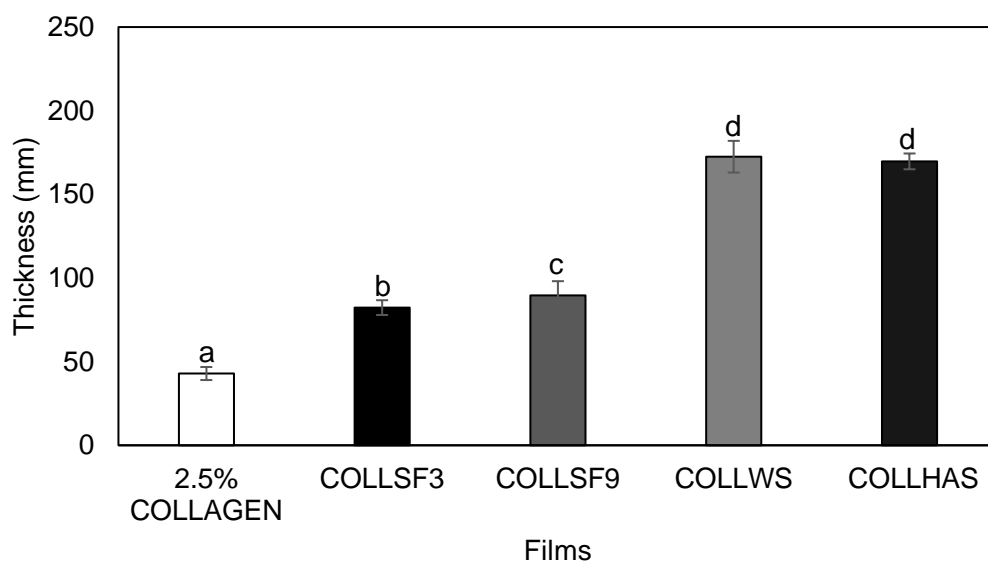


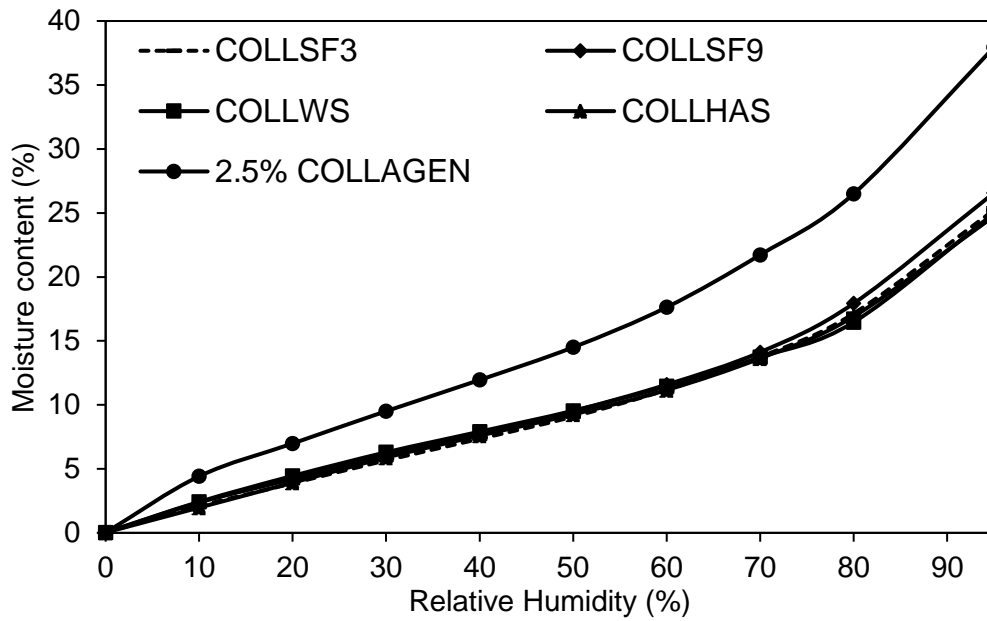
Figure 6-3: Thickness of collagen with cellulose (COLLSF3 and COLLSF9), Collagen with starch (COLLWS and COLLHAS) and pure collagen films at (A) 3.5% (B) 2.5% collagen concentrations. The different letter means significant ($P < 0.05$) difference between the pastes. The error bars represent the standard deviation.

6.5.3 Water interaction determined by dynamic vapour sorption

Collagen protein is highly hydrophilic; therefore, collagen film behaviour must be assessed when exposed to several conditions of equilibrium relative humidity to assess its feasibility as a food packaging. Figure 6-4 shows the sorption and desorption isotherm of collagen films with and without cellulose fibres/starch granules. All the film samples had a sigmoidal shape isotherm, a slow increase in moisture uptake is observed at relative humidities up to 70% RH. With a further increase in relative humidity, the moisture uptake increases rapidly. This behaviour has been widely reported for many hydrophilic polymer materials (Brunauer et al., 1938; Bilbao-Sáinz et al., 2010; Belbekhouche et al., 2011). A similar trend is observed for the desorption isotherms too. The sorption isotherm profile obtained in this study was similar to those seen in films made from type 1 collagen and gelatin (Tanioka et al., 1974; Yakimets et al., 2007; Wolf et al., 2009; Pępczyńska et al., 2019). Pure collagen films show the highest equilibrium moisture content compared to blend films at all the relative humidities studied, supporting results found when equilibrated over saturated salt solutions. The inclusion of cellulose fibres and starch granules reduced the equilibrium moisture content of collagen films at all RH studied. A possible explanation for the lower intake of blend films is that cellulose/starch molecules may interact with the polar sites of collagen molecules. As a result, fewer polar sites are available for interaction with water molecules, resulting in lower water intake of films. Also, the interaction between the cellulose/starch and the hydrophilic sites of collagen might have replaced the collagen-water interaction that existed in pure collagen films, which is thought to provide stability to the ordering of collagen fibrils during film formation. If the presence of the dispersion prevents this process, then the impact on water intake and release seems to be affected. Similar behaviour was reported when sucrose,

glucose and Maltodextrin were individually incorporated into salmon gelatin films. The composite films showed lower equilibrium moisture content compared to pure gelatin films (Pępczyńska et al., 2019). It was suggested that gelatin hydrophilic sites were occupied by polysaccharide molecules, so active sites were less available to water molecules. Notably, however, collagen hierarchical structures differ from molecular interactions afforded by gelatin triple helices.

(A)



(B)

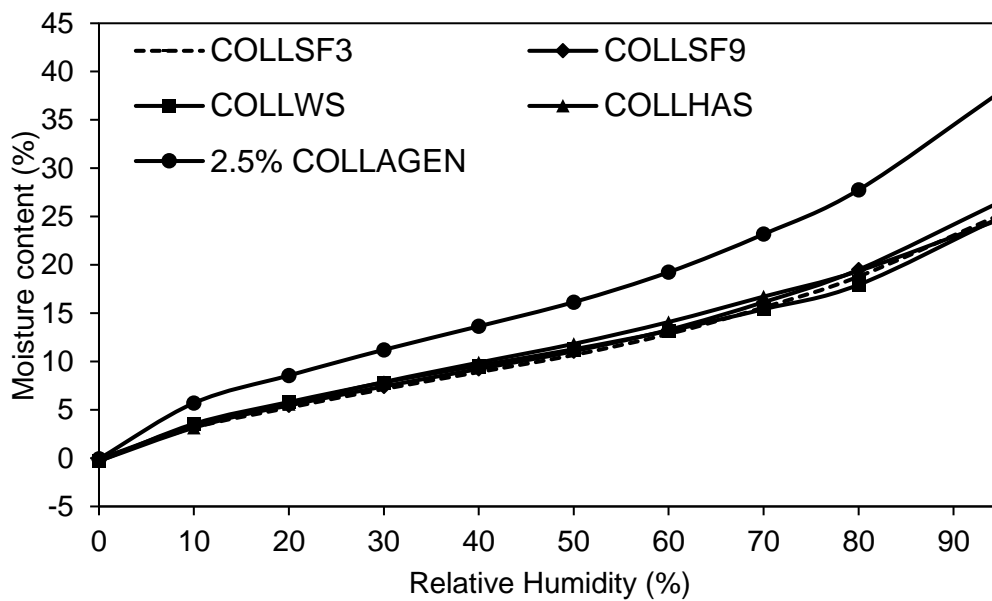


Figure 6-4: (A) Sorption isotherm, and (B) Desorption isotherms of pure collagen, collagen- cellulose (COLLSF3 and COLLSF9) and collagen-starch (COLLWS and COLLHAS) films at 2.5% collagen concentration at 25 °C. The graph presented here is an average of duplicate measurements.

To describe films water sorption behaviour, experimental sorption data of collagen with and without cellulose/starch films were fitted to the GAB model, and the calculated GAB parameters are given in Table 6-1. The GAB model provides an excellent fit for all the films with R^2 values > 0.999 . The monolayer water content (M_0) indicates the amount of water that is strongly adsorbed to active sites, and it is at this value that the film is most stable (Bilbao-SáInz et al., 2010). C indicates the binding strength of water molecules to the sorption site: higher C values indicate stronger interactions between water molecule and hydrophilic sites (Kristo and Biliaderis, 2007). Pure collagen film shows the highest monolayer water content (M_0) value. This is consistent with the high equilibrium moisture content observed at all the RH's, indicating that with increasing RH, pure collagen film can take up more water than the blend films and can retain the highest amount of water upon drying. However, the addition of cellulose fibres and starch granules reduced the M_0 values of the blend films. Lower monolayer moisture content (M_0) values are not surprising as it is explained earlier; the interaction between the hydroxyl groups of cellulose fibres/starch granules and collagen hydrophilic sites reduced the active sites accessible for adsorption of water molecules. In addition, it is plausible that cellulose fibres/starch interrupted the water bridges stabilising the collagen structure. As a result, the collagen structure became less ordered, resulting in lower water uptake by the films. The addition of cellulose fibres and starch granules reduced the C values of the films. Thus, lower C values of blend films indicate reduced sorption sites resulting in lower water sorption energy interaction with the film matrix. Furthermore, the K parameter, which is related to sorption enthalpy of the subsequent layers, was < 1 for all the samples, which indicates the predominance of monolayer absorption and the formation of multilayers of water on the monolayer is similar for all the films (Basiak et al., 2017; Díaz-Calderón et al., 2017). This result agrees with

moisture content data and suggests that adding cellulose fibres and starch granules reduce collagen film hydrophilicity.

Table 6-1: GAB fitting parameters of sorption isotherm of collagen films with and without cellulose fibres/starch granules. SF9 (Solka floc 900), SF3 (Solka floc 300), WS (Waxy starch) and HAS (high amylose starch).

Films	M_0	K	C	R^2
COLLSF3	8.49	0.75	3.08	0.9992
COLLSF9	8.28	0.76	4.77	0.9999
COLLHAS	8.40	0.75	4.44	0.9999
COLLWS	7.30	0.77	4.26	0.9992
2.5% COLLAGEN	11.92	0.74	5.79	0.9995

6.5.4 Mechanical properties

Table 6-2 shows tensile strength (TS), Young's modulus (YM) and elongation at break (EAB) of collagen films with and without cellulose fibres. The tensile strength represents the maximum stress supported by the film before breaking, percentage elongation at break represents the flexibility of the films before breaking, while the young modulus indicates the stiffness or rigidity of the films (Cazón et al., 2017; Askari et al., 2018). The mechanical properties of films are related to film microstructure and possibly cohesion forces between different components in the film matrix (Acosta et al., 2015). The tensile strength and Young's modulus of collagen films made from pastes at 2.5 and 3.5% wt/wt collagen concentration were 8.81-12.79 MPa, and 711.63 - 842.27 MPa, respectively. Films made from collagen and starch were too

brittle after drying and were hitherto not considered for mechanical tests. The brittleness was due to ungelatinised starch granules that caused film defects. The TS and YM of collagen with cellulose films are higher, and values were significantly different ($p < 0.05$) than those of the pure collagen films. However true, values also increased with increasing collagen concentration in films. Cellulose fibres have a high mechanical strength due to several intermolecular and intramolecular hydrogen bonding in their fibrillar structure (Kowalczyk and Baraniak, 2014). . Cellulose fibres may interweave with collagen fibres, resulting in fibril entanglement and a network structure with increased strength and stiffness. Mathew et al. (2012) observed that the physical entanglements of cellulose nanofibres with collagen fibres could increase the tensile strength of collagen films. Aside from the filler effect, collagen on its own as a function of how it can stabilise itself upon drying also contributes to the improvement. The pure collagen films at different concentrations show differences in their mechanical properties. This implies that collagen's concentration influences the collagen's ability to stabilise itself upon drying, thus influencing the tensile property of the resulting films. Therefore, the mechanical properties of the composites are a complex result of polymer blending, and the complexity of these composites will need much more understanding and experimentation. Also, the difference in pure collagen and collagen/cellulose films moisture content may also explain differences in mechanical properties. Generally, water acts as a plasticiser by reducing the hydrogen bond interactions between the biopolymer chains, thus resulting in films with weak tensile strength and stiffness (Chang et al., 2000). As observed in the moisture content results (Figure 6-2), collagen films show higher moisture intake than blend films. Thus, higher moisture in the pure collagen films would be expected to exert a more plasticising effect, resulting in lower tensile strength and stiffness.

The elongation at break (%) of collagen/cellulose films was significantly higher ($p < 0.05$) than that of pure collagen films, indicating increased extensibility and flexibility of the films. In general, for biopolymer films, an increase in TS is followed by a decrease in EAB, but this is not the case in this study. Lower EAB values for pure collagen may be due to the strong interactions between the collagen triple α -chains, which prevented the stretching of the chains (Chen et al., 2008). The addition of plasticisers has been reported to increase the EAB of biopolymer films due to decreased intermolecular bonds between polymer chains, consequently resulting in greater flexibility of the films (Olivas and Barbosa-Cánovas, 2008). Moreover, Andonegi et al. (2020) reported that strong hydrogen bonds and van der Waals interactions in the collagen structure gives collagen its tensile strength, but disruption can lead to increased stretching. Based on this, it is proposed that cellulose fibres might interfere with the hydrogen bond stabilising the collagen structure, as indicated in the FTIR analysis (section 6.4.5). From a molecular level perspective, it is speculated that the interactions between collagen and cellulose can prevent the hydrogen bonds from stabilising the collagen triple helices formed upon drying, thus allowing the chains to stretch more easily, and as a consequence, the flexibility of the films increases (Chen et al., 2008). These findings are consistent with those of Ding et al. (2015), who reported an increase in TS and EAB in collagen films modified with hydroxypropylmethylcellulose. They ascribed the increase in TS and EAB to hydrogen bonding interaction between the two polymers. Similarly, Ahmad et al. (2016) reported that the addition of chitosan led to an increase in the EAB of collagen films and drew a conclusion that chitosan produced a plasticisation effect which weakened the collagen chain interaction and promoted chain mobility in the collagen-chitosan composite films, which in turn led to the increased flexibility of the film matrix. In

contrast, the reinforcement of collagen films with carboxylated cellulose nanofibres (CNFs) decreased the EAB of collagen films (Wang et al., 2018). This was due to both strong interactions between biopolymers and CNF stiffness. Furthermore, comparison of the cellulose with different fibre length showed that Young's modulus of collagen with cellulose of long fibre length (COLLSF9) was higher than collagen with short fibre lengths (COLLSF3) films, although this difference was not significant ($p > 0.05$). This slight difference may be due to the aspect ratio of the cellulose fibres. (Bouafif et al., 2009; Migneault et al., 2009). Hence, it is concluded that the increased mechanical properties of the blend films result from reinforcement in the microstructure of the films by cellulose and an alteration in the collagen matrix due to differences in fibril stabilisation upon drying.

Table 6-2: Mechanical properties of collagen films with and without cellulose fibres/starch granules at different collagen concentrations.

Films	Tensile strength (MPa)	Elongation at break (%)	Young's modulus (MPa)
3.5% COLLAGEN	12.8 ± 1.9 ^a	1.8 ± 0.6 ^a	842.3 ± 177.7 ^a
COLLSF9	26.6 ± 2.2 ^b	2.8 ± 0.5 ^b	1246.9 ± 123.4 ^b
COLLSF3	26.0 ± 2.7 ^b	3.6 ± 0.8 ^b	1137.9 ± 231.4 ^b
2.5% COLLAGEN	8.8 ± 1.3 ^a	1.4 ± 0.2 ^a	711.6 ± 89.8 ^a
COLLSF9	20.1 ± 2.5 ^b	3.7 ± 1.0 ^b	1004.4 ± 163.7 ^b
COLLSF3	20.7 ± 2.8 ^b	3.4 ± 0.9 ^b	856.5 ± 270.3 ^{ab}

6.5.5 Attenuated total reflectance-Fourier Transform Infrared Spectroscopy (ATR-FTIR)

The ATR-FTIR was used to probe chemical group interaction between biopolymers present in films at a molecular and supramolecular level. The spectra of the collagen films with and without cellulose fibres and starch granules in the range of 500 - 4000 cm^{-1} are shown in Figure 6-5, and the wavenumber of absorption bands are summarised in Table 6-3. The assignments of absorption peaks associated with the major functional groups of collagen were based upon the study of Ahmad et al. (2016). The spectra of pure collagen films made from 3.5% and 2.5 % (w/w) collagen paste concentration show five characteristic absorption bands of collagen at 3292, 2928, 1626, 1542, 1237 cm^{-1} and 3292, 2928, 1626, 1542, 1237 cm^{-1} , which corresponds to Amide A, B, I, II and III bands of collagen, respectively (Jakobsen et al., 1983; Muyonga et al., 2004). The characteristic bands of collagen arise from the vibrational motions of peptide bonds that link together the amino acids that constitute the collagen

protein (Guzzi Plepis et al., 1996; Pępczyńska et al., 2019). The amide A band is associated with N-H stretching coupled with O-H vibrations. Amide B arises from asymmetric stretching vibration of =C-H as well as NH_3^+ . The amide I band represents the stretching vibrations of carbonyl groups (C=O) along the polypeptide backbone, while the amide II comprises about 60% amide N-H bending vibrations coupled with about 40% C-N stretching vibrations. The amide III bands represent intermolecular interactions in collagen. It consists of C-N stretching and N-H plane bending from amide linkages and absorptions arising from wagging vibrations from CH_2 groups from the glycine backbone and proline side chains (Payne and Veis, 1988; Sionkowska et al., 2004). The amide I, II and III bands are associated with the triple helical structure of collagen, and amide I is sensitive to the changes in the conformational state of the protein (Lazarev et al., 1985; Heu et al., 2010). The FTIR spectra of the collagen/cellulose and collagen/starch blend films show characteristic peaks of collagen, cellulose, and starch, respectively. The bands associated with cellulose and starch were located between 995 and 1031 cm^{-1} and are associated with C-O and C-C stretching vibrations of cellulose and starch molecules (Zhijiang and Guang, 2011; Wang et al., 2017a).

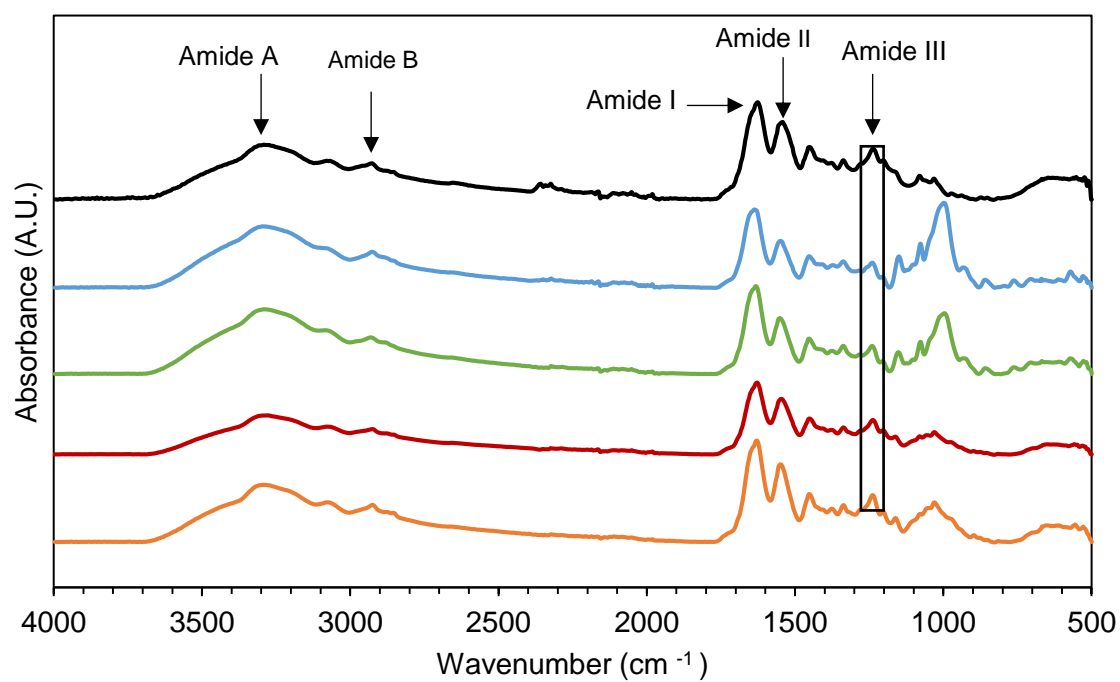
Previous literature has reported that a shift of the amide A, amide B, amide I, amide II and amide III bands to lower wavenumbers indicates increased hydrogen bonding potential and increased collagen stability (Doyle et al., 1975; Liu et al., 2016; Riaz et al., 2018; Noorzai, 2020). Also, a shift to higher wavenumbers indicates an alteration in collagen helical structure (Xie et al., 2006). Regardless of the starting paste collagen concentration, the amide A, amide I, amide II, and amide III bands of collagen films with cellulose fibres or starch granules shifted to higher wavenumbers when compared to that of the pure collagen films with collagen-starch showing the highest amide I, II

and III values. According to (Doyle et al., 1975; Li et al., 2013), amide A shifts to lower frequency when the NH group of a peptide is involved in hydrogen bonding, and a lower amide I wavenumber corresponds to a higher hydrogen bonding potential of C=O groups with adjacent chains. Therefore, the shift to higher wavenumbers of the collagen films in the presence of cellulose fibres and starch granules would indicate an interruption of hydrogen bonding between the amino (NH) and carbonyl (C=O) groups of the peptide chain during the drying process, thus resulting in a less ordered structure (also shown by the XRD data – section 6.5.6). Similar results were obtained for collagen-corn starch composite films (Wang et al., 2017a) and collagen modified with alginate di-aldehyde (Hu et al., 2014). The authors concluded that the shift to higher wavenumbers showed a conformational change in collagen structure due to altered hydrogen-bonding interactions in collagen structure and/or polymer molecules. Furthermore, the Amide III band's absorbance peak is affected by changes in the triple helical structure; the extent of the decrease in the intensity is therefore used to quantify the degree of ordering or stabilisation of the collagen structure (Chen et al., 2019). It was observed that the intensity of the Amide III peak of the collagen films decreased in the presence of cellulose fibres and starch granules. However, the decrease was more evident in collagen-starch films, indicating a higher degree of disorder in the collagen triple helix structure in the dried film state.

The absorption ratio of Amide III to 1450 cm^{-1} is used to investigate the integrity of the collagen triple helix structure. The structure of pure collagen is considered intact if the ratio is greater than or equal to 1, whereas the ratio of gelatin, the denatured collagen has been reported as 0.6 (Hu et al., 2014). The absorption ratio for collagen with and without cellulose/starch films are presented in Table 6-4. The absorption intensity ratio for collagen/cellulose films was between the range of 0.85 – 0.95, indicating that the

triple helix of collagen was preserved in the presence of cellulose. However, collagen/starch film values were below 0.6, suggesting that the starch granules affected the integrity of collagen's hierarchical structure. This data correlates with the X-ray data, where less ordered structure was observed for collagen-starch films.

(A)



(B)

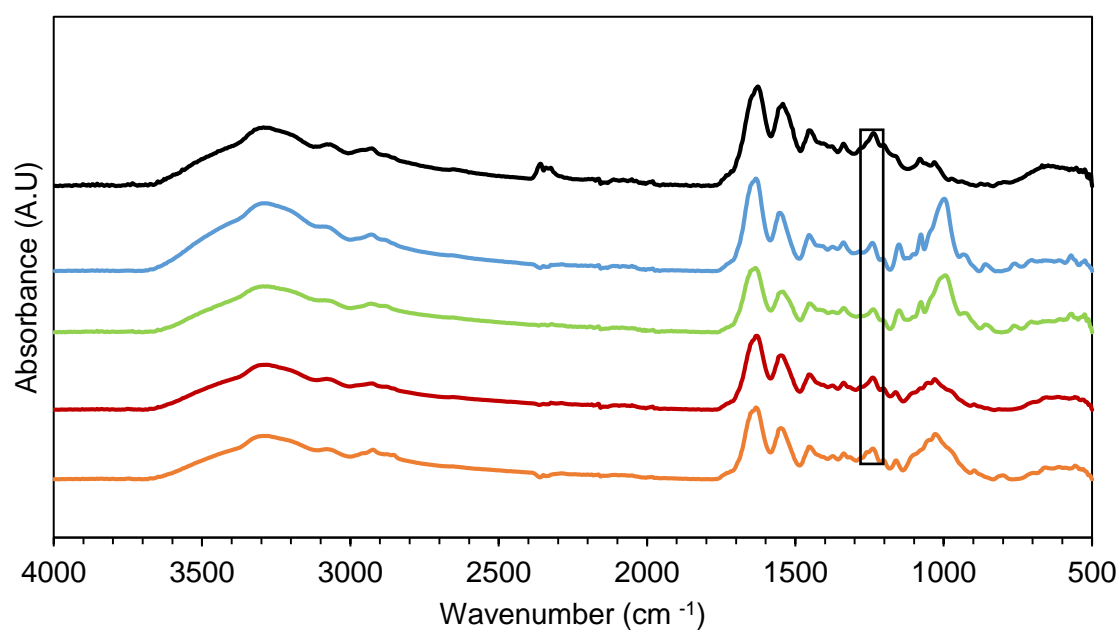


Figure 6-5: FTIR spectra of COLLSF3 (orange line), COLLSF9 (red line), COLLWS (green line), COLLHAS (blue line) and pure collagen (black) films at (A) 3.5% (B) 2.5% collagen concentrations.

Table 6-3. Wavenumber of the bands in the FTIR spectra of the films.

Films	Amide					
	A	Amide B	Amide I	Amide II	Amide III	C-O-C
3.5% COLLAGEN	3292	2928	1626	1542	1237	
COLLWS	3290	2931	1632	1551	1240	996
COLLHAS	3290	2925	1633	1550	1240	998
COLLSF9	3293	2928	1628	1547	1239	1031
COLLSF3	3292	2925	1629	1549	1238	1030
2.5% COLLAGEN	3292	2928	1626	1542	1237	
COLLWS	3292	2930	1634	1544	1240	995
COLLHAS	3293	2929	1635	1551	1240	997
COLLSF9	3292	2927	1630	1547	1239	1030
COLLSF3	3292	2924	1632	1547	1238	1029

Table 6-4. FTIR absorption ratios of A_{III}/A₁₄₅₀ for collagen films with and without cellulose fibres/starch granules at different collagen concentrations.

Films	A _{III} /A ₁₄₅₀ cm ⁻¹ Ratio
3.5% COLLAGEN	0.96 ± 0.0 ^b
COLLWS	0.53 ± 0.2 ^a
COLLHAS	0.47 ± 0.2 ^a
COLLSF3	0.95 ± 0.0 ^b
COLLSF9	0.95 ± 0.0 ^b
2.5% COLLAGEN	0.94 ± 0.2 ^b
COLLWS	0.49 ± 0.2 ^a
COLLHAS	0.48 ± 0.1 ^a
COLLSF3	0.89 ± 0.2 ^b
COLLSF9	0.85 ± 0.3 ^b

^{a-b} Mean ± standard deviation. Means in the same column with different superscript letter are significantly different (P < 0.05).

6.5.6 X-ray Diffraction of films

The X-ray diffractograms of pure collagen and collagen films blended with either cellulose or starch are shown in Figure 6-6 and Figure 6-7, respectively. Their corresponding percentage crystallinity is also reported in Table 6-5. Pure collagen films made from pastes at 3.5% and 2.5% wt/wt concentrations both present an intense peak at $\sim 2\theta = 7.9^\circ, 8.1^\circ$ and a broad peak at $2\theta = 15 - 26^\circ$. The first peak indicates the crystalline triple-helix structure of collagen, the intensity of the peak relates to the triple helix content, and the broad peak relates to the amorphous fraction of collagen (Tanioka et al., 1976; Pępczyńska et al., 2019; Xu et al., 2020b). For

collagen-cellulose films (COLLSF3 and COLLSF9), the collagen peak appeared at diffraction angle $2\theta = 7.7^\circ - 7.9^\circ$, while the broad, amorphous peak of collagen was suppressed by characteristic crystalline peaks of cellulose I at about $2\theta = 16.1^\circ - 22.5^\circ$ are related to (101) and (002) crystallographic plane of cellulose I (Koganti et al., 2011; El Oudiani et al., 2011; Khan et al., 2012). An additional small peak was also observed for all collagen-cellulose films at $2\theta = 35^\circ$, and this is associated with (040) crystallographic plane of cellulose I (De Morais Teixeira et al., 2011; Oun and Rhim, 2016). Collagen-starch films (COLLWS and COLLHAS) showed both collagen and starch peaks. The collagen crystal diffraction peak of COLLHAS and COLLWS appeared at $2\theta = 7.7 - 7.9^\circ$. However, the broad, amorphous collagen peak was overlapped by diffraction peaks of amylopectin and amylose peaks. COLLWS films exhibited sharp peaks at diffraction angles ca. $2\theta = 15^\circ$ and 23° , corresponding to A-pattern diffraction peaks of high amylopectin corn starch. Whereas COLLHAS films showed a strong peak at around $2\theta = 17^\circ$ and a few smaller peaks at 20° , 22° , 23° , which are characteristic peak patterns of B-type starch (Zobel, 1988; Cheetham and Tao, 1998). Interestingly, irrespective of the collagen concentration in the blends, the intensity of the collagen films diffraction peak at around $2\theta = 7.9^\circ$ reduces with the incorporation of cellulose fibres or starch granules. This indicates that the collagen crystalline structure decreases with the addition of cellulose fibres and starch granules. Additionally, it was observed that the intensity of the collagen is lower for collagen-starch films compared with blends of collagen-cellulose films, indicating that starch granules have a higher degree of interference on the ordered structure of collagen. The estimated percentage crystallinity of pure collagen films with and without cellulose fibres/starch granules are presented in Table 6-5. As expected, the crystallinity of pure collagen films was higher due to the highly ordered triple helical structure. However,

with the introduction of cellulose fibres and starch granules, the crystallinity of the blend films was significantly reduced ($p < 0.05$). As previously explained, the reduced crystallinity of the blend films is due to the cellulose fibres and starch granules preventing the stabilised ordered arrangement of collagen structure during the drying process and disrupting the bonds stabilising the collagen structure. Collagen-starch films show the lowest values consistent with reducing melting enthalpy observed by DSC (section 6.4.7). The decrease in crystallinity corresponds to the decreased thermal stability of the blend films, as observed by TGA analysis (Table 6-7). Similar results were reported for collagen-CMC films (Wu et al., 2020). They suggested that biopolymers altered protein triple helical structure formation by disrupting hydrogen-bonding interactions between collagen molecules. The disruption results from an interaction between the hydroxyl (-OH) groups of the biopolymers and amine (-NH₂) groups of the collagen and a decrease in the water bridge stabilising the triple helices.

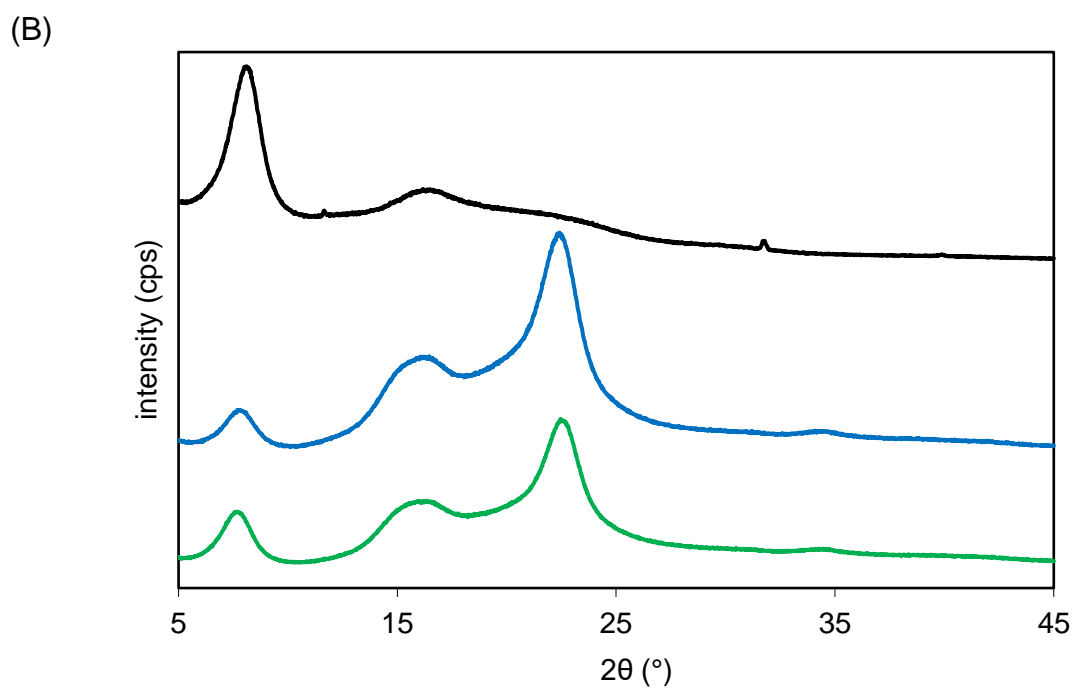
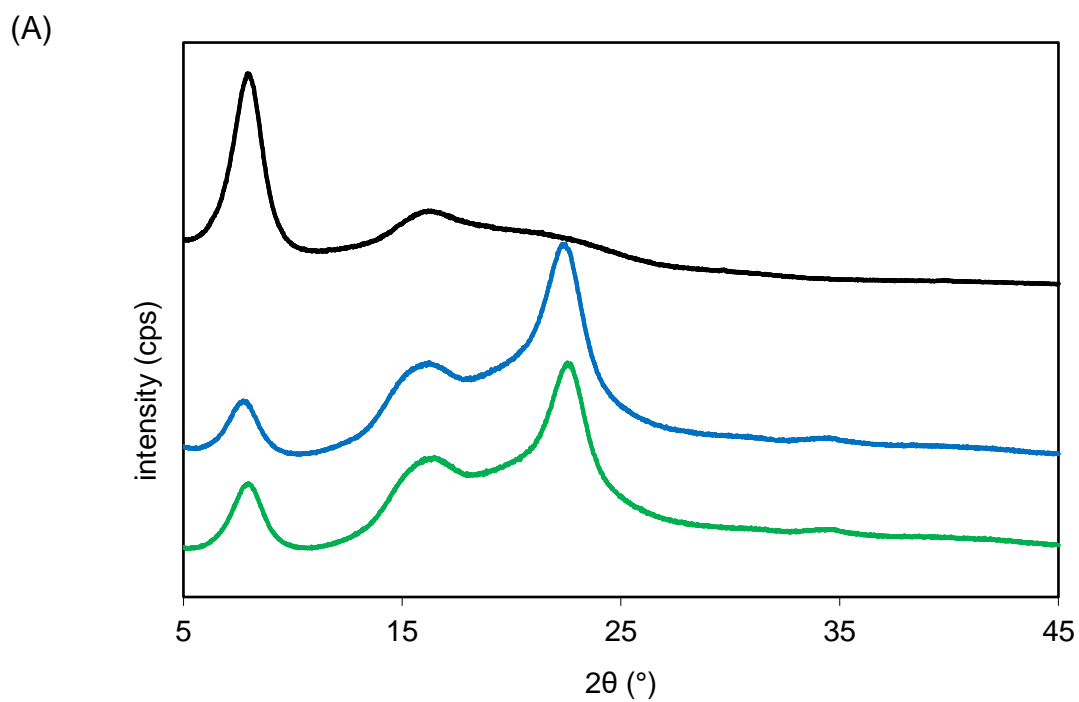
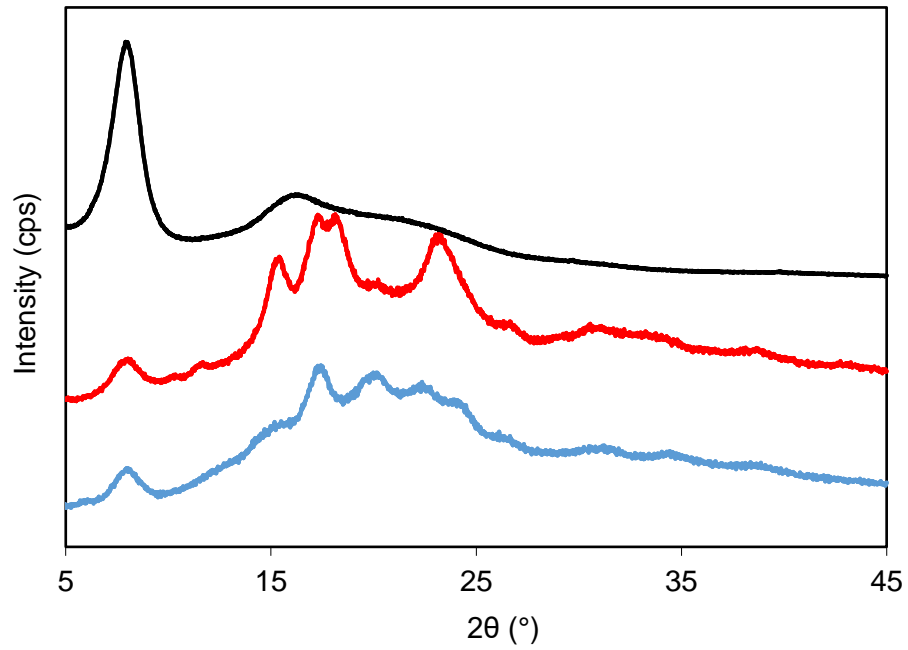


Figure 6-6. X-ray diffraction patterns of pure collagen (black line) COLLSF3 (blue line) and COLLSF9 (green line) films at (A) 2.5% (B) 3.5% collagen concentration.

(A)



(B)

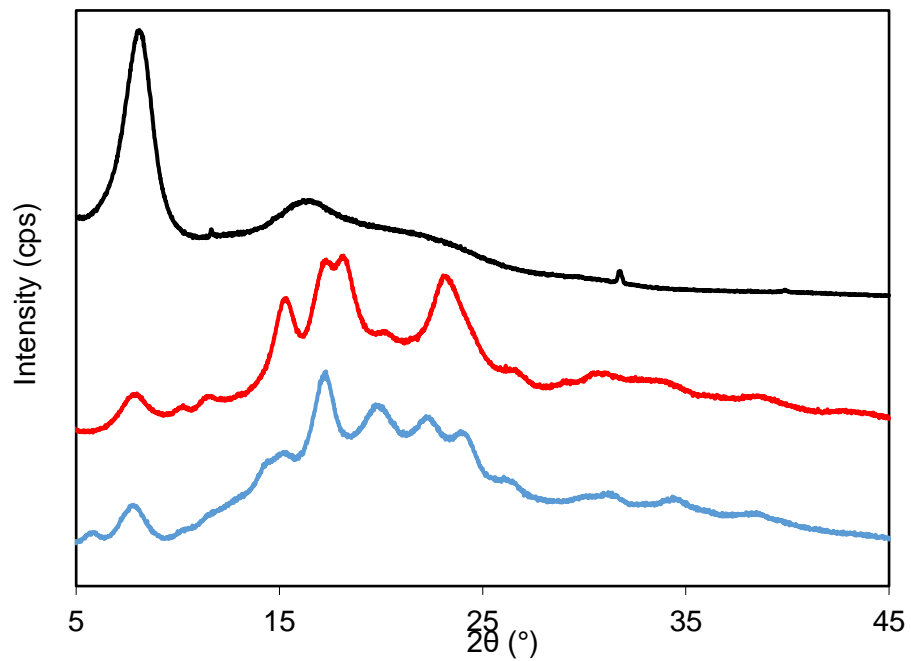


Figure 6-7. X-ray diffraction patterns of pure collagen (black line) COLLWS (red line) and COLLHAS (blue line) films at (A) 2.5% (B) 3.5% collagen concentration.

Table 6-5: Percentage crystallinity of collagen films with and without cellulose/starch at different collagen concentrations.

Film	% Crystallinity
3.5% COLLAGEN	73.8 ± 2.3 ^c
COLLWS	44.3 ± 1.2 ^a
COLLHAS	47.8 ± 1.0 ^a
COLLSF3	66.3 ± 0.1 ^b
COLLSF9	66.0 ± 1.1 ^b
2.5% COLLAGEN	71.9 ± 4.5 ^b
COLLWS	44.7 ± 1.2 ^a
COLLHAS	45.3 ± 1.1 ^a
COLLSF3	67.6 ± 1.3 ^b
COLLSF9	66.7 ± 1.2 ^b

^{a-c}Mean ± standard deviation. Means in the same column with different superscript letter are significantly different (P < 0.05).

6.5.7 Differential Scanning Calorimetry

The DSC thermograms of collagen with and without cellulose/starch films are depicted in Figure 6-8 and their melting transition temperatures and enthalpies are presented in Table 6-6. All the films show an endotherm at peak temperatures (T_{Peak}) > 100 °C. These temperatures is attributed to the disruption of collagen chains from their highly ordered structure due to the breakdown of intra and intermolecular bonds of the collagen molecules (Bigi et al., 2001; Chen et al., 2014; Ahmad et al., 2016). Pure collagen films made from collagen paste at 2.5 and 3.5 % wt/wt shows intense

endotherm at peak temperature (T_{peak}) values of 104.86 °C and 106.02 °C, respectively. Thus, collagen stabilisation upon drying of the pure collagen films depends on the starting paste concentration. The values reported in this study for pure collagen films were different from those reported by Wang et al. (2017c) and (Xu et al., 2020b) for collagen films formed from acid swollen collagen fibres. The differences in the endothermic peak temperature of collagen films of this study and those reported in literature might arise from differences in collagen concentrations, film preparation methods and the moisture content of the films. However, in the presence of cellulose fibres and starch granules, the intensity of the endothermic peak relating to the helix-coil melting temperature (T_{peak}) was reduced.

As observed in Table 6-6, at higher paste collagen concentration, at 3.5% collagen concentration the denaturation temperatures (T_{peak}) of collagen/cellulose films (COLLF3 and COLLSF9) were not significantly different ($p > 0.05$) compared to pure collagen films alone. Whereas, in the case of collagen-starch films, the peak temperature values were significantly lower ($p < 0.05$) than pure collagen films, indicating a reduction in the thermal stability of the collagen in the films. However, at lower paste collagen concentration, the T_{Peak} values of collagen/cellulose (COLLSF9 and COLLSF3) films were significantly ($p < 0.05$) higher than pure collagen film alone. The T_{Peak} value of COLLWS was not significantly ($p > 0.05$) than that of pure collagen film. However, COLLHAS show significantly lower T_{peak} value.. A possible explanation for the increase in peak temperatures of the blend films at lower levels of collagen might be because, at lower collagen concentration, the collagen fibrils could align to a greater extent in the presence of the fillers, with cellulose fibrils aligning better with collagen fibres, irrespective of cellulose fibre length. In general, collagen starch films had lower denaturation temperatures compared to collagen-cellulose films. This result

suggests that collagen molecules were less thermally stable in starch granules than cellulose fibres. As explained earlier, spherical starch granules disrupted collagen fibril re-alignment more during drying, resulting in less stable films. The presence of starch granules, causing an alteration in the triple helical structure, was confirmed by FTIR data (Table 6-4). Similarly, reduced melting temperatures of collagen-starch blend films may be related to lower film crystallinity index. According to Lecorre et al. (2012), semi-crystalline biopolymers with a higher crystallinity melt at higher temperatures. A similar result was reported by Ahmad et al. (2015) for composite films of fish gelatin with rice flour. It was found that the lower crystallinity of the fish gelatin/rice flour films led to a decrease in the melting temperature and enthalpy of fish gelatin.

The total heat of fusion, commonly referred to as the enthalpy (ΔH), indicates the energy required to disrupt the hydrogen bonds stabilising the collagen triple helices, and the values can be related to the relative amount of triple helical structure in the samples (Bigi et al., 2004). Cellulose fibres and starch granules reduced the melting enthalpies of collagen films at each paste collagen concentration (Table 6-6). This suggests that starch and cellulose affected the ordered structure of collagen upon drying and matched previous results. Collagen-starch films show the lowest enthalpy values, and this correlates with reduced crystallinity. It is widely accepted that collagen structure is stabilised by direct and water-mediated hydrogen bonds located within the triple helices (Bella et al., 1995; Brodsky and Ramshaw, 1997; Zhang et al., 2007). Two hypotheses are proposed to explain the reduction in enthalpy of collagen films in the presence of cellulose fibres and starch granules. The first hypothesis is that starch granules and cellulose fibre prevents the alignment of collagen fibrils during drying while the second hypothesis is that cellulose/starch are acting as physical crosslinkers with collagen molecules. In the first hypothesis, the fillers (cellulose/starch) could

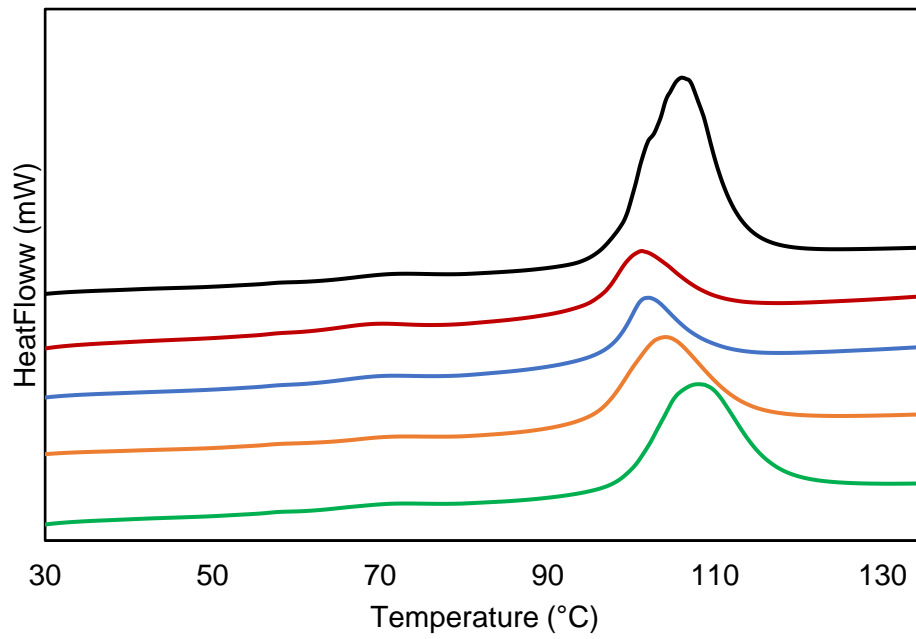
physically deter the re-alignment of the collagen chains in an orderly manner during the drying process. Consequently, collagen molecules cannot come together to form water bridges, thus, resulting in a less stabilized triple helical structure and a decrease in the enthalpies. The aspect ratios of cellulose fibres and starch granules and their concentrations at comparable phase volumes might also affect the ordered rearrangement of collagen triple helices. Cellulose fibrils can align with the collagen fibres, resulting in a slightly less impeded ordered structure. On the contrary, the spherical starch granules hindered the realignment of collagen fibres due to the smaller aspect ratios of the starches and the higher amount required at comparable phase volume. Also, the type of starches used in this study did not affect as similar enthalpy values were observed. However, in the case of cellulose, higher enthalpies were observed for cellulose with higher aspect ratios. This could be explained by the need for less long cellulose fibre that may align more effectively with collagen fibres upon drying.

The second hypothesis is that starch and cellulose molecules might be acting as physical cross-linkers. Schroepfer and Meyer (2017) investigated cross-linked and non-cross-linked bovine collagen by DSC. They showed that the enthalpy of denaturation of collagen decreased with the addition of chemical cross-linkers. They concluded that the cross-linkers disturbed the water network stabilising the collagen triple helices, thereby causing a decrease in enthalpy. According to Schroepfer and Meyer (2017), water molecules not directly linked to collagen molecules acted as spacers in hydrated collagen samples by preventing direct contact of collagen molecules. However, upon drying, the water is removed, and the collagen helices are drawn closer via direct water bridges, thereby increasing the denaturation enthalpies. It is proposed that the water bridges between the collagen molecules were affected by

the presence of the fillers due to a possible cross-linking interaction between collagen and cellulose/starch molecules. These interactions may prevent hydrogen-bonded water bridges within collagen chains and rearrange the triple helix structure during drying. Starch is very efficient at preventing water bridge formation because a higher dry mass is used and potentially provides more hydrogen bonding sites for water molecules; the hydroxyl groups on the starch will interact with the water molecules. As a result, there is a net decrease in water available for water bridge formation because the hydroxyl groups of starch occupy the surface of the collagen.

The collagen films enthalpy value with smaller cellulosic fibres (COLLSF3) is higher than collagen films with starch granules, though the values are still lower than pure collagen films alone. Higher enthalpy was seen with cellulose with a higher aspect ratio; however, it is still lower than collagen on its own. Thus, the difference in enthalpy values of collagen films in the presence of the various fillers could be due to differences in aspect ratios and concentrations required at comparable phase volume and the anhydrous nature of the fillers. Previous studies by Sionkowska (2003) and Chen et al. (2008) reported that the addition of poly (vinyl) pyrrolidone and chitosan nanofibres to collagen blends reduced the denaturation enthalpy of collagen, this was due to an intermolecular interaction between the different macromolecules which 'replaced' collagen-collagen interactions. They concluded that intermolecular hydrogen bond formation between macromolecules interrupted and competed to form hydrogen bonds between collagen molecules. This is an interesting proposition, but the hierarchical nature of swollen collagen fibres needs to be considered a potential steric barrier to 'molecular' interactions, indicating that this could only be a surface effect.

(A)



(B)

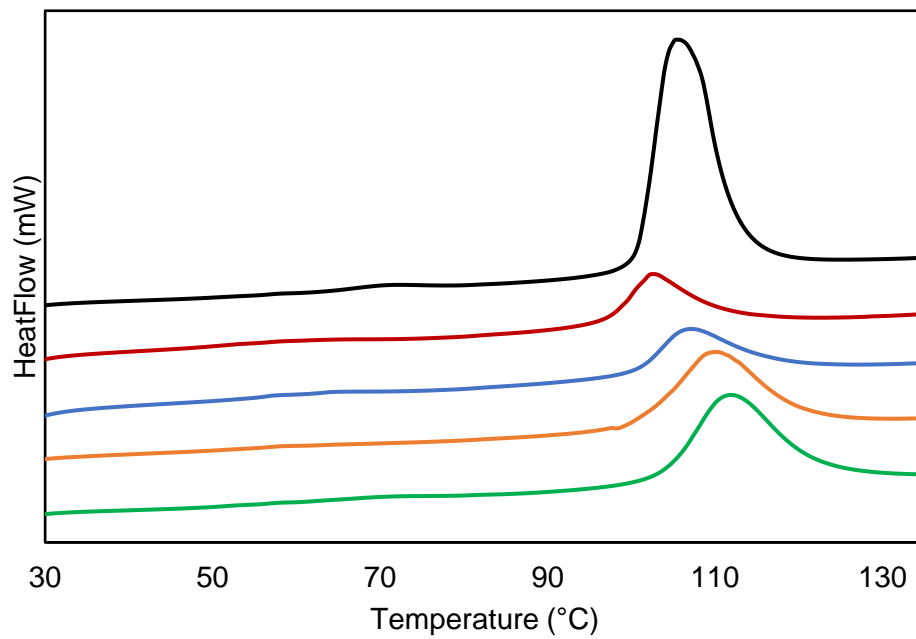


Figure 6-8. DSC thermograms of pure collagen (black line), COLLSF9 (green line), COLLSF3 (orange line), COLLWS (Blue line) and COLLHAS (red line) collagen with

and without cellulose fibres/starch granules at (A) 3.5% (B) 2.5% collagen concentrations.

Table 6-6. Onset temperature (T_o), endothermic peak (T_{peak}), Endset (T_{end}), enthalpy (ΔH) of collagen with and without cellulose/starch films at different collagen concentrations.

Samples	T_{onset} ($^{\circ}C$)	T_{peak} ($^{\circ}C$)	T_{end} ($^{\circ}C$)	$\Delta H(J/g)$
3.5% COLLAGEN	98.0 ± 0.5^a	106.0 ± 1.0^c	112.9 ± 0.2^{bc}	30.0 ± 1.0^d
COLLWS	97.0 ± 0.3^a	101.8 ± 0.5^a	109.9 ± 0.2^a	9.7 ± 0.2^a
COLLHAS	95.3 ± 0.1^a	101.0 ± 0.5^a	110.3 ± 0.7^{ab}	9.8 ± 0.3^a
COLLSF9	102.6 ± 3.9^b	106.9 ± 1.3^c	117.5 ± 1.0^d	21.8 ± 0.6^c
COLLSF3	95.7 ± 0.2^a	104.0 ± 0.2^b	113.9 ± 2.9^c	16.9 ± 0.7^b
2.5% COLLAGEN	96.7 ± 7.5^a	104.9 ± 0.7^b	113.1 ± 6.1^a	30.9 ± 2.1^d
COLLWS	100.9 ± 1.4^a	106.9 ± 1.7^b	117.8 ± 2.8^{ab}	8.9 ± 0.4^a
COLLHAS	97.1 ± 0.4^a	102.6 ± 0.0^a	112.1 ± 1.0^a	8.6 ± 0.2^a
COLLSF9	103.8 ± 0.6^a	111.8 ± 0.5^c	122.2 ± 0.0^b	17.9 ± 0.3^c
COLLSF3	101.0 ± 3.2^a	110.3 ± 1.8^c	120.5 ± 1.9^b	15.4 ± 0.4^b

6.5.8 Thermogravimetric analysis

Thermogravimetric analysis (TGA) was performed to study the thermal stability of collagen with and without cellulose/starch films at various collagen concentrations. The TGA and derivative thermogravimetric (DTG) curves are shown in Figure 6-9, and Figure 6-10 and their parameters are presented in Table 6-7. The DTG curves show two distinct weight loss stages for pure collagen and collagen/cellulose films, while

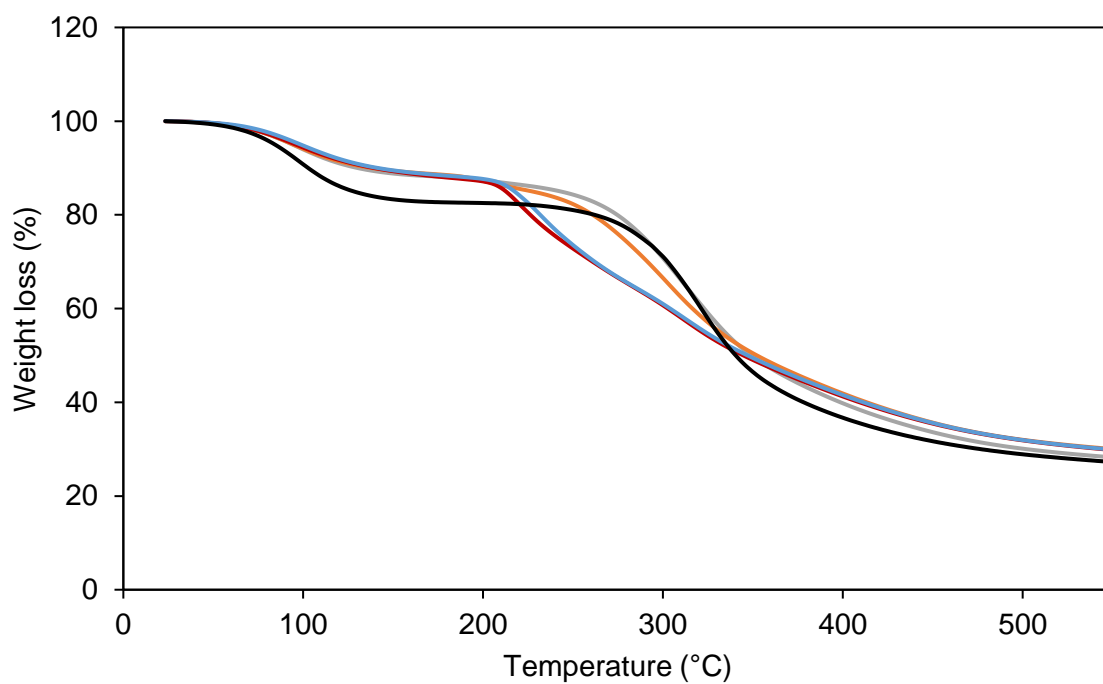
collagen/starch films show three main degradation stages. The first weight-loss stage for all the films occurred between 23 °C and 150 °C, and it relates to the evaporation of structural and bound water (Ding et al., 2015). The corresponding weight loss values for pure collagen films made from 2.5% and 3.5% (w/w) collagen pastes are about 17.2% and 18.8%, respectively, whilst the weight loss values of the blend films are between 13.0% - 15.5% at the levels of collagen paste studied (consistent with Figures 2A and 2B). The difference in the percentage weight loss is due to the films moisture content (Sahraee et al., 2017). The second stage of weight loss ($\Delta w_2 = 56.2 - 56.5\%$) occurs at degradation temperatures of 323.4 and 325.9 °C for pure collagen films made from 2.5% and 3.5% (w/w) collagen paste concentration, respectively. For collagen-cellulose (COLLSF3 and COLLSF9) films, the second degradation step occurred at degradation temperatures between 306.8 °C - 313.7 °C with weight loss of about ($\Delta w_2 = 54.5 - 56.9\%$). The second degradation stage of pure collagen films and collagen-cellulose films (COLLSF3 and COLLSF9) is attributed to the decomposition of collagen (Ma et al., 2018). The degradation profile and temperatures for collagen films are in line with previous studies (Jose et al., 2009; Ding et al., 2015). COLLSF3 and COLLSF9 films show small weight loss at temperatures between 205.0 and 213.4 °C, which might indicate a small amount of disordering of the collagen chains.

In collagen-starch films, the second stage weight loss ($\Delta w_2 = 21.9 - 24.6\%$) appeared at a much lower degradation temperature of 226.6 °C - 240.3 °C and is attributed to the degradation of collagen molecules. Interestingly, collagen films with high amylose starch (COLLHAS) showed higher degradation temperatures than those with waxy starch (COLLWS). This may be due to different levels of crystallinity within a starch granule, affecting the anhydrous nature of the granule itself. Higher levels of amylose

would infer a lower anhydrous nature to the granule, increasing (slightly) the water available to stabilise the collagen upon drying. A third weight-loss stage with smaller peaks with weight loss ($\Delta w_3 = 30.3 - 33.5\%$) appeared at degradation temperatures of about 315.6 - 325.2 °C. TGA analysis was performed on powdered waxy and high amylose corn-starch, and their main degradation temperature was observed at temperatures about 306.6 °C – 313.3 °C (data are not shown). Therefore, collagen degradation temperatures with starch film at higher temperatures may be related to residual stabilised collagen and starch granules since they both degraded at similar temperatures.

Comparing the collagen degradation temperatures of pure collagen and the blend films shows that pure collagen films, regardless of the starting paste collagen concentration, showed higher degradation temperatures. Strong hydrogen bonding interaction among collagen chains yielded a highly ordered structure, resulting in higher heat resistance of the resulting collagen films. However, the addition of cellulose fibres and starch granules reduces the thermal stability of collagen films, with collagen-starch films showing the lowest thermal stability, which is in line with the DSC result (Table 6-6). Zhang et al. (2020b) reported that a film's crystallinity is closely related to material stability. Winkworth-Smith (2015) reported that reduced crystallinity of microcrystalline cellulose fibres due to ball milling led to lower cellulose degradation temperatures. Thus, the lower crystallinity of the blend films indicates a less orderly structure that results in less thermally stable films. The lower thermal stability of the collagen-starch films can be attributed to a more disordered film structure compared to collagen-cellulose films.

(A)



(B)

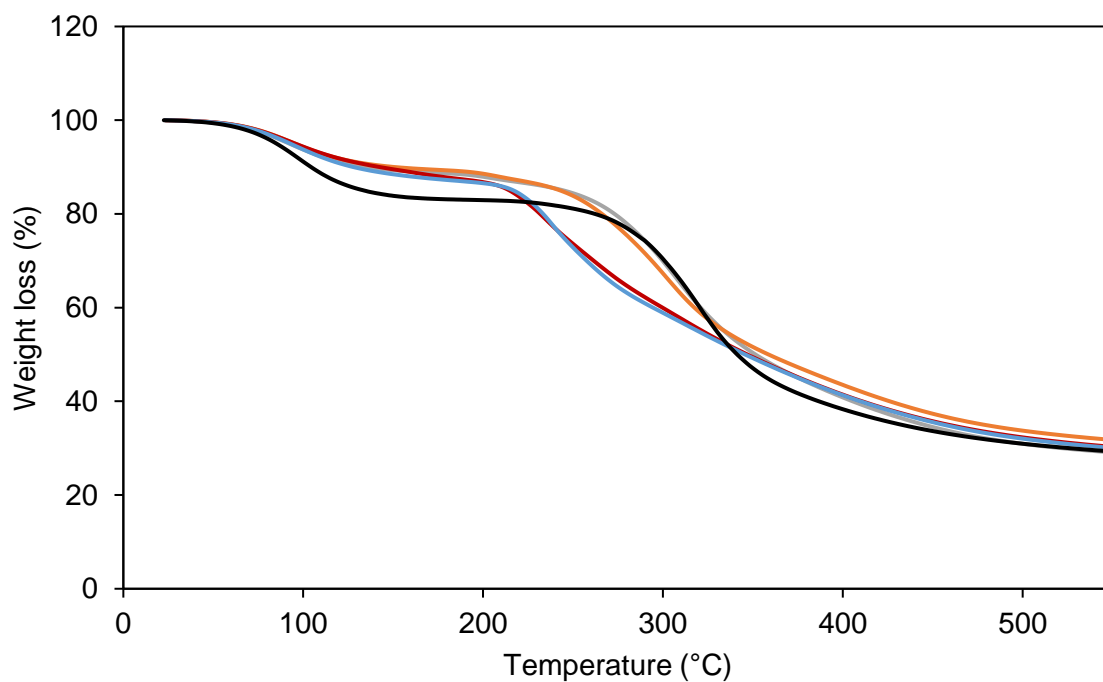


Figure 6-9. . TGA curves of pure collagen (black line), COLLSF3 (orange line), COLLSF9 (grey line), COLLWS (red line) and COLLHAS (blue line) films at (A) 2.5% (B) 3.5% collagen concentrations.

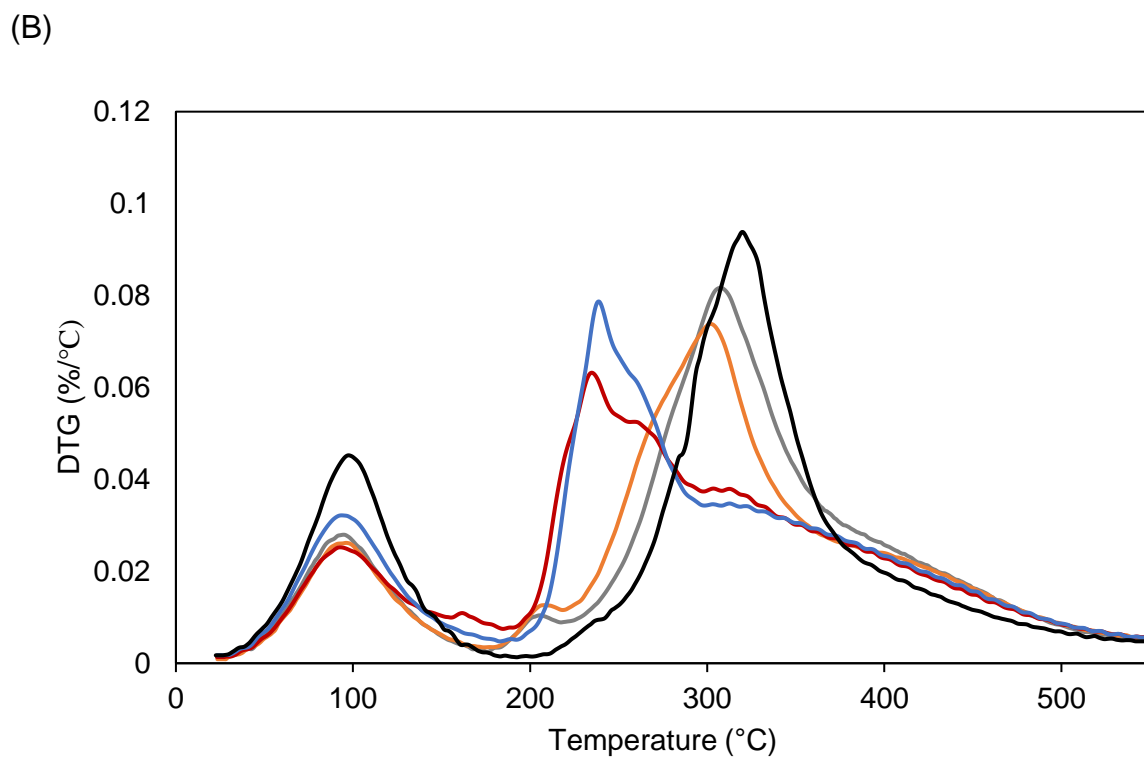
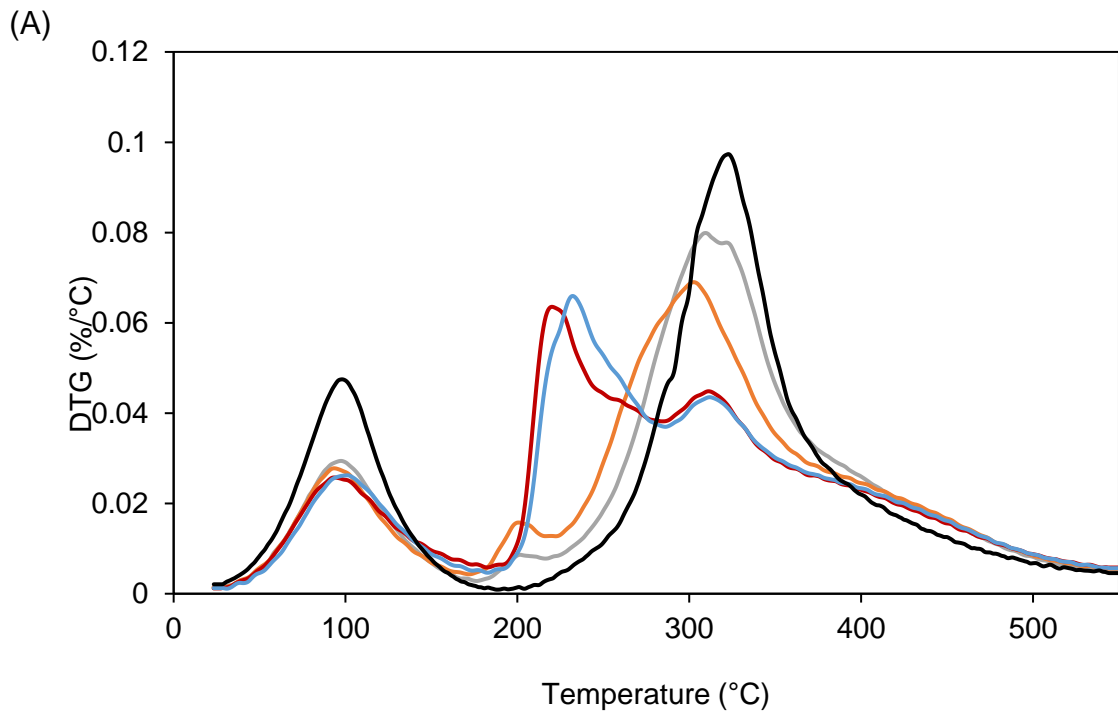


Figure 6-10. DTG curves of pure collagen (black line), COLLSF3 (orange line), COLLSF9 (grey line), COLLWS (red line) and COLLHAS (blue line) films at (A) 2.5% (B) 3.5% collagen concentrations.

Table 6-7. Thermal degradation temperature (Td) and weight loss (%) of collagen with and without cellulose fibres/starch granules at different collagen concentrations.

Samples	Δ_1		Δ_2		Δ_3	
	T _{d1} (°C)	Δ_{w1} (%)	T _{d2} (°C)	Δ_{w2} (%)	T _{d3} (°C)	Δ_{w3} (%)
3.5% COLLAGEN	103.5± 1.4	18.0 ± 0.6	325.9 ± 0.6	56.5 ± 0.2		
COLLWS	99.2 ± 0.4	15.0 ± 0.1	226.6 ± 0.1	21.9 ± 0.2	315.6 ± 0.5	32.4± 0.2
COLLHAS	104.5± 1.3	15.5 ± 1.1	235.6 ± 1.9	22.1 ± 0.1	316.9 ± 0.5	33.5 ± 0.4
COLLSF9	100.4± 0.5	14.7 ± 0.3	313.7 ± 1.9	56.9 ± 0.4		
COLLSF3	97.1 ± 0.5	13.0 ± 0.4	306.8 ± 0.4	54.5 ± 0.7		
2.5% COLLAGEN	103.2± 0.2	17.2 ± 1.3	323.4 ± 1.4	56.2 ± 0.5		
COLLWS	98.8 ± 0.9	15.7 ± 0.6	235.1 ± 1.9	22.8 ± 2.8	317.3 ± 0.9	31.8 ± 0.5
COLLHAS	100.1± 2.8	14.9 ± 0.1	240.3 ± 0.9	24.6 ± 1.4	325.2 ± 1.0	30.3 ± 0.5
COLLSF9	98.5 ± 1.3	14.8 ± 0.1	311.4 ± 0.6	56.8 ± 0.4		
COLLSF3	100.5± 0.5	14.0 ± 3.8	309.3 ± 1.0	53.4 ± 2.2		

Note: Δ_1 , Δ_2 and Δ_3 denote the first, second and third weight loss stages respectively of the films.

6.6 Conclusions

This study aimed to assess the effect of cellulose fibres and starch granules (assumed as fillers) at comparable dispersed phase volume on collagen film structure, thermal, mechanical and sorption properties. It was shown that by fixing the dispersed phase volume, the cellulose and starch affected the rearrangement of collagen fibres during drying, which affected the properties of the resulting films. The microstructures of the films by SEM showed the addition of the cellulose fibres/starch granules affected the self-alignment of the collagen fibres, consequently resulting in rough surfaces and increased thickness of the blend films. The addition of starch granules has a more significant influence on preventing the rearrangement of collagen chains and leads to higher thickness values, which might be due to the spherical nature and the concentration of starch required at comparable phase volumes with cellulose. The inclusion of cellulose fibres strengthened the collagen films by increasing the tensile properties and stiffness of the collagen films, which can be attributed to the entanglement of cellulose fibres with collagen fibres. Whereas, the presence of starch granules in collagen films made them too brittle and untested. FTIR and XRD results helped to understand the structural changes and interactions between collagen and cellulose/starch at a molecular and supramolecular level. The incorporation of cellulose fibres and starch granules was shown to alter collagen ordering, which reduced the crystallinity of blend films. Changes in collagen structure were shown to depend on filler morphology, as spherical starch granules had a greater effect on collagen structure disordering.

Furthermore, as evidenced in TGA, incorporation of cellulose fibres and starch granules reduced the thermal stability of collagen films; this was correlated with reduced film crystallinity. DSC results showed that collagen/cellulose films had more

thermally stable molecules than collagen/starch films, and values increased with lower collagen concentrations attributed to a more orderly arrangement. The enthalpy of collagen film denaturation decreased with the inclusion of cellulose fibres and starch granules. The decrease was more pronounced in the presence of starch granules. Two hypotheses are proposed to explain reduced enthalpy, crystallinity and thermal stability in starch and cellulose: 1) the particulates prevent the collagen fibre structure re-organisation during the drying process, which is thought to be dependent on the shape and concentration of fillers used; 2) relies on the prevention of the hydrogen-bonded water bridge stabilising the collagen triple helical structure due to a physical cross-linking effect of cellulose/starch with collagen molecules and or the hydration state of the fillers. Additionally, as revealed by DVS and moisture content results, cellulosic fibre and starch granules decreased collagen film moisture uptake, improving film potential as a packaging material. In summary, this comparative study results provide insight into understanding how different polysaccharide dispersions matched at the same dispersed phase volume affect the properties of collagen within a film, which could provide fundamental data for producing films with modified properties for commercial applications.

**7 EFFECT OF ACID-SWOLLEN COLLAGEN PASTE ON
STARCH GELATINISATION USING STANDARD AND
HIGH-TEMPERATURE HEATING MODES**

7.1 Abstract

Starch is the most versatile food ingredient used as a thickener, gelling agent, and rheology modifier across food industry applications and beyond, including composite materials for coating and packaging applications. This study aims to investigate the effect of different concentrations of acid-swollen collagen pastes on the pasting properties of starches with different amylose and amylopectin content; normal (NS), waxy (WS), and high amylose (HAS) corn starches using both standard (95 °C) and high-temperature Rapid Visco-Analysis (RVA) mode (140 °C). Under standard heating mode (95 °C), NS pasting temperature shifted to lower temperatures at higher collagen levels (4% and 3.5%). Increasing concentration of collagen paste caused an increase in the peak viscosities of all the starches. Breakdown and setback viscosities of WS and NS increased, especially at higher collagen concentrations. Final and trough viscosities increased for NS, but the opposite effect was observed for WS. These changes contrast with high amylose starch behaviour with and without collagen that did not show a distinct pasting profile. Likewise, the addition of acid-swollen collagen paste did not affect the pasting temperature of waxy starch, suggesting that potential competition for water between NS starch and collagen is a potential driving factor for the observed changes.

This hypothesis is tested at the high-temperature heating mode (140 °C); a similar trend was observed with NS and WS's pasting temperature. The peak viscosity and break viscosity of WS and NS increased with increasing collagen concentrations in a similar way to the standard temperature. Conversely, the trough, setback, and final viscosities decreased with increasing collagen concentrations. Values were significantly lower than those observed at standard temperatures. Heating at high temperatures allowed the complete gelatinisation of high-amylose starch. The pasting

temperature of HAS shifted to lower temperatures, but peak and breakdown viscosities increased with increasing collagen levels. Final viscosity and setback viscosity decreased with increasing collagen pastes concentration. These findings offer exciting views on the use of collagen pastes in modifying starch paste properties and the effect of heating temperature on the pasting properties of corn-starch with and without additives.

7.2 Introduction

Starch is the main storage polysaccharide in higher plants and is widely used in processed foods, textiles, paper/packaging, and pharmaceuticals due to its unique functional properties, abundance, biodegradability, and low cost. In the food industry, starch is used as a rheology and texture modifier, stabiliser, and binding agent (Biliaderis et al., 1997). It consists of two polymers: amylose, a linear chain of (1-4)-linked α -D-glucopyranose residues, and amylopectin, highly branched with much shorter chains (1-4) α -D glucose residues and the branched chains are connected by α -(1-6) linkages (Jane et al., 1999). The physicochemical properties of starch granules are affected by amylose's ratio to amylopectin and the macromolecules' organisation into granular structures (Hong et al., 2015). When starch granules are heated in excess water, they undergo a process known as gelatinisation, which involves the dissociation of the amylopectin crystalline structures followed by a series of irreversible process such as loss of birefringence, swelling of the granules, and leaching of amylose (Tester and Morrison, 1990a; Cooke and Gidley, 1992). Upon cooling, the leached amylose re-associates to form a viscoelastic gel, a process known as retrogradation. The pasting and gelatinisation properties of starch are essential for their applications in the food industry (Sun et al., 2014). However, native starch pastes have some disadvantages, such as low stability when subjected to extended cooking time, high shear forces, and high retrogradation tendency (Sullo, 2012).

The blending of starch with hydrocolloids is a widely explored approach for improving the texture/rheology of starch gels, retarding retrogradation, increasing moisture retention in addition to other functionalities (Christianson et al., 1981; Appelqvist and Debet, 1997; Chaisawang and Supphantharika, 2005; Achayuthakan and Supphantharika, 2008; Sullo and Foster, 2010; Bemiller, 2011), without the need to use

chemical crosslinking within the starch granule which also imparts either granule stability or controls retrogradation. Most research on the modification of starch pasting properties has focused on using hydrocolloid gums due to their thickening properties. Nonetheless, while the effect of proteins, especially animal proteins such as gelatin, has been explored with regard to polymer incompatibility (Abdulmola et al., 1997), no data for collagen have been reported (to the best of our knowledge). This might be due to the insoluble nature of collagen.

Collagen is the most abundant fibrous protein and found in connective tissues such as skins, bones, cartilages, and tendons of mammals; it comprises approximately 30% of the total protein in the body of mammals and fish. The collagen molecule known as tropocollagen is a triple helix structure made up of three alpha chains, each consisting of a predominance of repeating units of GLY-X-Y amino acid sequences, whereas X and Y are proline and hydroxyproline, respectively. The alpha chains interact together via intermolecular hydrogen bonding and further intertwine to form a right-handed triple helix structure (Stenzel et al., 1974; Friess, 1998). Four to eight collagen molecules aggregate through fibrillogenesis into microfibrils and subsequently into collagen fibrils (diameters between 10 nm – 500 nm) with extra strength and stability resulting from further self-aggregation and intermolecular crosslinks (Stenzel et al., 1974; Gelse et al., 2003). These fibrils further assemble to form collagen fibres, which gives tensile strength and elasticity to animal tissue. Collagen can be obtained from bovine and porcine skins, and depending upon the extraction pre-treatments, the degree of 'native' fibre to fibrillar structure remains, making its study rather complex and more difficult to interpret than gelatin. Additionally, collagen is made into various forms such as powders, solutions and pastes/gels, which are viscoelastic. They are commonly

used for industrial applications in food, pharmaceutical, cosmetics, and biomaterial applications.

Starches pasting properties are commonly analysed using the rapid viscous analyser (RVA) technique at heating temperatures up to 95 °C to avoid artefacts that occur during boiling. However, some industrial starch applications, such as canned and extruded products, are processed at high temperatures (Liu et al., 2019). Also, high amylose starches require a high temperature (> 110 °C) to gelatinise. The present RVA heating (up to 95 °C) mode does not permit the analysis of starch performance in the abovementioned food applications. Therefore, it is necessary to perform RVA analysis at temperatures that mimic such industrial applications. Recently, a new Rapid Visco analyser (RVA-4800) equipped with a good sealing canister that can be pressurised up to 100 psi (6.9 bar) was developed. This allows the measurement of the starches' pasting properties to be carried out at 140°C without boiling (Perten Instruments, 2018).

Therefore, it can assess starch properties under high-temperature conditions associated with high-temperature processing. Presently, only a few publications have reported the pasting properties of starches from different botanical sources at a high-temperature range (>100 °C) (Liu et al., 2019; Zhang et al., 2020a; Liu et al., 2020; Li et al., 2020). Therefore, this study is the first to investigate the effect of acid-swollen collagen paste on maize starches' pasting properties with different amylose and amylopectin contents (normal, waxy, and high amylose maize starches) using the conventional and high-temperature RVA modes.

7.3 Material and Methods

7.3.1 Materials

Amioca (waxy maize starch - WS) and (Hylon VII - HAS) high amylose starch in powder form were kindly provided by Ingredion Incorporated (UK). Normal maize starch (NS) was purchased from Sigma Aldrich (Germany) in powder form. Acid-swollen collagen pastes at about pH 2 were donated by Devro plc (Scotland, UK).

7.3.2 Measurement of pasting properties

Pasting properties of waxy, normal, and high amylose maize starches in the presence and absence of collagen pastes were determined using a Rapid Visco-Analyser RVA Super 4 (Newport Scientific, Australia) for standard temperature and RVA 4800 (Perten Instruments, Sweden) for high temperature ($> 100\text{ }^{\circ}\text{C}$). For the control samples, each starch powder (1.75g) was weighed in a canister and distilled water added to reach a total weight of 25g to prepare a starch suspension of 7% w/w. For the blend preparation, the required amount of acid-swollen collagen paste corresponding to a final collagen concentration of 4 %w/w, 3.5 % w/w, and 2.5% w/w was added to each starch powder (to a final suspension concentration matching the control) with the required amount of distilled water added to a final weight of 25g. The dispersions were stirred manually using a plastic spatula before immediate loading into the RVA instrument. The samples were analysed using the following temperature profiles: equilibrating at $20\text{ }^{\circ}\text{C}$ for 1 min before heating to $95\text{ }^{\circ}\text{C}$ (Standard temperature) or $140\text{ }^{\circ}\text{C}$ (high temperature) at $12\text{ }^{\circ}\text{C}/\text{min}$, holding at $95/140\text{ }^{\circ}\text{C}$ for 2.5 min before cooling to $20\text{ }^{\circ}\text{C}$ at $12\text{ }^{\circ}\text{C}/\text{min}$ and holding at 20 for 2 min. The samples were initially mixed at 960 rpm for 1 min, and the measurements were performed under constant stirring at 160 rpm. All measurements were performed in triplicate. The pasting

properties: pasting temperature (the temperature of the onset of viscosity increase due to starch granule swelling upon the absorption of water), peak viscosity (the maximum viscosity obtained during heating), trough viscosity (the maximum viscosity during hold at maximum temperature), breakdown viscosity (the difference between peak and trough viscosities), final viscosity (viscosity at the end of the run) and setback viscosity (the difference between final and trough viscosities) were calculated from the pasting curve using the ThermoLine version 2.2 software Newport Scientific (Warriewood, Australia).

7.3.3 Microscopy

After cooling at standard and high-temperature heating modes, the paste structure was observed using an EVOS phase-contrast light microscope. Samples were mounted on a glass slide; a coverslip was placed on the sample, and another slide was used to press the pastes to make it thin for easy imaging. Images were taken at magnifications of 10X.

7.3.4 Statistical Analysis

The data were analysed using Statistical Package for Social Sciences (SPSS) version 26.0 (SPSS Inc., Chicago, IL, USA). One-way analysis of variance (ANOVA) was performed, and Tukey's mean comparison test compared the samples' means. The differences between starch and starch/collagen blends were considered significant when $p < 0.05$. Results were presented as mean \pm standard deviation.

7.4 Results and discussions

7.4.1 Pasting properties of starch/collagen blends measured in standard heating mode (up to 95 °C)

Figure 7-1 shows the pasting curves of the NS, WS, and HAS with and without collagen pastes when pasted to 95 °C, and their pasting parameters are summarised in Table 7-1. As expected, HAS alone shows no pasting response in water as it requires a higher temperature > 110 °C to undergo gelatinisation (Kibar et al., 2010; Genkina et al., 2014). WS alone exhibits a lower pasting temperature, final and setback viscosities, higher peak, trough, and breakdown viscosities than NS alone. These results are consistent with Hong et al. (2015) and Liu et al. (2019), who observed a similar trend for NS and WS. The difference in pasting profile of the starches can be attributed to differences in their amylose/amylopectin content; WS contains a small proportion of amylose (<1%), NS contains about 21-24 % amylose, while HAS contains about 70 % amylose (Kibar et al., 2010). The swelling of maize starch granules is dependent on amylopectin content (Tester and Morrison, 1990a; Tester and Morrison, 1993; Fredriksson et al., 1998). Containing mainly amylopectin, WS could swell more easily and develop high peak viscosity at low temperature. The amylose content in NS will form complexes with the internal lipids present in the granules, restricting the granule swelling (Tester and Morrison, 1990a; Tester and Morrison, 1990c).

The amylose-lipid complex is insoluble and requires high temperatures to disassociate (Jane et al., 1999). Fredriksson et al. (1998) reported similar results in that the gelatinisation temperatures of maize starches increased with increasing amylose content. NS shows higher setback and final viscosity than WS due to the higher

content of leached amylose during the gelatinisation. The increase in viscosity of the paste upon cooling is attributed to a retrogradation process involving the re-association of amylose molecules into an ordered structure (Atwell, 1988). The first (short-term) phase of retrogradation involves network formation through entanglements and/or formation of junction zones between amylose molecules (Gidley, 1989; Doublier and Choplin, 1989; Eidam et al., 1995), thereby forming a viscoelastic gel with granule ghosts and remnants acting as fillers (Miles et al., 1985; Ring, 1985; Keetels et al., 1996). In starches that do not contain amylose, the amylopectin molecules can associate to form weak gels (Cameron et al., 1994), which is slower due to the shorter chain lengths and steric restrictions imposed by the branched molecular structure (Gidley and Bulpin, 1987). The addition of collagen pastes at different concentrations results in modifying the pasting properties of the starches (Table 7-1).

The viscosity curves of the starches in the presence of collagen paste shows a drop in the viscosity profile at temperatures of about 38 °C, which is attributed to the thermal denaturation of collagen triple helices and the breakdown of the fibrillar structures. It is worth noting that some residual collagen fibrous structures at the standard heating temperature mode were still present upon heating to 95 °C. Upon cooling, the melted structures will renature, referred to as 'renatured collagen'. The curve of HAS in the presence of collagen (Figure 7-1C) did not show defined peak viscosity during heating and cooling at 95 °C; hence the trough, breakdown and setback viscosities could not be determined. Since HAS cannot be pasted under traditional RVA mode, the observed changes were attributed to only collagen.

The pasting temperature is the temperature at which the initial onset of viscosity increase of the starch is observed. For WS, the pasting temperature did not change significantly ($p < 0.05$) with the addition of collagen pastes at the concentrations studied. In contrast, NS with 4% and 3.5% collagen paste shows a slight shift to lower pasting temperatures ($p < 0.05$) but the opposite effect was obtained at 2.5% collagen paste. The lowering of the pasting temperature of starches in the presence of hydrocolloids has been attributed to the interactions between the hydrocolloids and leached amylose (Christianson et al., 1981; Shi and Bemiller, 2002; Funami et al., 2005). Considering the difference in collagen paste impact on the pasting temperature on WS and NS, this result implores the question of why WS behaves differently from NS corn-starch in the presence of collagen. It could be assumed that during the gelatinisation process, the leached linear amylose chains would interact with the collagen to a greater extent than the branched amylopectin chains still present within the granule ghosts (Debet and Gidley, 2007).

Conversely, for WS, the absence of amylose may explain why the pasting temperature was not affected in the presence of collagen. This result agrees with the study of Diaz-Calderon et al. (2018) and Sullo and Foster (2010), who reported a decrease in the pasting temperature of the wheat and maize starches in the presence of bacterial cellulose fibrils and hydrocolloid solutions. The authors suggested that when starch granules are embedded in hydrocolloid solution, the composite viscosity would be affected by changes in the two phases and how the phases interact with each other. They also suggested that the mutual exclusion of the hydrocolloids and starch molecules increases the effective concentration of starch, promoting interactions between the starch granules. Also, the higher viscosity of the continuous phase might allow early-stage swelling of the granules, not detected when starch is dispersed in

water. Also, Sullo (2012) showed that WS behaves differently from NS in the presence of guar gum, MC and HPMC. Thus, the detection of early onset of viscosity increase between NS/collagen pastes may arise from both phenomena. Therefore, the amylose presence appears to determine whether collagen delays or hasten viscosity onset increases.

The peak viscosity, which is the maximum viscosity, is attributed to the starch's ability to swell freely before it begins to break down under the imposed shear profile. The WS and NS peak viscosity in the presence of collagen pastes are significantly ($p < 0.05$) higher than those of WS and NS starches alone, and the extent of increase is more pronounced as the concentration of collagen increases. The increase in peak viscosity of various starches in the presence of hydrocolloids has been widely reported in the literature (Christianson et al., 1981; Achayuthakan and Supphantharika, 2008; Sullo and Foster, 2010; Diaz-Calderon et al., 2018; Zhang et al., 2020a). Several explanations have been proposed for the increasing starch peak viscosity with the addition of hydrocolloids, including phase separation and intermolecular interactions between the starch component and hydrocolloids (Christianson et al., 1981; Alloncle and Doublier, 1991). For NS with high amylose levels, the interaction between leached amylose molecules and hydrocolloid molecules was suggested to increase starch viscosity.

Conversely, for WS with hydrocolloids, the improvement in peak viscosities was attributed to the phase separation phenomenon (Zhang et al., 2020a). Applying Alloncle et al. (1989) reasoning, the starch/collagen blends can be considered a biphasic system with the starch granules located in the continuous collagen phase. The effective collagen concentration would increase as the volume of the phase

accessible to the collagen reduces as the granules absorb water and swell. Therefore, the swelling of the starch granule and the increase of collagen concentration in its phase will increase the system's overall viscosity. Similar results were reported by Sullo and Foster (2010) for WS and NS with MC and HPMC, who concluded that starch-hydrocolloid viscosity blends depend not only on the viscosity of the starch and hydrocolloid phase but also on how the two phases interact with each other. Thus, the increase in WS and NS's peak viscosities upon heating with increasing collagen concentration may be explained by two mechanisms: (1) an interaction between collagen and leached amylose, further experiments would need to be carried out in order to confirm the specific interaction and (2) an increase in the effective starch concentration in the starch domain upon the addition of collagen. The second mechanism is more plausible for WS with collagen blend due to the considerably lower amylose content.

During the holding period, the disruption of the granules results in a decrease in the paste viscosity. The minimum viscosity reached is known as the trough viscosity, and the difference between the trough and peak viscosities is referred to as the breakdown viscosity. Therefore, breakdown viscosity measures swollen granules resistance to disintegration (Achayuthakan and Suphantharika, 2008). Compared to WS alone, the trough viscosity decreases with increasing collagen concentration, but the opposite is seen for NS, where the trough viscosity values increase with higher collagen concentration than NS alone. It may be plausible that the increase of collagen viscosity in its phase prevents the amylose leaching, thereby strengthening the granule ghost. WS and NS's breakdown increases with collagen, except for NS/collagen blends containing 2.5 %wt of collagen. According to Christianson et al. (1981), an increase

in starch's breakdown viscosity when mixed with hydrocolloids is due to increased shear forces exerted on the swollen granules. Therefore, the increase in the starches breakdown viscosity in the collagen presence suggests that the swollen granules are less resistant to heat and shear forces during the pasting process.

The setback measures the retrogradation potential of the starch upon cooling. The viscosity increase resulting from starch chains reassociation, particularly amylose molecules during cooling and the final viscosity, reflects the cold paste (Jane et al., 1999). Upon cooling, starch molecules, particularly leached amylose re-associates to form a strong gel, increasing the final viscosity. The addition of collagen paste increases the setback viscosity for WS. Similarly, the setback viscosity of NS increases with 4% and 3.5% (except for 2.5%) collagen concentrations. The setback viscosity values are lower for WS/collagen pastes, and this was attributed to the less amylose in waxy maize starch. The increase in the starches setback viscosity indicates that the re-natured collagen increases the starches early-stage retrogradation tendency. This may be explained by an increase in the effective concentration of starch or, more specifically, the amylose in the starch phase (Cooke and Gidley, 1992). Based on this, collagen's addition to starch would not be useful for products in which staling and syneresis pose a major concern.

WS/collagen pastes final viscosity values decreased with increasing collagen paste concentration. The increase in the effective concentration of collagen in the continuous phase may prevent the re-association of the amylopectin chains to a lower extent, resulting in weaker gels, which are collagen concentration-dependent. On the contrary, the incorporation of collagen pastes in NS result in an increase in final viscosity except for 2.5% collagen. Some authors have related the increase in final

viscosity of starches in the presence of hydrocolloids results from two phenomena, first a phase separation process due to thermodynamic incompatibility between dissimilar polymers, and intermolecular interactions, which could either be hydrocolloid-amylose or amylose-amylose interactions (Alloncle et al., 1989; Biliaderis et al., 1997; Shi and Bemiller, 2002; Ptaszek and Grzesik, 2007). The higher final viscosity of NS in the presence of re-natured collagen may be attributed to a synergistic effect due to the mutual segregation of amylose molecules and re-natured collagen due to their thermodynamic incompatibility. This leads to an increase in their respective domains' concentrations, enhancing the blend system's viscosity. Alternatively, the increase in final viscosity may be explained by an interaction between renatured collagen and amylose molecules upon cooling, which increases the final viscosity, which seems to be collagen concentration-dependent. The reasons for the increase in final viscosity are still unclear, as little is known of the mechanism by which renatured collagen (gelatin) interacts with starch. In a study by Diaz-Calderon et al. (2018), bacterial cellulose fibrils were found to increase the final viscosity of amylose-containing starches, and this was attributed to the binding of amylose to the bacterial cellulose. A similar effect was also reported for rice starches in the presence of *Plantago* mucilage polysaccharides (Cowley, 2020). This study's data showed that the effect of renatured collagen on the final viscosity of starch followed a similar hypothesis. During the cooling process, the re-association of the amylose chains and the reformation of the triple helices of the denatured collagen may have resulted in the formation of a complex network with stronger gel properties. Also, the gelling ability of the denatured collagen upon cooling may have contributed to the increase in final viscosity. According to Goel et al. (1999), the hydrophilic groups in

proteins such as OH, NH₂, and COOH can form crosslinks with starch, resulting in an enhancement in paste viscosity compared to starch alone.

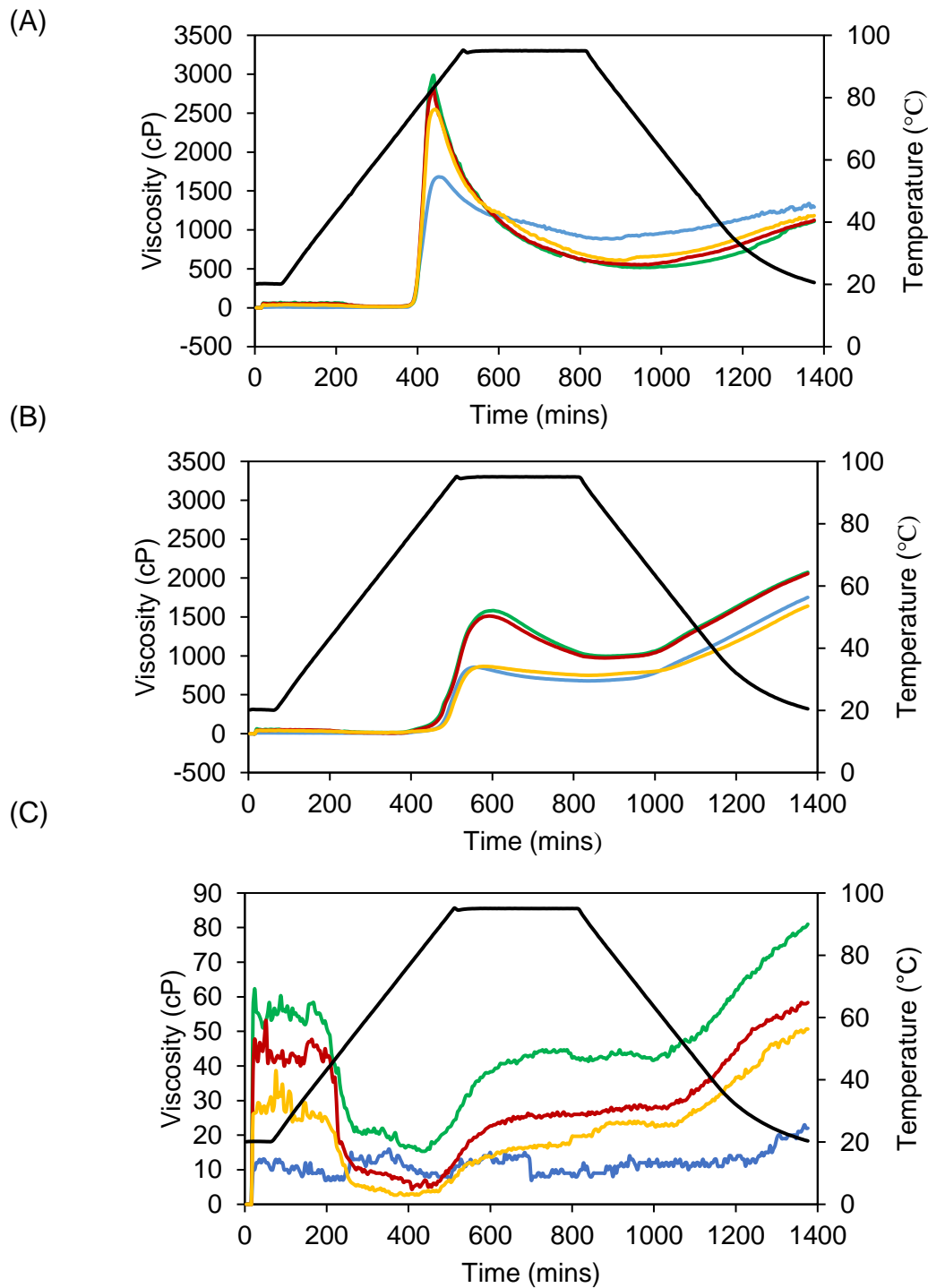


Figure 7-1: Pasting profile of (A) WS (B) NS (C) HAS in water (blue line) and different collagen concentrations: 4%w/w (green line), 3.5%w/w (red line) and 2.5%w/w (yellow line) studied under standard RVA heating mode (to 95 °C). The temperature profile (black line).

Table 7-1: Pasting parameters of WS, NS and HAS with and without different collagen concentrations at standard RVA heating mode (95 °C).

Samples	Peak viscosity (cP)	Trough Viscosity (cP)	Breakdown viscosity (cP)	Final viscosity (cP)	Setback viscosity (cP)	Pasting temperature (°C)
WS	1682 ± 4 ^a	851 ± 34 ^c	807 ± 8 ^a	1293 ± 8 ^c	418 ± 15 ^a	74.5 ± 0.7 ^a
WS +4% Collagen	2981 ± 29 ^d	513 ± 27 ^a	2468 ± 36 ^d	1110 ± 13 ^a	597 ± 24 ^b	74.4 ± 0.8 ^a
WS +3.5% Collagen	2828 ± 12 ^c	551 ± 29 ^{ab}	2277 ± 22 ^c	1125 ± 36 ^a	573 ± 13 ^b	75.2 ± 0.4 ^a
WS + 2.5% Collagen	2550 ± 13 ^b	603 ± 15 ^b	1946 ± 27 ^b	1184 ± 18 ^b	580 ± 31 ^b	75.3 ± 0.6 ^a
HAS	ND	ND	ND	81.0	ND	ND
HAS +4% Collagen	ND	ND	ND	58.3	ND	ND
HAS +3.5% Collagen	ND	ND	ND	50.7	ND	ND
HAS + 2.5% Collagen	ND	ND	ND	20.5	ND	ND
NS	854 ± 3 ^a	679 ± 2 ^a	176 ± 4 ^b	1752 ± 8 ^a	1073 ± 8 ^b	89.2 ± 0.0 ^b
NS +4% Collagen	1582 ± 39 ^b	996 ± 12 ^b	586 ± 27 ^d	2075 ± 7 ^b	1098 ± 19 ^b	87.2 ± 0.1 ^a
NS + 3.5% Collagen	1513 ± 17 ^b	973 ± 16 ^b	540 ± 5 ^c	2059 ± 29 ^b	1084 ± 23 ^b	87.2 ± 0.1 ^a
NS + 2.5% Collagen	865 ± 62 ^a	749 ± 55 ^a	116 ± 7 ^a	1640 ± 128 ^a	891 ± 74 ^a	89.9 ± 0.1 ^c

^{ac} Mean ± standard deviation. Different letters in the same column indicate significant differences ($P < 0.05$). ND = not detected.

7.4.2 Pasting properties of starch/collagen blends measured in High-Temperature mode (up to 140 °C)

Figure 7-2 displays the pasting curves of NS, WS, and HAS with and without collagen pastes under high heating temperature (140 °C). HAS now shows a more common pasting profile, and the higher gelatinisation temperatures are due to amylose-lipid complex dissociation (Kibar et al., 2010). However, when compared with WS and NS alone, HAS exhibits lower peak, trough, breakdown, final, and setback viscosities (Table 7-2). This is due to the high amylose content of the HAS and the melting of the amylose-lipid complex, which leads to a higher loss in the integrity of the swollen granules and remnants (Liu et al., 2019). NS pasting temperature is consistent with that of the standard temperature (up to 95 °C). However, the pasting temperature of WS alone increased slightly. The trough and final viscosities of NS and WS decreased with high heating temperature, whereas breakdown viscosities increased compared to the standard temperature (95 °C).

Interestingly, as the heating temperature increased from 95 to 140 °C, the final viscosity of WS becomes higher than NS, which is contrary to that seen when heated to the 'standard' temperature. The starches final viscosity decreased with an increase in amylose content, with HAS showing the lowest final viscosity. Li et al. (2020) reported that the final viscosity of high amylose wheat flour and starches with varying amylose content decreased with an increase in amylose content. The suggestion was made that at 140 °C, the swollen granules and remnants' integrity were destroyed, and the amylose molecules were dispersed among amylopectin molecules that failed to form a strong gel network. Also, due to the longer duration needed to cool the pastes

from 140 – 20 °C, the lipids present in the HAS could form single-helical complexes with amylose, and the formed amylose-lipid complexes could leach out of the medium. Thereby preventing the starch molecules from re-associating with each other, resulting in a lower final viscosity. The increase in breakdown viscosity, decrease in the trough, and final viscosities of the starches at 140 °C could be due to the thixotropic breakdown because of prolonged cooking and shear and possibly thermal degradation of the starch molecules resulting from the high heating temperature (Liu et al., 2019). The effect of collagen pastes at the various concentration on the pasting properties of WS, NS, and HAS at high heating temperature (140 °C) are shown in Figure 7-2. Notably, at high heating temperature, collagen chains are entirely melted into random coil conformations, and there was no evidence of residual fibrous structures. However, some residual structure is present at the onset of viscosity increase of NS and WS. The impact of collagen pastes on WS and NS's pasting temperatures under high heating temperature is consistent with the trend observed at standard temperature (95 °C). The addition of collagen did not affect the pasting temperature of WS. Likewise, for NS, the addition of 4% and 3.5% collagen paste did not affect NS's pasting temperature. However, the values increased significantly ($p < 0.05$) with 2.5% collagen concentration. For HAS, pasting temperature is lowered with increasing collagen concentration, indicating that collagen presence identifies early gelatinisation (Sullo and Foster, 2012), and higher collagen concentration has a more pronounced effect. As noted earlier, the intermolecular interactions between collagen and amylose molecules may be responsible for the early onset of the viscosity increase. The effect of collagen on the peak and breakdown viscosities of WS and NS is consistent with the trend observed at standard heating temperature. The viscosity values increased with increasing collagen concentrations. Similarly, for

HAS, the peak and breakdown viscosities increase with higher collagen concentration. The trough, setback, and final viscosities of NS decrease with increasing collagen concentration compared to NS alone, contrary to the trend observed at 95 °C. At a high temperature (140 °C), the swollen starch granules' integrity is destroyed (Liu et al., 2019). This may lead to a lack of interaction between the starch and denatured collagen molecules. Consequently, leading to an increase of the denatured collagen in its phase which may hinder the strong association of the amylose chains from providing a high final viscosity.

For WS/collagen blends, trough and setback viscosities decrease with increasing collagen content. Whereas the opposite effect is seen with the final viscosity, where the values increased with decreasing collagen concentration compared to WS alone, indicating that lower collagen concentration promoted the gel formation of amylopectin molecules. For HAS, the trough and breakdown viscosity decrease with lower collagen concentration, while the final and setback viscosities decrease with increasing collagen concentration compared to HAS alone. This indicates that an increase of denatured collagen in its phase may interfere with amylose-amylose re-association and reduces the gel formation of high amylose starch granules after destruction under shear. Overall, it is worth noting that trough, setback, and final viscosities of starch/collagen pastes are lower than viscosities measured under standard heating (95 °C). This corroborates with the study of Cowley (2020) who observed a considerable reduction in rice flour's trough and final viscosity containing *Plantago* when pasted to 140 °C. As previously mentioned, this is attributed to the thixotropic and granular breakdown due to more prolonged cooking and shearing and full thermal denaturation of the collagen fibrillar structures.

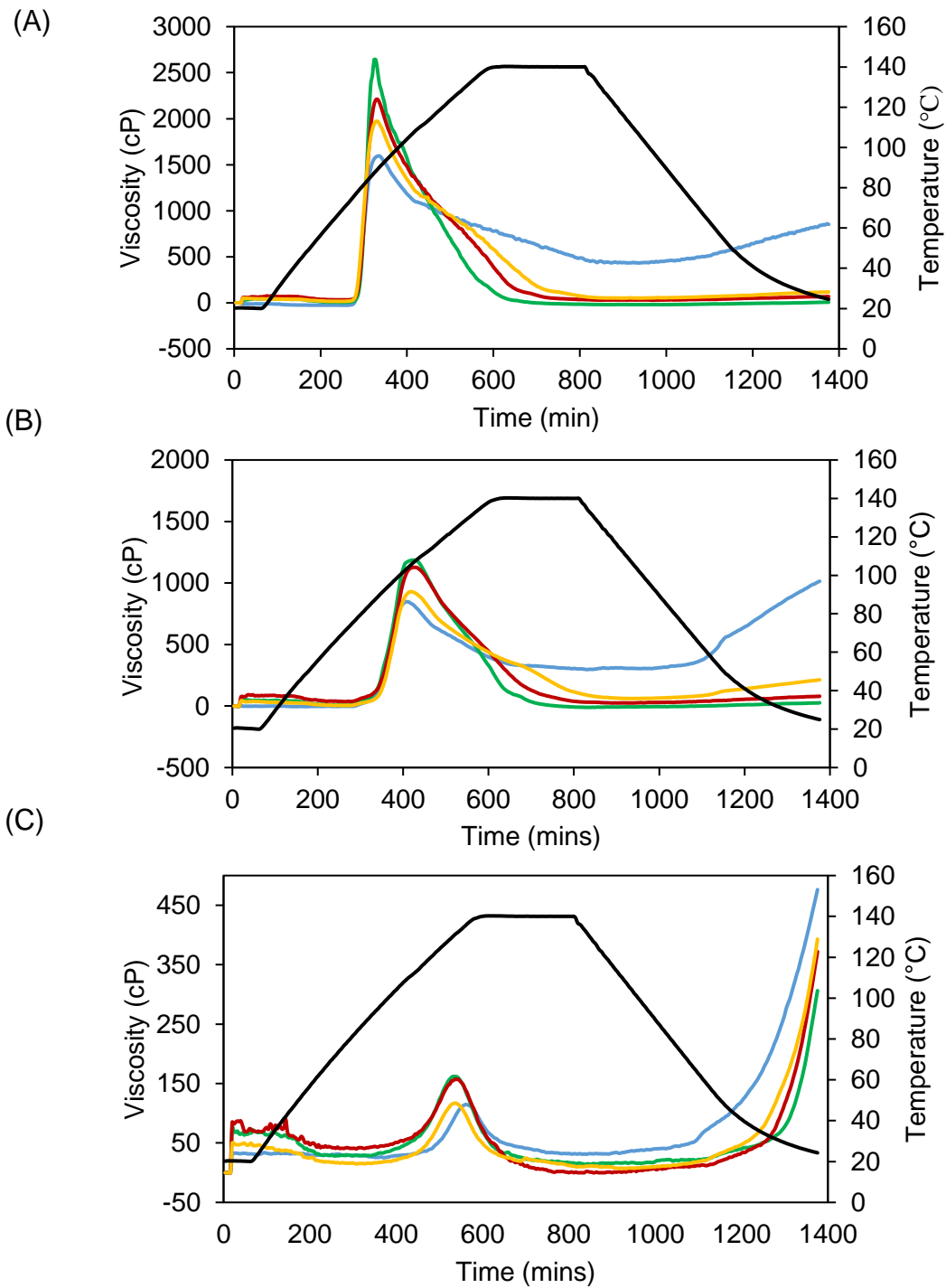


Figure 7-2: Pasting profile of (A) WS (B) NS (C) HAS in water (blue line) and different collagen concentrations: 4%w/w (green line), 3.5%w/w (red line) and 2.5%w/w (yellow line) studied under standard RVA heating mode (to 140 °C). The temperature profile is (black line).

Table 7-2: Pasting parameters of WS, NS and HAS with and without different collagen concentrations at high-temperature RVA heating mode (140 °C).

Samples	Peak viscosity (cP)	Trough viscosity (cP)	Breakdown viscosity (cP)	Final viscosity (cP)	Setback viscosity (cP)	Pasting temperature (°C)
WS	1597 ± 32 ^a	425 ± 32 ^c	1172 ± 13 ^a	852 ± 45 ^c	427 ± 13 ^c	77.6 ± 0.3 ^a
WS +4% Collagen	2879 ± 31 ^c	20 ± 23 ^a	2900 ± 17 ^c	23 ± 19 ^a	26 ± 10 ^a	77.7 ± 0.6 ^a
WS + 3.5% Collagen	2216 ± 28 ^{bc}	28 ± 19 ^{ab}	2188 ± 24 ^{ab}	68 ± 21 ^{ab}	40 ± 3 ^a	78.0 ± 1.0 ^a
WS + 2.5% Collagen	1979 ± 32 ^{ab}	50 ± 16 ^b	1928 ± 23 ^b	118 ± 21 ^b	67 ± 7 ^b	78.1 ± 0.8 ^a
HAS	115 ± 23 ^a	30 ± 19 ^a	85 ± 4 ^a	476 ± 20 ^c	447 ± 12 ^b	113.9 ± 2.8 ^b
HAS +4% Collagen	165 ± 16 ^b	14 ± 18 ^a	151 ± 6 ^c	308 ± 53 ^a	291 ± 42 ^a	92.7 ± 0.5 ^a
HAS + 3.5% Collagen	161 ± 13 ^b	13 ± 13 ^a	148 ± 10 ^c	395 ± 32 ^b	382 ± 21 ^b	94.5 ± 2.5 ^a
HAS + 2.5% Collagen	117 ± 3 ^a	7 ± 7 ^a	111 ± 9 ^b	393 ± 68 ^{ab}	386 ± 17 ^b	96.6 ± 2.9 ^a
NS	850 ± 10 ^a	297 ± 18 ^c	553 ± 26 ^a	717 ± 4 ^d	1014 ± 19 ^d	89.0 ± 0.3 ^a
NS +4% Collagen	1189 ± 48 ^c	11 ± 10 ^a	1200 ± 35 ^d	38 ± 3 ^a	34 ± 9 ^a	89.2 ± 0.3 ^a
NS + 3.5% Collagen	1132 ± 33 ^c	23 ± 20 ^{ab}	1109 ± 21 ^c	57 ± 12 ^b	79 ± 32 ^b	89.5 ± 0.8 ^a
NS + 2.5% Collagen	934 ± 27 ^a	61 ± 6 ^b	873 ± 32 ^b	152 ± 7 ^c	213 ± 13 ^c	92.0 ± 1.2 ^b

To further investigate the pastes structure after standard and high-temperature heating modes, their structures were observed using optical microscopy (Figure 7-3 and

Figure 7-4). Figure 7-3 shows micrographs of WS, HAS and NS starches with and without collagen paste obtained after the standard heating mode. The starch granules remained visibly intact for HAS alone and with collagen (Figure 7-3A and Figure 7-3B), confirming that the amylose starch did not dissociate under the standard heating mode. This is not surprising as literature has reported that high amylose starch granules dissociate at temperatures $> 100\text{ }^{\circ}\text{C}$. For NS alone and in the presence of collagen (Figure 7-3C and D), the granules increased to twice the original volume, indicating swelling of the amylopectin. However, the granules were not completely dissociated because of the amylose region. In WS alone and collagen, the granules were not evident, indicating swelling and complete melting of the crystallites. Also, in Figure 7-3F, the triple helical structure of collagen is evident (marked by a circle), which might be residual fibrous collagen that was not completely melted. At the high-temperature heating mode $140\text{ }^{\circ}\text{C}$, HAS with and without collagen (Figure 7-4A and Figure 7-4B) lost their granular structures compared to when heated to $95\text{ }^{\circ}\text{C}$, and the granules became dispersed in the continuous phase. The dispersed amylose molecules re-associated with each other during cooling to develop a strong gel network. Similar micrographs are seen for NS alone, and in the presence of collagen (Figure 7-4C and Figure 7-4D), the granules/remnants completely lost their integrity, and the linear amylose chains were dispersed in the continuous phase of the system. In the case of WS alone and in the presence of collagen (Figure 7-4E and Figure 7-4F), the granules were not evident, indicating swelling and complete melting of the crystallites. This is similar to what was observed for standard heating temperature. Furthermore, no evidence of collagen's triple helical structure is seen at high heating temperature, suggesting that the fibrous collagen is melted completely and no re-association upon cooling.

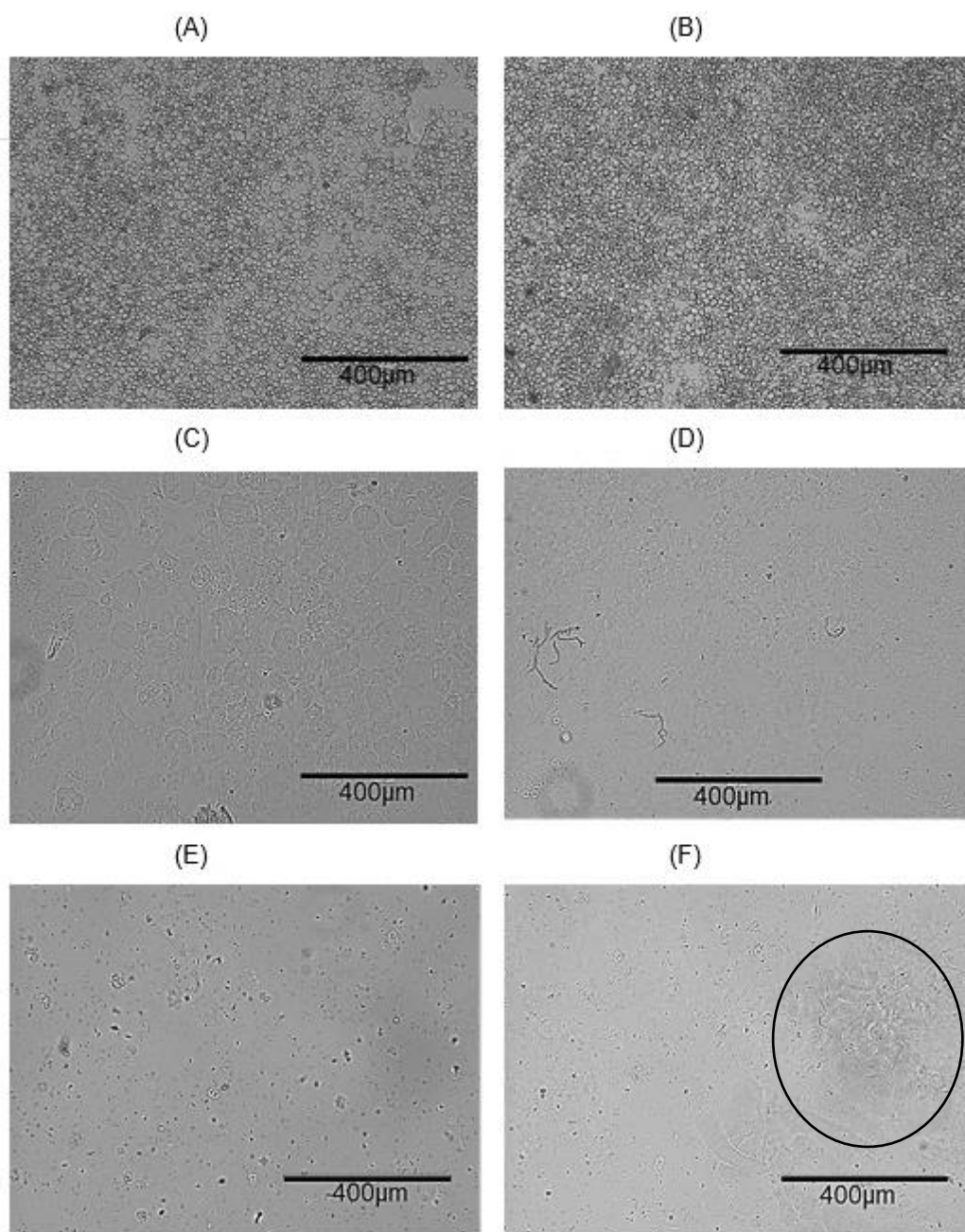


Figure 7-3: Light microscopy of (A) HAS + WATER (B) HAS + 4% COLL (C) NS + WATER (D) NS + 4% COLL (E) WS + WATER (F) WS + 4% COLL after standard-temperature RVA mode (up to 95 °C).

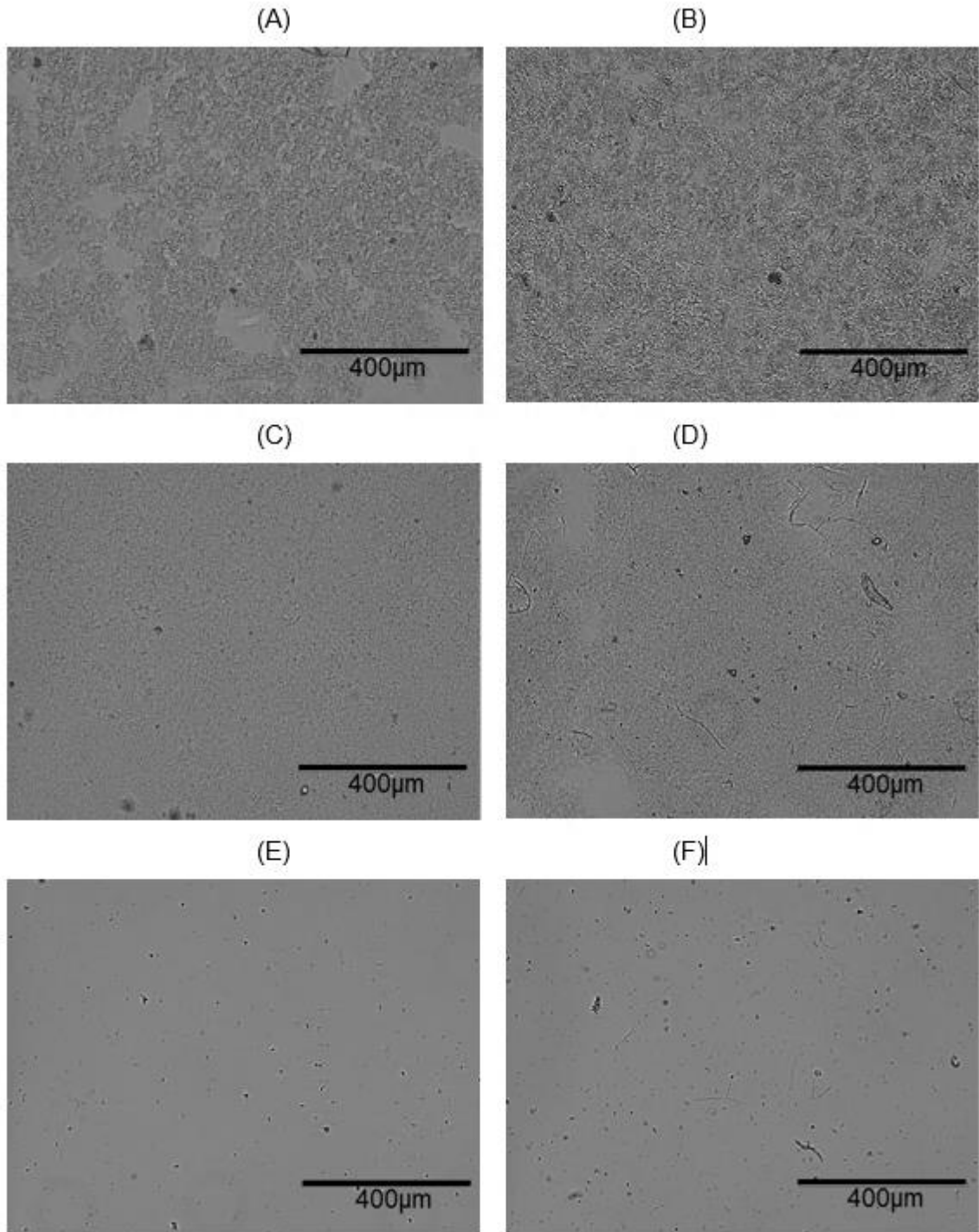


Figure 7-4: Light microscopy of (A) HAS + WATER (B) HAS + 4% COLL (C) NS + WATER (D) NS + 4% COLL (E) WS + WATER (F) WS + 4% COLL after high-temperature RVA mode (up to 140 °C).

7.5 Conclusion

In this study, the effect of different collagen pastes concentrations on the pasting properties of NS, WS, and HAS was studied under standard (95 °C) and high temperature (140 °C) RVA heating modes. The addition of collagen pastes modified the pasting behaviour of the different maize starches. The extent of modification depends on the collagen pastes concentration and the amylose/amylopectin ratio of the starches. Under standard heating mode, high amylose starch with and without collagen pastes did not show a noticeable pasting profile due to amylose: lipid complexes which prevented the starch granules from swelling. Collagen pastes did not affect the pasting temperature of WS.

In contrast, increasing concentrations (4% and 3.5%) of collagen lowers NS pasting temperature. The peak, setback, and breakdown viscosities of NS and WS increased significantly with increasing collagen concentrations. Increasing the retrogradation potential of starches upon the addition of collagen paste would suggest that adding collagen to starch would not be useful for products where staling and syneresis pose a major concern. WS final viscosity decreased with increasing collagen levels. The absence of interaction between collagen and amylose in waxy maize starch may explain the lower final viscosity and the lack of difference in the waxy maize starch's pasting temperature.

The presence of collagen increased the final viscosity of NS, attributed to the interaction between leached amylose and collagen molecules and the resulting competition of water. At high-heating temperature (140°C), HAS with and without collagen pastes developed a noticeable pasting profile. The pasting temperature of HAS reduced with increasing collagen concentrations due to the interaction between

leached amylose and collagen molecules allows early granules swelling. The effect of collagen on NS and WS at the high heating temperature induced the final, trough, and setback viscosity of the starches to decrease significantly, attributed to the thixotropic breakdown and thermal degradation of starches and plausibly the complete melting of the collagen triple helices. Interestingly, the final viscosity of WS alone increased with high heating temperature. Simultaneously, that of NS decreased, contrary to the standard mode indicating that the fuller breakdown of the granular starch structure promotes amylopectin retrogradation. In contrast, with increased amylose content, the molecules create either a complex phase-separated microstructure and/or the amylopectin molecules now 'dilute' the effectiveness of amylose retrogradation (in which the amylopectin granular ghosts would have been embedded under standard heating protocols). This begins to cast new light and challenges on understanding starch gel structures after 'complete' gelatinisation and molecular mixing due to enhanced granular breakdown and will undoubtedly be areas of further study and in-depth understanding.

The hypotheses proposed to explain the acid-swollen collagen paste effect on the pasting behaviour of starches are (1) Interaction of collagen with leached amylose. However, there is no comprehensive evidence describing the interaction of denatured collagen and amylose molecules, and thus, further studies will be needed to understand the mechanism of interaction better. A similar conclusion was reported by Cowley (2020), who indicated that the pasting properties of rice flour in the presence of *Plantago* mucilage polysaccharides interacting with the helical amylose, (2) a phase separation, which occurred due to thermodynamic incompatibility of the macromolecules. The heating temperature also has a significant effect on starches pasting behaviour with and without collagen pastes. The biggest difference between

the standard and high-temperature heating mode for the starches with and without collagen is the extent to which collagen impacts the granular integrity, which ultimately affects the measured retrogradation and gel formation of the starches. This was seen to be 'inhibited' when heated to the higher temperatures, which begins to unlock further the understanding of hydrocolloid mixtures with starch, be it through molecular interactions or a new insight into molecular incompatibilities.

In conclusion, this study offers new insights into fibrous acid-swollen collagen's effect on the pasting properties of corn starches with different amylose and amylopectin content during various heating regimens. Also, the information obtained from this study will be important for industrial applications of starches with and without additives in different products, particularly for high-temperature processing.

8 CONCLUSIONS AND FUTURE WORK

8.1 Conclusions

The weak mechanical and thermal properties of collagen film (casing) compared to the casing from the animal intestine for sausage manufacturing have led to the growing interest of casing manufacturers and researchers in designing collagen casings that can provide similar strength and thermal stability as intestinal casings. Very little is known about the effect of polysaccharides on collagen films made from acid-swollen collagen paste. Therefore, this work has focused on exploring the possibility of using different polysaccharides to enhance collagen films made from acid-swollen collagen pastes. In this work, polysaccharides including cellulose, starches, HPMC, MC, CMC and guar gum were chosen because of their abundance, low cost and functional properties (gelling and viscosifying).

It can be concluded from the first experimental that the addition of uncharged hydrocolloids (HPMC, MC and high/low molecular weight guar gum) and negatively charged (CMC) at comparable low-shear viscosity (300 mPa.s) increased the elastic and viscous moduli of acid-swollen collagen paste, at various collagen concentrations. The storage modulus increased to a similar extent for all the hydrocolloids. Simultaneously, the G'' was different at a higher frequency, indicating that the hydrocolloids dominate the viscoelastic properties at higher angular frequencies. On the contrary, the addition of negatively charged CMC decreased the elastic and viscous properties of the acid-swollen collagen paste. It is proposed that the charge interaction between the cationic collagen and anionic CMC result in the de-swelling of the fibrous collagen structure. As such, the blending of CMC solution to acid-swollen collagen paste would not be recommended for collagen film (casing) manufacturing. Furthermore, as determined by DSC, the denaturation of collagen was largely unaffected by the presence of the hydrocolloids. In contrast, CMC increased the

collagen denaturation temperature due to the increased aggregation of collagen fibres due to the de-swelling of the collagen paste. Thus, it appears that the hydrocolloid charge influences the viscoelastic and thermal stability of fibrous acid-swollen collagen paste.

The effect of uncharged hydrocolloids (HPMC, MC and guar gums) on the mechanical, thermal, sorption and structural properties of collagen films was discussed in chapter 4. As observed by the DSC data, adding the hydrocolloids increased the melting temperature and decreased the enthalpy of melting the composite films. It was suggested that collagen-collagen interactions were replaced by collagen-hydrocolloid interactions when drying the films, leading to the formation of stable film networks. Another possibility is that the hydrocolloids, while potentially phase concentrating the collagen fibres, create a more thermally stable collagen structure. The reduced enthalpy values were ascribed to the fact that the presence of hydrocolloids prevents the collagen fibrils from coming close together to form intense interactions, resulting in less energy required to disrupt the collagen chains. XRD data and FTIR spectra of the films showed slight alterations in the ordered collagen structure in the composite films. This was related to the fact that hydrocolloids affect the thermodynamics and kinetics of the realignment of the collagen fibres upon drying. However, the change in the nature of collagen upon drying in the presence of hydrocolloids needs to be explored further using techniques such as circular dichroism, a spectroscopic technique used to study structural changes and molecular order of collagen (Bhumber et al., 2019). This proposed change in collagen structure resulted in reduced water uptake by the composite films, as seen in the sorption and moisture content data. TGA of the films shows that collagen thermal stability was not affected by the hydrocolloids. In addition, the tensile strength, stiffness and elongation of the collagen films increase

with the incorporation of the hydrocolloids and with increasing levels of collagen fibre content. This is a positive finding as increased mechanical properties are essential for sausage casing manufacturers. The increase in tensile strength of the composite films is related to the ability of collagen fibres to stabilise themselves and the effect the individual polymer is having upon drying the films. It was suggested that the mutual exclusion of collagen and hydrocolloids would increase each component in their domains, which might promote the formation of a stronger film network. Collagen films with derivatised cellulose (COLLMC and COLLHPMC) showed higher tensile strength and stiffness than composite films with guar gums. This is understood because the higher concentrations of derivatised cellulose in the films, the more interaction forces available, thereby resulting in the formation of a stronger film network. Furthermore, attempts were made to use SEM to obtain the film's morphology; however, the micrographs did not show the detailed structure expected; therefore, future work should explore this further.

Chapter 5 concludes that adding the cellulose with different fibres lengths and starches: waxy and high amylose starch at comparable phase volumes increased the elastic and loss modulus of the acid-swollen collagen paste. Moreover, collagen paste with the starches (waxy and high amylose) shows greater enhancement, possibly due to the higher amount of starch used at comparable phase volume. The fillers did not influence the collagen pastes thermal stability as observed by the DSC, which correlated with the temperature sweep results. Additionally, there was no substantial difference between the different fibre lengths of the cellulose and the type of starch used. Interestingly, upon reheating the collagen paste, the enthalpy of the denatured collagen (gelatin) reduces in the presence of starches. It was hypothesised that an unexpected molecular interaction between denatured collagen chains and starch

might reduce the formation of the gelatin-like structure. Further work is needed to elucidate the specific interaction between denatured collagen and starch molecules.

In chapter 6, the effect of the fillers (cellulose and starches) on the mechanical, structural, thermal and sorption properties of acid swollen collagen films were investigated. The surface morphology of the composite films was rough due to the protrusion of the cellulose fibres and starch granules on the surface of the films. Upon drying, the aggregation of the starch granules and cellulose fibres prevented the re-arrangement of the collagen fibres in the films. This resulted in increased thickness values of the composite films than the pure collagen films. The addition of cellulose fibres reduces the film moisture uptake as indicated by sorption properties and moisture content data, lower thermal stability as shown by the TGA, and reduced composite films melting enthalpy shown by the DSC data.

Furthermore, FTIR spectra and XRD data of the composite films reveals some interruption in the ordered arrangement of collagen fibre structure in the composite films. Two hypotheses are proposed to explain changes observed in the composite films: 1) the fillers prevent the collagen fibre structure re-organisation during the drying process, which is thought to be dependent on the shape and concentration of fillers used; and 2) relies on the prevention of the hydrogen-bonded water bridge stabilising the collagen triple helical structure due to a physical cross-linking effect of cellulose/starch with collagen fibre chains. Composite films with starch granules are found to affect the properties of collagen fibre films greatly. The difference in cellulose and starch morphology, packing, and size may affect collagen fibres arrangement during drying. Cellulose fibrils can align to an extent with the rearranged collagen fibres upon drying. In contrast, the spherical starch granules do not align with the collagen

fibrils, thereby interfering with the ordered arrangement of collagen fibrils to a large extent.

Additionally, it was shown that cellulose fibres increased the mechanical properties (tensile strength, stiffness and elongation at break) of the composite films. This was attributed to the entanglement of cellulose fibres and collagen fibres which strengthened the structural integrity by increasing the tensile strength and stiffness of the composite films. However, the addition of starch granules results in very brittle films which could not be tested. The film brittleness is due to the heterogeneity of the films in relation to the effect of the granules disordering the collagen fibre structure. However, to increase the potential of starch as reinforcement in collagen films (casings), plasticisers need to be added to the film-forming pastes.

Chapter 7 concludes that adding collagen paste at different addition levels modifies the pasting properties of waxy, high amylose and normal maize starches studied using conventional (up to 95 °C) and high-temperature (up to 140 °C) RVA heating modes. The extent of modification of the pasting properties depends on the type of starches and the concentration of the levels of collagen paste. All three starches show a synergistic increase in the peak viscosity on collagen paste addition. The extent of this effect is dependent on the starch type and concentration of the added collagen paste. The pasting temperature of waxy maize starch is unaffected.

In contrast, the pasting temperature was lowered on the incorporation of collagen pastes. A greater effect was seen with increasing levels of collagen paste. The increase in peak viscosity may increase starch concentration in the starch phase upon collagen paste addition and possibly interactions between amylose and collagen. The lack of the second mechanism for waxy maize starch may explain why the pasting

temperature is not affected. The heating temperature had a significant effect on starches pasting behaviour with and without collagen pastes. The most significant difference between the standard and high-temperature heating mode for the starches with and without collagen is the extent to which collagen impacts the granular integrity, which ultimately affects the measured retrogradation and gel formation of the starches. This effect was more pronounced when the starches were heated to higher temperatures (up to 140 °C), attributed to the thixotropic breakdown of the starch network and possibly thermal degradation (Liu et al., 2019)

To conclude, this work has shown that the presence of polysaccharides depending on type, shape, hydrodynamic volume, chain stiffness, molecular weight, charge distribution, hydrophobicity, and structure will affect the nature of collagen fibre structure upon drying and the overall film properties. Additionally, this study has demonstrated that the hydrocolloids investigated are promising candidates for improving collagen properties, particularly mechanical properties, which will significantly interest collagen casings manufacturers. Also, it provides direction for collagen casing manufacturers on the choice of hydrocolloids for enhancing collagen properties.

8.2 Future work

The results obtained in this research project will provide scientific knowledge and background to promote further the potential use of hydrocolloid for enhancing collagen film properties for industrial application. A logical continuation of this work is to assess the impact of the hydrocolloids on collagen films/casings cooking and eating properties.

As indicated in this study, some interactions exist between the collagen fibres and hydrocolloids molecules which impacted the resultant film properties. More research would be needed to help gain more knowledge of the specific interactions and the mechanism governing these interactions. This work shows that the hydrocolloids charge affects the swelling of the acid-swollen paste, which impacts the film formation. The addition of negatively charged CMC caused a de-swelling of the collagen paste, resulting in an aggregation of collagen fibres and a decrease in the viscoelasticity of collagen paste. It would be interesting in future work to investigate other negatively charged water-soluble polymers such as carboxylated alginate, pectin, and xanthan, and the sulphated lambda carrageenan, as well as positively charged such as chitosan on acid-swollen collagen paste properties, which might provide a new route to designing collagen casings with new or improved properties. Mixtures/blends of the hydrocolloids mentioned above might offer further tunability of properties once the underlying mechanisms are affirmed.

Some unanswered questions from the non-charged water-soluble polymers are the effect of molecular weight, degree of substitution and chain stiffness. It would be opportune to extend the findings of this study to compare the derivatised celluloses

and, e.g. guar at the same molecular weight / hydrodynamic volume, such that the same low shear viscosities are produced from identical concentrations of the comparative polymers.

For edible films manufacturing, the addition of plasticisers is important as they would help reduce the films brittleness. This study did not cover the effects of the plasticisers on the properties of the films. Therefore, further work would need to investigate the impact of various plasticisers such as glycerol and sorbitol on collagen/hydrocolloid fibre film properties, which would be a major industrial interest.

Aside from mechanical properties, another important functional property of collagen casing for sausage manufacturing that was not considered in this study is its barrier property, which is simply permeability to water vapour, smoke and gases. The migration of water and other materials into and out of the sausage is important as it produces complex effects on the texture, nutritive and marketing value of sausage (Savic and Savic, 2016). Changes in moisture content, governed by the casing permeability properties and water activity, influences the sensory quality and shelf-life of sausages. Permeability to smoke is also important as smoke can improve flavour and extend the shelf-life of the sausages by reducing microbial growth. Therefore, it is suggested that collagen/hydrocolloid films permeability properties are investigated in further studies.

Finally, although small oscillation, rheological measurements have provided a valuable tool for understanding structural changes; extensional flow measurement would help understand the composite paste behaviour under processing operations such as extrusion.

REFERENCES

- Achayuthakan, P. & Suphantharika, M. (2008). Pasting and rheological properties of waxy corn starch as affected by guar gum and xanthan gum. *Carbohydrate Polymers*, 71(1), 9-17.
- Acosta, S., Jiménez, A., Cháfer, M., González-Martínez, C. & Chiralt, A. (2015). Physical properties and stability of starch-gelatin based films as affected by the addition of esters of fatty acids. *Food Hydrocolloids*, 49135-143.
- Adzaly, N. Z. 2014. *Development of a novel sausage casing made of chitosan and its performance under traditional sausage manufacturing conditions*. Michigan State University.
- Agrawal, A. M., Manek, R. V., Kolling, W. M. & Neau, S. H. (2004). Water distribution studies within microcrystalline cellulose and chitosan using differential scanning calorimetry and dynamic vapor sorption analysis. *Journal of Pharmaceutical Sciences*, 93(7), 1766-1779.
- Ahmad, M., Hani, N. M., Nirmal, N. P., Fazial, F. F., Mohtar, N. F. & Romli, S. R. (2015). Optical and thermo-mechanical properties of composite films based on fish gelatin/rice flour fabricated by casting technique. *Progress in Organic Coatings*, 84115-127.
- Ahmad, M., Nirmal, N. P., Danish, M., Chuprom, J. & Jafarzedeh, S. (2016). Characterisation of composite films fabricated from collagen/chitosan and collagen/soy protein isolate for food packaging applications. *RSC Advances*, 6(85), 82191-82204.
- Ahmed, S. & Jones, F. (1990). A review of particulate reinforcement theories for polymer composites. *Journal of Materials Science*, 25(12), 4933-4942.

- Alloncle, M. & Doublier, J.-L. (1991). Viscoelastic properties of maize starch/hydrocolloid pastes and gels. *Food Hydrocolloids*, 5(5), 455-467.
- Alloncle, M., Lefebvre, J., Llamas, G. & Doublier, J. (1989). A rheological characterization of cereal starch-galactomannan mixtures. *Cereal Chemistry*, 66(2), 90-93.
- Alves, M. M., Antonov, Y. A. & Gonçalves, M. P. (1999). On the incompatibility of alkaline gelatin and locust bean gum in aqueous solution. *Food Hydrocolloids*, 13(1), 77-80.
- Amin, S. & Ustunol, Z. (2007). Solubility and mechanical properties of heat-cured whey protein-based edible films compared with that of collagen and natural casings. *International Journal of Dairy Technology*, 60(2), 149-153.
- Andonegi, M., Las Heras, K., Santos-Vizcaíno, E., Igartua, M., Hernandez, R. M., De La Caba, K. & Guerrero, P. (2020). Structure-properties relationship of chitosan/collagen films with potential for biomedical applications. *Carbohydrate Polymers*, 237116159.
- Ang, J. & Miller, W. (1991). Multiple functions of powdered cellulose as a food ingredient. *Cereal foods world (USA)*.
- Antonov, Y. A. & Gonçalves, M. (1999). Phase separation in aqueous gelatin–κ-carrageenan systems. *Food Hydrocolloids*, 13(6), 517-524.
- Antonov, Y. A. & Gonçalves, M. P. (2015). Phase separation in water-gelatin-locust bean gum system. *Journal of Nature Science and Sustainable Technology*, 9(1), 257-264.
- Anvari, M. & Chung, D. (2016). Dynamic rheological and structural characterization of fish gelatin–Gum arabic coacervate gels cross-linked by tannic acid. *Food Hydrocolloids*, 60516-524.

- Appelqvist, I. A. & Debet, M. R. (1997). Starch-biopolymer interactions—a review. *Food Reviews International*, 13(2), 163-224.
- Arfat, Y. A., Benjakul, S., Prodpran, T. & Osako, K. (2014). Development and characterisation of blend films based on fish protein isolate and fish skin gelatin. *Food Hydrocolloids*, 3958-67.
- Arvanitoyannis, I., Psomiadou, E., Nakayama, A., Aiba, S. & Yamamoto, N. (1997). Edible films made from gelatin, soluble starch and polyols, Part 3. *Food Chemistry*, 60(4), 593-604.
- Askari, F., Sadeghi, E., Mohammadi, R., Rouhi, M., Taghizadeh, M., Hosein Shirgardoun, M. & Kariminejad, M. (2018). The physicochemical and structural properties of psyllium gum/modified starch composite edible film. *Journal of Food Processing and Preservation*, 42(10), e13715.
- Atwell, W. (1988). The terminology and methodology associated with basic starch phenomena. *Cereal foods world*, 33306-311.
- Aymard, P., Martin, D. R., Plucknett, K., Foster, T. J., Clark, A. H. & Norton, I. T. (2001). Influence of thermal history on the structural and mechanical properties of agarose gels. *Biopolymers: Original Research on Biomolecules*, 59(3), 131-144.
- Badea, E., Della Gatta, G. & Usacheva, T. (2012). Effects of temperature and relative humidity on fibrillar collagen in parchment: A micro differential scanning calorimetry (micro DSC) study. *Polymer Degradation and Stability*, 97(3), 346-353.
- Bae, I., Osatomi, K., Yoshida, A., Osako, K., Yamaguchi, A. & Hara, K. (2008). Biochemical properties of acid-soluble collagens extracted from the skins of underutilised fishes. *Food Chemistry*, 108(1), 49-54.

- Bahnassey, Y. A. & Breene, W. M. (1994). Rapid Visco-Analyzer (RVA) Pasting Profiles of Wheat, Corn, Waxy Corn, Tapioca and Amaranth Starches (*A. hypochondriacus* and *A. cruentus*) in the Presence of Konjac Flour, Gellan, Guar, Xanthan and Locust Bean Gums. *Starch-Stärke*, 46(4), 134-141.
- Bakker, W., Houben, J., Koolmees, P., Bindrich, U. & Sprehe, L. (1999). Effect of initial mild curing, with additives, of hog and sheep sausage casings on their microbial quality and mechanical properties after storage at difference temperatures. *Meat Science*, 51(2), 163-174.
- Barbut, S. (2010). Microstructure of natural extruded and co-extruded collagen casings before and after heating. *Italian Journal of Food Science*, 22(2), 126-133.
- Basiak, E., Lenart, A. & Debeaufort, F. (2017). Effect of starch type on the physico-chemical properties of edible films. *International Journal of Biological Macromolecules*, 98348-356.
- Belbekhouche, S., Bras, J., Siqueira, G., Chappey, C., Lebrun, L., Khelifi, B., Marais, S. & Dufresne, A. (2011). Water sorption behavior and gas barrier properties of cellulose whiskers and microfibrils films. *Carbohydrate Polymers*, 83(4), 1740-1748.
- Bella, J., Brodsky, B. & Berman, H. M. (1995). Hydration structure of a collagen peptide. *Structure*, 3(9), 893-906.
- Bemiller, J. N. (2011). Pasting, paste, and gel properties of starch–hydrocolloid combinations. *Carbohydrate Polymers*, 86(2), 386-423.
- Ben Slimane, E. & Sadok, S. (2018). Collagen from cartilaginous fish by-products for a potential application in bioactive film composite. *Marine drugs*, 16(6), 211.
- Benchabane, A. & Bekkour, K. (2008). Rheological properties of carboxymethyl cellulose (CMC) solutions. *Colloid and Polymer Science*, 286(10), 1173.

- Bhuimbar, M. V., Bhagwat, P. K. & Dandge, P. B. (2019). Extraction and characterization of acid soluble collagen from fish waste: Development of collagen-chitosan blend as food packaging film. *Journal of Environmental Chemical Engineering*, 7(2), 102983.
- Bigi, A., Cojazzi, G., Panzavolta, S., Rubini, K. & Roveri, N. (2001). Mechanical and thermal properties of gelatin films at different degrees of glutaraldehyde crosslinking. *Biomaterials*, 22(8), 763-768.
- Bigi, A., Panzavolta, S. & Rubini, K. (2004). Relationship between triple-helix content and mechanical properties of gelatin films. *Biomaterials*, 25(25), 5675-5680.
- Bilbao-Sáinz, C., Avena-Bustillos, R. J., Wood, D. F., Williams, T. G. & Mchugh, T. H. (2010). Composite edible films based on hydroxypropyl methylcellulose reinforced with microcrystalline cellulose nanoparticles. *Journal of Agricultural and Food Chemistry*, 58(6), 3753-3760.
- Biliaderis, C., Arvanitoyannis, I., Izydorczyk, M. & Prokopowich, D. (1997). Effect of hydrocolloids on gelatinization and structure formation in concentrated waxy maize and wheat starch gels. *Starch-Stärke*, 49(7-8), 278-283.
- Bledzki, A. K. & Gassan, J. (1999). Composites reinforced with cellulose based fibres. *Progress in Polymer Science*, 24(2), 221-274.
- Bouafif, H., Koubaa, A., Perré, P. & Cloutier, A. (2009). Effects of fiber characteristics on the physical and mechanical properties of wood plastic composites. *Composites Part A: Applied Science and Manufacturing*, 40(12), 1975-1981.
- Bourbon, A. I., Pinheiro, A. C., Cerqueira, M. A., Rocha, C. M. R., Avides, M. C., Quintas, M. a. C. & Vicente, A. A. (2011). Physico-chemical characterization of chitosan-based edible films incorporating bioactive compounds of different molecular weight. *Journal of Food Engineering*, 106(2), 111-118.

- Brodsky, B. & Ramshaw, J. A. (1997). The collagen triple-helix structure. *Matrix Biology*, 15(8-9), 545-554.
- Brown Jr, R. M. & Saxena, I. M. (2000). Cellulose biosynthesis: a model for understanding the assembly of biopolymers. *Plant Physiology and Biochemistry*, 38(1-2), 57-67.
- Brunauer, S., Emmett, P. H. & Teller, E. (1938). Adsorption of gases in multimolecular layers. *Journal of the American chemical society*, 60(2), 309-319.
- Buléon, A., Colonna, P., Planchot, V. & Ball, S. (1998). Starch granules: structure and biosynthesis. *International Journal of Biological Macromolecules*, 23(2), 85-112.
- Calahorra, M., Cortazar, M., Eguiazabal, J. & Guzmán, G. (1989). Thermogravimetric analysis of cellulose: effect of the molecular weight on thermal decomposition. *Journal of Applied Polymer Science*, 37(12), 3305-3314.
- Cameron, R. E., Durrani, C. M. & Donald, A. M. (1994). Gelation of amylopectin without long range order. *Starch-Stärke*, 46(8), 285-287.
- Carlson, W., Overton, J. & Ziegenfuss, E. (1962). Compatibility and manipulation of guar gum. *Food Technology*, 16(10), 50-&.
- Cazón, P., Velazquez, G., Ramírez, J. A. & Vázquez, M. (2017). Polysaccharide-based films and coatings for food packaging: A review. *Food Hydrocolloids*, 68136-148.
- Chaisawang, M. & Supphantharika, M. (2005). Effects of guar gum and xanthan gum additions on physical and rheological properties of cationic tapioca starch. *Carbohydrate Polymers*, 61(3), 288-295.
- Chak, V., Kumar, D. & Visht, S. (2013). A review on collagen based drug delivery systems. *Int J Pharm Teach Pract*, 4(4), 811-820.

- Chang, Y., Cheah, P. & Seow, C. (2000). Plasticizing—antiplasticizing effects of water on physical properties of tapioca starch films in the glassy state. *Journal of Food Science*, 65(3), 445-451.
- Cheetham, N. W. H. & Tao, L. (1998). Variation in crystalline type with amylose content in maize starch granules: an X-ray powder diffraction study. *Carbohydrate Polymers*, 36(4), 277-284.
- Chen, L., Ma, L., Zhou, M., Liu, Y. & Zhang, Y. (2014). Effects of pressure on gelatinization of collagen and properties of extracted gelatins. *Food Hydrocolloids*, 36316-322.
- Chen, X., Zhou, L., Xu, H., Yamamoto, M., Shinoda, M., Tada, I., Minami, S., Urayama, K. & Yamane, H. (2019). The structure and properties of natural sheep casing and artificial films prepared from natural collagen with various crosslinking treatments. *International Journal of Biological Macromolecules*, 135959-968.
- Chen, Z., Mo, X., He, C. & Wang, H. (2008). Intermolecular interactions in electrospun collagen–chitosan complex nanofibers. *Carbohydrate Polymers*, 72(3), 410-418.
- Cheng, H., Takai, M. & Ekong, E. A. Rheology of carboxymethylcellulose made from bacterial cellulose. *Macromolecular Symposia*, 1999. Wiley Online Library, 145-153.
- Cheng, S., Wang, W., Li, Y., Gao, G., Zhang, K., Zhou, J. & Wu, Z. (2019). Cross-linking and film-forming properties of transglutaminase-modified collagen fibers tailored by denaturation temperature. *Food chemistry*, 271527-535.
- Choi, D. W. & Chang, Y. H. (2012). Steady and dynamic shear rheological properties of buckwheat starch-galactomannan mixtures. *Preventive Nutrition and Food Science*, 17(3), 192.

- Christianson, D., Hodge, J., Osborne, D. & Detroy, R. W. (1981). Gelatinization of wheat starch as modified by xanthan gum, guar gum, and cellulose gum. *Cereal Chemistry*, 58(6), 513-517.
- Clark, A. H. & Ross-Murphy, S. B. 1987. Structural and mechanical properties of biopolymer gels. *Biopolymers*. Springer.
- Clasen, C. & Kulicke, W.-M. (2001a). Determination of viscoelastic and rheo-optical material functions of water-soluble cellulose derivatives. *Progress in Polymer Science*, 26(9), 1839-1919.
- Clasen, C. & Kulicke, W. M. (2001b). Determination of viscoelastic and rheo-optical material functions of water-soluble cellulose derivatives. *Progress in Polymer Science*, 26(9), 1839-1919.
- Cooke, D. & Gidley, M. J. (1992). Loss of crystalline and molecular order during starch gelatinisation: origin of the enthalpic transition. *Carbohydrate Research*, 227103-112.
- Copeland, L., Blazek, J., Salman, H. & Tang, M. C. (2009a). Form and functionality of starch. *Food Hydrocolloids*, 23(6), 1527-1534.
- Copeland, L., Blazek, J., Salman, H. & Tang, M. C. (2009b). Form and functionality of starch. *Food Hydrocolloids*, 23((6)), 1527-1534.
- Coultate, T. P. 2009. *Food: the chemistry of its components*, Royal Society of Chemistry.
- Cowley, J. M. 2020. *Exploiting natural variation in Plantago seed composition for food and human health applications*.
- Crooks, H. B. 1985. Method of preparing collagen extrusion gels. US4526580 A.

- De Morais Teixeira, E., Bondancia, T. J., Teodoro, K. B. R., Corrêa, A. C., Marconcini, J. M. & Mattoso, L. H. C. (2011). Sugarcane bagasse whiskers: extraction and characterizations. *Industrial Crops and Products*, 33(1), 63-66.
- Debet, M. R. & Gidley, M. J. (2007). Why do gelatinized starch granules not dissolve completely? Roles for amylose, protein, and lipid in granule “ghost” integrity. *Journal of Agricultural and Food Chemistry*, 55(12), 4752-4760.
- Derkach, S. R., Kuchina, Y. A., Kolotova, D. S. & Voron'ko, N. G. (2020). Polyelectrolyte Polysaccharide–Gelatin Complexes: Rheology and Structure. *Polymers*, 12(2), 266.
- Desbrieres, J., Hirrien, M. & Ross-Murphy, S. (2000). Thermogelation of methylcellulose: rheological considerations. *Polymer*, 41(7), 2451-2461.
- Devro 2019. Annual report and accounts 2018. Devro plc, England. Devro plc, England.
- Díaz-Calderón, P., Flores, E., González-Muñoz, A., Pepczynska, M., Quero, F. & Enrione, J. (2017). Influence of extraction variables on the structure and physical properties of salmon gelatin. *Food Hydrocolloids*, 71118-128.
- Diaz-Calderon, P., Macnaughtan, B., Hill, S., Foster, T., Enrione, J. & Mitchell, J. (2018). Changes in gelatinisation and pasting properties of various starches (wheat, maize and waxy maize) by the addition of bacterial cellulose fibrils. *Food Hydrocolloids*, 80274-280.
- Ding, C., Zhang, M. & Li, G. (2014a). Rheological properties of collagen/hydroxypropyl methylcellulose (COL/HPMC) blended solutions. *Journal of Applied Polymer Science*, 131(7).

- Ding, C., Zhang, M. & Li, G. (2015). Preparation and characterization of collagen/hydroxypropyl methylcellulose (HPMC) blend film. *Carbohydrate Polymers*, 119194-201.
- Ding, C., Zhang, M., Wu, K. & Li, G. (2014b). The response of collagen molecules in acid solution to temperature. *Polymer*, 55(22), 5751-5759.
- Donovan, J. W. (1979). Phase transitions of the starch–water system. *Biopolymers*, 18(2), 263-275.
- Doublier, J.-L. & Choplin, L. (1989). A rheological description of amylose gelation. *Carbohydrate research*, 193215-226.
- Doyle, B. B., Bendit, E. & Blout, E. R. (1975). Infrared spectroscopy of collagen and collagen-like polypeptides. *Biopolymers: Original Research on Biomolecules*, 14(5), 937-957.
- Dufresne, A. & Vignon, M. R. (1998). Improvement of starch film performances using cellulose microfibrils. *Macromolecules*, 31(8), 2693-2696.
- Eidam, D., Kulicke, W. M., Kuhn, K. & Stute, R. (1995). Formation of maize starch gels selectively regulated by the addition of hydrocolloids. *Starch-Stärke*, 47(10), 378-384.
- El Ghzaoui, A., Trompette, J. L., Cassanas, G., Bardet, L. & Fabregue, E. (2001). Comparative rheological behavior of some cellulosic ether derivatives. *Langmuir*, 17(5), 1453-1456.
- El Oudiani, A., Chaabouni, Y., Msahli, S. & Sakli, F. (2011). Crystal transition from cellulose I to cellulose II in NaOH treated *Agave americana* L. fibre. *Carbohydrate Polymers*, 86(3), 1221-1229.

- Esteghlal, S., Niakousari, M. & Hosseini, S. M. H. (2018). Physical and mechanical properties of gelatin-CMC composite films under the influence of electrostatic interactions. *International Journal of Biological Macromolecules*, 1141-9.
- Feddersen, R. L. & Thorp, S. N. 1993. Chapter 20 - sodium carboxymethylcellulose. *In: Whistler, R. L. & Bemiller, J. N. (eds.) Industrial Gums (Third Edition)*. London: Academic Press.
- Feiner, G. 2006. *Meat products handbook: Practical science and technology*, Elsevier.
- Florjancic, U., Zupancic, A. & Zumer, M. (2002). Rheological characterization of aqueous polysaccharide mixtures undergoing shear. *Chemical and Biochemical Engineering quarterly*, 16(3), 105-118.
- Fredriksson, H., Silverio, J., Andersson, R., Eliasson, A.-C. & Åman, P. (1998). The influence of amylose and amylopectin characteristics on gelatinization and retrogradation properties of different starches. *Carbohydrate Polymers*, 35(3-4), 119-134.
- French, D. (1972). Fine structure of starch and its relationship to the organization of starch granules. *Journal of the Japanese Society of starch Science*, 19(1), 8-25.
- Friess, W. (1998). Collagen–biomaterial for drug delivery. *European Journal of Pharmaceutics and Biopharmaceutics*, 45(2), 113-136.
- Funami, T., Kataoka, Y., Omoto, T., Goto, Y., Asai, I. & Nishinari, K. (2005). Food hydrocolloids control the gelatinization and retrogradation behavior of starch. 2a. Functions of guar gums with different molecular weights on the gelatinization behavior of corn starch. *Food Hydrocolloids*, 19(1), 15-24.

- Gałkowska, D., Pycia, K., Juszcak, L. & Pająk, P. (2014). Influence of cassia gum on rheological and textural properties of native potato and corn starch. *Starch-Stärke*, 66(11-12), 1060-1070.
- Gelse, K., Pöschl, E. & Aigner, T. (2003). Collagens—structure, function, and biosynthesis. *Advanced Drug Delivery Reviews*, 55(12), 1531-1546.
- Genkina, N. K., Kozlov, S. S., Martirosyan, V. V. & Kiseleva, V. I. (2014). Thermal behavior of maize starches with different amylose/amylopectin ratio studied by DSC analysis. *Starch-Stärke*, 66(7-8), 700-706.
- Ghanbarzadeh, B., Almasi, H. & Entezami, A. A. (2010). Physical properties of edible modified starch/carboxymethyl cellulose films. *Innovative food science & emerging technologies*, 11(4), 697-702.
- Ghannam, M. T. & Esmail, M. N. (1997). Rheological properties of carboxymethyl cellulose. *Journal of Applied Polymer Science*, 64(2), 289-301.
- Ghosh, A. K. & Bandyopadhyay, P. (2012). Polysaccharide-protein interactions and their relevance in food colloids. *The Complex World of Polysaccharides*, 14395-406.
- Gibis, M., Schuh, V. & Weiss, J. (2015). Effects of carboxymethyl cellulose (CMC) and microcrystalline cellulose (MCC) as fat replacers on the microstructure and sensory characteristics of fried beef patties. *Food Hydrocolloids*, 45236-246.
- Gidley, M. J. (1989). Molecular mechanisms underlying amylose aggregation and gelation. *Macromolecules*, 22(1), 351-358.
- Gidley, M. J. & Bulpin, P. V. (1987). Crystallisation of malto-oligosaccharides as models of the crystalline forms of starch: minimum chain-length requirement for the formation of double helices. *Carbohydrate Research*, 161(2), 291-300.

- Gilsenan, P. M. & Ross-Murphy, S. B. (2000). Viscoelasticity of thermoreversible gelatin gels from mammalian and piscine collagens. *Journal of Rheology*, 44(4), 871-883.
- Gioffrè, M., Torricelli, P., Panzavolta, S., Rubini, K. & Bigi, A. (2012). Role of pH on stability and mechanical properties of gelatin films. *Journal of Bioactive and Compatible Polymers*, 27(1), 67-77.
- Goel, P. K., Singhal, R. S. & Kulkarni, P. R. (1999). Studies on interactions of corn starch with casein and casein hydrolysates. *Food Chemistry*, 64(3), 383-389.
- Gómez-Guillén, M., Giménez, B., López-Caballero, M. A. & Montero, M. (2011). Functional and bioactive properties of collagen and gelatin from alternative sources: A review. *Food hydrocolloids*, 25(8), 1813-1827.
- Goycoolea, F. M., Morris, E. R. & Gidley, M. J. (1995). Viscosity of galactomannans at alkaline and neutral pH: evidence of 'hyperentanglement' in solution. *Carbohydrate Polymers*, 27(1), 69-71.
- Greene, D. M. 2003. *Use of Poultry Collagen Coating and Antioxidants as Flavor Protection for Cat Foods Made with Rendered Poultry Fat*. Virginia Tech.
- Guggenheim, E. A. (1966). Applications of statistical mechanics.
- Guzzi Plepis, A. M. D., Goissis, G. & Das-Gupta, D. K. (1996). Dielectric and pyroelectric characterization of anionic and native collagen. *Polymer Engineering & Science*, 36(24), 2932-2938.
- Haniffa, M., Cader, M. A., Ching, Y. C., Abdullah, L. C., Poh, S. C. & Chuah, C. H. (2016). Review of bionanocomposite coating films and their applications. *Polymers*, 8(7), 246.
- Haque, A. & Morris, E. R. (1993). Thermogelation of methylcellulose. Part I: molecular structures and processes. *Carbohydrate Polymers*, 22(3), 161-173.

- Haque, A., Richardson, R. K., Morris, E. R., Gidley, M. J. & Caswell, D. C. (1993a). Thermogelation of methylcellulose. Part II: effect of hydroxypropyl substituents. *Carbohydrate Polymers*, 22(3), 175-186.
- Harper, B., Barbut, S., Lim, L.-T. & Marcone, M. (2012). Microstructural and textural investigation of various manufactured collagen sausage casings. *Food Research International*, 49(1), 494-500.
- Harper, B., Barbut, S., Lim, L.-T. & Marcone, M. (2013). Characterization of 'wet' alginate and composite films containing gelatin, whey or soy protein. *Food research international*, 52(2), 452-459.
- Harrington, J. C. & Morris, E. R. (2009). Conformational ordering and gelation of gelatin in mixtures with soluble polysaccharides. *Food Hydrocolloids*, 23(2), 327-336.
- Harris, P. J. & Smith, B. G. (2006). Plant cell walls and cell-wall polysaccharides: structures, properties and uses in food products. *International Journal of Food Science & Technology*, 41(12), 129-143.
- Hashim, P., Sofberi, M., Ridzwan, M., Bakar, J. & Mat Hashim, D. (2015). Collagen in food and beverage industries. *International Food Research Journal*, 22(1), 1-8.
- Haug, I., Williams, M. A., Lundin, L., Smidsrød, O. & Draget, K. I. (2003). Molecular interactions in, and rheological properties of, a mixed biopolymer system undergoing order/disorder transitions. *Food Hydrocolloids*, 17(4), 439-444.
- He, L., Lan, W., Zhao, Y., Chen, S., Liu, S., Cen, L., Cao, S., Dong, L., Jin, R. & Liu, Y. (2020). Characterization of biocompatible pig skin collagen and application of collagen-based films for enzyme immobilization. *RSC Advances*, 10(12), 7170-7180.

- He, L., Mu, C., Shi, J., Zhang, Q., Shi, B. & Lin, W. (2011). Modification of collagen with a natural cross-linker, procyanidin. *International Journal of Biological Macromolecules*, 48(2), 354-359.
- Heinze, T. & Petzold, K. 2008. Cellulose chemistry: novel products and synthesis paths. *Monomers, polymers and composites from renewable resources*. Elsevier.
- Hemar, Y., Lebreton, S., Xu, M. & Day, L. (2011). Small-deformation rheology investigation of rehydrated cell wall particles–xanthan mixtures. *Food Hydrocolloids*, 25(4), 668-676.
- Hernandez, R. (1997). Polymer properties. *The Wiley encyclopedia of packaging technology*, 2738-764.
- Heu, M. S., Lee, J. H., Kim, H. J., Jee, S. J., Lee, J. S., Jeon, Y.-J., Shahidi, F. & Kim, J.-S. (2010). Characterization of acid-and pepsin-soluble collagens from flatfish skin. *Food Science and Biotechnology*, 19(1), 27-33.
- Heymann, E. (1935). Studies on sol-gel transformations. I. The inverse sol-gel transformation of methylcellulose in water. *Transactions of the Faraday society*, 31846-864.
- Hong, Y., Wu, Y., Liu, G. & Gu, Z. (2015). Effect of amylose on pasting and rheological properties of corn starch/xanthan blends. *Starch-Stärke*, 67(1-2), 98-106.
- Hoover, R. (2001). Composition, molecular structure, and physicochemical properties of tuber and root starches: a review. *Carbohydrate polymers*, 45(3), 253-267.
- Hoque, M. S., Benjakul, S., Prodpran, T. & Songtipya, P. (2011). Properties of blend film based on cuttlefish (*Sepia pharaonis*) skin gelatin and mungbean protein isolate. *International Journal of Biological Macromolecules*, 49(4), 663-673.

- Hsu, S., Lu, S. & Huang, C. (2000). Viscoelastic changes of rice starch suspensions during gelatinization. *Journal of Food Science*, 65(2), 215-220.
- Hu, Y., Liu, L., Gu, Z., Dan, W., Dan, N. & Yu, X. (2014). Modification of collagen with a natural derived cross-linker, alginate dialdehyde. *Carbohydrate polymers*, 102324-332.
- loi, M. 2013. *An Investigation of Commercial Collagen Dispersions and their use in Co-Extrusion Sausage Manufacturing*. MSc, The University of Guelph.
- Jakobsen, R., Brown, L., Hutson, T., Fink, D. & Veis, A. (1983). Intermolecular interactions in collagen self-assembly as revealed by Fourier transform infrared spectroscopy. *Science*, 220(4603), 1288-1290.
- Jane, J., Chen, Y., Lee, L., Mcpherson, A., Wong, K., Radosavljevic, M. & Kasemsuwan, T. (1999). Effects of amylopectin branch chain length and amylose content on the gelatinization and pasting properties of starch. *Cereal Chemistry*, 76(5), 629-637.
- Jones, A. K. (1992). Hydrophobicity in polysaccharide gelation.
- Jose, M. V., Thomas, V., Dean, D. R. & Nyairo, E. (2009). Fabrication and characterization of aligned nanofibrous PLGA/Collagen blends as bone tissue scaffolds. *Polymer*, 50(15), 3778-3785.
- Joséfonseca, M., Alsina, M. A. & Reig, F. (1996). Coating liposomes with collagen (Mr 50 000) increases uptake into liver. *Biochimica et Biophysica Acta (BBA)-Biomembranes*, 1279(2), 259-265.
- Kanmani, P. & Lim, S. T. (2013). Development and characterization of novel probiotic-residing pullulan/starch edible films. *Food Chemistry*, 141(2), 1041-1049.
- Kaufman, H. E., Steinemann, T. L., Lehman, E., Thompson, H. W., Varnell, E. D., Jacob-Labarre, J. T. & Gebhardt, B. M. (1994). Collagen-based drug delivery

- and artificial tears. *Journal of Ocular Pharmacology and Therapeutics*, 10(1), 17-27.
- Keetels, C., Van Vliet, T. & Walstra, P. (1996). Gelation and retrogradation of concentrated starch systems: 2. Retrogradation. *Food hydrocolloids*, 10(3), 355-362.
- Kent, M. & Meyer, W. (1984). Complex permittivity spectra of protein powders as a function of temperature and hydration. *Journal of Physics D: Applied Physics*, 17(8), 1687.
- Khan, A., Khan, R. A., Salmieri, S., Le Tien, C., Riedl, B., Bouchard, J., Chauve, G., Tan, V., Kamal, M. R. & Lacroix, M. (2012). Mechanical and barrier properties of nanocrystalline cellulose reinforced chitosan based nanocomposite films. *Carbohydrate Polymers*, 90(4), 1601-1608.
- Khutoryanskiy, V. V., Cascone, M. G., Lazzeri, L., Nurkeeva, Z. S., Mun, G. A. & Mangazbaeva, R. A. (2003). Phase behaviour of methylcellulose–poly (acrylic acid) blends and preparation of related hydrophilic films. *Polymer International*, 52(1), 62-67.
- Kibar, E. a. A., Gönenç, İ. & Us, F. (2010). Gelatinization of waxy, normal and high amylose corn starches. *The Journal of Food*, 35(4), 237-244.
- Kim, W. & Yoo, B. (2011a). Rheological and thermal effects of galactomannan addition to acorn starch paste. *LWT-Food Science and Technology*, 44(3), 759-764.
- Kim, W. W. & Yoo, B. (2011b). Rheological and thermal effects of galactomannan addition to acorn starch paste. *LWT - Food Science and Technology*, 44(3), 759-764.

- Klemm, D., Heublein, B., Fink, H. P. & Bohn, A. (2005). Cellulose: fascinating biopolymer and sustainable raw material. *Angewandte Chemie International Edition*, 44(22), 3358-3393.
- Koganti, N., Mitchell, J. R., Ibbett, R. N. & Foster, T. J. (2011). Solvent effects on starch dissolution and gelatinization. *Biomacromolecules*, 12(8), 2888-2893.
- Komsa-Penkova, R., Koynova, R., Kostov, G. & Tenchov, B. G. (1996). Thermal stability of calf skin collagen type I in salt solutions. *Biochimica et Biophysica Acta (BBA)-Protein Structure and Molecular Enzymology*, 1297(2), 171-181.
- Koolmees, P., Tersteeg, M., Keizer, G., Van Den Broek, J. & Bradley, R. (2004). Comparative histological studies of mechanically versus manually processed sheep intestines used to make natural sausage casings. *Journal of Food Protection*, 67(12), 2747-2755.
- Kowalczyk, D. & Baraniak, B. (2014). Effect of candelilla wax on functional properties of biopolymer emulsion films – A comparative study. *Food Hydrocolloids*, 41195-209.
- Kristo, E. & Biliaderis, C. G. (2006). Water sorption and thermo-mechanical properties of water/sorbitol-plasticized composite biopolymer films: Caseinate–pullulan bilayers and blends. *Food Hydrocolloids*, 20(7), 1057-1071.
- Kristo, E. & Biliaderis, C. G. (2007). Physical properties of starch nanocrystal-reinforced pullulan films. *Carbohydrate Polymers*, 68(1), 146-158.
- Krochta, J. M. (2002). Proteins as raw materials for films and coatings: definitions, current status, and opportunities. *Protein-Based Films And Coatings*, 1-41.
- Kroon-Batenburg, L. & Kroon, J. (1997). The crystal and molecular structures of cellulose I and II. *Glycoconjugate Journal*, 14(5), 677-690.

- Krystyjan, M., Ciesielski, W., Khachatryan, G., Sikora, M. & Tomasik, P. (2015). Structure, rheological, textural and thermal properties of potato starch – Inulin gels. *LWT - Food Science and Technology*, 60(1), 131-136.
- Krystyjan, M., Khachatryan, G., Ciesielski, W., Buksa, K. & Sikora, M. (2017). Preparation and characteristics of mechanical and functional properties of starch/*Plantago psyllium* seeds mucilage films. *Starch-Stärke*, 69(11-12), 1700014.
- Lai, G., Li, Y. & Li, G. (2008). Effect of concentration and temperature on the rheological behavior of collagen solution. *International Journal of Biological Macromolecules*, 42(3), 285-291.
- Langmaier, F., Mokrejs, P. & Mladek, M. (2010). Heat-treated biodegradable films and foils of collagen hydrolysate crosslinked with dialdehyde starch. *Journal of Thermal Analysis and Calorimetry*, 102(1), 37-42.
- Lapasin, R. & Prici, S. (1995). *Rheology of Industrial Polysaccharides; Theory and Applications*.
- Lazarev, Y. A., Grishkovsky, B. & Khromova, T. (1985). Amide I band of IR spectrum and structure of collagen and related polypeptides. *Biopolymers: Original Research on Biomolecules*, 24(8), 1449-1478.
- Lecorre, D., Bras, J. & Dufresne, A. (2012). Influence of native starch's properties on starch nanocrystals thermal properties. *Carbohydrate Polymers*, 87(1), 658-666.
- Lee, C. H., Singla, A. & Lee, Y. (2001). Biomedical applications of collagen. *International Journal of Pharmaceutics*, 221(1-2), 1-22.

- Lee, S.-Y., Mohan, D. J., Kang, I.-A., Doh, G.-H., Lee, S. & Han, S. O. (2009). Nanocellulose reinforced PVA composite films: effects of acid treatment and filler loading. *Fibers and Polymers*, 10(1), 77-82.
- Lee, Y. & Chang, Y. H. (2015). Effects of galactomannan addition on rheological, pasting and physical properties of water chestnut starch. *Journal of Texture Studies*, 46(1), 58-66.
- Lemus M, R. (2011). Models of sorption isotherms for food: uses and limitations. *Vitae*, 18(3), 325-334.
- Li, C., Dhital, S., Gilbert, R. G. & Gidley, M. J. (2020). High-amylose wheat starch: structural basis for water absorption and pasting properties. *Carbohydrate Polymers*, 116557.
- Li, L., Wang, Q. & Xu, Y. (2003). Thermoreversible association and gelation of methylcellulose in aqueous solutions. *Nihon Reoroji Gakkaishi*, 31(5), 287-296.
- Li, W., Guo, R., Lan, Y., Zhang, Y., Xue, W. & Zhang, Y. (2014). Preparation and properties of cellulose nanocrystals reinforced collagen composite films. *Journal of Biomedical Materials Research Part A*, 102(4), 1131-1139.
- Li, Y., Li, Y., Du, Z. & Li, G. (2008). Comparison of dynamic denaturation temperature of collagen with its static denaturation temperature and the configuration characteristics in collagen denaturation processes. *Thermochimica Acta*, 469(1-2), 71-76.
- Li, Z.-R., Wang, B., Chi, C.-F., Zhang, Q.-H., Gong, Y.-D., Tang, J.-J., Luo, H.-Y. & Ding, G.-F. (2013). Isolation and characterization of acid soluble collagens and pepsin soluble collagens from the skin and bone of Spanish mackerel (*Scomberomorus niphonius*). *Food Hydrocolloids*, 31(1), 103-113.

- Liu, H., Yu, L., Xie, F. & Chen, L. (2006). Gelatinization of cornstarch with different amylose/amylopectin content. *Carbohydrate Polymers*, 65(3), 357-363.
- Liu, L., Kerry, J. & Kerry, J. (2007). Application and assessment of extruded edible casings manufactured from pectin and gelatin/sodium alginate blends for use with breakfast pork sausage. *Meat Science*, 75(2), 196-202.
- Liu, S., Reimer, M. & Ai, Y. (2020). In vitro digestibility of different types of resistant starches under high-temperature cooking conditions. *Food Hydrocolloids*, 105927.
- Liu, S., Yuan, T. Z., Wang, X., Reimer, M., Isaak, C. & Ai, Y. (2019). Behaviors of starches evaluated at high heating temperatures using a new model of Rapid Visco Analyzer – RVA 4800. *Food Hydrocolloids*, 94217-228.
- Liu, X., Dan, N. & Dan, W. (2016). Preparation and characterization of an advanced collagen aggregate from porcine acellular dermal matrix. *International Journal of Biological Macromolecules*, 88179-188.
- Long, K., Cha, R., Zhang, Y., Li, J., Ren, F. & Jiang, X. (2018). Cellulose nanocrystals as reinforcements for collagen-based casings with low gas transmission. *Cellulose*, 25(1), 463-471.
- Lorén, N., Hermansson, A.-M., Williams, M., Lundin, L., Foster, T., Hubbard, C., Clark, A., Norton, I., Bergström, E. & Goodall, D. (2001). Phase separation induced by conformational ordering of gelatin in gelatin/maltodextrin mixtures. *Macromolecules*, 34(2), 289-297.
- Lucas, P. A., Laurencin, C., Syftestad, G. T., Domb, A., Goldberg, V. M., Caplan, A. I. & Langer, R. (1990). Ectopic induction of cartilage and bone by water-soluble proteins from bovine bone using a polyanhydride delivery vehicle. *Journal of Biomedical Materials Research*, 24(7), 901-911.

- Ma, Y., Wang, W., Wang, Y., Guo, Y., Duan, S., Zhao, K. & Li, S. (2018). Metal ions increase mechanical strength and barrier properties of collagen-sodium polyacrylate composite films. *International Journal of Biological Macromolecules*, 11915-22.
- Machado, A. S., Martins, V. & Plepis, A. (2002). Thermal and Rheological Behavior of Collagen. Chitosan blends. *Journal of Thermal Analysis and Calorimetry*, 67(2), 491-498.
- Mathew, A. P., Oksman, K., Pierron, D. & Harnad, M.-F. (2012). Crosslinked fibrous composites based on cellulose nanofibers and collagen with in situ pH induced fibrillation. *Cellulose*, 19(1), 139-150.
- Meng, Z., Zheng, X., Tang, K., Liu, J., Ma, Z. & Zhao, Q. (2012). Dissolution and regeneration of collagen fibers using ionic liquid. *International Journal of Biological Macromolecules*, 51(4), 440-448.
- Mezger, T. G. 2006. *The rheology handbook: for users of rotational and oscillatory rheometers*, Vincentz Network GmbH & Co KG.
- Michon, C., Cuvelier, G., Relkin, P. & Launay, B. (1997). Influence of thermal history on the stability of gelatin gels. *International Journal of Biological Macromolecules*, 20(4), 259-264.
- Migneault, S., Koubaa, A., Erchiqui, F., Chaala, A., Englund, K. & Wolcott, M. P. (2009). Effects of processing method and fiber size on the structure and properties of wood-plastic composites. *Composites Part A: Applied Science and Manufacturing*, 40(1), 80-85.
- Miles, C. & Bailey, A. (2001). Thermally labile domains in the collagen molecule. *Micron*, 32(3), 325-332.

- Miles, C. A. & Ghelashvili, M. (1999). Polymer-in-a-Box Mechanism for the Thermal Stabilization of Collagen Molecules in Fibers. *Biophysical Journal*, 76(6), 3243-3252.
- Miles, M. J., Morris, V. J., Orford, P. D. & Ring, S. G. (1985). The roles of amylose and amylopectin in the gelation and retrogradation of starch. *Carbohydrate Research*, 135(2), 271-281.
- Mohammed, I., Ahmed, A. R. & Senge, B. (2011). Dynamic rheological properties of chickpea and wheat flour dough's. *Journal of Applied Sciences*, 11(19), 3405-3412.
- Mohanty, S., Verma, S. K. & Nayak, S. K. (2006). Dynamic mechanical and thermal properties of MAPE treated jute/HDPE composites. *Composites Science and Technology*, 66(3), 538-547.
- Morris, E. R., Cutler, A., Ross-Murphy, S., Rees, D. & Price, J. (1981). Concentration and shear rate dependence of viscosity in random coil polysaccharide solutions. *Carbohydrate Polymers*, 1(1), 5-21.
- Morris, V. (1990). Starch gelation and retrogradation. *Trends in Food Science & Technology*, 12-6.
- Mu, C., Li, D., Lin, W., Ding, Y. & Zhang, G. (2007). Temperature induced denaturation of collagen in acidic solution. *Biopolymers: Original Research on Biomolecules*, 86(4), 282-287.
- Mudgil, D., Barak, S. & Khatkar, B. S. (2012). X-ray diffraction, IR spectroscopy and thermal characterization of partially hydrolyzed guar gum. *International Journal of Biological Macromolecules*, 50(4), 1035-1039.

- Mudgil, D., Barak, S. & Khatkar, B. S. (2014). Guar gum: processing, properties and food applications—a review. *Journal of food science and technology*, 51(3), 409-418.
- Muyonga, J., Cole, C. & Duodu, K. (2004). Fourier transform infrared (FTIR) spectroscopic study of acid soluble collagen and gelatin from skins and bones of young and adult Nile perch (*Lates niloticus*). *Food Chemistry*, 86(3), 325-332.
- Nicoletti, J. & Telis, V. (2009). Viscoelastic and thermal properties of collagen–xanthan gum and collagen–maltodextrin suspensions during heating and cooling. *Food Biophysics*, 4(3), 135.
- Noorzai, S. 2020. *Extraction and characterization of collagen from bovine hides for preparation of biodegradable films*. The University of Waikato.
- Noorzai, S. & Verbeek, C. J. 2020. Collagen: From Waste to Gold. *Biomass*. IntechOpen.
- Oechsle, A. M., Bugbee, T. J., Gibis, M., Kohlus, R. & Weiss, J. (2017). Modification of extruded chicken collagen films by addition of co-gelling protein and sodium chloride. *Journal of Food Engineering*, 20746-55.
- Oechsle, A. M., Häupler, M., Gibis, M., Kohlus, R. & Weiss, J. (2015). Modulation of the rheological properties and microstructure of collagen by addition of co-gelling proteins. *Food Hydrocolloids*, 49118-126.
- Olivas, G. I. & Barbosa-Cánovas, G. V. (2008). Alginate–calcium films: water vapor permeability and mechanical properties as affected by plasticizer and relative humidity. *LWT-Food Science and Technology*, 41(2), 359-366.
- Oliveira, V. D. M., Assis, C. R. D., Costa, B. D. a. M., Neri, R. C. D. A., Monte, F. T. D., Freitas, H. M. S. D. C. V., França, R. C. P., Santos, J. F., Bezerra, R. D. S.

- & Porto, A. L. F. (2021). Physical, biochemical, densitometric and spectroscopic techniques for characterization collagen from alternative sources: A review based on the sustainable valorization of aquatic by-products. *Journal of Molecular Structure*, 1224129023.
- Osburn, W. N. (ed.) 2002. *Collagen casings*, USA: CRC Press.
- Oun, A. A. & Rhim, J.-W. (2016). Isolation of cellulose nanocrystals from grain straws and their use for the preparation of carboxymethyl cellulose-based nanocomposite films. *Carbohydrate Polymers*, 150187-200.
- Panduranga Rao, K. (1996). Recent developments of collagen-based materials for medical applications and drug delivery systems. *Journal of Biomaterials Science, Polymer Edition*, 7(7), 623-645.
- Pankaj, S. K., Bueno-Ferrer, C., Misra, N., O'Neill, L., Tiwari, B., Bourke, P. & Cullen, P. (2015). Dielectric barrier discharge atmospheric air plasma treatment of high amylose corn starch films. *LWT-Food Science and Technology*, 63(2), 1076-1082.
- Pataridis, S., Eckhardt, A., Mikulikova, K., Sedlakova, P. & Mikšik, I. (2008). Identification of collagen types in tissues using HPLC-MS/MS. *Journal of Separation Science*, 31(20), 3483-3488.
- Pati, F., Adhikari, B. & Dhara, S. (2010). Isolation and characterization of fish scale collagen of higher thermal stability. *Bioresource Technology*, 101(10), 3737-3742.
- Pauling, L. & Corey, R. B. (1951). The structure of fibrous proteins of the collagen-gelatin group. *Proceedings of the National Academy of Sciences of the United States of America*, 37(5), 272.

- Payne, K. & Veis, A. (1988). Fourier transform IR spectroscopy of collagen and gelatin solutions: deconvolution of the amide I band for conformational studies. *Biopolymers: Original Research on Biomolecules*, 27(11), 1749-1760.
- Pępczyńska, M., Díaz-Calderón, P., Quero, F., Matiacevich, S., Char, C. & Enrione, J. (2019). Interaction and fragility study in salmon gelatin-oligosaccharide composite films at low moisture conditions. *Food Hydrocolloids*, 105207.
- Pérez, O. E., Sánchez, C. C., Rodríguez Patino, J. M. & Pilosof, A. M. (2006). Thermodynamic and Dynamic Characteristics of Hydroxypropylmethylcellulose Adsorbed Films at the Air– Water Interface. *Biomacromolecules*, 7(1), 388-393.
- Pérez, S. & Bertoft, E. (2010). The molecular structures of starch components and their contribution to the architecture of starch granules: A comprehensive review. *Starch-Stärke*, 62(8), 389-420.
- Pérez, S. & Mazeau, K. (2005). Conformations, structures, and morphologies of celluloses. *Polysaccharides: Structural diversity and functional versatility*, 2.
- Perten Instruments. 2018. *Assessing ingredient performance using the RVA 4800* [Online]. Available: <https://www.perten.com/Publications/Articles/Assessing-ingredient-performanceusing-> [Accessed 2 November 2020].
- Perumal, R. K., Perumal, S., Thangam, R., Gopinath, A., Ramadass, S. K., Madhan, B. & Sivasubramanian, S. (2018). Collagen-fucoidan blend film with the potential to induce fibroblast proliferation for regenerative applications. *International Journal of Biological Macromolecules*, 1061032-1040.
- Petersen, N. & Gatenholm, P. (2011). Bacterial cellulose-based materials and medical devices: current state and perspectives. *Applied Microbiology and Biotechnology*, 91(5), 1277-1286.

- Phillips, G. & Williams, P. (2009). Handbook of hydrocolloids. *Handbook of hydrocolloids*.
- Pietrucha, K. (2005). Changes in denaturation and rheological properties of collagen–hyaluronic acid scaffolds as a result of temperature dependencies. *International Journal of Biological Macromolecules*, 36(5), 299-304.
- Piez, K. A. 1984. Molecular and aggregate structures of the collagens. *Extracellular matrix biochemistry*. Elsevier New York.
- Prockop, D. J. & Kivirikko, K. I. (1995). Collagens: molecular biology, diseases, and potentials for therapy. *Annual Review of Biochemistry*, 64(1), 403-434.
- Ptaszek, P. & Grzesik, M. (2007). Viscoelastic properties of maize starch and guar gum gels. *Journal of Food Engineering*, 82(2), 227-237.
- Ramachandran, G., Bansal, M. & Bhatnagar, R. (1973). A hypothesis on the role of hydroxyproline in stabilizing collagen structure. *Biochimica et Biophysica Acta (BBA)-Protein Structure*, 322(1), 166-171.
- Ramachandran, G. & Kartha, G. (1954). Structure of collagen. *Nature*, 174(4423), 269-270.
- Ratanavaraporn, J., Kanokpanont, S., Tabata, Y. & Damrongsakkul, S. (2008). Effects of acid type on physical and biological properties of collagen scaffolds. *Journal of Biomaterials Science, Polymer Edition*, 19(7), 945-952.
- Riaz, T., Zeeshan, R., Zarif, F., Ilyas, K., Muhammad, N., Safi, S. Z., Rahim, A., Rizvi, S. A. & Rehman, I. U. (2018). FTIR analysis of natural and synthetic collagen. *Applied Spectroscopy Reviews*, 53(9), 703-746.
- Ring, S. (1985). Some studies on starch gelation. *Starch-Stärke*, 37(3), 80-83.

- Rivero, S., García, M. & Pinotti, A. (2010). Correlations between structural, barrier, thermal and mechanical properties of plasticized gelatin films. *Innovative Food Science & Emerging Technologies*, 11(2), 369-375.
- Robinson, G., Ross-Murphy, S. B. & Morris, E. R. (1982). Viscosity-molecular weight relationships, intrinsic chain flexibility, and dynamic solution properties of guar galactomannan. *Carbohydrate Research*, 107(1), 17-32.
- Rodrigues Filho, G., De Assunção, R. M., Vieira, J. G., Meireles, C. D. S., Cerqueira, D. A., Da Silva Barud, H., Ribeiro, S. J. & Messaddeq, Y. (2007). Characterization of methylcellulose produced from sugar cane bagasse cellulose: Crystallinity and thermal properties. *Polymer degradation and stability*, 92(2), 205-210.
- Ross-Murphy, S. B. (1995). Rheological characterisation of gels. *Journal of Texture Studies*, 26(4), 391-400.
- Rössler, B., Kreuter, J. & Ross, G. (1994). Effect of collagen microparticles on the stability of retinol and its absorption into hairless mouse skin in vitro. *Die Pharmazie*, 49(2-3), 175-179.
- Saha, D. & Bhattacharya, S. (2010). Hydrocolloids as thickening and gelling agents in food: a critical review. *Journal of Food Science and Technology*, 47(6), 587-597.
- Sahraee, S., Ghanbarzadeh, B., Milani, J. M. & Hamishehkar, H. (2017). Development of gelatin bionanocomposite films containing chitin and ZnO nanoparticles. *Food and Bioprocess Technology*, 10(8), 1441-1453.
- Sarkar, N. (1979). Thermal gelation properties of methyl and hydroxypropyl methylcellulose. *Journal of Applied Polymer Science*, 24(4), 1073-1087.

- Sarkar, N. (1995). Kinetics of thermal gelation of methylcellulose and hydroxypropylmethylcellulose in aqueous solutions. *Carbohydrate Polymers*, 26(3), 195-203.
- Savic, Z. & Savic, I. 2002. Sausage Casings . Vienna, Austria: Victus. Inc.
- Savic, Z. & Savic, I. 2016. *Sausage Casings*, Vienna, Austria, VICTUS International GmbH.
- Schirmer, M., Jekle, M. & Becker, T. (2015). Starch gelatinization and its complexity for analysis. *Starch-Stärke*, 67(1-2), 30-41.
- Schroepfer, M. & Meyer, M. (2017). DSC investigation of bovine hide collagen at varying degrees of crosslinking and humidities. *International Journal of Biological Macromolecules*, 103120-128.
- Schuh, V., Allard, K., Herrmann, K., Gibis, M., Kohlus, R. & Weiss, J. (2013). Impact of carboxymethyl cellulose (CMC) and microcrystalline cellulose (MCC) on functional characteristics of emulsified sausages. *Meat Science*, 93(2), 240-247.
- Sherman, V. R., Yang, W. & Meyers, M. A. (2015). The materials science of collagen. *Journal of the mechanical behavior of biomedical materials*, 5222-50.
- Shi, D., Liu, F., Yu, Z., Chang, B., Goff, H. D. & Zhong, F. (2019). Effect of aging treatment on the physicochemical properties of collagen films. *Food Hydrocolloids*, 87436-447.
- Shi, X. & Bemiller, J. N. (2002). Effects of food gums on viscosities of starch suspensions during pasting. *Carbohydrate polymers*, 50(1), 7-18.
- Shit, S. C. & Shah, P. M. (2014). Edible polymers: challenges and opportunities. *Journal of Polymers*, 2014.

- Silva, S. M., Pinto, F. V., Antunes, F. E., Miguel, M. G., Sousa, J. J. & Pais, A. A. (2008). Aggregation and gelation in hydroxypropylmethyl cellulose aqueous solutions. *Journal of colloid and interface science*, 327(2), 333-340.
- Silvipriya, K., Kumar, K. K., Bhat, A., Kumar, B. D., John, A. & Lakshmanan, P. (2015a). Collagen: Animal sources and biomedical application. *Journal of Applied Pharmaceutical Science*, 5(3), 123-127.
- Silvipriya, K., Kumar, K. K., Bhat, A., Kumar, B. D., John, A. & Lakshmanan, P. (2015b). Collagen: Animal sources and biomedical application. *J. Appl. Pharm. Sci*, 5(3), 123-127.
- Simelane, S. & Ustunol, Z. (2005). Mechanical Properties of Heat-cured Whey Protein-based Edible Films Compared with Collagen Casings under Sausage Manufacturing Conditions. *Journal of Food Science*, 70(2), E131-E134.
- Singh, N., Singh, J., Kaur, L., Sodhi, N. S. & Gill, B. S. (2003). Morphological, thermal and rheological properties of starches from different botanical sources. *Food Chemistry*, 81(2), 219-231.
- Sionkowska, A. (2003). Interaction of collagen and poly (vinyl pyrrolidone) in blends. *European Polymer Journal*, 39(11), 2135-2140.
- Sionkowska, A., Wisniewski, M., Skopinska, J., Kennedy, C. J. & Wess, T. J. (2004). Molecular interactions in collagen and chitosan blends. *Biomaterials*, 25(5), 795-801.
- Soares, R., Lima, A., Oliveira, R., Pires, A. & Soldi, V. (2005). Thermal degradation of biodegradable edible films based on xanthan and starches from different sources. *Polymer degradation and stability*, 90(3), 449-454.

- Sobanwa, M., Foster, T. & Watson, N. (2020). The effect of cellulose and starch on the viscoelastic and thermal properties of acid-swollen collagen paste. *Food Hydrocolloids*, 101105460.
- Stenzel, K. H., Miyata, T. & Rubin, A. L. (1974). Collagen as a biomaterial. *Annual Review of Biophysics and Bioengineering*, 3(1), 231-253.
- Stephen, A. M. 1995. *Food polysaccharides and their applications*, CRC press.
- Sullo, A. 2012. *Self-association of cellulose ethers and its effect on the starch gelatinisation*. University of Nottingham.
- Sullo, A. & Foster, T. J. (2010). Characterisation of Starch/Cellulose blends. *Annual Transactions of the Nordic Rheology*, 181-7.
- Sullo, A., Wang, Y., Koschella, A., Heinze, T. & Foster, T. J. (2013). Self-association of novel mixed 3-mono-O-alkyl cellulose: Effect of the hydrophobic moieties ratio. *Carbohydrate Polymers*, 93(2), 574-581.
- Sun, Q., Xing, Y., Qiu, C. & Xiong, L. (2014). The pasting and gel textural properties of corn starch in glucose, fructose and maltose syrup. *PLoS One*, 9(4), e95862.
- Sun, S., Mitchell, J. R., Macnaughtan, W., Foster, T. J., Harabagiu, V., Song, Y. & Zheng, Q. (2009). Comparison of the mechanical properties of cellulose and starch films. *Biomacromolecules*, 11(1), 126-132.
- Suurs, P. & Barbut, S. (2020). Collagen use for co-extruded sausage casings—A review. *Trends in Food Science & Technology*.
- Tan, B. K., Ching, Y. C., Poh, S. C., Abdullah, L. C. & Gan, S. N. (2015). A review of natural fiber reinforced poly (vinyl alcohol) based composites: Application and opportunity. *Polymers*, 7(11), 2205-2222.

- Tanioka, A., Miyasaka, K. & Ishikawa, K. (1976). Reconstitution of collagen-fold structure with stretching of gelatin film. *Biopolymers: Original Research on Biomolecules*, 15(8), 1505-1511.
- Tanioka, A., Tazawa, T., Miyasaka, K. & Ishikawa, K. (1974). Effects of water on the mechanical properties of gelatin films. *Biopolymers: Original Research on Biomolecules*, 13(4), 753-764.
- Tatsumi, D., Ishioka, S. & Matsumoto, T. (2002). Effect of fiber concentration and axial ratio on the rheological properties of cellulose fiber suspensions. *Nihon Reoroji Gakkaishi*, 30(1), 27-32.
- Tester, R. & Morrison, W. (1993). Swelling and gelatinization of cereal starches. VI. Starches from waxy hector and hector barleys at four stages of grain development. *Journal of Cereal Science*, 17(1), 11-18.
- Tester, R. F., Karkalas, J. & Qi, X. (2004). Starch—composition, fine structure and architecture. *Journal of Cereal Science*, 39(2), 151-165.
- Tester, R. F. & Morrison, W. R. (1990a). Swelling and gelatinization of cereal starches. I. Effects of amylopectin, amylose, and lipids. *Cereal chem*, 67(6), 551-557.
- Tester, R. F. & Morrison, W. R. (1990b). Swelling and gelatinization of cereal starches. I. Effects of amylopectin, amylose, and lipids. *Cereal Chemistry*, 67(6), 551-557.
- Tester, R. F. & Morrison, W. R. (1990c). Swelling and gelatinization of cereal starches. II. Waxy rice starches. *Cereal Chem*, 67(6), 558-563.
- Timmermann, E., Chirife, J. & Iglesias, H. (2001). Water sorption isotherms of foods and foodstuffs: BET or GAB parameters? *Journal of Food Engineering*, 48(1), 19-31.

- Van Den Berg, C. & Bruin, S. (1981). Water activity: influence on food quality. *Academic Press: New York*, 198(1), 1-6.
- Villalobos, R., Hernández-Muñoz, P. & Chiralt, A. (2006). Effect of surfactants on water sorption and barrier properties of hydroxypropyl methylcellulose films. *Food Hydrocolloids*, 20(4), 502-509.
- Waigh, T. A., Gidley, M. J., Komanshek, B. U. & Donald, A. M. (2000). The phase transformations in starch during gelatinisation: a liquid crystalline approach. *Carbohydrate Research*, 328(2), 165-176.
- Wallace, D. G. & Rosenblatt, J. (2003). Collagen gel systems for sustained delivery and tissue engineering. *Advanced Drug Delivery Reviews*, 55(12), 1631-1649.
- Wang, K., Wang, W., Ye, R., Liu, A., Xiao, J., Liu, Y. & Zhao, Y. (2017a). Mechanical properties and solubility in water of corn starch-collagen composite films: Effect of starch type and concentrations. *Food Chemistry*, 216209-216.
- Wang, K., Wang, W., Ye, R., Xiao, J., Liu, Y., Ding, J., Zhang, S. & Liu, A. (2017b). Mechanical and barrier properties of maize starch–gelatin composite films: effects of amylose content. *Journal of the Science of Food and Agriculture*, 97(11), 3613-3622.
- Wang, W., Liu, Y., Liu, A., Xiao, J., Wang, K., Zhao, Y., Zhang, S. & Zhang, L. (2017c). Fabrication of acid-swollen collagen fiber-based composite films: Effect of nano-hydroxyapatite on packaging related properties. *International Journal of Food Properties*, 20(5), 968-978.
- Wang, W., Liu, Y., Liu, A., Zhao, Y. & Chen, X. (2016a). Effect of in situ apatite on performance of collagen fiber film for food packaging applications. *Journal of Applied Polymer Science*, 133(44).

- Wang, W., Wang, Y., Wang, Y., Zhang, X., Wang, X. & Gao, G. (2016b). Fabrication and characterization of microfibrillated cellulose and collagen composite films. *Journal of Bioresources and Bioproducts*, 1(4), 162-168.
- Wang, W., Zhang, X., Li, C., Du, G., Zhang, H. & Ni, Y. (2018). Using carboxylated cellulose nanofibers to enhance mechanical and barrier properties of collagen fiber film by electrostatic interaction. *Journal of the Science of Food and Agriculture*, 98(8), 3089-3097.
- Wang, W., Zhang, Y., Ye, R. & Ni, Y. (2015). Physical crosslinkings of edible collagen casing. *International Journal of Biological Macromolecules*, 81920-925.
- Wang, Z., Hu, S. & Wang, H. (2017d). Scale-up preparation and characterization of collagen/sodium alginate blend films. *Journal of Food Quality*, 2017.
- Williams, P. A. & Phillips, G. O. 2009. 1 - Introduction to food hydrocolloids. In: Phillips, G. O. & Williams, P. A. (eds.) *Handbook of Hydrocolloids (Second Edition)*. Woodhead Publishing.
- Winkworth-Smith, C. G. 2015. *Cellulose composite structures—by design*. University of Nottingham.
- Wolf, K., Sobral, P. & Telis, V. (2009). Physicochemical characterization of collagen fibers and collagen powder for self-composite film production. *Food Hydrocolloids*, 23(7), 1886-1894.
- Wright, N. & Humphrey, J. (2002). Denaturation of collagen via heating: an irreversible rate process. *Annual Review of Biomedical Engineering*, 4(1), 109-128.
- Wu, J., Liu, F., Yu, Z., Ma, Y., Goff, H. D., Ma, J. & Zhong, F. (2020). Facile preparation of collagen fiber–glycerol-carboxymethyl cellulose composite film by immersing method. *Carbohydrate Polymers*, 229115429.

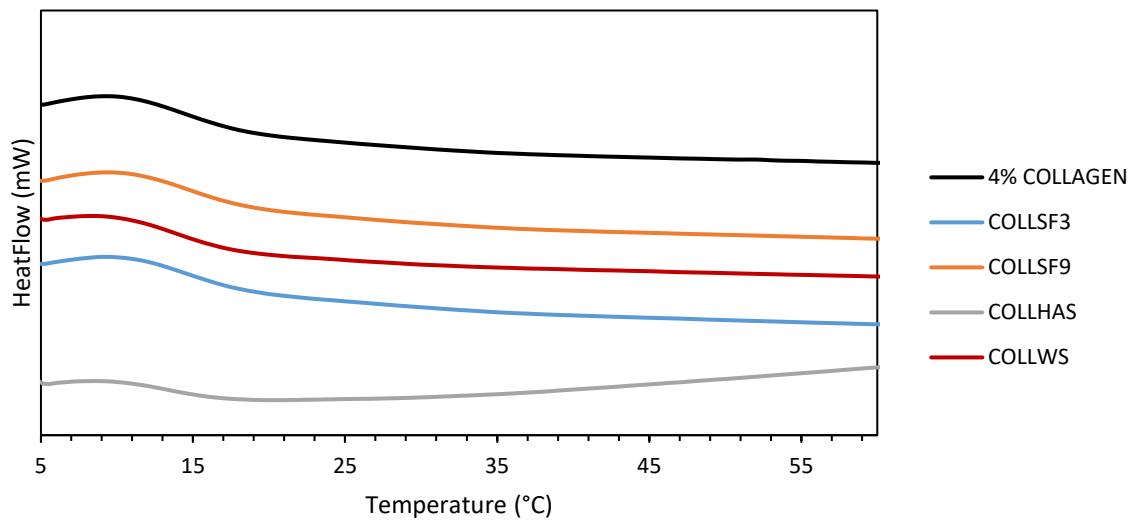
- Wu, X., Liu, A., Wang, W. & Ye, R. (2018). Improved mechanical properties and thermal-stability of collagen fiber based film by crosslinking with casein, keratin or SPI: Effect of crosslinking process and concentrations of proteins. *International Journal of Biological Macromolecules*, 1091319-1328.
- Wu, X., Liu, Y., Liu, A. & Wang, W. (2017). Improved thermal-stability and mechanical properties of type I collagen by crosslinking with casein, keratin and soy protein isolate using transglutaminase. *International journal of biological macromolecules*, 98292-301.
- Wu, X., Luo, Y., Liu, Q., Jiang, S. & Mu, G. (2019). Improved structure-stability and packaging characters of crosslinked collagen fiber-based film with casein, keratin and SPI. *Journal of the Science of Food and Agriculture*, 99(11), 4942-4951.
- Xiao, J., Ma, Y., Wang, W., Zhang, K., Tian, X., Zhao, K., Duan, S., Li, S. & Guo, Y. (2020). Incorporation of gelatin improves toughness of collagen films with a homo-hierarchical structure. *Food Chemistry*, 128802.
- Xie, Y. L., Zhou, H. M. & Qian, H. F. (2006). Effect of addition of peach gum on physicochemical properties of gelatin-based microcapsule. *Journal of Food Biochemistry*, 30(3), 302-312.
- Xu, J., Liu, F., Wang, T., Goff, H. D. & Zhong, F. (2020a). Fabrication of films with tailored properties by regulating the swelling of collagen fiber through pH adjustment. *Food Hydrocolloids*, 108106016.
- Xu, J., Liu, F., Wang, T., Goff, H. D. & Zhong, F. (2020b). Fabrication of films with tailored properties by regulating the swelling of collagen fiber through pH adjustment. *Food Hydrocolloids*, 106016.

- Yakimets, I., Paes, S. S., Wellner, N., Smith, A. C., Wilson, R. H. & Mitchell, J. R. (2007). Effect of water content on the structural reorganization and elastic properties of biopolymer films: a comparative study. *Biomacromolecules*, 8(5), 1710-1722.
- Yang, C., Hillas, P. J., Báez, J. A., Nokelainen, M., Balan, J., Tang, J., Spiro, R. & Polarek, J. W. (2004). The application of recombinant human collagen in tissue engineering. *BioDrugs*, 18(2), 103-119.
- Yang, H., Xu, S., Shen, L., Liu, W. & Li, G. (2016). Changes in aggregation behavior of collagen molecules in solution with varying concentrations of acetic acid. *International Journal of Biological Macromolecules*, 92581-586.
- Yang, X. H. & Zhu, W. L. (2007). Viscosity properties of sodium carboxymethylcellulose solutions. *Cellulose*, 14(5), 409-417.
- Yaşar, F., Toğrul, H. & Arslan, N. (2007). Flow properties of cellulose and carboxymethyl cellulose from orange peel. *Journal of Food Engineering*, 81(1), 187-199.
- Yin, J., Luo, K., Chen, X. & Khutoryanskiy, V. V. (2006). Miscibility studies of the blends of chitosan with some cellulose ethers. *Carbohydrate Polymers*, 63(2), 238-244.
- Yoon, K. & Lee, C. (1990). Effect of powdered cellulose on the texture and freeze-thaw stability of surimi-based shellfish analog products. *Journal of food science*, 55(1), 87-91.
- Zhang, D., Chippada, U. & Jordan, K. (2007). Effect of the structural water on the mechanical properties of collagen-like microfibrils: a molecular dynamics study. *Annals of Biomedical Engineering*, 35(7), 1216-1230.

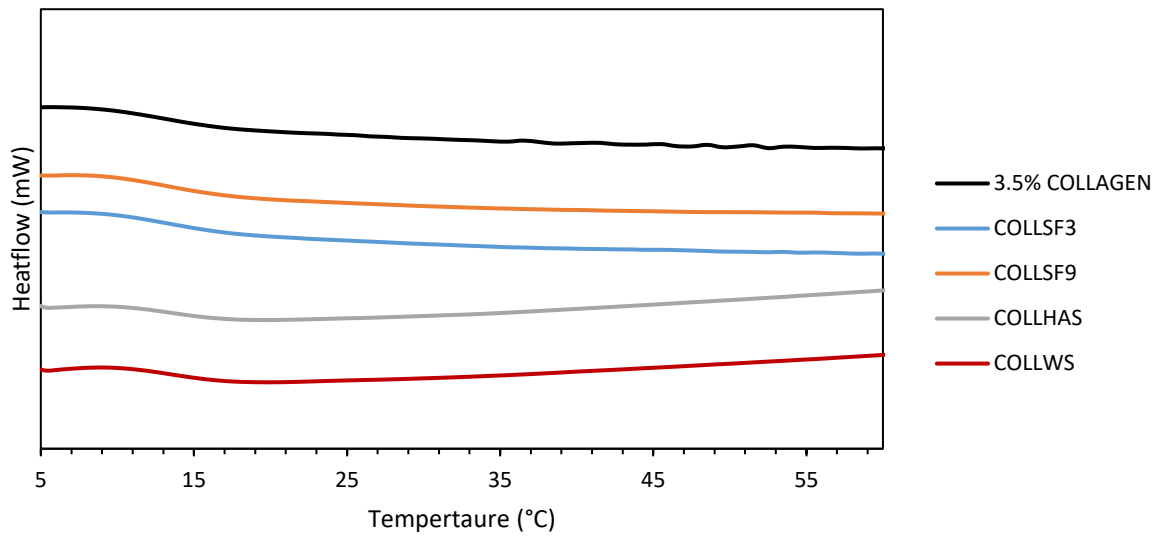
- Zhang, M., Chen, Y., Li, G. & Du, Z. (2010). Rheological properties of fish skin collagen solution: Effects of temperature and concentration. *Korea-Australia Rheology Journal*, 22(2), 119-127.
- Zhang, M., Li, J., Ding, C., Liu, W. & Li, G. (2013). The rheological and structural properties of fish collagen cross-linked by N-hydroxysuccinimide activated adipic acid. *Food Hydrocolloids*, 30(2), 504-511.
- Zhang, Y., Li, M., You, X., Fang, F. & Li, B. (2020a). Impacts of guar and xanthan gums on pasting and gel properties of high-amylose corn starches. *International Journal of Biological Macromolecules*, 1461060-1068.
- Zhang, Y., Zhou, L., Zhang, C., Show, P. L., Du, A., Fu, J. & Ashokkumar, V. (2020b). Preparation and characterization of curdlan/polyvinyl alcohol/ thyme essential oil blending film and its application to chilled meat preservation. *Carbohydrate Polymers*, 116670.
- Zheng, T., Tang, P., Shen, L., Bu, H. & Li, G. (2021). Rheological behavior of collagen/chitosan blended solutions. *Journal of Applied Polymer Science*, 50840.
- Zhijiang, C. & Guang, Y. (2011). Bacterial cellulose/collagen composite: characterization and first evaluation of cytocompatibility. *Journal of Applied Polymer Science*, 120(5), 2938-2944.
- Zobel, H. (1988). Starch crystal transformations and their industrial importance. *Starch-Stärke*, 40(1), 1-7.
- Zohuriaan, M. J. & Shokrolahi, F. (2004). Thermal studies on natural and modified gums. *Polymer Testing*, 23(5), 575-579.

APPENDICES

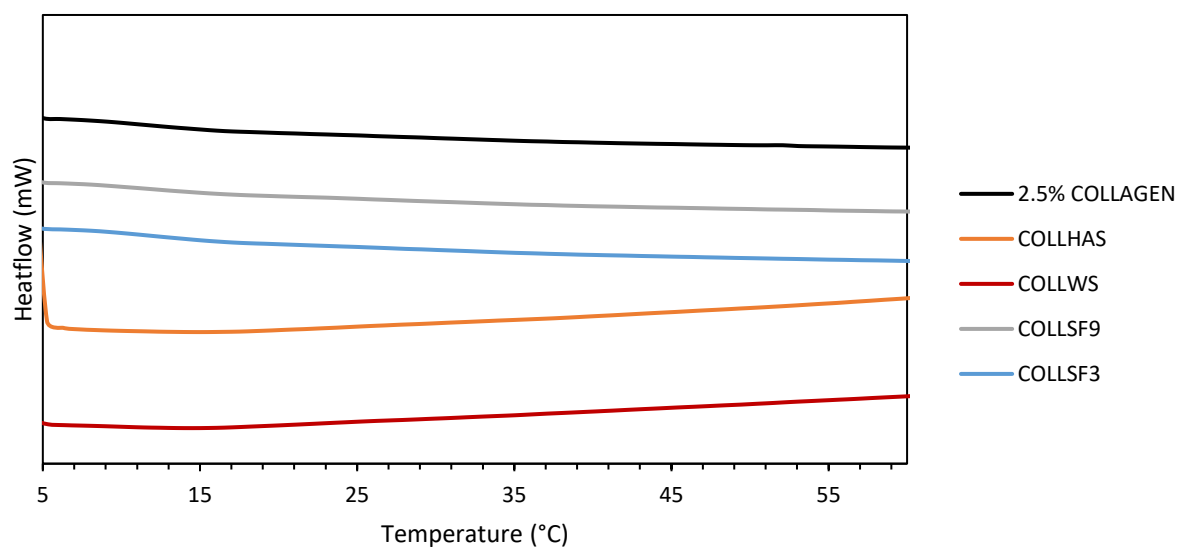
(A)



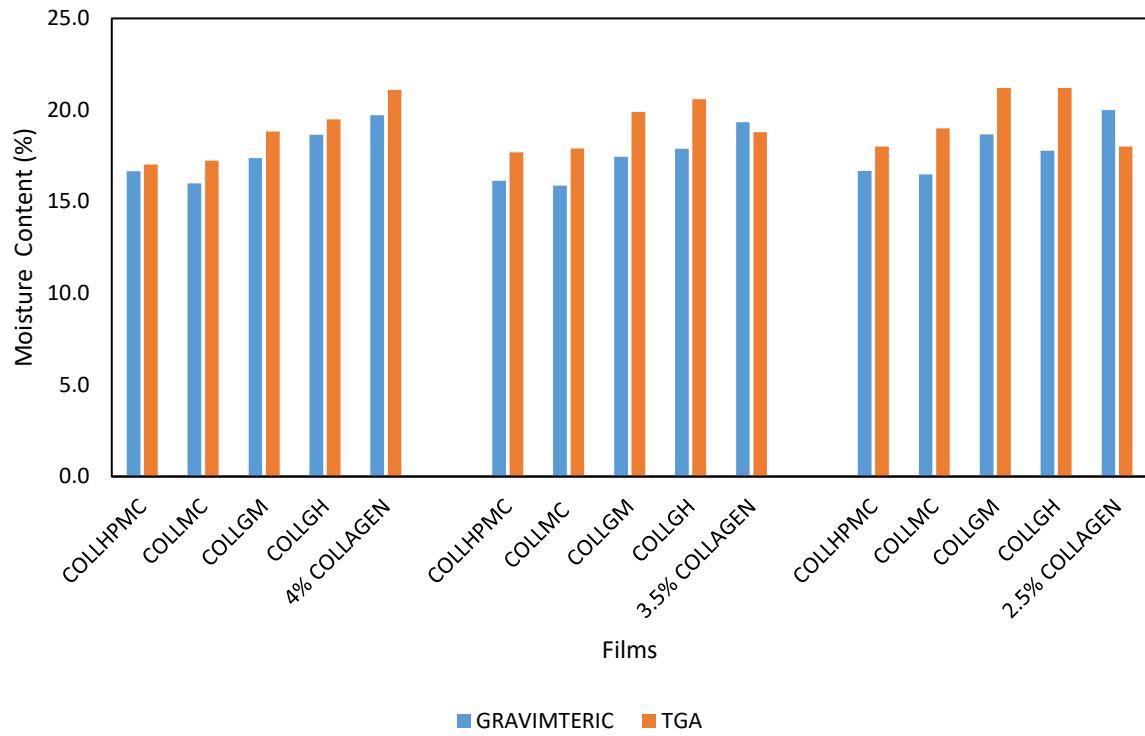
(B)



(C)



Supplementary figure 1. Cooling curve of collagen with and cellulose/starch at different collagen concentrations.



Supplementary figure 2 Comparison of moisture content of collagen films with and without hydrocolloids at different collagen concentrations determined gravimetrically and TGA.